

IONIC LIQUIDS AND DEEP EUTECTIC SOLVENTS AND
THEIR POTENTIAL USE IN PRODUCTION OF SODIUM

FATEMEH SAADAT GHAREH BAGH

A THESIS SUBMITTED IN FULFILMENT OF THE
REQUIREMENTS FOR THE DEGREE OF DOCTOR OF
PHILOSOPHY

DEPARTMENT OF CHEMICAL ENGINEERING
FACULTY OF ENGINEERING
UNIVERSITY OF MALAYA
KUALA LUMPUR

2014

ORIGINAL LITERARY WORK DECLARATION

Name of Candidate: Fatemeh saadat ghareh Bagh (Passport No. L9523678)

Registration/Matric No.: KHA100015

Name of Degree: Doctor of Philosophy (Ph.D.)

Title of Project Paper/Research Report/Dissertation/Thesis (“this Wrok”):

**NOVEL DEEP EUTECTIC SOLVENTS AND THEIR POTENTIAL USE IN
THE PRODUCTION OF SODIUM METAL**

Field of Study: Chemical Engineering

I do solemnly and sincerely declare that:

- (1) I am the sole author/writer of this Work;
- (2) This Work is original;
- (3) Any use of any work in which copyright exists was done by way of fair dealing and for permitted purposes and any excerpt or extract from, or reference to or reproduction of any copyright work has been disclosed expressly and sufficiently and the title of the work and its authorship have been acknowledged in this Work;
- (4) I do not have any actual knowledge or ought I reasonably to know that the making of this Work constitutes an infringement of any copyright work;
- (5) I hereby assign all and every rights in the copyright to this Work to the University of Malaya (“UM”), who henceforth shall be owner of the copyright in this Work and that any reproduction or use in any form or by any means whatsoever is prohibited without the written consent of UM having been the first had and obtained;
- (6) I am fully aware that if in the course of making this Work I have infringed any copyright whether intentionally or otherwise, I may be subject to legal action or any other action as may be determined by UM.

Candidate’s Signature

Date:

Subscribed and solemnly declared before,

Witness’s signature

Name:

Date:

Designation: Department of Chemical Engineering,

Faculty of Engineering, University of Malaya, Kuala Lumpur, 50603, Malaysia

Tel./Fax.:

ACKNOWLEDGMENT

My first and sincere appreciation goes to Professor Ali Hashim, Dr Inas M. Alnashef and Dr Farouq M. Jalli ,my senior supervisors for all I have learned from them and for their continuous help and support in all stages of this thesis. I would also like to thank them for being an open person to ideas, and for encouraging and helping me to shape my interest and ideas.

I would like to express my deep gratitude and respect to my love, dearest friend, and husband who sacrificed his life for me and provided unconditional love and care. I would not have made it this far without him. My daughter has been my best friend during these years of PhD. I love her dearly and thank God for her presence in my life.

My greatest appreciation and friendship goes to my closest friend, Mukhtar Aljadri, who was always a great support in all my struggles and frustrations in studies in this country. Cheers to Mukhtar for being a great reliable person to whom I could always talk about my problems and excitements. Thanks him for questioning me about my ideas, helping me think rationally and even for hearing my problems.

I would like to thank my family, especially my mother and father for always believing in me, for their continuous love and their supports in my decisions. Without whom I could not have made it here.

ABSTRACT

Sodium metal is an essential reducing agent, and it has a wide range of applications. In the present study ionic liquids (ILs) and their analogues known as deep eutectic solvents (DESs) have been proposed as electrolytes for sodium metal production at moderate temperatures of 90°C to 150°C. These electrolytes can be recognized as “green” solvents as they can potentially replace hazardous and polluting organic solvents.

In using ILs or DESs as electrolytes for the production of sodium, three factors are of paramount importance: the solubility of commercially available sodium salts in the IL or DES, the conductivity of the solution of sodium salt in IL or DES, and the stability of the sodium metal in the IL or DES. DESs possess additional advantages over ILs especially because of the ease of synthesizing them and due to the lower cost of preparation. The evaluation of DESs as new electrolytes requires an insight of their main physical properties. For this purpose, some physical properties of specially-prepared DESs were measured and the results were reported. Zinc chloride-based DESs were characterized for their melting temperatures, viscosities, electrical conductivities and refractive indices.

Subsequently, the solubility of different commercially available sodium salts were measured in different DESs and ILs at different temperatures. The solubility of sodium chloride increased with temperature in all the investigated ILs. The chemical structure of cations and anions in the ILs affected the solubility. The effect of the cation was larger than that of the anion. Different DESs were prepared by mixing ammonium or phosphonium salts, with different hydrogen bond donors (HBDs), or metal halides at several molar ratios. The effect of temperature on the solubility of sodium salts was found to be different from one DES to another. In certain DESs, the solubility of sodium salts increased with increasing temperature. The constituents of the DES and the molar

ratios affected the solubility of sodium salts. DESs based on HBDs had very low solubility of NaCl in comparison to those that used metal halides as complexing agents. Sodium metal reacted with DESs containing HBDs; however, sodium metal was stable and did not react with DESs synthesized by utilizing metal halides.

NRTL model was used to correlate the solubility of NaCl in some ILs as well as DESs at different temperatures. In most cases the experimental and calculated solubilities for NaCl in DESs and ILs were in good agreement.

Cyclic voltammetry analysis was used to study the stability of sodium within the potential range found for metal halide-based DESs at different salt:metal halide molar ratios under different temperatures. It was found that the electrical windows of DESs dropped with the increase in ZnCl_2 molar composition in the DES and increased as the temperature increased. Reduction peak was observed for sodium ion in some ZnCl_2 -based DESs at certain temperatures.

This work shows that DESs are superior to conventional molten salt electrolytes of Downs Process for the production of sodium metal due to lower operational temperature and less negative effects on the environment.

ABSTRAK

Logam natrium merupakan agen penurunan yang penting. Ianya mempunyai pelbagai kegunaan. Dalam kajian ini, IL dan DES telah dicadangkan sebagai elektrolit untuk penghasilan logam natrium pada suhu sederhana antara 90 °C hingga 150 °C. Elektrolit-
elektrolit ini boleh dikenali sebagai “pelarut hijau” memandangkan mereka berpotensi untuk menggantikan pelarut organik yang berbahaya dan mencemarkan.

Dalam penggunaan cecair ionik (ionic liquids atau ILs) atau analog mereka yang dikenali sebagai pelarut “deep eutectic” (Deep Eutectic Solvents atau DES) sebagai pelarut dan elektrolit untuk penghasilan logam natrium, tiga faktor penting untuk proses tersebut termasuklah: keterlarutan garam natrium komersil dalam IL atau DES, kekonduksian larutan garam natrium dalam IL atau DES, dan kestabilan logam natrium dalam IL atau DES. DES mempunyai kelebihan berbanding IL terutamanya kerana penghasilan yang mudah dan berkos rendah. Penilaian DES sebagai elektrolit baru memerlukan pemahaman terhadap sifat fizikal mereka. Untuk tujuan ini, sebahagian ciri-ciri fizikal DES yang disediakan khas telah didapatkan dan keputusannya dilaporkan. DES berasaskan zink klorida telah dikarakterisasikan berdasarkan suhu lebur, kelikatan, konduktiviti elektrik, dan indeks biasan pada julat suhu yang besar.

Seterusnya, keterlarutan garam natrium komersil yang berlainan telah diukur dalam DES dan IL yang berlainan pada suhu berlainan. Keterlarutan natrium klorida meningkat dengan suhu dalam semua IL yang dikaji. Struktur kimia kation dan anion dalam IL mempengaruhi keterlarutan. Kesan kation lebih besar berbanding anion. DES berlainan dihasilkan dengan mencampurkan garam ammonium dan fosfonium, dengan penderma ikatan hidrogen (hydrogen bond donors atau HBD) yang berlainan, atau logam halida pada beberapa nisbah molar. Kesan suhu pada keterlarutan garam natrium telah didapati berbeza daripada satu DES dengan yang lain. Dalam sesetengah DES,

keterlarutan garam natrium meningkat dengan peningkatan suhu. Konstituen-konstituen DES dan nisbah molar mempengaruhi keterlarutan garam natrium. DES berasaskan HBD mempunyai keterlarutan NaCl yang sangat rendah berbanding DES yang menggunakan logam halida sebagai agen pengkompleksan. Logam natrium bertindakbalas dengan DES yang mengandungi etilena glikol dan gliserol sebagai HBD; namun, logam natrium adalah stabil dan tidak bertindakbalas dengan DES yang disintesis menggunakan logam halida.

Pekali aktiviti termodinamik model “non-random two-liquid” (NRTL) telah digunakan untuk mengkorelasi keterlarutan NaCl dalam beberapa IL dan DES pada suhu berlainan. Dalam kebanyakan kes, keterlarutan yang didapati daripada eksperimen dengan yang dikira untuk NaCl dalam DES dan IL adalah hampir sama.

Analisis "cyclic voltammetry" telah digunakan untuk mengkaji kestabilan natrium dalam julat berpotensi yang ditemukan untuk DES berasaskan logam halida pada pelbagai nisbah molar garam:logam halida pada suhu yang berbeza. Keputusan menunjukkan bahawa julat elektrik untuk DES berkurangan dengan meningkatnya komposisi molar $ZnCl_2$ dalam DES dan meningkat seiring peningkatan suhu. Pengurangan puncak diperhatikan untuk ion natrium dalam sebahagian DES berasaskan $ZnCl_2$ pada suhu tertentu.

Kajian ini menunjukkan DES mempunyai kelebihan berbanding elektrolit larutan garam konvensional dalam proses Down's untuk penghasilan logam natrium oleh sebab suhu operasi yang lebih rendah dan kurang kesan negative terhadap alam sekitar.

TABLE OF CONTENTS

ACKNOWLEDGMENT		iii
ABSTRACT		iv
ABSTRAK		vi
TABLE OF CONTENTS		viii
LIST OF FIGURES		xii
LIST OF TABLES		xvii
LIST OF ABBREVIATIONS		xix
NOMENCLATURE		xx
1	CHAPTER I INTRODUCTION	1
1.1	INTRODUCTION	1
1.2	IONIC LIQUIDS AND THEIR IMPORTANCE	3
1.3	PROBLEM STATEMENT	5
1.4	RESEARCH OBJECTIVES	7
1.5	RESEARCH METHODOLOGY	7
1.6	THESIS OUTLINE	8
2	CHAPTER II LITERATURE REVIEW	9
2.1	SODIUM METAL	9
	2.1.1 Chemical Properties of Sodium Metal	10
	2.1.2 Production of Sodium Metal	11
	2.1.3 Product Grade and Quality Levels	19
	2.1.4 Factors Affecting Pricing	19
	2.1.5 Drawbacks of Downs Process	19
2.2	GREEN ELECTROLYTES (GREEN SOLVENTS)	21
2.3	INTRODUCTION TO IONIC LIQUIDS	23
	2.3.1 Physical properties of ILs	24
	2.3.2 History of ILs	26
	2.3.3 Synthesis of ILs	27
	2.3.4 Applications of ILs	28
	2.3.4.1 Applications of ILs as electrolytes	29
	2.3.4.2 ILs in fuel cells	31
	2.3.4.3 ILs in Electrochemical Sensors and Biosensors	31
	2.3.4.4 ILs in supercapacitors	32
	2.3.4.5 Application of ILs in batteries	33
	2.3.5 ILs at extreme temperatures	35
	2.3.6 Limitations of the use of ILs	36
2.4	DEEP EUTECTIC SOLVENTS (DESS)	37

2.4.1	Synthesis of DESs	43
2.4.2	Physical properties of DESs	43
2.4.2.1	Freezing point (melting point)	44
2.4.2.2	Viscosity	44
2.4.2.3	Electrical conductivity	45
2.4.2.4	Refractive index	46
2.4.2.5	Density	47
2.4.3	Applications of DESs	48
2.4.3.1	DESs in CO ₂ capture process	49
2.4.3.2	Dissolution of metal oxides	50
2.4.3.3	Purification of biodiesel	51
2.4.3.4	DESs for ionic conductivity enhancement	52
2.4.3.5	DESs as solvents for extraction of aromatic hydrocarbons from naphtha	52
2.4.3.6	DESs as catalysts	53
2.4.3.7	DESs as electrolytes	54
2.5	ILs/DESs ELECTROLYTE as MOLTEN SALT in DOWNS PROCESS	58
2.5.1	Solubility	59
2.5.2	Stability	61
3	CHAPTER III METHODOLOGY	62
3.1	SYNTHESIS OF DESs	62
3.1.1	Chemicals	62
3.1.2	Synthetic procedure	63
3.2	CHARACTERIZATION OF DESs	64
3.3	MEASURING THE SOLUBILITY OF SODIUM SALTS IN DESs AND ILs	68
3.4	MEASURING THE CONDUCTIVITIES OF SODIUM SOLUTIONS	69
3.5	MEASURING THE STABILITY OF SODIUM METAL IN DESs	70
3.6	CYCLIC VOLTAMMETRY	70
4	CHAPTER IV RESULTS AND DISCUSSION	72
4.1	SYNTHESIS AND CHARACTERIZATION OF DIFFERENT DESs	74
4.1.1	Melting temperatures	74
4.1.2	Viscosities	76

	4.1.3	Electrical conductivity	81
	4.1.4	Refractive index	92
4.2		SOLUBILITY OF DIFFERENT SODIUM SALTS IN ILs AND DESs	96
	4.2.1	Solubility of sodium chloride, sodium bromide, and sodium carbonate in ammonium-based DESs	97
	4.2.1.1	Stability of sodium metal in DESs 1 – 9	107
	4.2.1.2	Solubility modelling	107
	4.2.2.	Solubility of sodium chloride in phosphonium-based DESs	111
	4.2.2.1	Stability of sodium metal in DESs 10 – 16	117
	4.2.2.2	Solubility modelling	117
	4.2.3	Solubility of sodium chloride in different ILs	123
	4.2.3.1	Solubility modelling	127
4.3		ELECTRICAL CONDUCTIVITY OF SODIUM CHLORIDE SATURATED IN DESs	131
4.4		THE ELECTROCHEMICAL POTENTIAL WINDOWS OF ZnCl₂ BASED DESs	141
5		CHAPTER V CONCLUSIONS	153
	5.1	A SIMPLE AND EFFICIENT METHOD CAN BE USED FOR THE SYNTHESIS OF DESs	153
	5.2	DIFFERENT CONDITIONS ARE NEEDED FOR THE SYNTHESIS OF DESs OF DIFFERENT COMBINATIONS	153
	5.3	PHYSICAL PROPERTIES OF DESs ARE TEMPERATURE AND COMPONENT DEPENDENT	154
	5.4	SOLUBILITY OF SODIUM SALTS IN ILs OR DESs DEPENDED ON VARIOUS PARAMETERS	154
	5.5	NRTL ACTIVITY COEFFICIENTS MODEL CAN BE APPLIED SUCCESSFULLY FOR THE STUDIED SYSTEMS	155
	5.6	ZnCl₂-2 -BASED DESs HAD A HIGH POTENTIAL FOR BEING ELECTROLYTES FOR SODIUM PRODUCTION	155

6 CHAPTER VI RECOMMENDATIONS FOR FUTURE WORK	156
BIBLIOGRPHY	157
APPENDIX A	169

LIST OF FIGURES

Figure 2.1	Castner's Cell	13
Figure 2.2	Down's Cell	14
Figure 2.3	Flowchart for sodium metal production process by DuPont	16
Figure 2.4	Schematic representation of eutectic mixture formation	37
Figure 2.5	Structure of anthracene and phenantherne	60
Figure 4.1	Melting temperatures of DES5 (●), DES8 (▼), DES12 (▲) and DES15 (■) as a function of salt:HBD mole ratio	76
Figure 4.2	Viscosity μ of DES5 1:1 (●), 1:2 (■) and 1:3 (▲) as a function of inversed temperature T^{-1} . Curves represent fitting by Equation 1	78
Figure 4.3	Viscosity μ of DES8 1:2 (●), 1:3 (■) and 1:4 (▲) as a function of inversed temperature, T^{-1} . Curves represent fitting by Equation 1	79
Figure 4.4	Viscosity μ of DES12 1:2 (●), 1:3 (■) and 1:4 (▲) as a function of inversed temperature, T^{-1} . Curves represent fitting by Equation 1	80
Figure 4.5	Viscosity μ of DES15 1:2 (●), 1:3 (■) and 1:4 (▲) as a function of inversed temperature, T^{-1} . Curves represent fitting by Equation 1.	80
Figure 4.6	Viscosity μ of DES5 1:2 (●), DES8 1:2 (■), DES12 1:2 (▲), DES15 1:2 (▼) as a function of inversed temperature, T^{-1} . Curves represent fitting by Equation 1	81
Figure 4.7	Electrical conductivity σ of DES1 1:1.75 (●), 1:2 (■), and 1:2.5 (▲) as a function of the inversed temperature. Curves represent fitting by Equation 4.2.	83
Figure 4.8	Electrical conductivity σ of DES2 1:1 (●), 1:2 (■), and 1:3 (▲) as a function of the inversed temperature. Curves represent fitting by Equation 4.2.	84
Figure 4.9	Electrical conductivity σ of DES3 1:2.5 (●), 1:3 (■), and 1:4 (▲) as a function of the inversed temperature. Curves represent fitting by Equation 4.2.	85
Figure 4.10	Electrical conductivity σ of DES4 1:2 (●), 1:3 (■), and 1:4 (▲) as a function of the inversed temperature. Curves represent fitting by Equation 4.2.	85
Figure 4.11	Electrical conductivity σ of DES5 1:1 (●), 1:2 (■), 1:3 (▲), and 1:4 (▼) as a function of the inversed temperature. Curves represent fitting by Equation 4.2.	86
Figure 4.12	Electrical conductivity σ of DES8 1:1 (●), 1:2 (■), 1:3 (▲), and 1:4 (▼) as a function of the inversed temperature. Curves represent fitting by Equation 4.2	87
Figure 4.13	Electrical Conductivity σ of DES10 1:3 (●), 1:4 (■), and 1:5 (▲) as a function of the inversed temperature. Curves represent fitting by Equation 4.2	88

Figure 4.14	Electrical conductivity σ of DES11 1:2 (●), 1:3 (■), and 1:4 (▲) as a function of the inversed temperature. Curves represent fitting by Equation 4.2.	88
Figure 4.15	Electrical conductivity σ of DES12 1:2 (●), 1:3 (■), 1:4 (▲), and 1:5 (▼) as a function of the inversed temp. Curves represent fitting by Equation 4.2	89
Figure 4.16	Electrical conductivity σ of DES12 1:2 (●), 1:3 (■), 1:4 (▲), and 1:5 (▼) as a function of the inversed temp. Curves represent fitting by Equation 4.2	90
Figure 4.17	Refractive index n_D of DES5 1:1 (●), 1:2 (■), 1:3 (▲), and 1:4 (▼) as a function of temperature. Lines represent fitting by Equation 4.4	95
Figure 4.18	Refractive index n_D of DES8 1:1 (●), 1:2 (■), 1:3 (▲), and 1:4 (▼) as a function of temperature. Lines represent fitting by Equation 4.4.	95
Figure 4.19	Refractive index n_D of DES12 1:2 (●), 1:3 (■), 1:4 (▲), and 1:5 (▼) as a function of temperature. Lines represent fitting by Equation 4.4	96
Figure 4.20	Refractive index n_D of DES15 1:2 (●), 1:3 (■), 1:4 (▲), and 1:5 (▼) as a function of temperature. Lines represent fitting by Equation 4.4	96
Figure 4.21	Solubility of NaCl, NaBr and Na ₂ CO ₃ in DES1 as a function of temperature. The continuous line is drawn through the experimental data of the same system for visual clarity	99
Figure 4.22	Solubility profiles of NaCl and NaBr in DES2 as a function of temperature. NaCl series, for salt:HBD ratios 1:1.5 (●), 1:2 (○), 1:2.5 (◆) and 1:3 (◇). NaBr series, for salt:HBD ratios 1:1.5 (▼), 1:2 (s), 1:2.5 (▲) and 1:3 (Δ)	100
Figure 4.23	Solubility profiles of NaCl in DES3 as a function of temperature. NaCl series, for salt:HBD ratios 1:2.5 (●), 1:3 (○), 1:4 (◆) and 1:4.5 (◇)	101
Figure 4.24	Solubility (Concentration) profiles of NaCl in DES4 as a function of temperature. NaCl series, for salt:HBD ratios 1:2.5 (●), 1:3 (○), 1:4 (◆)	102
Figure 4.25	Solubility profiles of NaCl and NaBr in DES5 as a function of temperature. NaCl series, for salt:HBD ratios 1:1 (●), 1:2 (○), and 1:3 (◆). NaBr series, for salt:metal halide ratios 1:1 (◇), 1:2 (▼), and 1:3 (s)	103
Figure 4.26	Comparison of solubility (Concentration) of NaCl in DES5, 6 and 7 at 60 °C	105
Figure 4.27	Solubility (Concentration) profiles of NaCl in DES8 as a function of temperature. NaCl series, for salt:metal halide ratios 1:1 (●), 1:2 (○), 1:3 (▲) and 1:4 (Δ)	106
Figure 4.28	Solubility profile of NaCl in DES9 (salt:metal halide molar ratio 1:3) as a function of temperature	107

Figure 4.29	Calculated (NRTL) vs experimental solubilities of sodium chloride in DES2, DES3, DES4, and DES5 for different ratios and at different temperatures. z is the ratio of the HBD in the DES considering that the salt's ratio is always 1	110
Figure 4.30	Solubility profiles of NaCl in DES10 as a function of temperature (passed lines are based on NRTL calculations)	111
Figure 4.31	Solubility profiles of NaCl in DES11 as a function of temperature (passed line is based on NRTL calculations)	113
Figure 4.32	Solubility profiles of NaCl in DES12 as a function of temperature (passed lines are based on NRTL calculations).	114
Figure 4.33	Solubility profiles of NaCl in DES13 as a function of temperature (passed lines are based on NRTL calculations)	115
Figure 4.34	Solubility profiles of NaCl in DES14 as a function of temperature (passed lines are based on NRTL calculations)	116
Figure 4.35	Solubility profiles of NaCl in DES15 as a function of temperature (passed lines are based on NRTL calculations)	116
Figure 4.36	Solubility profiles of NaCl in DES16 as a function of temperature (passed lines are based on NRTL calculations)	117
Figure 4.37	Experimental solubility (Concentration) of NaCl in imidazolium-based ILs. (Δ) IL1, (o) IL2, (\square) IL3, (∇) IL4, (s) IL5, (\blacktriangle) IL6, (l) IL7, (\blacksquare) IL8, (\llcorner) IL9, (q) IL10	124
Figure 4.38	Experimental solubility (Concentration) of NaCl in pyrrolidinium-based ILs. (Δ) IL11, (o) IL12, (\square) IL13	125
Figure 4.39	Experimental solubility (Concentration) of NaCl in pyridinium-based ILs. (Δ) IL14, (o) IL15	126
Figure 4.40	Experimental solubility of NaCl in IL16 (Δ)	127
Figure 4.41	Experimental and calculated solubilities (mole fraction) by NRTL for NaCl in imidazolium-based ILs. (Δ) IL1, (o) IL2, (\square) IL3. Line represents NRTL data	130
Figure 4.42	Experimental and calculated solubilities (mole fraction) by NRTL for NaCl in (Δ) IL10, (\square) IL16. Lines represent NRTL data	131
Figure 4.43	Electrical conductivity, σ , of saturated NaCl in DES1 1:1.75 (\bullet), 1:2 (\blacksquare), and 1:2.5 (\blacktriangle) as a function of the inversed temperature. Curves represent fitting by Equation 4.2	134
Figure 4.44	Electrical conductivity, σ , of saturated NaCl in DES2 1:1 (\bullet), 1:2 (\blacksquare), and 1:3 (\blacktriangle) as a function of the inversed temperature. Curves represent fitting by Equation 4.2	134
Figure 4.45	Electrical conductivity, σ , of saturated NaCl in DES3 1:2.5 (\bullet), 1:3 (\blacksquare), and 1:4 (\blacktriangle) as a function of the inversed temperature. Curves represent fitting by Equation 4.2	135
Figure 4.46	Electrical conductivity, σ , of saturated NaCl in DES4 1:2 (\bullet), 1:3 (\blacksquare), and 1:4 (\blacktriangle) as a function of the inversed temperature. Curves represent fitting by Equation 4.2	136

Figure 4.47	Electrical conductivity, σ , of saturated NaCl in DES5 1:1 (●), 1:2 (■), 1:3 (▲), and 1:4 (▼) as a function of the inversed temperature. Curves represent fitting by Equation 4.2	137
Figure 4.48	Electrical conductivity, σ , of saturated NaCl in DES8 1:1 (●), 1:2 (■), 1:3 (▲), and 1:4 (▼) as a function of the inversed temperature. Curves represent fitting by Equation 4.2	137
Figure 4.49	Electrical Conductivity, σ , of saturated NaCl in DES10 1:3 (●), 1:4 (■), and 1:5 (▲) as a function of the inversed temperature. Curves represent fitting by Equation 4.2	138
Figure 4.50	Electrical conductivity, σ , of saturated NaCl in DES11 1:2 (●), 1:3 (■), and 1:4 (▲) as a function of the inversed temperature. Curves represent fitting by Equation 4.2	139
Figure 4.51	Electrical conductivity, σ , of saturated NaCl in DES12 1:2 (●), 1:3 (■), 1:4 (▲), and 1:5 (▼) as a function of the inversed temp. Curves represent fitting by Equation 4.2	140
Figure 4.52	Electrical conductivity, σ , of saturated NaCl in DES15 1:2 (●), 1:3 (■), 1:4 (▲), and 1:5 (▼) as a function of the inversed temp. Curves represent fitting by Equation 4.2	140
Figure 4.53	Electrochemical window of DES5(1:1) as a function of temperature on a GC (3 mm) working electrode/ Ag reference electrode/ Pt counter electrode at scan rate of 100 mVs ⁻¹	144
Figure 4.54	Electrochemical window of DES5(1:3) as a function of temperature on a GC (3 mm) working electrode/ Ag reference electrode/ Pt counter electrode at scan rate of 100 mVs ⁻¹	145
Figure 4.55	Cyclic voltammety for the reduction of saturated sodium chloride in DES5(1:1) at 130oC on a GC (3 mm) working electrode/ Ag reference electrode/ Pt counter electrode at scan rate of 100 mVs ⁻¹	145
Figure 4.56	Electrochemical window of DES8(1:1) as a function of temperature on a GC (3 mm) working electrode/ Ag reference electrode/ Pt counter electrode at scan rate of 100 mVs ⁻¹	146
Figure 4.57	Electrochemical window of DES8(1:2) as a function of temperature on a GC (3 mm) working electrode/ Ag reference electrode/ Pt counter electrode at scan rate of 100 mVs ⁻¹	146
Figure 4.58	Electrochemical window of DES8(1:3) as a function of temperature on a GC (3 mm) working electrode/ Ag reference electrode/ Pt counter electrode at scan rate of 100 mVs ⁻¹	147
Figure 4.59	Electrochemical window of DES12(1:2) as a function of temperature on a GC (3 mm) working electrode/ Ag reference electrode/ Pt counter electrode at scan rate of 100 mVs ⁻¹	149

Figure 4.60	Electrochemical window of DES12(1:3) as a function of temperature on a GC (3 mm) working electrode/ Ag reference electrode/ Pt counter electrode at scan rate of 100 mVs ⁻¹	149
Figure 4.61	Cyclic voltammetry for the reduction of saturated sodium in DES12(1:2) at 100 °C on a GC (3 mm) working electrode/ Ag reference electrode/ Pt counter electrode at scan rate of 100 mVs ⁻¹	150
Figure 4.62	Electrochemical window of DES15(1:2) as a function of temperature on a GC (3 mm) working electrode/ Ag reference electrode/ Pt counter electrode at scan rate of 100 mVs ⁻¹	151
Figure 4.63	Electrochemical window of DES15(1:3) as a function of temperature on a GC (3 mm) working electrode/ Ag reference electrode/ Pt counter electrode at scan rate of 100 mVs ⁻¹	151
Figure 4.64	Cyclic voltammetry for the reduction of saturated sodium in DES15(1:2) under 130°C on a GC (3 mm) working electrode/ Ag reference electrode/ Pt counter electrode at scan rate of 100 mVs ⁻¹	152

LIST OF TABLES

Table 1.1	Main sodium metal producers in China in 2012	2
Table 2.1	Physical properties of sodium metal	9
Table 2.2	Sodium metal grades and specifications by DuPont and MSSA	19
Table 2.3	Common cations and anions in ILs	25
Table 2.4	Properties of some ionic liquids suitable for electrochemistry	30
Table 2.5	Typical structures of the quaternary salts and HBDs used for DES synthesis	41
Table 3.1	Equipment used in the DESs synthesis	63
Table 3.2	Devices used for characterization of DESs with their uncertainties	64
Table 4.1	DESs studied in this work with their abbreviations	72
Table 4.2	ILs studied for the solubility of NaCl	73
Table 4.3	Melting temperatures for DESs 5, 8, 12 and 15	75
Table 4.4	Experimental results for viscosity (Pa.S) of DESs 5,8,12, and 15 at different molar ratios and temperatures	77
Table 4.5	Values of μ_o and E_μ for the fitting by Equation 4.1	78
Table 4.6	Experimental results of electrical conductivity (mS cm^{-1}) for DESs 1 and 2 at different molar ratios	83
Table 4.7	Experimental results of electrical conductivity (mS cm^{-1}) for DESs 3 and 4 at different molar ratios	84
Table 4.8	Experimental results of electrical conductivity (mS cm^{-1}) for DESs 5 and 8 at different molar ratios	86
Table 4.9	Table 4.9: Experimental results of electrical conductivity (mS cm^{-1}) for DESs 10 and 11 at different molar ratios	87
Table 4.10	Experimental results of electrical conductivity (mS cm^{-1}) for DESs 12 and 15 at different molar ratios.	89
Table 4.11	Values of σ_∞ and E_σ for the fitting by Equation 4.2	91
Table 4.12	Experimental refractive indices n_D of DESs 5, 8, 12, and 15 at different molar ratios	93
Table 4.13	Values of a and b for the fitting by Equation 4.4	94
Table 4.14	Solubility(wt%) of sodium chloride, sodium carbonate, and sodium bromide in DES1 at different temperatures	98
Table 4.15	Solubility(wt%) of sodium chloride and sodium bromide in DES2 at different temperatures.	99
Table 4.16	Solubility of sodium chloride in DES3 at different temperatures	101
Table 4.17	Solubility of sodium chloride in DES4 at different temperatures	101
Table 4.18	Solubility of sodium chloride and sodium bromide in DES5 at different temperatures	103
Table 4.19	Comparison of solubility of sodium chloride in DESs 5, 6, and 7 at 60 °C	104
Table 4.20	Solubility of sodium chloride in DES8 at different temperatures	106

Table 4.21	Solubility of sodium chloride in DES9 at different temperatures	106
Table 4.22	NRTL binary interaction parameters between NaCl and DES2 to DES5 for different molar ratios ($i \equiv \text{NaCl}$ and $j \equiv \text{DES}$)	110
Table 4.23	NRTL binary interaction parameters between NaCl and DES10, DES12 – DES16 for different molar ratios ($i \equiv \text{DES}$ and $j \equiv \text{NaCl}$).	118
Table 4.24	Comparison of NRTL and experimental solubilities of NaCl in DES10 at different molar ratios	119
Table 4.25	Comparison of NRTL and experimental solubilities of NaCl in DES11 at 1:3.5 molar ratio	119
Table 4.26	Comparison of NRTL and experimental solubilities of NaCl in DES12 at different molar ratios.	120
Table 4.27	Comparison of NRTL and experimental solubilities of NaCl in DES13 at different molar ratios	120
Table 4.28	Comparison of NRTL and experimental solubilities of NaCl in DES14 at different molar ratios	121
Table 4.29	Comparison of NRTL and experimental solubilities of NaCl in DES15 at different molar ratios	121
Table 4.30	Comparison of NRTL and experimental solubilities of NaCl in DES16 at different molar ratios	122
Table 4.31	Experimental solubilities of NaCl in studied ILs	123
Table 4.32	NRTL binary interaction parameters between NaCl and different ILs ($1 \equiv \text{NaCl}$ and $2 \equiv \text{IL}$)	130
Table 4.33	Experimental electrical conductivity (mS cm^{-1}) of saturated NaCl in DESs 1 and 2 at different molar ratios.	133
Table 4.34	Experimental electrical conductivity (mS cm^{-1}) of saturated NaCl in DESs 3 and 4 at different molar ratios.	135
Table 4.35	Experimental electrical conductivity (mS cm^{-1}) of saturated NaCl in DESs 5 and 8 at different molar ratios.	136
Table 4.36	Experimental electrical conductivity (mS.cm^{-1}) of saturated NaCl in DESs 10 and 11 at different molar ratios.	138
Table 4.37	Experimental electrical conductivity (mS cm^{-1}) of saturated NaCl in DESs 12 and 15 at different molar ratios	139
Table 4.38	Values of σ_{∞} and $E\sigma$ for the fitting by Equation 4.2 in the system of NaCl(saturated)/DES	141
Table 4.39	Electrochemical windows obtained at Pt counter electrode, glassy carbon working electrode, and a silver wire quasi reference electrode for DESs 5, 8, 12, and 15	142

LIST OF ABBREVIATIONS

[bmim][BF ₄]	1-Butyl-3-methylimidazolium tetrafluoroborate
[bmim][Cl]	1-Butyl-3-methylimidazolium chloride
[bmim][DCA]	1-Butyl-3-methylimidazolium dicyanamide
[bmim][Tf ₂ N]	1-Butyl-3-methylimidazolium bis (trifluoromethylsulfonyl)- imide
[bmim][TfO]	1-Butyl-3-methylimidazolium trifluoromethanesulfonate
[bmp][DCA]	1-Butyl-1-methylpyrrolidinium dicyanamide
[bmp][TfA]	1-Butyl-1-methylpyrrolidinium trifluoroacetate
[bmpyr][CF ₃ SO ₃]	1-Butyl-1-methylpyrrolidinium trifluoromethanesulfonate
[bmpyr][DCA]	N-Butyl-3-methylpyridinium dicyanamide
[bmpyr][MSO ₄]	N-Butyl-3-methylpyridinium methylsulfate
[C8mim][Cl]	1-Octyl-3-methylimidazolium chloride
[edmi][Cl]	1-Ethyl-2,3-dimethylimidazolium chloride
[emim][DMP]	1-Ethyl-3-methylimidazolium dimethylphosphate
[emim][EtSO ₄]	1-Ethyl-3-methylimidazolium ethylsulfate
[emim][MeSO ₃]	1-Ethyl-3-methylimidazolium methanesulfonate
[EtOHNMe ₃][Me ₂ PO ₄]	(2-Hydroxy ethyl) trimethylammonium dimethylphosphate
ChCl	Choline Chloride
DES	Deep Eutectic Solvent
EPA	Environment Protection Agency
FTIR	Fourier Transform Infrared
GC	Glassy Carbon
HBD	Hydrogen Bond Donor
ICP-AES	Inductively Coupled Plasma-Atomic Emission Spectrometer
IL	Ionic Liquid
MSSA	Métaux Spéciaux SA
NMR	Nuclear Magnetic Resonance
RTIL	Room Temperature Ionic Liquid
XRD	X-ray Diffraction

NOMENCLATURE

E_{μ}	Activation Energy of Viscosity(Pa.m ³ .mol ⁻¹)
γ	Activity Coefficient
τ_{ij}	Binary Interaction Parameters
k	Boltzmann's constant (meVK ⁻¹)
x_i	Composition of Component i in Binory Mixture
I	Current (A)
ρ	Density (g cm ⁻³)
ΔC_p	Difference in Heat Capacity Between the Solute in the Two States (kJ mol ⁻¹ K ⁻¹)
σ_{∞}	Electrical Conductivity as T reaches infinity (mScm ⁻¹)
σ	Electrical Conductivity (mS cm ⁻¹)
E_{σ}	Electron Mobility (meV)
a, b	Fitting parameters in Equation 4.4
R	Ideal Gas Constant (Pa.m ³ mol ⁻¹ K ⁻¹)
ΔH^{fus}	Latent Heat of Fusion of NaCl (kJ mol ⁻¹)
m.p.	Melting Point (K)
T_m	Melting Temperature (K)
z	Mole ratio of HBDs whereby mole ratio of salt is 1
τ_{ij0} , τ_{ijT}	Optimized Parameters in Equation 4.9
E	Potential Voltage (V)
n_D	Refractive Index
s	Solubility (wt%)
v	Speed of Light in the Medium of Concern (m s ⁻¹)
c	Speed of Light in Vacuum (m s ⁻¹)
T	Temperature
Tr	Triple Point Temperature
μ	Viscosity (Pa.s)
μ_0	Viscosity Constant (Pa.s)

CHAPTER I

INTRODUCTION

1.1 Introduction

Sodium (Na) metal is an essential alkali metal having wide technical and commercial applications, such as its utilization as an intermediate product in the manufacturing of chemicals and pharmaceuticals, and as metal refiner (Thayer, 2008, Pearson *et al.*, 2008). These wide applications are possible due to the fact that sodium metal is a strong reducing agent (Banks, 1989, Pearson *et al.*, 2008, Thayer, 2008). Sodium is one of the most effective coolants in nuclear reactors since the operating temperatures of these reactors are less than the boiling point of sodium (Pearson *et al.*, 2008). Sodium as well as its alloys with potassium are utilized as heat transfer agents in chemical heat transfer units. Furthermore, sodium is an important substance for producing artificial rubber (Pearson *et al.*, 2008, Thayer, 2008) .

It is interesting to know that sodium metal in its pure form is a hazardous material. It is highly reactive with many compounds available naturally in the environment, such as water (Kroschwitz, 1995, Banks, 1990). Upon contact with different compounds, sodium metal can combust spontaneously resulting in an enormous amount of heat. Therefore, it is a problematic and expensive matter to store or transport this pure metal (Kroschwitz, 1995, Thayer, 2008).

According to the United States International Trade Commission report in 2008, the main producers of sodium metal in the world are DuPont from the United States, Métaux Spéciaux SA (MSSA) from France, and three Chinese companies. In 2008, MSSA with production rate of 27000 metric tons per year was the world's largest producer. The global demand of sodium metal at the end of 2008 was 80,000 to 90,000

metric tons per year and it has been anticipated that by end of 2013, the global demand would rise to 100,000 to 120,000 metric tons per year. Declining tax incentives, rising energy cost and quality concerns are limiting Chinese sodium exports, leaving MSSA and DuPont as the main global suppliers. MSSA is also the only producer of highly purified sodium used as a coolant for fast-breeder nuclear reactors. MSSA exports most of its product, while DuPont uses much of its sodium output itself for producing biodiesel catalysts or sells it at a contracted price to Rohm and Haas, its largest customer for sodium borohydride and other chemicals (Pearson *et al.*, 2008).

In 2012, according to the global and Chinese sodium metal industry report, China in parallel with the United States and France became not only one of the big producers of sodium metal but also a big consumer. China's demand for sodium metal was expected to drive up owing to the growing consumption worldwide and the development of domestic atomic energy industry. Table 1.1 introduces the main sodium metal producers in China in 2012 (Pearson *et al.*, 2008).

Table 1.1: Main sodium metal producers in China in 2012 (Pearson *et al.*, 2008).

Manufacture	Capacity(Tons /Year)
Inner Mongolia Lantai Industrial Co., Ltd	45,000
Wanji Holding Group Co., Ltd	22,500
Ningxia Yinchuan Sodium Factory	4,000
Yinchuan Jingying Fine Chemistry Co., Ltd	3,500
Zunbao Titanium Co., Ltd	10,000(still not in production)

Currently, Downs process based on electrolysis of sodium salts, in particular sodium chloride (NaCl), is broadly used by the main producing companies (Thompson, 2004, Pearson *et al.*, 2008). Since the melting point of sodium chloride is 804 °C, the electrolysis process at this temperature can cause corrosion of the cell because of the produced sodium fog. Moreover, there is a high possibility of short electrical circuits. Hence, calcium chloride (CaCl₂) is added to NaCl at a ratio of 2:3 by mass to decrease

the fusion temperature to about 600 °C and increases the electrical conductivity. This lowering in fusion temperature makes the process feasible. The mixture is electrolyzed in a cylindrical outer iron cell lined with fire bricks. The cell is fitted with a central graphite anode and a surrounding iron cathode. The two electrodes are separated by a cylindrical iron gauze diaphragm which screens the graphite anode from the ring-shaped iron cathode. This keeps away the molten sodium metal which floats to the top of the cathode compartment from gaseous chlorine formed at the anode. In addition, the molten sodium metal must be prevented from contacting with oxygen because the metal would be oxidized instantaneously under the high-temperature conditions of the cell reaction. The sodium metal collects in the inverted trough placed over the cathode, rises up the pipe and is tapped off through the iron vessel (Keppler *et al.*, 2003, Thompson *et al.*, 2004, Pearson *et al.*, 2008).

1.2 Ionic Liquids And Their Importance

ILs have been accepted as key role players in modern green chemistry (Petkovic *et al.*, 2011). This has excited the interest of both the academia and the chemical industries. These chemicals can reduce the use of hazardous and polluting organic solvents as well as taking part in various new syntheses due to their unique characteristics (Seddon *et al.*, 2006). The terms room temperature ionic liquid (RTIL), nonaqueous ionic liquid, molten salt, liquid organic salt and fused salt have all been used to describe these salts in the liquid phase. ILs are known as salts that are liquid at room temperature in contrast to high-temperature molten salts. They have a unique array of physico-chemical properties, such as low vapor pressure and non flammability which make them suitable in numerous applications in which conventional organic solvents are not sufficiently effective or not applicable (Earle and Seddon, 2000).

In the late 1990s, there was a significant increase in research on ILs, from synthesis and characterization to their possible applications. They are now a major topic

of academic and industrial interest with numerous existing and potential applications. The number of scientific papers, books, and patents covering the latest advances in ionic liquids are available in the literature (Hagiwara and Ito, 2000, Petkovi *et al.*, 2009) .

The main advantage of ILs is the profiles of their physical and chemical properties, resulting from the complex interplay between hydrogen bonding and Van Der Waal interactions. Remarkably, many ILs' properties can be controlled by structurally modifying their cations and anions (Plechkova and Seddon, 2008). ILs are such a class of potentially useful liquids in environmental friendly applications (Gan *et al.*, 2006, Arce *et al.*, 2007, Petkovic *et al.*, 2011). Therefore, they have been explored for use in various research and industrial applications, from electronic applications, including electrolytes for batteries and capacitors to separation processes, such as extraction of metals or matrices for mass spectrometry. One drawback of utilizing ILs is that they are usually expensive and unavailable at industrial scale (Keskin *et al.*, 2007, Petkovic *et al.*, 2011) .

ILs analogous, known as deep eutectic solvents (DESs), have been recognized as an alternative to traditional solvents and ILs (Hou *et al.*, 2008). A DES is generally composed of two or three components which are capable of associating with each other, through hydrogen bond interactions, to form a eutectic mixture (Abbott *et al.*, 2003a). These components are cheap and environmentally safe (Chen *et al.*, 2010). The resulting DES is characterized by a melting point lower than those of the individual components. In 2004, Professor Andrew Abbott and his group reported the synthesis of the first deep eutectic solvent from a mixture of choline chloride (ChCl) as a salt and urea as hydrogen-bond donor (HBD), with a salt:HBD molar ratio of 1:2. The melting point of ChCl is 302°C and that of urea is 133°C while the above mentioned eutectic liquid melts at 12 °C (Abbott *et al.*, 2004a).

It was reported that these ILs analogues or DESs can seriously compete with ILs in terms of physical properties, synthesis, and more importantly in price (Earle *et al.*, 2000, Abbott *et al.*, 2003a, Kareem *et al.*, 2010). As mentioned above, it is possible to choose their components to be biodegradable and non-toxic, adding more advantages to them. Additionally, most DESs are non-reactive with water (Chen *et al.*, 2010). Since the time that Abbott and his colleagues reported the first choline chloride:urea DES, numerous researches on DESs synthesis and applications have been carried out (Abbott *et al.*, 2004b). New DESs were introduced and numerous applications were studied (Kareem *et al.*, 2010, Hayyan *et al.*, 2012). To date, numerous research papers, patents, and books have been published covering various possible applications of DESs. In Chapter Two, a comprehensive literature review on ILs and DESs is presented.

1.3 Problem Statement

Energy crisis and global warming are the major challenges of 21st century. These crises have risen up due to (i) limited energy resources and energy security, (ii) sustainability of utilized energy resources, as well as (iii) environmental impact of conventional fuels and climate change (Akella *et al.*, 2007, Zheng *et al.*, 2010).

The demands on energy became incredibly huge, and the resources of conventional energy, such as coal, oil, petroleum and natural gas are limited. These resources are estimated to last until 2040 (Hayward, 2010). On the other hand, it has been recognised that the nuclear energy can have serious harmful impact on the environment if accidents happen. This was clear in both Chernobyl and Fukushima disasters, where radiation leaked out of the reactors due to accidental events (Hayward, 2010). All of these factors necessitated the wise use of alternative forms of energy. Renewable sources of energy, such as solar energy, wind energy, geothermal energy, bioenergy, ocean energy, and hydropower are completely clean, natural and harmless. The obvious problem concerning utilizing renewable energy resources lies in their high

costs of generation. The high cost of these forms of energy originated from two facts. Firstly, the technology of renewable energy, such as solar panels, is newer in comparison to the conventional ones. Secondly, the materials used in the manufacturing of renewable energy systems are often rare and costly (Namovicz, 2011).

The manufacturers in developed countries terminated the production of sodium metal, including the leading manufacturers, DuPont, MSSA and some Russian manufacturers. This is due to the fact that Down's Process features high energy consumption (Global and China Sodium Metal Industry Report, 2012).

Several concepts have been proposed to reduce emissions and energy consumption, but none have been successfully applied on an industrial scale. Developing an electrolytic process that can be used to produce sodium metal more economically is increasingly important. The operability of the process must also be improved, making automation possible. Suitable processing techniques are limited because sodium has a strong affinity to oxygen and water due to its negative reduction potential. Therefore, sodium chloride cannot be electrolyzed in aqueous solutions. All processes must also comply with existing environmental regulations. Therefore, a novel process that electrolyzes sodium chloride at or near ambient temperatures has numerous industrial potential applications (Paterson, 1966, Keppler *et al.*, 2003, Anastas, 2010).

The concept of green solvents was adopted to represent the efforts spent to minimize the industrial impact on the environment by utilizing safer and friendlier solvents than the conventional ones. This adoption led to the development of four direct implementations for this concept. They are: i) replacing the hazardous solvents by solvents of better environmental, health and safety properties, ii) using bio-solvents produced from renewable sources, iii) replacing the volatile organic compounds used as solvents by benign solvents, and iv) using ionic liquids (ILs) as well as their analogues

known as deep eutectic solvents (DESs) which are considered as non-volatile because they showed negligible vapor pressure.(Keskin *et al.*, 2007, Anastas, 2010)

The work elaborated in this thesis is an attempt to overcome the problem of high-energy consumption in sodium metal production by introducing ILs and DESs as low-temperature electrolytes for this process.

1.4 Research Objectives

In using ILs or DESs as electrolytes for the production of sodium, three factors are of paramount importance for the process: the solubility of commercially available sodium salts in the IL or DES, the conductivity of the solution of sodium salt in IL or DES, and the stability of the sodium metal in the IL or DES. Additionally, the pertinent physical properties of these DESs are important to be characterized if these DESs are planned to be used industrially. Thus, in summary, the objectives of this work are as follow:

- 1- Synthesis of different DESs including new metal halide-based DESs in the laboratory.
- 2- Measuring the physical properties for some of these DESs.
- 3- Studying the solubility of some commercially available sodium salts in ILs and DESs.
- 4- Studying the conductivity of sodium chloride (NaCl) in DESs.
- 5- Investigating the stability of sodium metal in selected DESs
- 6- Applying thermodynamic models to correlate the experimental data.
- 7- Evaluating of cyclic voltammetry of selected DESs

1.5 Research Methodology

The methodology followed to achieve the objectives of this project will be dealt with comprehensively in Chapter Three. However, a brief introduction to the methodology is given here:

- 1- Synthesis of DESs.
- 2- Characterization of physical properties of these solvents using various equipment.
- 3- Preparation of solubility experiments.
- 4- Addition of sodium salts to ILs and DESs.
- 5- Sampling of the experimental mixtures for the measurement of solubility.
- 6- Analysis of the samples using Induced Coupled Plasma (ICP) analysis.
- 7- Final results are drawn from the ICP results.
- 8- Estimation of the stability of sodium metal inside DESs.
- 9- Applying the non-random two liquid (NRTL) model for activity coefficients to correlate the experimental results.
- 10- Cyclic voltammetry analysis using a computer-controlled *i*-Autolab potentiostat

1.6 Thesis Outline

This thesis comprises the following main chapters:

1. Chapter One - INTRODUCTION
2. Chapter Two - LITERATURE REVIEW
3. Chapter Three - METHODOLOGY
4. Chapter Four - RESULTS AND DISCUSSIONS
5. Chapter Five - CONCLUSIONS

CHAPTER II

LITERATURE REVIEW

2.1 Sodium Metal

Sodium or Natrium in Latin has been used for centuries in both organic and inorganic industries (Thayer, 2008). Alkali metals or group I in the Periodic Table consists of lithium, sodium, potassium, rubidium, cesium, and francium. This group of metals possess lower densities than other metals, one loosely bound valence electron, the largest atomic radii in their periods, lower ionization energies, low electronegativities and highly reactive than common metals (Banks, 1990). Atomic sodium possesses 11 protons, 11 electrons and 12 neutrons that lead to its atomic number of 11 and atomic mass of 22.98977 g/mol. Table 2.1 represents the physical properties of sodium metal (Banks, 1990, Eggeman, 2007).

Table 2.1: Physical properties of sodium metal (Eggeman, 2007).

Phase at room temp.	solid
Density at 20 °C	0.968 g/cm ³
Hardness	0.5 Mohs
Liquid density at f.p.	0.927 g/cm ³
Melting point	97.72 °C
Boiling point	883 °C
Heat of fusion	2.60 kJ/mol
Heat of vaporization	97.42 kJ/mol
Molar heat capacity	28.230 kJ/ mol K
Energy of first ionisation	495.7 kJ/mol
Standard potential	- 2.71 V
Colour	Silvery white

Sodium has a body centered cubic (bcc) structure and is found in the form of a solid metallic substance at room temperature. Due to its softness, it can be easily cut with a

table knife. When it is exposed to air, it reacts rapidly with oxygen and oxidizes to a dull and gray coating (Eggeman, 2007). Sodium is a good conductor of electricity which means that electric current can pass through this element without high resistance (Pearson *et al.*, 2008).

2.1.1 Chemical Properties of Sodium Metal

Sodium is more reactive than lithium and less reactive than potassium (Banks, 1990, Klemm *et al.*, 2005). In the presence of air, it reacts with oxygen instantly to form sodium oxide coating. This coating prevents any further reaction of the oxygen with the underlying metal layers. Therefore, it is often stored by immersing in nitrogen atmosphere or inside inert liquids like naphtha or kerosene (Wells, 1984). When it is burnt in the open atmosphere, sodium peroxide (Na_2O_2) will be produced whereas upon burning in limited supply of oxygen, it forms sodium oxide (Na_2O). If this burning process is carried out under high pressure, sodium superoxide (NaO_2) would be formed (Wells, 1984, Greenwood, 1997). At a temperature over $200\text{ }^\circ\text{C}$, sodium reacts with hydrogen to produce sodium hydride (NaH) (Holleman *et al.*, 2001). Sodium reacts with water through an exothermic reaction and produces sodium hydroxide (NaOH) and hydrogen gas. The released heat often ignites the hydrogen gas and a fire may break out to the extent that a loud explosion would occur if a big piece of sodium is brought in contact with water (Klemm *et al.*, 2005). Sodium is able to react with ammonia either in the presence of pure carbon or cobalt. In the presence of carbon, it produces sodium cyanide (NaCN) and hydrogen, and in the presence of cobalt, it produces sodium amide (NaNH_2) and hydrogen (Greenlee *et al.*, 1946). Sodium amalgam, which is an alloy of sodium and mercury, is formed by the reaction of sodium and mercury (Renfrow *et al.*, 1939). On addition of sodium into alcohol, alkoxide is produced. This reaction is similar to sodium's reaction with water since in both cases it replaces one hydrogen atom (Chandran *et al.*, 2006). Sodium halides can be produced by vigorous reaction of

sodium metal with fluorine and chlorine at room temperature to produce sodium fluoride (NaF) and sodium chloride (NaCl), respectively. However, it reacts potentially with vaporized bromine and iodine to produce sodium bromide (NaBr) and sodium iodide (NaI). When sodium comes in contact with alkenes and dienes, it forms additional products. One such product formed the basis of making an early synthetic rubber known as Buna Rubber. Sodium reacts with organic halides in order to produce sodium organic compounds (Greenwood *et al.*, 1997, Klemm *et al.*, 2005).

After aluminium, magnesium, calcium and iron, sodium is the fifth most abundant element on earth, comprising 2.6 % of the earth's crust (Banks, 1990). Sodium metal in its pure form is a hazardous material. This is because it is highly reactive due to its extremely low ionization energy. It may combust spontaneously if it comes into contact with air or water. These facts make it a hazardous material that is difficult and expensive to transport and store (Kroschwitz, 1995, Thayer, 2008).

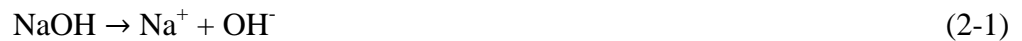
2.1.2 Production of Sodium Metal

The most common source for the production of sodium metal is sodium chloride (NaCl) (Banks, 1990). It is found in nature as rock salt and in sea water. Other sources of sodium metal are minerals, among which are soda niter (NaNO₃), cryolite (Na₃AlF₆), zeolites (NaAlSi₂O₆-H₂O), and sodalite (Na₄Al₃(SiO₄)₃Cl) (Banks, 1990, Pearson *et al.*, 2008).

Sodium metal is not found in its pure form in nature due to its vigorous reactivity (Banks, 1990, Keppler *et al.*, 2003, Thompson *et al.*, 2004). In October 1807, Humphrey Davy isolated sodium by electrolyzing molten soda (NaOH) (Banks, 1990). The next year, Gay-Lussac and Louis Jacques Thénard produced sodium metal by reducing sodium hydroxide with iron at high temperatures (Banks, 1990). More than four decades later, in 1855, Henri Étienne Sainte-Claire Deville developed the first

commercial process to produce sodium metal from its carbonate by carbon as catalyst at temperatures over 1100 °C (Wallace, 1953). However, in 1890, Hamilton Castner distilled off sodium metal by electrolysis of fused caustic soda at 330 °C in Oldbury, England, at a rate of two tons/week. Later on, Castner's cell was used to produce sodium at a rate of 105 tons/week until late in 1952 when the producing plant was finally discontinued. Figure 2.1 illustrates a schematic diagram of Castner's cell (Wallace, 1953). Castner's process is principally based on the electrolysis of caustic soda (NaOH) involving three steps:

- a) Producing individual ions through fusing NaOH



- b) In the electrolysis cell, Na^+ ion tends to move toward the iron cathode and the molten sodium is formed.



- c) At the nickel anode, H_2O and O_2 are evolved due to oxidation of OH^- :



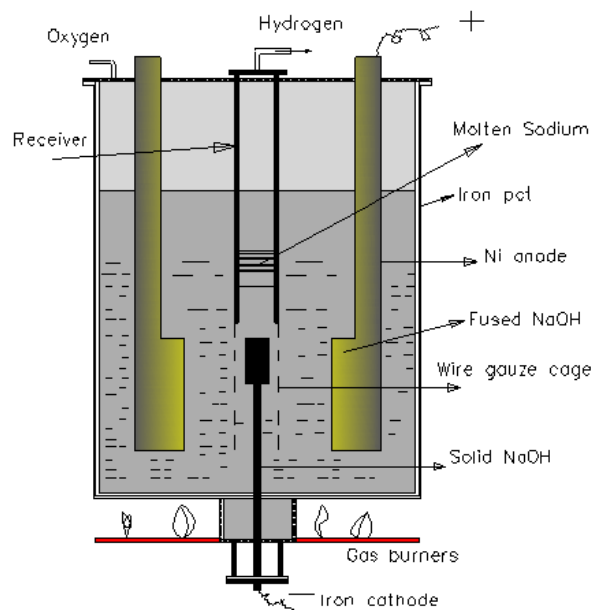


Figure 2.1: Castner's Cell (Wallace, 1953).

In 1921, a process involving the electrolysis of a mixture of fused sodium chloride (NaCl), calcium chloride (CaCl₂), and barium chloride (BaCl₂) in Downs cell was introduced to reduce the melting point of the electrolyte to slightly below 600 °C (Thompson *et al.*, 2004, Keppler *et al.*, 2003). This made the process more practical compared to using pure NaCl which has a higher melting point of about 804 °C. This change was applied because operating an electrolytic process at 804 °C was difficult and presented numerous operating constraints. During electrolysis, calcium was also obtained at the cathode but sodium and calcium were separated from each other due to the difference in density. The density of sodium is 0.67 g/cm³ and the density of calcium is 2.54 g/cm³ at operating temperature, making molten sodium and calcium immiscible (Keppler *et al.*, 2003, Thompson *et al.*, 2004, Pearson *et al.*, 2008).

As the decomposition potential of calcium is close to that of sodium, calcium co-deposits with sodium at the cathode during the electrolysis. This is the reason for having traces of calcium in sodium metal produced by Downs process (Pearson *et al.*, 2008). A schematic diagram of Downs cell is shown in Figure 2.2. Downs cell consists of a large steel tank lined with a refractory material containing one or more carbon anodes, each

surrounded by a cathode. The small gap between the cathode and anode is filled with a molten mixture of NaCl, CaCl₂ and BaCl₂. When electrical current is applied across the gap, NaCl produces sodium metal, which is collected at the cathode, and chlorine gas (Cl₂), which is collected at the anode. A fine metal mesh between the cathode and anode prevents the sodium and chlorine from reacting again to form NaCl. The chlorine gas bubbles up through the molten salt and is collected in the chlorine dome at the top center of the vessel (Pearson *et al.*, 2008). It is then liquified to be used for various industrial purposes. Being less dense than the molten salts, the sodium metal floats up from the cathodes into a collector, then goes up a riser and into a holding container (Pearson *et al.*, 2008).

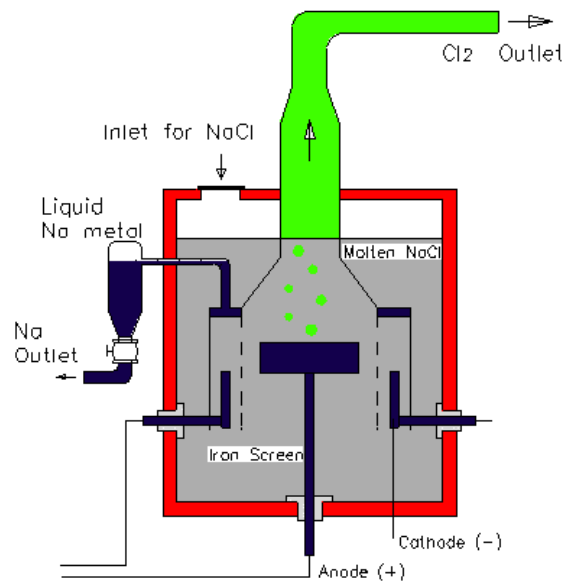


Figure 2.2: Downs Cell (Pearson *et al.*, 2008).

The chemistry of reaction in Downs Cell is:

- a) Fused NaCl contains sodium and chloride ions



- b) At the cathode: Na⁺ ions migrate to the cathode where they are reduced to Na



c) At the anode: Cl^- ions migrate to the anode and oxidised to form chlorine gas



d) Overall Reaction



The reduced sodium metal in the iron cathode of Downs cell is required to be filtered while it is cooled. Afterwards, the excess calcium would be precipitated by adjusting with a mixture of an inert gas containing 0.1% - 2% of nitrogen (N_2) and 0.1% - 0.5% of oxygen (O_2) at a temperature below 300 °C. The separation method is based on the oxidation of calcium to calcium oxide during the purification of sodium (Pearson *et al.*, 2008).

Downs process shown in figure 2.3 produces sodium with 99.8% purity, is the currently utilized method in industry worldwide (Keppler *et al.*, 2003, Thompson *et al.*, 2004, Pearson *et al.*, 2008, Thayer, 2008). The major producers are DuPont and MSSA companies (Thayer, 2008). It has been stated that the production process for manufacturing sodium metal from the Downs cells is essentially the same for the two manufacturers (Pearson *et al.*, 2008, Thayer, 2008).

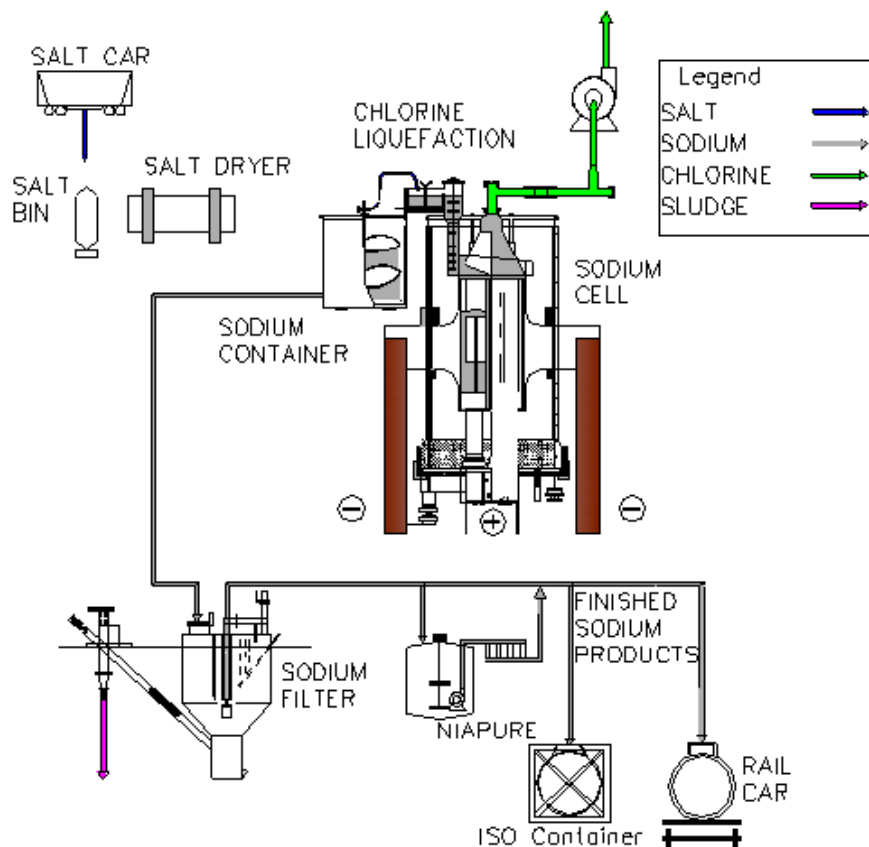


Figure 2.3: Flow chart for sodium metal production process by DuPont
(Pearson *et al.*, 2008).

Several important sources of demand for sodium metal have declined or disappeared entirely, although new applications are under development. Its largest end use was as a raw material in the production of tetraethyl lead and tetramethyl lead used to formulate anti-knock additives for gasoline in automobiles. Consumption for this application was dramatically reduced with the phasing out of leaded gasoline during the 1970s and 1980s (Davies, 1996, Citron *et al.*, 1977, Gatti *et al.*, 2010). Sodium metal was principally used in a wide range of applications, such as an input in the production of chemicals and pharmaceuticals, indigo fuel, pesticide, rare and precious metal smelting, nuclear industries and in metal refining (Fanning, 2007, Pearson *et al.*, 2008, Thayer, 2008). It has also been applied in the manufacture of different chemicals including sodium borohydride, sodium azide, sodium methylate, sodium tertbutoxide,

agricultural chemicals; such as herbicides and insecticides, dyes; such as synthetic indigo, nylon synthetic fibers, rubber compounds, and flavorings and fragrances. Sodium metal is also used to produce pharmaceutical products such as barbiturate, vitamins A and C, ibuprofen, and sulfa methoxizane (Klemm *et al.*, 2005). In metal manufacturing, sodium metal is used as a reducing agent to produce pure metals such as titanium, tantalum, hafnium, and zirconium (Thayer, 2008, Pearson *et al.*, 2008). Possessing vast difference in its melting and boiling points, 98 °C to 882 °C, it has been used as heat transfer medium in atomic reactors and in die casting machines. Other metal industry uses include silicon manufacturing, refining metallic lead; silver; and zinc, alloying metals and steel de-scaling via sodium hydride. Additionally, sodium metal is useful as a scavenging agent in smelting processes (Fanning, 2007).

Three downstream products of sodium metal are of special interest due to the potential for strong growth in the future. Firstly, sodium methylate is a catalyst used in the production of biodiesel fuel (Thayer, 2008), which will likely witness an increased production due to regulations mandates for biofuel usage in some countries. Secondly, polysilicon wafers used in solar cells may benefit from the United States' government support for alternative energy (Pearson *et al.*, 2008). Lastly, titanium metal primarily used in aircraft manufacturing could be produced in a less expensive manner via a new production process that uses sodium metal (Thayer, 2008).

Since the sodium metal industry features high energy consumption, manufacturers in developed countries including leading industrial manufacturers in America, France, and Russia, have halted its production, according to a global sodium metal report in 2012. In China, by contrast, major sodium metal enterprises are expanding their capacities and many start-ups emerged, helping worldwide sodium capacity to be transferred to China in phases. Recently, the sodium metal production capacity of China has exceeded 100,000 tons/yr, offering a surplus in the market.

China is not only a big producer of sodium metal now, but also a big consumer. In 2006, the demand for sodium metal in China hit 82,000 tons/yr, and then in 2010 the figure was close to 100,000 tons/yr. China's demand for sodium metal is expected to drive up due to the increasing consumption worldwide as well as the skyrocketing development of domestic atomic energy industry (Global and China Sodium Metal Industry Report, 2012).

Indigo Fuel is the key consumer of sodium, occupying 60% of the total demand. Indigo Fuel LTD was incorporated in 2005 to provide convenient quality fuel oil service at a higher quality than the industrial standard (Pearson *et al.*, 2008). The development of nuclear power industry has in recent years fuelled the demand for nuclear-grade sodium which features higher specific heat than vast majority of metals and good thermal insulation properties and serves as an ideal coolant for fast reactors (Fanning, 2007). Thus far, fast reactors are in service worldwide, including Phenix, Super-Phenix, Russian BN-600 and Chinese CEFR, which are all employing nuclear-grade sodium as coolant (IAEA, 2007).

It is expected that the demand for nuclear-grade sodium will show incredible growth with the application of the fourth generation nuclear power technology. In the upcoming three to five years, the demand for nuclear grade sodium will mainly be contributed by two fast reactors, i.e. Fujian Sanming and Russian BN-1200, with the targeted demand hitting 8,000 tons/yr and 6,000 tons/yr, respectively (IAEA, 2007).

According to the United States International Trade Commission's Report in November 2008 (Pearson *et al.*, 2008), the Chinese exportation of sodium metal reached a total of 16,917,000 pounds in 2007.

2.1.3 Product Grade and Quality Levels

Table 2.2 depicts various sodium metal grades by DuPont and MSSA in the period January 2005 - June 2008. DuPont offers three quality levels, while MSSA offers four.

Table 2.2: Sodium metal grades and specifications by DuPont and MSSA (Pearson *et al.*, 2008).

DuPont		MSSA	
Commercial Name	Specifications	Commercial Name	Specifications
Technical	99.89% pure; 400 ppm Ca	Technical (S+)	99.8% pure; 400 ppm Ca
Niapure	99.89% pure; 400 ppm Ca	Sopure	99.8% pure; 200 ppm Ca
Niapure select	99.91% pure; 200 ppm Ca	Refined	99.9% pure; 10 ppm Ca
		Extra Refined	99.98% pure; 10 ppm Ca

2.1.4 Factors Affecting Pricing

Numerous factors influence the purchaser's decision regarding the suppliers of sodium metal. DuPont asserted that price was the largest single factor affecting purchase decisions in the market for sodium metal (Thayer, 2008, Pearson *et al.*, 2008).

Prices of sodium metal may fluctuate based on demand factors such as general economic activity as well as shifts in demand for products in the sectors where sodium metal is used. They can also fluctuate based on supply side factors, most notably the costs of sodium chloride and energy (Pearson *et al.*, 2008). In addition, the form and the purity of the sodium metal may have an effect on the overall cost of production, and subsequently the price. Other factors that may affect the price are the order size, length of the contract, and the mode of transportation.

2.1.5 Drawbacks of Downs Process

Downs process is considered as the major process for producing sodium metal, as elaborated in previous subsections. It is a minor source for producing industrial chlorine as well. The major drawback of this process is the high energy consumption due to the

elevated temperatures at which it operates. The electrolyte mixture has a melting temperature of about 580 °C to 600 °C (Banks, 1990, Paterson, 1966, Keppler *et al.*, 2003, Thompson *et al.*, 2004). As a result, cell freeze-ups and other upsets are frequent, leading to an increase in the overall costs of production. For this reason, a smooth operation of the cell is found to be difficult and the process is not amenable to automation (Thompson *et al.*, 2004). Operating an electrolytic process at such temperature is difficult and presents a serious operational constraint. Additionally, the concentric cylindrical cell design of the Downs process (Figure 2.2) imposes a poor space efficiency. This translates directly into high capital and operating costs per ton produced.

Several concepts have been proposed to reduce emissions and energy consumption, but none has been successfully applied on an industrial scale. There is an increasing need to develop an electrolytic process that can be used to produce sodium metal in a more economical way. There is also a need to develop a process that can improve the operability, for instance, making automation possible (Paterson, 1966, Keppler *et al.*, 2003, Thompson *et al.*, 2004). The options for new processing techniques are limited because sodium has a strong affinity to both oxygen and water (Klemm *et al.*, 2005). Thus, considering production of sodium metal, NaCl cannot be electrolysed in aqueous solutions. Furthermore, any new process should comply with existing environmental regulations. A new process in which NaCl would be electrolyzed at or near ambient temperatures would have a good industrial potential (AlNashef, 2010). Hence, it is of paramount importance to introduce new electrolytes in which the production of sodium from its common salts such as NaCl is possible at low to moderate temperatures. These electrolytes will be considered as “green” materials if they succeed in reducing the operation temperature (AlNashef, 2010).

2.2 Green Electrolytes (Green Solvents)

Organic solvents are important in chemical industry. They were utilized as media for reactions in the synthesis of various compounds, as extraction solvents for separation and purification, as well as in drying. They are also very important in analytical methodologies, spectrometry and measurements of physico-chemical properties (Plechkova and Seddon, 2007). The majority of traditional organic solvents are hazardous, with problems of toxicity, cost, and waste by-products resulting from their use in the chemical industry. Using these solvents in chemical laboratories and chemical industries is raising an important issue for the health and safety of workers as well as pollution for the environment. Green chemistry deals with research focused on finding solutions for issues related to excessive use of non-renewable energy and hazardous or toxic materials with greener alternatives (Anastas *et al.*, 2003, Plechkova and Seddon, 2007, Anastas, 2010). Paul Anderson, a senior chemist in the Environment Protection Agency (EPA), developed the principles of green solvents during 1990s and introduced them as a set of guidelines. These guidelines were intended to be followed by the chemical manufacturers to reduce pollution in their plants and to make chemical processes safer and more sustainable. The main target was that the products and processes should be cost-competitive and be designed to include as many as possible of the following:

- a) Source reduction/prevention of chemical hazards, which includes
 - Design chemical products to be less hazardous to human health and environment. This meant that these products should be less toxic to organisms and ecosystems, not persistent or bioaccumulative in organisms or the environment, and inherently safer with respect to handling and use.
 - Use feedstocks and reagents that are less hazardous to human health and environment.

- Design syntheses and other processes to consume less energy and materials.
 - Use feedstock derived from renewable resources or from abundant waste.
 - Design chemical products that can be reused or recycled.
- b) Treat hazardous chemicals and convert them to safe end materials.
- c) Proper disposal of chemicals not of more use (Anantas *et al.*, 2003).

The most popular green solvents are water and supercritical carbon dioxide. Recently, room temperature ionic liquids (RTILs) were also recognized by many researchers as green solvents, mainly due to the fact that they possess negligible vapour pressure. This means that they do not emit any hazardous vapours when they are used, eliminating the opportunity for the formation of combustible or toxic clouds (Anantas *et al.*, 2003).

All three of the above mentioned green solvents have their benefits and drawbacks. Water is abundant, nontoxic, and intensive compound. However, it is a poor solvent for most organic compounds and it is difficult to be removed from end products. Supercritical carbon dioxide is abundant, can dissolve most organic solvents, and can be removed easily. The main problem of utilizing it is the requirement for large energy input to generate the pressure needed to liquefy it. RTILs are non flammable, non volatile, and easy to recycle. However, most of these solvents are derived from petroleum products and thus are toxic to aquatic organisms (Pandey, 2006, Plechkova and Seddon, 2007). Therefore, there was an urgent need to develop new type of green solvents that can be prepared from abundant, inexpensive, innocuous, and biorenewable components and can be reused or recycled. Ionic liquids (ILs) analogues known as deep eutectic solvents (DESs) possess the former principles mentioned earlier in this section (Zhang *et al.*, 2012).

In the following Sections, ILs and DESs are presented and discussed comprehensively.

2.3 Introduction to ILs

An ionic liquid is a liquid which is composed entirely of ions, such as KCl and KOH at high temperatures. If a compound is in liquid state at or near room temperature and is composed of ions only, then it is called “room temperature ionic liquid” or RTIL (Rui, 2010). In practice, the concept of RTIL is extended to include ILs within the temperature range 0-100 °C (Galiński *et al.*, 2006).

The attractive force between the anion and the cation in ILs is coulombic force. The magnitude of this force is related to the charge number and radius of anion and cation. Ionic compounds have a larger ionic radius and smaller force between them, thus an ionic compound has a low melting point (George *et al.*, 2011). Their ability to be liquid at or around room temperature initiated a big interest in them within the chemical society.

The application of common organic solvents, such as toluene, diethyl ether or methanol is limited nowadays due to more strict regulations imposed on the industry. In contrast, ILs due to their specific properties and their potential as green solvents do not encounter this problem. An intriguing characteristic is to fine tune the physical and chemical properties by suitable choice of cations and anions (Zhang *et al.*, 2012). Therefore, ILs are recognized as designer solvents, which means that their properties such as viscosity, melting point, hydrophobicity, and density can be easily adjusted to suit the requirements of a particular process. ILs have been the subject of considerable interest due to their very low volatility and their ability to dissolve a wide variety of compounds, which makes them useful as “green” solvents for energy applications and industrial processes. ILs involving fully quarternized nitrogen cations have negligible

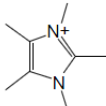
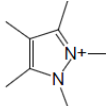
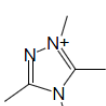
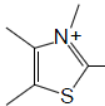
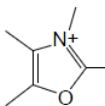
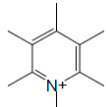
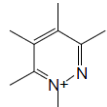
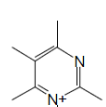
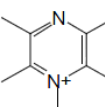
vapor pressure and are non-flammable. These properties are important when addressing the health and safety concerns for the working personnel. Negligible vapor pressure means that the solvent will not evaporate at normal temperatures, eliminating the risk of the formation of combustible clouds or the risk of suffocation (Huang *et al.*, 2001, Stewart *et al.*, 2004).

2.3.1 Physical Properties of ILs

ILs possess numerous important favorable properties in physics and chemistry, such as their low melting points, moderate viscosities and densities, and high thermal stability. Different cations and anions can be selected to prepare different ILs, and their compatibility with water is thus controllable (Wang, 2007). They are little denser than water, miscible with substances having very wide range of polarities, and can simultaneously dissolve organic and inorganic substances.

The negligible vapor pressure, wide electrochemical window (between 2 V and 4.5 V except for Bronsted acidic system), large liquid range, and high electrical conductivity are other favorable physical properties of ILs. The molecule of an IL is composed of a large asymmetric cation and an organic or inorganic anion (Johnson, 2007, Forsyth *et al.*, 2004). The most common cations and anions that compromise the well-known ILs are presented in Table 2.3.

Table 2.3: Common cations and anions in ILs (Wilkes *et al.*, 1982, Wasserscheid and Keim, 2000, Tsuda and Hussey, 2007).

Cations					
	Imidazolium	Pyrazolium	Triazolium	Thiazolium	Oxazolium
Cations					
	Pyridinium	Pyridazinium	Pyridinium	Pyrazinium	
Anions	NO_3^- Nitrate	Cl^- Chloride	Br^- Bromide	CuCl_2^-	ClO_4^- Perchlorate
	BF_4^- Tetrafluoroborate	PF_6^- Hexafluorophosphate	CF_3SO_3^- Trifluoromethanesulfonate	$\text{N}(\text{SO}_2\text{CF}_3)_2^-$	$\text{N}(\text{SO}_2\text{CF}_2\text{CF}_3)_2^-$

The physical behavior of ILs was found to be dependent largely on the utilized cation and anion. Additionally, this behavior can be easily changed by utilizing various cations and anions. The solubility of ILs in water depends significantly on the structure of the anion (Plechkova and Seddon, 2007, Holbrey *et al.*, 2003). For instance, most of the chloride-based ILs are miscible with water, while the ILs composed of the anions hexafluorophosphate (PF_6^-) or bis(trifluoromethylsulfonyl)imide (Tf_2N^-) are hydrophobic. This shows an advantage for ILs over conventional solvents, which is the possibility of anion replacement that enables designing compounds with properties required for a particular application. Thus, the solvent properties of ILs can be tuned for a specific application by varying the anion-cation combinations (Shvedene *et al.*, 2005, Plechkova and Seddon, 2007, Zhou *et al.*, 2012).

ILs can replace hazardous and polluting organic solvents in industrial applications. They are receiving an increasing interest as environmental-friendly solvents for many synthetic and catalytic processes. Having high electrical conductivity due to their ionic structure is the essential character of ILs that predisposes them as potential efficient electrolytes. This is an advantage for their potential to serve as electrolytes in electrochemical processes (Tsuda and Hussey, 2007).

In ILs, a combination of bulky and asymmetrical cations and evenly shaped anions form a regular structure of liquid phase. This means that the anion of ILs cannot pack well. The combination of larger asymmetric organic cation and smaller inorganic counterparts lower the lattice energy and hence the melting point of the formed ILs. In some ILs, the anions are relatively large and playing a role in decreasing the melting point. For instance, the melting point of 1-butyl-3-methylimidazolium tetrafluoroborate ([bmim][BF₄]) is -71°C in comparison with that of 1-butyl-3-methylimidazolium hexafluorophosphate ([bmim][PF₆]) which is 11°C (Coll *et al.*, 2005, Ganjali *et al.*, 2009). Consequently, ILs are often liquid at ambient temperature (Keskin *et al.*, 2007, Plechkova and Seddon, 2007).

ILs are polar solvents and consist of loosely coordinating bulky ions. They are able to dissolve various organic, inorganic, and organo metallic materials. They are immiscible with many organic solvents. Furthermore, they are nonaqueous polar alternatives for phase transfer processes (Cooper and O'Sullivan, 1992, Keskin *et al.*, 2007).

What was discussed above is general and valid for the most commonly used ILs. However, it must be noted that there are many ILs containing different anions and cations and their properties cover a vast range. Therefore, the above statements should not be generalized for all existing ILs and for those designed in the future (Keskin *et al.*, 2007).

2.3.2 History of ILs

The use of the first IL goes back to 1914 when ethylammonium nitrate, [EtNH₃][NO₃], with melting point of 12 °C was synthesised. However, ILs did not achieve a decent interest until the discovery of binary ionic liquids synthesised from mixtures of aluminium chloride and N-alkylpyridinium or 1,3-dialkylimidazolium

chloride. The most problematic factor of chloroaluminate based ILs was their instability in the presence of air and water. Moreover, they are not inert towards various organic compounds and this limited their applications. In 1970, a work was presented for developing ILs as electrolytes for nuclear warhead batteries and space probes (Chen, 2001, Keskin et al., 2007).

These type of batteries and space probes required molten salts to operate. These molten salts were hot enough to damage the nearby materials. Therefore, chemists searched for salts which remain liquid at lower temperatures and eventually they identified alkyl-substituted imidazolium and pyridinium cations, with halide or tetrahalogenoaluminate anions that initially could use as electrolytes in battery applications. Wilkes and his colleagues improved specific ILs for the use as battery electrolytes (Wilkes *et al.*, 1982). In 1980s, imidazolium-based cations were found to have better properties, such as air/moisture stability and more potential variations (Carmichael and Seddon, 2000, Aki *et al.*, 2001, Sheldon *et al.*, 2002, Kölle and Dronskowski, 2004). In 1990s, applications of air-stable ILs, such as 1-n-butyl-3-methylimidazolium tetrafluoroborate ([bmim][BF₄]) and 1-n-butyl-3-methylimidazolium hexafluorophosphate ([bmim][PF₆]) as well as water-stable ILs were increased rapidly to the extent that ILs became among the most promising chemicals as solvents in chemical processes (Aki *et al.*, 2001, Wasserscheid *et al.*, 2002).

2.3.3 Synthesis of ILs

There are three basic methods to synthesis the ILs, namely: the metathesis reactions, acid-base neutralization, and direct combination.

a) Metathesis Reactions

Numerous ILs are prepared by a metathesis reaction from a halide or similar salt of the desired cation. Pyridinium and imidazolium halides can be obtained according to

this method. Generally, these kinds of reactions are divided into two categories depending on the water solubility of the targeted IL: metathesis by free acids or ammonium salts of alkali metals, and metathesis by silver (Ag) salt. For example, in 1996, the synthesis of water immiscible ILs, such as dialkylimidazolium bis(triflyl)amides and dialkylimidazolium nonafluorobutanesulphonate were reported by reacting a halide or triflate with lithium bis(triflyl)amide. The production of water miscible ILs is an important and difficult task since it requires separation of the by-products from the desired IL. For instance 1-ethyl-3-methylimidazolium tetrafluoroborate [C₂mim][BF₄] was produced in 1992 by metathesis reaction of 1-ethyl-3-methylimidazolium iodide [C₂mim]I and silver tetrafluoroborate (AgBF₄) in methanol.

Metathesis reaction is suitable for synthesizing new ILs. However, the prepared ILs are usually contaminated with small amounts of halide ions that may react with solute materials (Wilkes and Zaworotko, 1992, Bao *et al.*, 2003).

b) Acid-base neutralization

Monoalkylammonium nitrates are produced by the neutralization of the aqueous solutions of the amine (base) with nitric acid. The by-product is water, which can be removed under vacuum. Similarly, tetraalkylammonium sulfonates are prepared by the reaction of sulfonic acid and tetraalkylammonium hydroxide. In order to purify the produced IL, it must be dissolved in either acetonitrile or tetrahydrofuran and treated with carbon active for at least 24 hours, and the organic solvent can be removed under vacuum (Wilkes and Zaworotko, 1992, Bao *et al.*, 2003).

c) Direct combination

Some ILs are prepared by direct combination of a metal salt and a metal halide, such as halogenaluminate(III) as well as chlorocuprate(I) based ILs. However, the

chlorocuprate(I) based ILs are sensitive to oxygen, and are not utilized widely in synthesis (Welton, 1999).

2.3.4 Applications of ILs

Apart from the fact that ILs are utilized as green solvents in different chemical and engineering processes (Plechkova and Seddon, 2007), they possess numerous other applications. Various electronic applications, such as electrolytes for batteries, capacitors and charge storage devices, as well as conducting and light emitting materials have utilized ILs as solvents. In the area of polymers, ILs have applications as grafted components, solvents for polymerization, and modifiers of polymer morphology. They were utilized as solvents for the synthesis as well as stabilization of nanomaterials.

ILs have been the focus of most researchers on nonaqueous electrodeposition and recovery of metals. Separations, spectroscopy, and mass spectrometry are other broad applications for ILs. They have also been employed widely in solvent extraction, particularly for recovery of metal salts. Moreover, ILs are being utilized recently as optical materials, lubricants, fuels for propulsion, and refrigerants (Plechkova and Seddon, 2007, Handy, 2011).

2.3.4.1 Applications of ILs as Electrolytes

Another useful aspect of some ILs is their wide window of electrochemical stability, which can be as large as 6 V. This wide window makes ILs promising candidates for use as electrolytes for electrochemistry. While materials with large voltage windows are desirable, they may also possess unacceptable viscosities and insufficient conductivities for use as electrolytes. High viscosities often result in higher oxidation potentials due to decreased mass transfer rates and longer reaction times (Tsuda and Hussey, 2007, Pinter et al., 2010). Examples of main physical and electrochemical properties of some IL electrolytes (ILEs) are shown in Table 2.4.

Table 2.4: Properties of some ionic liquids suitable for electrochemistry. (Stenger-Smith and Irvin, 2009)

Ionic Liquid	M.P. (°C)	Viscosity (Pa s) at 25 °C	Conductivity (S/cm)	Electrochemical window (V)
1-ethyl-3-methylimidazolium bis (trifluoromethylsulfonyl)imide	-17	18	8.8	4.1
1-ethyl-3-methylimidazolium trifluoromethanesulfonate	-9	43	9.2	4.1
1-butyl-1-methylpyrrolidinium bis(trifluoromethylsulfonyl)imide	-50	71	2.2	5.5
1-hexyl-3-methylimidazolium hexafluorophosphate	-80	548	1	5.5
1-ethyl-3-methylimidazolium dicyanamide	-21	17	27	5.9
1-methyl-3-octylimidazolium tetrafluoroborate	-88	422	0.43	6

The ILs shown in Table 2.4 have attracted significant attention as alternative electrolytes in industrial processes. They can be used in a pure form or in combination with other solvents (Stenger-Smith *et al.*, 2002, Pringle *et al.*, 2005, Zakeeruddin and Graetzel, 2009). Advantages of ILs include a broad temperature range of application, low volatility, and good electrochemical and thermal stabilities (Armand *et al.*, 2009).

Wide electrochemical windows and negligible vapor pressures make ILs advantageous for the electroplating of metals and semiconductors (Tsuda and Hussey, 2007, Keskin *et al.*, 2007, Palmieri *et al.*, 2009). ILs are also promising in enabling the technology of high-temperature fuel cells (Greaves, 2008, Handy, 2011). ILs offer an excellent alternative to conventional aqueous proton transfer systems at temperatures exceeding 100 °C, i.e. when water as a solvent is not an option. ILs have been showing an enhancement for long-term stability of electromechanical actuators utilizing electroactive or ion exchange polymers (Ding *et al.*, 2003). The most prominent illustration of stability enhancement using ILs is in the electrochromic devices. When 1-butyl-3-methylimidazolium tetrafluoroborate ([bmim][BF₄]) was used as the electrolyte in a polyaniline-based electrochromic display, there was no significant loss in electroactivity after 1,000,000 cycles (Armand *et al.*, 2009, Handy, 2011). ILs were

also utilized as electrolytes in the synthesis of electrochemical sensors, biosensors and supercapacitors (Handy, 2011).

2.3.4.2 ILs in Fuel Cells

Many factors had encouraged researchers to utilize ILs as electrolytic solvents in fuel cells (Handy, 2011, Ke *et al.*, 2012). Examples are the high demand to improve the anhydrous proton conducting electrolytes used in fuel cells, and the need for developing electrolytes able to operate at temperatures above 120 °C, especially in polymeric-electrolyte membrane fuel cells. ILs were required to act as protonic solvents or be capable to conduct protons. The developed fuel cells were categorized in five categories: i) molten carbonate, ii) solid oxide, iii) phosphoric acid, iv) polymeric electrolyte membrane, and v) alkaline fuel cells (Handy, 2011, Ke *et al.*, 2012). The non-Bronsted acid-base room temperature imidazolium ionic liquids, such as 1-n-butyl-3-methylimidazolium tetrafluoroborate, were found to be outstanding electrolytes for fuel cells (Noda and Susan, 2003).

2.3.4.3 ILs in Electrochemical Sensors and Biosensors

Due to the entire ionic composition, the intrinsic conductivity, and the negligible vapor pressure of ILs, they have been utilized as electrochemical sensors for gaseous analytes, such as oxygen (O₂), carbon dioxide (CO₂), sulfur dioxide (SO₂) and ammonia (NH₃) (Buzzeo *et al.*, 2004, Peng *et al.*, 2008). Cai and colleagues (Cai *et al.*, 2001) had developed an SO₂ gas sensor resembling the Clark model that employs an IL as the electrolyte. Furthermore, several groups have used different kinds of ILs in electrode modification for the design of electrochemical sensors or as novel electrolytic materials. For instance, Lu *et al.* in 2001 utilized a novel chitosan/1-butyl-3-methylimidazolium hexafluorophosphate composite material as a new immobilization matrix to entrap proteins, in addition they studied the electrochemical behaviors of hemoglobin (Hb) on glassy carbon electrode (Singh *et al.*, 2012).

Biosensors are small devices employing biochemical molecular recognition properties as the basis for a selective analysis. The major processes involved in any biosensor system are (i) analyte recognition, (ii) signal transduction, and (iii) readout. In an electrochemical biosensor, a molecular sensing device couples a biological recognition element to an electrode transducer, which converts the biological recognition event into an electrical signal (Singh et al., 2012). ILs have shown good compatibility with biomolecules and enzymes and even whole cells are active in various ILs. 1-Butyl-3-methylimidazolium chloride ([bmim][Cl]) was found miscible with silk, which is an attractive biomaterial with excellent mechanical properties and biocompatibility (Singh et al., 2012, Buzzeo et al., 2004).

2.3.4.4 ILs in Supercapacitors

Electrochemical capacitors (ECs), also known as supercapacitors, are power leveling charge storage devices in which oxidation and reduction of electroactive polymers, metal oxides, or carbonaceous materials are taking place to store electrical energy. They require an electrolyte for their operation. During the charging process, the EC cathode is reduced and the anode is oxidized to store electrical energy. Later on, this charge is released during discharge, as electrode materials return to their neutral states (Namisnyk, 2003).

The most promising applications of ECs are memory protection systems for portable electronics, load leveling for electric utilities and energy storage for electric vehicles. ECs generally provide more power per unit mass than batteries and store more energy per unit mass than traditional capacitors. Consequently, they are used to supply burst power for electric vehicles (Namisnyk, 2003).

The most common commercial electrolytes used in ECs are organic solvents containing a salt, typically an alkylammonium salt dissolved in acetonitrile. These mixtures have good conductivity and ion transport properties, but also have high

volatility, flammability and toxicity (Stenger-Smith, 2002). These characteristics raise safety and environmental concerns. Moreover, the use of acetonitrile generally limits their applications above 70 °C due to the risk of cell rupture. It also has a very low flash point, i.e. 10 °C, and emits toxic gases such as cyanogen (CN₂) and nitrogen oxides (NO_x) as combustion products.

The use of ILs (Frackowiak *et al.*, 2005, Kim *et al.*, 2011) in ECs allows volatile and hazardous conventional solvents to be eliminated and improves the operational stability of these devices. Therefore, their utilization opens up the possibility of utilizing energy storage devices for applications at higher temperatures such as military equipment, hand-held surgical tools for sterile surgical environments, subterranean probes and other power systems exposed to high temperature environments (Kim *et al.*, 2011, Balducci *et al.*, 2004, Frackowiak *et al.*, 2005) .

2.3.4.5 Application of ILs in Batteries

For a long period of time, battery cells used caustic and hazardous electrolytes. By the introduction of ILs as electrolytes in these cells, scientists believe that numerous new types of batteries can be introduced. This is due to the fact that ILs are non-volatile and thermally-stable in contrast to the common electrolytes (Stenger-Smith and Irvin, 2009).

Generally, conventional batteries are composed of an organic electrolyte, a graphite anode and a lithium transition metal oxide as cathode, such as lithium cobalt oxide (LiCoO₂) and lithium nickel oxide (LiNiO₂). The used electrolytes consist of an electrochemically stable lithium salt, such as lithium hexafluorophosphate (LiPF₆) and ethylene carbonate (C₃H₄O₃) dissolved in an organic solvent such as dimethyl carbonate (C₃H₄O₃). The dissolved C₃H₄O₃ plays a role by forming a film on the anode to protect the electrolyte against reduction while it is ionically-conductive. The

drawback of these batteries is the low boiling point and flammability of the organic solvent which cause a safety risk (Lewandowski and Swiderska-Mocek, 2009)

Unlike highly acidic conventional electrolytes, ILs due to their unique properties have fostered the interest in battery applications to develop novel types of solid state rechargeable batteries such as lithium-ion batteries. These kinds of batteries are broadly used in portable electrical and electronic products such as laptops and cell phones owing to the highest energy density among rechargeable energy storage systems. The utilized electrolyte in a lithium ion battery consists of a lithium salt dissolved in the IL, such as 1-ethyl-3-methylimidazolium bis(trifluoromethylsulfonyl)imide ($[\text{C}_2\text{mim}][\text{NTf}_2]$) (Abu-lebdeh and Davidson, 2013).

Various ILs were studied for this application, such as 1-ethyl-3-methylimidazolium chloride and 1-methylbutylpyridinium chloride due to their incombustibility. In addition, other ILs based on tetrafluoroborate $[\text{BF}_4]$, bis(trifluoromethylsulfonyl)imide $[\text{NTf}_2]$, and hexafluorophosphate $[\text{PF}_6]$ as anions and ethylmethylimidazolium $[\text{EtMeIm}]$, $[\text{Et}_2\text{Me}_2\text{Im}]$, $[\text{BuMe}_2\text{Im}]$, and $[\text{Me}_3\text{HexN}]$ as cations have been reported for this application (Clare *et al.*, 2008).

Furthermore, ILs have been used as alternative electrolytes in nickel-metal hydride (NiMH) batteries, the standard lead-acid battery, and flow batteries. In 2012, researchers at the Queen's University Belfast have developed a novel battery technology based on a design of a flow battery which stores and releases energy by the electrochemical reactions of ILs as they pass through a membrane.

The purity of the electrolytes used in energy storage applications is crucial for the stability and performance of electrochemical devices. ILs are no exception. Depending on the synthetic routes employed for the preparation of ILs, impurities in these materials may include water, superfluous cations or anions, or other solvents. Even trace amounts of contaminants can result in undesirable side reactions and hamper the performance of

electroactive polymer-based devices. Chloride and water impurities have been shown to influence the viscosity of ionic liquids (Seddon *et al.*, 2000, Zhang and Bond, 2005). Small amounts, i.e. few ppm's, of sorbents such as alumina and silica can also result in reduced electrochemical performance of ILs (Clare *et al.*, 2008, Stenger-Smith and Irvin, 2009). Purification approaches that produce ILs suitable for use in electrochemistry often involve column chromatography or vacuum distillation of impurities.

2.3.5 ILs at Extreme Temperatures

As the focus on energy production and storage attained an increasing pattern, there is a growing demand for charge storage devices that operate at a wide range of temperatures. For instance, charge storage devices are ideally operational at temperatures as low as -30 °C in the automotive industry (Pesaran *et al.*, 2007). Other requirements for these devices are even more severe, as the temperatures reach -60 °C. It has been reported that batteries undergo severe performance deficiency at low temperatures (Stenger-Smith and Irvin, 2009). Low temperatures slow down the kinetics of the charge/discharge process and increase the viscosity of the electrolytes leading to a reduced ability of charge transportation. These changes in the property lead to performance deficiency or failure upon long exposure to low temperatures. One of the most serious effects of low temperatures on solution-based electrolytes is the reduction in the solubility of the electrolyte material, which in turn leads to precipitation of the salt and destruction of the EC or battery (Stenger-Smith and Irvin, 2009).

ILs as electrolytes are used at the moderately low temperatures required by the automotive industry. However, few of these can operate at extremely low temperatures (Stenger-Smith and Irvin, 2009). What is more challenging is the fact that these electrolytes should support various electrochemical processes in a variety of reaction systems across a broad temperature interval. There are very few ILs that remain liquid

at extremely low temperatures and their viscosities may become relatively high for most of the electrochemical applications. To overcome this challenge, the use of mixtures of different ILs and the use of viscosity-reducing additives have been proposed. Not only the low temperatures are of concern to researchers, but also the elevated temperatures, i.e. up to 60 °C (Pesaran et al., 2007). As most solvent-based electrolytes have high solvent volatility at elevated temperatures, solvent evaporation can result in numerous unfavoured issues. These issues include fire and explosion in sealed systems and in electrolyte precipitation, destruction of the charge storage materials, and loss of charge storage capability in open systems. Thus, the negligible vapour pressure of ILs makes them excellent electrolytes for use at elevated temperatures (Stenger-Smith and Irvin, 2009).

2.3.6 Limitations of the Use of ILs

To date, cations such as N-alkylimidazolium, N-alkylpyridinium, N-alkylthiazolium, N,N-dialkylpyrazolium, tetraalkylammonium, and coordinating inorganic bulky anions such as BF_4^- , PF_6^- , F_3CSO_3^- and $(\text{F}_3\text{CSO}_2)_2\text{N}^-$, ZnCl_3^- , are the most investigated components of traditional ILs (Endres, 2002, Endres, 2004). Imidazolium based ILs for their micro-by phasic structure composed of polar and non-polar domains had undergone numerous simulations and experimental research (Santos *et al.*, 2007). Drawbacks that hindered the full utilization of ILs are mostly connected to their toxicity (Morrison et al., 2009). Possible drain of the ILs to the soil or water channels make them persistent pollutants and pose environmental risks. Not forgetting to mention the cost factor, drawbacks are now obvious for the industrial management bodies in considering ILs for complete utilization.

Even though ultrasonic irradiation ostensibly can break down traditional ILs into more environmentally benign non-toxic compounds, such as biurea and acetoxyacetic

acid (Xuehui, *et al.*, 2007), this irradiation requires high frequency sound waves on solutions of hydrogen peroxide and acetic acid to be implemented.

Other main challenging issues are not only the synthesis, but also the drying and purifying steps of traditional ILs. Moreover, the equipment used in processes utilizing ILs necessitate certain skills, owing to the complicated reaction mechanism of traditional ILs. Lastly, physico-chemical properties of ILs can simply be influenced by small amounts of impurities especially in catalytic activities and electrochemical applications.

Recently, Abbott and his colleagues (Abbott *et al.*, 2001) demonstrated that a mixture of solid organic salt and a complexing agent can form a liquid at temperatures below 100°C, known as deep eutectic solvent (DES).

2.4 Deep Eutectic Solvents (DESs)

The term “deep eutectic solvent” refers to liquids close to the eutectic composition of the mixtures and is represented diagrammatically in Figure 2.4. The eutectic point of a mixture refers to the molar ratio of the components which gives the lowest melting point.

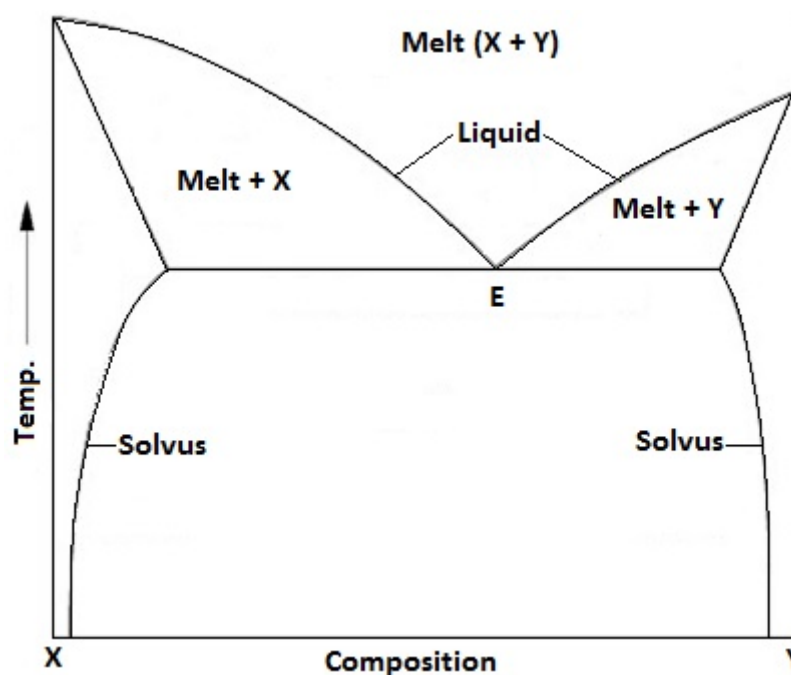
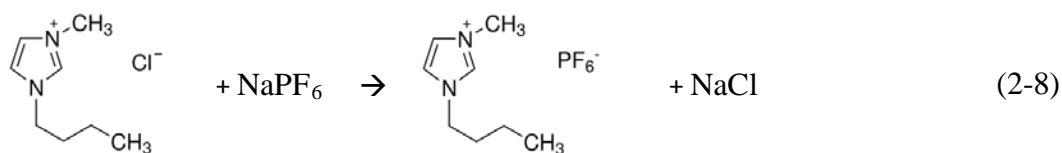


Figure 2.4: Schematic representation of eutectic mixture formation

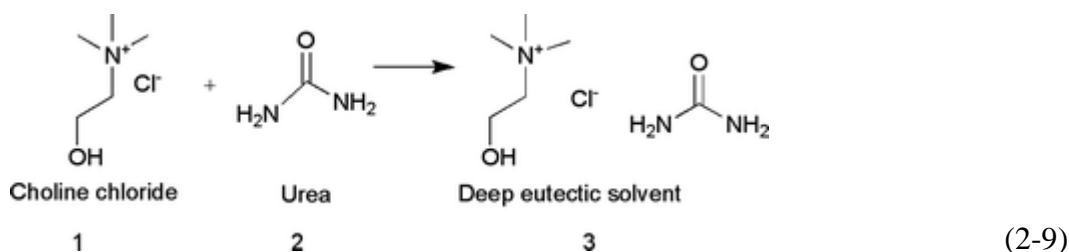
It is found in the literature that DESs are mostly synthesized by mixing a quaternary salt (X) with a hydrogen bond donor (HBD) or a complexing agent (Y). Professor Andrew Abbott and co-workers have introduced the first research article on the synthesis of DESs in 2004 (Abbott *et al.*, 2004a). Their initial view was that it is possible to synthesize a DES from a quaternary salt and a HBD. Their research was focused on quaternary ammonium salt, (2-hydroxyethyl)trimethylammonium chloride, which is known commercially as choline chloride. It is a well-known vitamin used in the diet of cows and chicken; thus, it possesses no harmful impact and is considered as a totally “green” compound (Aquilina *et al.*, 2011). The selected HBD was carbamide (urea) which is a fertilizer used in agriculture. Obviously both components are harmless and green, resulting in a totally green DES upon their mixing (Mavrovic *et al.*, 2010)

DESs are now a class of solvents that possess desirable characteristics such as low cost, high solute solubility, wide potential window, and negligible impacts on the environment (Abbott *et al.*, 2003a, Abbott *et al.*, 2006a, Kareem *et al.*, 2010, Ju *et al.*, 2012). The possibility to design their structure by choosing the proper salt and HBD as well as the similar solvation properties to ILs made them analogues for ILs. Added advantage is the ease of the preparation in comparison with ILs. DESs are produced from physical mixing of the salt and HBD with acute heating involving neither chemical reaction nor the need for catalysts (Yu *et al.*, 2008, Weaver *et al.*, 2010, Ilgen *et al.*, 2009, Reinhardt *et al.*, 2008); while, the production of ILs involves chemical reactions of the raw materials. Side products will form impurities to the IL and require additional purification (Keskin *et al.*, 2007). An example is given for the production of 1-butyl-3-methylimidazolium hexafluorophosphate according to the following reaction (Swatloski *et al.*, 2003):



Sodium chloride (NaCl) as a side product is an impurity to the IL and its removal is essential to improve the quality of the product.

The combination of the salt and the HBD or the complexing agent in DES synthesis creates a new compound with a melting point lower than that of its constituent components. The mechanism by which a DES is formed is not complicated. The HBD or the complexing agent interacts with the anion of the salt and increases its effective size, which in turn reduces the anion interaction with the cation. Thus, the melting point of the mixture is decreased (Zhang *et al.*, 2012, Carriazo *et al.*, 2012). Generally, DESs are characterized by a large depression of freezing point and by being liquids at temperatures lower than 150 °C (Carriazo *et al.*, 2012). However, most of them are liquid between room temperature and 70 °C (Zhang *et al.*, 2012, Carriazo *et al.*, 2012). A classic example is the mixture of choline chloride/urea DES. The melting points of ChCl and urea are 302 °C and 133 °C, respectively. When mixed at a 1:2 molar ratio of ChCl:urea, a liquid eutectic mixture was formed which has a melting temperature of 12 °C (Abbott *et al.*, 2003a, Zhao and Baker, 2013).



As mentioned earlier in this Section, DESs have advantages in the preparation procedure over ILs. Firstly, the preparation procedure of these eutectic mixtures, unlike traditional ILs, is simple and needs only to mix two different compounds mechanically

with acute heating without the need for a catalyst. Secondly, a total mass efficiency and zero emission in the synthesis are achieved. This means that all the masses of the salt and HBD or complexing agent involved are converted to DES, which is environmentally benign as there is no side products, especially in the form of vapours. Lastly, substance density and energy density in the preparation process is lower in comparison to ILs synthesis (Kareem et al., 2010, Hayyan et al., 2012, Zhao and Baker, 2013). All these advantages of the DESs make them suitable for strict industrial requirements and large-scale production in comparison to the traditional ILs synthesized by metathesis and ion exchange.

In 2007, DESs were defined using the general formula $R_1R_2R_3R_4N^+X^-:Y^-$, (Abbott et al., 2007a) where X is generally a halide ion (often Cl^-), Y is a complexing agent. Four general types of DESs were given as below:

Type I DES: $Y = MCl_x$, $M = Zn, Sn, Fe, Al, Ga$

Type II DES: $Y = MCl_x \cdot yH_2O$, $M = Cr, Co, Cu, Ni, Fe$

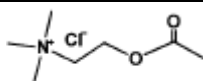
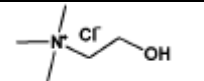
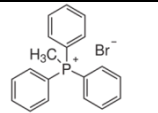
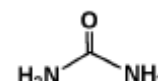
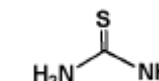
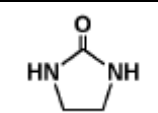
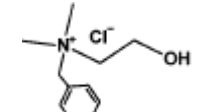
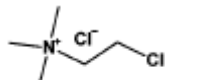
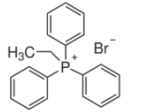
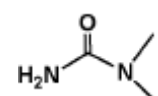
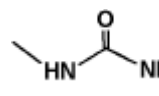
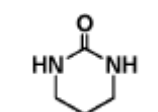
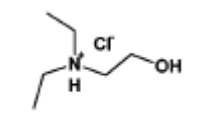
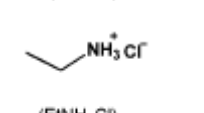
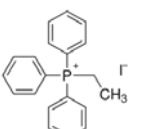
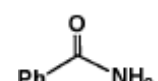
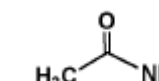
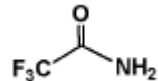
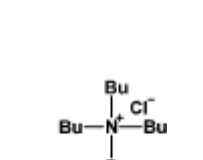
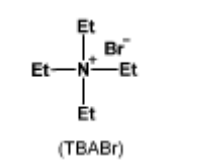
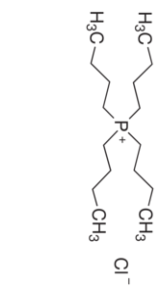

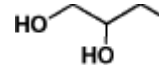
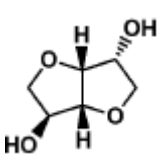

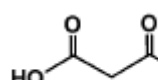
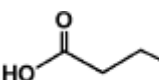
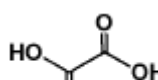
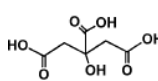
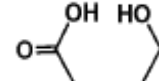
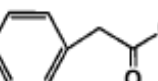
Type III DES: $Y = R_5Z$ with $Z = CONH_2^-, COOH^-, OH^-$

Type IV DES: MCl_x , such as $ZnCl_2$, mixed with a HBD such as urea, ethylene glycol, acetamide or hexanediol.

Like ILs, most of the DESs possess ionic species, especially choline chloride-based ones. However, they cannot be considered as ILs because they are not completely composed of cations (Abbott et al., 2003a).

Since the time the interest on DESs became obvious in the literature, many combinations of salts and HBDs or complexing agents were reported. Table 2.5 shows a summary of typical quaternary salts as well as some HBDs utilized by different researchers (Abbott et al., 2003b, Abbott et al., 2009, Kareem et al., 2010, Shahbaz et al., 2010, Hayyan et al., 2012, Kareem et al., 2012a, Kareem et al., 2012b).

Table 2.5: Typical structures of the quaternary salts and HBDs used for DES synthesis (Zhang et al., 2012, Zhao and Baker, 2013)

Quaternary salts			HBDs		
					
					
					
					
					
					

Choline chloride ($C_5H_{14}ClNO$) is widely available in the market at low prices. It is biodegradable and non-toxic. These characteristics favour its use as an organic salt to produce eutectic solvents with safe HBDs, such as urea, glycerol, carboxylic acids, or carbohydrate-derived polyols (Zhang *et al.*, 2012). In comparison with traditional ILs, DESs derived from choline chloride possess numerous superiorities which reinforce the greenness of these solvents, such as low price, ease of storage, ease of preparation, biodegradability, biocompatibility and non-toxicity. In addition, choline chloride-based DESs are very similar to traditional imidazolium-based ILs from both physical and chemical aspects. Intensive investigations were carried out by different researchers (Zhao and Baker, 2013, Zhang *et al.*, 2012) to characterize these types of DESs. Properties such as density, viscosity, refractive index, electrical conductivity, surface tension, and chemical inertness were found to be close to those of ILs. Consequently, applications of imidazolium ILs can be replaced by DESs. Moreover, in contrast with traditional organic solvents, storing DESs is easy due to their non flammability and non volatility properties (Zhao and Baker, 2013, Zhang *et al.*, 2012). From the view point of green chemistry, apart from their biodegradability and water stability, some DESs are compatible with enzymes, making them even more attractive. Choline chloride based DESs were successfully applied in numerous chemical and biochemical applications, such as metal oxide processing (Abbott *et al.*, 2006a), electropolishing (Abbott *et al.*, 2006b) and extraction of glycerol from biodiesel (Shahbaz *et al.*, 2010). Similar to ILs, ChCl-based DESs are studied for their potential application in carbon dioxide (CO_2) absorption. Li and co-workers (Li *et al.*, 2008, Zhang *et al.*, 2012) reported the absorption of CO_2 in a wide range of DESs from ChCl:urea and the solubility of CO_2 in ChCl:urea DES with water content.

2.4.1 Synthesis of DESs

DESs as “advanced ILs” (Gorke et al., 2010) are favorable solvents in comparison to ILs. One of the favoring factors is the ease of their synthesis. They can be easily prepared in high purity with very limited resources. The requirements are only a jacketed vessel with mechanical mixer and a mixing temperature of lower than 100°C. Additionally, their components can be selected from biodegradable and environmentally benign materials that possess low or no toxicity. (Abbott *et al.*, 2003a, Abbott *et al.*, 2009, Kareem *et al.*, 2010, Shahbaz *et al.*, 2010, Kareem *et al.*, 2012a, Kareem *et al.*, 2012b, Hayyan *et al.*, 2012).

The mechanism in which a DES is formed is that the complexing agent, typically a HBD, interacts with the anion of the salt and increases its effective size. This interaction reduces the anion interaction with the cation and thus decreases the freezing point of the mixture. DESs are characterized by a very large depression of freezing point and by being liquids at temperatures lower than 150 °C. Abbott et al. (2004a) have described a method for synthesizing DESs. This method also was adopted by Kareem *et al.* (2010, 2012a, 2012b) and Shahbaz *et al.* (2011a, 2011b, 2011c, 2012a, 2012b).

The mixing time and the temperature required to cause a complete interaction between the salt and the HBD are not systematically calculated. They are acquired through laboratory experience. The DES is said to be formed completely when the salt and HBD change to a homogeneous liquid (Abbott *et al.*, 2004a).

2.4.2 Physical Properties of DESs

As a similarity to ILs, DESs can be designed by combining desired components in various molar ratios to tune their physicochemical properties (Zhang *et al.*, 2012). In this way, different task-specific DESs with different physicochemical properties, such

as freezing point, viscosity, conductivity, and pH can be derived. Owing to their promising applications, numerous efforts have been devoted to the physicochemical characterization of DESs.

2.4.2.1 Freezing Point (Melting Point)

DESs are distinguished for their unique properties, essentially low melting points which make them favorable to traditional conventional solvents. The interest in their applications is influenced by liquid phase under 100°C, thus they are suitable to replace traditional molten salts that operate at very high operational temperatures. Abbott *et al.* (2003a) showed that DESs of choline chloride (ChCl) + urea had some unique solvent's properties. It was shown that the self-association taking place between the salt and the HBD depends on the type of components, and additionally their molar ratios play a key role in controlling the melting point of the DES. Kareem *et al.* (2010) and Shahbaz *et al.* (2010) presented similar findings to those of Abbott *et al.* (2003b) for phosphonium-based DESs and choline-based DES, respectively. A melting point of – 66 °C was achieved for ChCl + ethylene glycol at a salt:HBD molar ratio of 1:2. Moreover, Hua *et al.* (2011) and Hayyan *et al.* (2013) authenticated the controlling role of salt:HBD molar ratio in glycerol and glucose based DESs, respectively.

2.4.2.2 Viscosity

Owing to the potential application of DESs as green media in chemical processes, the development of DESs with low viscosity is critically important.

Viscosity is defined as the resistivity of a fluid to flow in streams. It is an important property, especially when fluids, generally, and liquids, specifically, are used as lubricants (Streeter *et al.*, 1998). Viscosity of a DES, similar to melting point, is strongly influenced by the atomic structure of its components, the molar ratio by which it is prepared, the operating temperature, and the water content. The ionic size of

components, void volume and interaction forces between components, such as electrostatic and Van der Waals, all significantly affect the viscosity of DESs (Abbott *et al.*, 1999).

Viscosity of most eutectic mixtures obviously changes as a function of the temperature. (Kareem *et al.*, 2010, Hayyan *et al.*, 2012):

Hayyan *et al.* (2012) presented a DES made of ChCl and D-fructose as a HBD. It was shown that the variation of the salt:HBD molar ratio influenced the viscosity of the resulting DES. The lowest viscosity attained was when the salt:HBD is 2:1 whereby the viscosity is 12 Pa.s at around 30 °C. Yet, the viscosity of this DES is higher than those reported for choline chloride-based DES by Kareem *et al.* (2010) with viscosities in the range of 0.068 and 0.14 Pa.s.

2.4.2.3 Electrical Conductivity

Electrical conductivity is one of the fundamental physical properties which represent how well a material can conduct electrical current. It is also an indication for how much a material is resistive for the motion of electrons within its molecules, i.e. resistivity (Ju *et al.*, 2012). The higher the value of the conductivity, the lower the resistance it provides to the flow of electric current (Ju *et al.*, 2012, Holbery *et al.*, 2003). In addition, it is a useful measurement, as in the case of using liquids as electrolytes in electrochemical processes, such as in batteries or in electroplating process. In engineering applications, it is crucial to measure the electrical conductivity of an electrolyte in order to design, control and optimize the electrolytic processes and the production of electrochemical power sources. For corrosion protection, electrical conductivity provides practical information for assessing the corrosivity of aqueous media and for cathodic protection system.(Holbery *et al.*, 2003).

Electrical conductivity of DESs is influenced by their relatively high viscosity. Therefore, DESs exhibit poor ionic electrical conductivity around or lower than 2 mS cm^{-1} at room temperature. In addition, due to the strong impact of the molecular structure and molar ratio of DES components on viscosity, the electrical conductivity of DESs is strongly influenced by these factors. A detailed description of electrical conductivity and its behavior with temperature for different ammonium and phosphonium based DES is presented in Chapter 4 of this work. Conductivities of DESs generally increase significantly as the temperature increases due to a decline in the viscosity.

2.4.2.4 Refractive Index

The index of refraction or refractive index is an important property, especially for optical identification of particular substances, inspecting the purity of materials and in measuring the concentration of solutes in solutions (Awwad and AlDujaili, 2001).

There are few recent studies that investigated the change in the refractive index of DESs with temperature. The work by Kareem *et al.* (2010) and Hayyan *et al.* (2013) showed that the refractive index of DESs decreases linearly as the temperature increases. Five different DESs were investigated, and it was found that the values of the refractive index for phosphonium salts-based DESs varied between 1.47 and 1.57 (Kareem *et al.*, 2010), for glucose-based DESs varied between 1.65 and 1.66 while for fructose-based DESs varied between 1.50 and 1.52 (Hayyan *et al.*, 2012, Hayyan *et al.*, 2013). A study by Shahbaz *et al.* (2013) proposed a predictive method to theoretically calculate the refractive indices of DESs. This method is based on the molar refraction method proposed by Wildman and Crippen (1999). The calculated refractive indices by this method were compared to the experimental values and the error percentages were estimated. The maximum error was 2.9918 % for ChCl:glycerol DES at salt:HBD molar

ratio of 1:1 while the minimum error was 0.2741 % for N,N-diethylethanol ammonium chloride:ethylene glycol DES at salt:HBD molar ratio of 1:3.

2.4.2.5 Density

Recent studies have reported the measurements of densities of DESs over various range of temperatures (Kareem *et al.*, 2010, Abbott *et al.*, 2011a, Shahbaz *et al.*, 2011c, Hayyan *et al.*, 2013). Density of a substance is the amount of mass in a unit volume. Most of the materials in liquid phase tend to follow the general rule, i.e. density varies in an inversely proportional pattern with temperature. The reported measurements for density of DESs showed the same behaviour. Some DESs possess low densities, such as N,N-diethylenethanol ammonium chloride: ethylene glycol (1:4) which has a density of 1.0590 gr/cm³ at 95 °C. Other DESs possess moderate densities, such as methyltriphenyl phosphonium bromide: glycerol (1:2) with a density of 1.2486 g cm⁻³ at 95 °C. The studies on DESs' densities showed that the density of a DES is similar to other physical properties in their dependence on the salt:HBD molar ratio. This means that the variation in salt:HBD molar ratio leads to a variation of the density of the resulting DES. This fact was illustrated by the work of Shahbaz *et al.* (2011c).

From the various works that dealt with the estimation of the densities of different DESs, it was shown that phosphonium-based DESs possess higher densities than water (Kareem *et al.*, 2010, Shahbaz *et al.*, 2012c). In the work of Abbott *et al.* (2011a), density's profile versus the salt's concentration in a DES made from ChCl and glycerol was reported. The density of this DES was 1.26 g/cm³ at zero % molar concentration of ChCl. The density started to decrease as the ChCl concentration increased until it reached 1.18 g/cm³ when the ChCl concentration became around 33 % mol.

2.4.3 Applications of DESs

Zhang *et al.* (2012) showed that the use of DESs not only allows the design of safer processes but also provides a straightforward access to new chemicals and materials.

The advantages of DESs over conventional ILs can be summarized as follows: ease in preparation, lower costs, the elimination of purification step and biodegradability. However, other than what has been reported in earlier sections, the applications of DESs are virtually unknown. This indicates the wide industrial horizon in which they can play essential roles. As DESs has emerged as an efficient, non-toxic and cheap replacement for conventional solvents, their potential applications in various chemical and electrochemical applications are significant. The electrodeposition of metals from zinc–tin alloys on ChCl:urea DESs was one of the first applications dealing with DESs (Abbott *et al.*, 2007a). Jhong *et al.* (2009) applied ChCl:glycerol DES as electrolyte for dye-sensitized solar cells. Biosett (2013) has reported physical properties of lithium bis[(trifluoromethyl)sulfonyl]imide:N-methylacetamide DES as superionic electrolyte for lithium ion batteries and electric double layer capacitors. It was found that, this DES possesses wide liquid-phase range from $-60\text{ }^{\circ}\text{C}$ to $280\text{ }^{\circ}\text{C}$, low vapor pressure, and high ionic conductivity up to 28.4 mS cm^{-1} at $150\text{ }^{\circ}\text{C}$ and at ratio of 1:4, therefore this solution can be practically used as electrolyte for electrochemical storage systems such as electric double-layer capacitors (EDLCs) and/or lithium ion batteries (LiBs).

The exponentially growing flow of research papers and patents concerning the synthesis and applications of DESs indicates the significant expansion in research on DESs.

2.4.3.1 DESs in CO₂ Capture Process

According to the Intergovernmental Panel on Climate Change (IPCC), global greenhouse gas emissions must be reduced by 50 to 80% by 2050 to avoid dramatic consequences of global warming (Metz et al., 2005). By the end of the 21st century, it is predicted that the emissions of greenhouse gases will increase the average global temperature by 1.1 to 6.4 °C. The consequences of elevated global temperatures will be melting of glaciers, leading to reduced water and food resources. The most important greenhouse gas is carbon dioxide (CO₂) because it is produced widely by the industry as a result of burning fossil fuels. Anthropogenic CO₂ emissions are mainly from fossil fuels, being the most important global energy sources. Therefore, it is of an urgent need to reduce CO₂ emissions from the industry (Metz *et al.*, 2005). CO₂ capture by washing the flue gases with amine solutions, such as monoethanol amine (MEA) and diethanol amine (DEA), has been proposed and studied widely (Gray *et al.*, 2008, Houshmand *et al.*, 2013, Song *et al.*, 2013). Although the utilization of amine solutions in CO₂ capture is efficient in terms of the yield of the process, drawbacks related to this utilization have been reported. High energy consumption and corrosion of process units due to the use of corrosive amine solutions as well as the degradation, toxicity and inefficient recyclability of these absorbents are among the drawbacks connected with CO₂ capture by amine solutions (Dawodu and Meisen, 1996, Schach *et al.*, 2010).

Li *et al.* (2008) reported that ChCl:urea DES has the potential in capturing CO₂. It was shown that ChCl:urea DES under different operating conditions of pressure and temperature has a high capacity to dissolve CO₂. The solubility was reported to be increasing with increasing pressure. Additionally, the different salt:HBD molar ratios did not give a significant difference in the solubility of CO₂ in the DES. Su *et al.* (2009) reported a work similar to the earlier work of Li *et al.*, whereby it was confirmed that CO₂ has a good solubility in the ChCl:urea DES.

2.4.3.2 Dissolution of Metal Oxides

Selective solubility of different metal oxides in “green” solvents under different temperatures is essentially important for metal extraction processes in hydrometallurgy or recovery of metals from waste materials produced by electric arc furnace (Cherginets, 2001, Fray and Chen, 2001). Electrowinning and liquid-liquid extraction have been used to recover and concentrate the metals, typically from their oxides (Abbott *et al.*, 2006b). Aqueous acids, alkalis and some high temperature molten salts have been used extensively in recovery of metals, such as titanium and aluminum (Cherginets, 2001, Abbott *et al.*, 2006a). Preliminary studies have shown that traditional imidazolium-based ILs are potentially applicable in metal recovery (Zhang and Bond, 2005, Wu *et al.*, 2002, McCluskey *et al.*, 2002). They have been applied for the extraction of the gold and silver from a mineral matrix and the recovery of uranium and plutonium from used nuclear fuel (Abbott *et al.*, 2006a). DESs as a potential replacement for ILs have shown the potential to dissolve metal oxides successfully (Abbott *et al.*, 2003a, Abbott *et al.*, 2006a). For example, ChCl:urea DES is capable of selectivity extracting zinc oxide (ZnO) and lead oxide (PbO) versus ferric oxide (Fe₂O₃) and aluminum oxide (Al₂O₃) from the waste of electric arc furnace (Abbott *et al.*, 2006a). Moreover, ChCl:urea DES is capable of dissolving a broad range of organic and inorganic compounds, even those which are not soluble in water, such as lithium chloride (LiCl), silver chloride (AgCl), aromatic acids, i.e. benzoic acid and amino acids (d-alanine). Abbott *et al.* (2003a) demonstrated the solubility of metal oxides in ChCl:urea DESs. It was shown that, for instance, the solubility of copper oxide (CuO) in a ChCl:urea eutectic mixture was 0.12 mol/L. In a later article (Abbott *et al.*, 2006a), the solubility of ZnO, CuO and Fe₃O₄ in different ChCl:carboxylic DESs was reported. It has been shown that the solubility of these oxides vary from 0.071 mol/L to 0.554

mol/L. It was also concluded that the solubility of different metal oxides would be dependent on the nature of the DES and metal oxides (Zhang *et al.*, 2012).

2.4.3.3 Purification of Biodiesel

Despite the use of liquid-liquid decantation to separate glycerol from biodiesel, the ASTM specification requires more purification for biodiesel prior to its use in vehicles (Shahbaz *et al.*, 2010). Unlike biodiesel, glycerol is highly polar. Abbott *et al.* (2007c) demonstrated the utilization of DESs to additionally treat biodiesel, owing to their compatible properties with ILs such as polarity. Ammonium-based DESs such as acetylcholine chloride:glycerol DES with ratio of 1:1 was used to separate glycerol from raw biodiesel. The results showed a significant decrease, 99%, of the content of glycerol in biodiesel. Evaluation of ammonium chloride DESs versus ammonium bromide DESs showed that the former DESs such as acetylcholine chloride-based DES was more efficient, i.e. 99% than ammonium bromide DES such as Pr_4NBr :glycerol DES (Abbott *et al.*, 2007c, Zhang *et al.*, 2012). This high efficiency of ammonium chloride-based DESs may be attributed to the higher electronegativity of the chloride agent. Similarly, Hayyan *et al.* (2010) showed that ChCl :glycerol based DESs can also be used as a solvent for the separation of glycerol from palm oil-derived biodiesel. Recently, Shahbaz *et al.* (2010) used other ChCl -based DESs for the extraction of residual glycerol from biodiesel. For example, ChCl :ethylene glycol and ChCl :2,2,2-trifluoroacetamide DESs were found to be efficient in this extraction. It has been shown that the best separation efficiency was achieved using a ChCl -ethylene glycol DES with a salt:HBD molar ratio of 1:2.5 with a DES:biodiesel ratio of 2.5:1. ChCl -2,2,2-trifluoroacetamide DES with a salt:HBD molar ratio of 1:1.75 was also highly efficient in the separation of glycerol from biodiesel at DES:biodiesel ratio of 3:1. In addition to ammonium based DESs, Shahbaz *et al.* (2010) utilized phosphonium-based DESs for

the purification of palm oil-derived biodiesel. Phosphonium-based DESs were synthesized from methyltriphenylphosphonium bromide as a salt with three different HDBs, i.e. glycerol, ethylene glycol or triethylene glycol. It was shown that ethylene glycol and triethylene glycol-based DESs were very efficient, over 90%, for removing residual glycerol from palm oil-derived biodiesel.

2.4.3.4 DESs for Ionic Conductivity Enhancement

Ramesh *et al.* (2012) used a ChCl:urea DES to improve the ionic transport mechanism and electrical conductivity as a suitable additive to the series of electrolytes of corn starch and lithium bis(trifluoromethanesulfonyl)imide. It was shown that the ionic conductivity of traditional ILs was increased by the amorphous elastomeric phase in corn starch: lithium bis(trifluoromethanesulfonyl)imide matrix. The ionic transport mechanism was found to be improved, and an appreciable amount of ion conducting polymer electrolytes was produced.

2.4.3.5 DESs as Solvents for Extraction of Aromatic Hydrocarbons from Naphtha

The removal of aromatic hydrocarbons from naphtha prior to the thermal cracking process to produce ethylene is a necessary process to gain economical and industrial benefits. It is a challenging process since these hydrocarbons have similar boiling points and cannot be separated by normal distillation. Solvent extraction is commonly used in industrial processes for aromatic hydrocarbon separation because of the mild operating conditions and due to its simplicity (Gaile *et al.*, 2004). Industrially used chemicals as extractants are mostly conventional polar organic solvents, such as with problems of toxicity and flammability. Meindersma (2005), Arce *et al.* (2007), Garcia *et al.* (2010), and Dominguez *et al.* (2013) utilized different ILs as extraction solvents in the separation of aromatics from naphtha. Different phosphonium-based DESs were

successfully used in ternary systems of benzene + hexane + DES and toluene + heptane + DES by Kareem et al. (2012a and 2012b). It was found that the DES of molar ratio of 1:6 methyltriphenylphosphonium bromide:ethylene glycol showed the best separation performance in comparison to sulfolane which is the commercial solvent for this extraction. In the system of toluene + heptane + DES, DESs composed of tetrabutylphosphonium bromide and two HBDs, i.e. ethylene glycol and sulfolane, were applied within a range of temperatures 30 °C to 60 °C. The results showed high selectivities of the DESs towards toluene, but not as high as those of sulfolane. However, the advantage was that the DESs investigated did not suffer a solvent loss to the raffinate phase.

2.4.3.6 DESs as Catalysts

Not only DESs were successful solvents in separation processes due to their low price and simplicity in synthesis but also they have been applied successfully as catalysts in different applications, similar to traditional ILs. Lindberg *et al.* (2010) used choline chloride-based DESs with ethane-diol, urea and ethylene glycol as HBDs in the hydrolysis of 1,2-trans-2-methylstyrene oxide. Recently, Hayyan *et al.* (2013) introduced phosphonium-based DESs as advantageous catalyst over ILs for the production of biodiesel from industrial low grade crude palm oil. In that work, Hayyan and colleagues used allyltriphenylphosphonium bromide as the phosphonium salt and p-toluenesulfonic acid monohydrate as HBD. The DES produced was jelly viscous under laboratory conditions, and the biodiesel produced from low grade crude palm oil met the international standards, i.e. ASTM D6751 and EN 14214. Durand *et al.* (2012) concentrated on analysing the advantages and limitations of several DESs as “green” solvents for biotransformation using immobilized *Candida antarctica lipase B* as a catalyst. Selected DESs for this utilization composed of two different ammonium salts,

i.e. choline chloride and ethylammonium chloride, with different HBDs, i.e. urea, glycerol, oxalic acid, malonic acid, and ethylene glycol. It was shown that the DESs composed of glycerol or urea combined with choline chloride as salt allowed the best initial specific activity of the lipase in comparison to those in conventional organic media. Azizi *et al.* (2012) introduced DESs as a dual catalyst and reaction medium for the efficient formation of aromatic amines without hazardous organic solvent and catalyst. Choline chloride-based DES with tin(II)chloride (SnCl_2) as a complexing agent was investigated as an environmental friendly catalyst for this application. The development of practical and harmless method to produce N,N-diarylamidines and formamides in the presence of DESs as catalyst and reaction medium was also investigated

2.4.3.7 DESs as Electrolytes

ILs are highly electrochemically stable which makes them promising candidates for electrolytic applications. Similarly, DESs became promising green electrolytes as proper replacement for high melting point molten salts and ILs in electrolysis and batteries applications. This is due to the fact that DESs share most of the favorable characteristics of ILs and more favorably they can be synthesized more easily than ILs (Zhang *et al.*, 2012). Some of the applications of DESs as electrolytes are summarized below:

a) Electrodeposition in DESs

ChCl-based DESs with HBDs such as urea or ethylene glycol have been widely applied as electrolytes in the electrodeposition of metals. Abbott *et al.* (2007a) introduced the electrodeposition of zinc (Zn)-tin (Sn) alloys in ChCl-based DESs. It has been shown that DESs composed of ChCl as salt and urea or ethylene glycol as HBD

are capable in depositing Sn, Zn and their alloys electrically. In addition, composite materials such as aluminium oxide (Al_2O_3) were found to be able to deposit in DESs media. Abbott *et al.* (2009) utilized the same DESs successfully in the electrodeposition of copper (Cu) with an efficiency of approximately 100%. It was found that the rate of electrodeposition is significantly dependent on the ratio of the DES and the concentration of the solvent. Additionally, Abbott *et al.* (2006c) studied the electrodeposition of stainless steel in ChCl based DESs.

Pollet *et al.* (2008) introduced possible utilization of ChCl:glycerol DES in the electrodeposition of Cu on platinum (Pt) electrodes. The electrodeposition process was carried out under three different conditions, i.e. without driving force; with driving force of 20 kHz; and with driving force of 850 kHz. Under normal conditions and without any driving force, the electrodeposition was driven only by diffusion. However, ultrasound waves served as the driving force to accelerate the electrodeposition.

ChCl-DESs were also successfully applied in producing CuGaSe_2 (CGS) semiconductors in thin film solar cells (Steichen *et al.*, 2011). It was found that ChCl:urea DES with salt:HBD molar ratio of 1:2 is capable in depositing Cu and gallium (Ga) to produce CGS economically.

The same DES was applied by Gómez and colleagues in the electrodeposition analysis of cobalt (Co), samarium (Sm) and samarium-cobalt (SmCo) system (Gómez *et al.*, 2011). In order to decrease the viscosity of DES to support less mass transfer rate and longer reaction time, the electrodeposition process took place at a high operating temperature of 70 °C. It was found that the DES had the capability to permit the electrodeposition in non-aggressive conditions for alloys containing some transition metals. In parallel, the same DES was applied for the electrodeposition of pure nickel (Ni) (Yang *et al.*, 2011). You *et al.* (2012) demonstrated facile electrodeposition of Ni-

Co alloys from ChCl:ethylene glycol DES containing $\text{NiCl}_2 \cdot 6\text{H}_2\text{O}$ and $\text{CoCl}_2 \cdot 6\text{H}_2\text{O}$ at room temperature.

Saravanan and Mohan (2011) introduced DESs synthesized from ChCl, chromium(III) chloride hexahydrate ($\text{CrCl}_3 \cdot 6\text{H}_2\text{O}$), nickel(II) chloride hexahydrate ($\text{NiCl}_2 \cdot 6\text{H}_2\text{O}$), iron (II) sulfate heptahydrate ($\text{FeSO}_4 \cdot 7\text{H}_2\text{O}$), potassium chloride (KCl) as well as ethylene glycol at specific ratios. These DESs were utilized in the electrodeposition of Fe-Ni-Cr alloy on mild steel substrate. Other studies on the electrodeposition of metals from DESs media were also reported by Bozzini *et al.* (2012), Abbott *et al.* (2011b), Yang *et al.* (2012), Gu *et al.* (2012), Wei *et al.* (2012), and Cojocaru *et al.* (2011).

Unlike the electrodeposition of metals in DESs media, the electrolytic deposition in DESs of ChCl and urea or ethylene glycol was introduced by Abbott *et al.* (2007b). The DESs were applied in the electrolytic deposition of metallic silver on copper substrates from a solution of silver ions (Ag^+). Silver deposits resulted from electrolytic deposition from DESs were at several microns through dip-coating. Electroless deposition of metals inside DESs was also studied by Abbott *et al.* (2008).

b) DESs in redox flow batteries

Bahadori *et al.* (2012) conducted the electrochemical screening of both ammonium and phosphonium-based DESs in their work on the potential applications of redox flow batteries. To select the best DES in their study, ferrocene/ferrocenium redox couple was chosen as the Nernstian redox probe. The investigated DESs for this application were ammonium salts, i.e. ChCl and N,N-diethylethanolammonium chloride, and phosphonium salt, i.e. methyltriphenylphosphonium bromide while the HBDs were glycerol, ethylene glycol and ferrocene. The potential windows of DESs were determined electrochemically at Pt (platinum) microelectrode and a GC (glassy carbon)

electrode. The reductive and oxidative potential limits were reported versus the Fc/Fc⁺ couple. It was observed that DESs synthesized from ammonium salts provided a larger potential window in comparison to the phosphonium-based ones when either Pt or GC working electrodes were employed. It was shown that N,N-diethylethanolammonium chloride:ethylene glycol DES with salt:HBD molar ratio of 1:2 possessed the highest standard heterogeneous rate constant of $5.44 \times 10^{-4} \text{ cm s}^{-1}$ and the compatible cyclic voltammetry with ILs as big as 5.7 V. It was concluded that this DES can be utilized as an electrolyte in redox flow batteries.

c) DESs in dye synthesized solar cells

Dye synthesized solar cells are low-cost solar cells belonging to the group of thin film solar cells. Jhong *et al.* (2009) investigated ammonium iodide-based DES with glycerol as HBD as electrolyte in dye-sensitized solar cells. DES-based electrolyte possesses numerous outstanding features in comparison to the traditional imidazolium-based ILs. It has been shown that current-voltage characteristics stand at 0.533 V on V_{oc} , 12.0 mAcm^{-2} on J_{sc} , 0.582 on fill factor, and 3.88% cell efficiency under AM 1.5, 100 mWcm^{-2} illuminations. The comparable cell performance with other advantages of DSEs makes glycerol-based DES a strong candidate for future electrolytic development of dye-sensitized solar cells.

d) DESs as electrolyte in lithium ion batteries and electric double layer capacitors

Biosset *et al.* (2013) investigated the potential application of N-methylacetamide: lithium bis[(trifluoromethyl)sulfonyl]imide DES as environmentally advantageous electrolyte in lithium ion batteries and electric double layer capacitors. Owing to the favorable properties of the DES for ratio of 4:1, such as wide liquid-phase range from -60°C to 280°C , low vapor pressure, and high ionic conductivity of up to 28.4 mS cm^{-1} at 150°C , it is suggested that this DES can be used as a promising electrolyte for EDLCs

(electrical double-layer capacitors) and LiBs (lithium bis[(trifluoromethyl)sulfonyl]imide) applications, especially for those requiring high safety and stability.

e) DESs in electropolishing of metals

Abbott *et al.* (2006b) utilized ChCl:ethylene glycol DES for the electropolishing of type 316 stainless steel, and the choice of this DES was due to its favorable characteristics, such as high current efficiencies, negligible gas evolution at the anode/solution interface during polishing, and being comparatively benign and non-corrosive in comparison to the traditional aqueous acid solutions. The electropolishing was successfully demonstrated and the dissolution mechanism was shown to be different from that found in aqueous acid solutions. Additionally, the dissolution of the oxide film was slow in the DES medium in comparison with aqueous solutions. The DES was not only non-corrosive but also air and moisture stable, adding one more advantage to the DES over the acid solutions.

2.5 ILs/DESs Electrolyte as Molten Salt in Downs Process

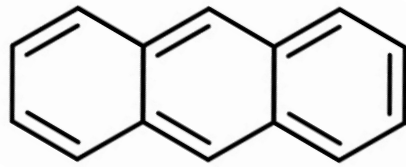
Earlier, the Downs process was introduced as the current industrial process for the production of sodium metal. The utilization of typical molten salt mixture of NaCl in a certain ratio with CaCl₂ and BaCl₂ is aimed at decreasing the melting temperature of NaCl from above 800°C to slightly below 600°C. This reduced temperature is still extremely high and therefore economically and environmentally unacceptable.

The high operating temperature of this process is considered as an operational drawback. Additionally, operating an electrolytic process at 600°C is difficult and presents numerous constraints. At such operating temperature, the process generates pollutants and consumes a high volume of energy (Keppler *et al.*, 2003, Thompson *et al.*, 2004). Moreover, the concentric cylindrical cell design of the Downs process necessitated by the high operating temperature leads to very poor space efficiency in the

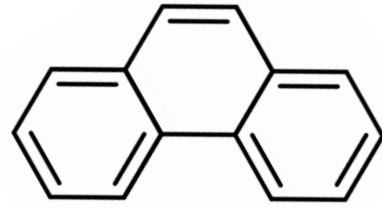
cell. This translates directly into high capital and operating costs per unit production. To overcome this difficulty, the utilization of a green efficient electrolyte has been proposed. The utilization of ILs and DESs instead of molten salts for the production of sodium, brings into focus three significant characteristics, namely solubility, electrical conductivity and stability. The solubility of commercially available sodium salts and the electrical conductivity of solution of sodium salt in IL or DES must be high, and the stability of sodium in IL or DES must be achieved (AlNashef, 2012).

2.5.1 Solubility

Solubility is in general a strong function of the intermolecular forces between solute and solvent. It is undeniable that in the absence of specific chemical effects, intermolecular forces between chemically similar species lead to a similar endothermic enthalpy of solution than those between dissimilar species (Prausnitz et al., 1998). However, factors other than intermolecular forces between solvent and solute also play a large role in determining the solubility of solid. To illustrate this, the solubilities of two isomers, such as anthracene and phenanthrene in benzene at 25°C are taken as an example (see Figure 2.6). Even though both solids are chemically similar to each other and to the solvent, the solubilities are different. The solubility of phenanthrene is 20.7 mol% which is about 25 times larger than that of anthracene, i.e. 0.81 mol%. It means that not only does solubility depend on the activity coefficient of the solute, which is a function of the intermolecular forces between solute and solvent, but also on the fugacity of the standard state to which that activity coefficient refers and on the fugacity of the pure solid (Prausnitz, *et al.*, 1998).



anthracene



phenanthrene

Figure 2.5: Structure of anthracene and phenanthrene

If the solute is designated by subscript 2, the equation of equilibrium would be:

$$f_{2(\text{pure solid})} = f_{2(\text{solute in liquid solution})} \quad (2.10)$$

Equation 2.10 is based on the assumption that there is no appreciable solubility of the liquid solvent in the solid phase, or

$$f_{2(\text{pure solid})} = \gamma_2 x_2 f_2^0 \quad (2.11)$$

where x_2 is the solubility in mole fraction of the solute in the solvent, γ_2 is the liquid-phase activity coefficient and f_2^0 the standard-state fugacity to which γ_2 refers.

From Equation 2.11, the solubility is

$$x_2 = \frac{f_{2(\text{pure solid})}}{\gamma_2 f_2^0} \quad (2.12)$$

Thus, the solubility depends not only on the activity coefficient but also on the ratio of the two fugacities as indicated by Equation 2.12.

Solubility of a solid in a liquid is strongly influenced by temperature. To a certain extent, the higher the temperature, the higher the solubility. As the temperature of a solution is increased, the average kinetic energy of the molecules that make up the

solution also increases. This increase in kinetic energy allows the molecules of the solvent to more effectively break apart the solute molecules that are held together by intermolecular attractions. The average kinetic energy of the solute molecules also increases, destabilizing the solid state. The increased vibration of the molecules causes them to be less able to hold together, and thus they dissolve more readily (Prausnitz *et al.*, 1998).

The electrical conductivity part has been presented in section 2.4.2.3.

2.5.2 Stability

It is well known that sodium metal is highly reactive when it is in its pure form. For this reason, sodium metal cannot be found pure in nature. It is therefore found in the form of compounds such as sodium halides, nitrites and oxides. Sodium has a fast and exothermic reaction when it comes into contact with atmospheric oxygen or water. It reacts with water to form sodium hydroxide and releases flammable hydrogen. Thus, the presence of any traces of water in the DES used for its production is not favorable (Pearson *et al.*, 2008)

As the proposed change to Downs process assumes the production of pure sodium metal in ILs or DESs as media, it is important to choose an IL or DES with which the pure sodium will not react. Thus, the stability of sodium metal inside various ILs and DESs must be studied.

CHAPTER III

METHODOLOGY

This chapter is composed of five sections. Section 3.1 discusses the synthesis of DESs. Section 3.2 explains the characterization procedure of the physical properties of some of the synthesized DESs. Section 3.3 shows the procedure followed for the measurement of the solubility of sodium salts in different DESs and ILs. Section 3.4 tackles the experimental work for measuring the electrical conductivity for solutions of sodium salts in DESs. Finally, Section 3.5 presents the experimental procedure for measuring the stability of sodium metal in some of the DESs. The whole of the experimental work was carried out under a glove box (Innovative Technology, USA) environment whereby the humidity was less than 0.4 ppm.

3.1 Synthesis of DESs

3.1.1 Chemicals

Various salts and HBDs or metal halides as complexing agents were utilized to synthesize the DESs. Choline chloride (ChCl), N,N-diethylethanolammonium chloride, methyltriphenylphosphonium bromide, ethyltriphenylphosphonium bromide, tetrabutylphosphonium bromide, ethylene glycol, glycerol, anhydrous zinc chloride (ZnCl_2), anhydrous tin chloride (SnCl_2), anhydrous iron (III) chloride (FeCl_3), sodium chloride (NaCl) and sodium bromide (NaBr) were acquired from Merck (Germany). All chemicals used were synthesis grade, i.e. highly pure, not less than 99% and were used without further purification.

3.1.2 Synthetic Procedure

Abbott *et al.* (2004a) reported that DESs can be synthesized by mixing predetermined amounts of a quaternary ammonium salt and hydrogen-bond donor at a certain temperature until a homogeneous colourless liquid is formed. This method was followed by many researches, and is utilized in this work to successfully synthesize different DESs. This method is easy to follow and less expensive in comparison to the synthesizing of ILs.

As the formation of DES depends in part on temperature and on the way the salt and HBD or metal halide are mixed, the mixing is an important operation in the synthesis of DES. The significant parameters are the type of mixing, mixing time, and mixing speed. Some DESs require mechanical stirring, some of them can be formed by shaking the mixing vessels while others can be stirred magnetically. The extent and type of mixing depend on the type and phase of the salt and the HBD or metal halide used in the synthesis of DES. In general, DES is said to be completely formed and is ready for use when the salt and HBD or metal halide combine together to give a homogenous liquid.

The equipment used in the synthesis of DESs are summarized in Table 3.1.

Table 3.1 : Equipment used in the DESs synthesis.

Stirring Type	Equipment and accessories	Model
Mechanical	Mechanical agitators, stirring speed controllers, jacketed vessels, oil/water bath.	Locally fabricated speed controller and mechanical agitators. Protech water bath.
Shaking	Incubating shaker, sealed vials.	Adolf Kühner AG, Schewir ASF-1-V incubating shaker
Magnetic	Hotplate magnetic stirrers, magnetic bars, sealed vessels.	IKA C-MAG HS7 S2 hotplate stirrer.

3.2 Characterization of DESs

Abbott et al. (2004a) reported that DES results from the formation of complex anions which decrease the lattice energy and the freezing point of the system. The mole ratio of salt: HBD or metal halide in the DES is an important factor that affect the physical properties of the resulting DES. This is obvious when the physical properties of different DESs synthesized from one combination of salt and HBD or metal halide at different mole ratios are compared.

A list for the characterization equipment and the measurements obtained along with the uncertainties in measurement are shown in Table 3.2.

Table 3.2 : Devices used for characterization of DESs with their uncertainties.

Property	Device	Estimated Uncertainty
Melting temperature	Mettler Toledo Differential Scanning Calorimetry	± 0.01 °C
Viscosity	Brookfield R/S plus Rheometer	(3 to 5) % of measured value*
Conductivity	Cheetah multi parameters meter	± 1 $\mu\text{S}\cdot\text{cm}^{-1}$
Refractive index	ABBE SASTEC ST-WYA-25 refractometer	± 0.00001

* As per the manufacturer guide

The detailed experimental procedures followed to measure the physical properties of some of the DESs are explained below.

a) Melting temperature

The melting temperature is defined as the temperature at which the substance changes from liquid phase to solid phase upon temperature depression. Identifying this exact temperature is possible by using visual methods. The capillary tube method is the common method used in organic chemistry laboratories. It utilises a magnifying lens that magnifies the vision of the glass tube which contains the sample. A light might be

used to provide better visibility. Upon heating or cooling the sample by an oil bath, the sample passes through its melting temperature at which the change in phases is detectable visually. This method is the one used in various analysis equipment such as Thomas Hoover melting point apparatus (advertised in Chemical and Engineering News Journal, 1961).

Although the above mentioned method is satisfactory for melting point analysis, another method of interest is the heat flow measurement method. The principle of this method is that when a sample passes through its melting temperature upon heating, it emits a certain amount of heat which is detectable by micro-scale sensors. The Differential Scanning Calorimetry (DSC) is an apparatus that measures the heat flow emitted from a sample upon heating over a range of temperatures.

To measure the melting temperature of a compound by DSC, a sample of less than 10 mg of this compound is placed inside a special pan made mainly from aluminium and a hole is made in the cover of that pan. The temperature of the sample is gradually raised. The hole allows the heat emitted to transfer outside the pan whereby special sensors measure this heat and record it. If the sample is liquid at room temperature, then it must be cooled down till it freezes. The measurement starts from a point at which the sample is in the solid state. If the sample is solid at room temperature, then the heating program may start from the ambient temperature to a temperature at which the sample is in the liquid state. The heating of the sample from below its melting temperature to above this temperature is carried out through a computerized program. On the initiation of the program the sample starts to emit a certain amount of heat till it reaches the glass transition point whereby only a few molecules of the sample change from the solid state to liquid state. At the glass transition point, the amount of heat emitted will be reduced sharply to assist in converting the state of the sample. The specialized sensors detect this sudden depression and it is drawn as a drop in the curve of the heat flow. When the

entire sample has melted down, the heat emission will be uniform again. This sudden drop in the heat flow curve will be identified on the x-axis which represents the temperature, and this temperature will be the melting temperature of the sample.

b) Viscosity

Viscosity is a measure of the resistance that the fluid shows to gradual deformation by shear or tensile stresses. The low viscosity of a fluid indicates an easy flow of that fluid in process streams, and vice versa.

Brookfield R/S Plus rheometer was used to measure viscosity. Temperature control was achieved by an external water bath that was connected to the jacket-like cell. A stainless steel testing tube was placed inside the jacket cell. A certain period of time was allowed after the desired temperature was reached in the water bath to ensure that the cell, test tube and the DES sample were all at the same desired temperature. Only then, the rheometer was run and measurements of the dynamic viscosity taken.

c) Electrical Conductivity

The conduction of electrical current through a medium requires the presence of charged atoms or ions. It is common knowledge that not all liquids contain ions, and thus not all liquids conduct electric current. Salty water conducts electricity due to the presence of the salt ions, but sugary water does not as there are no such ions. As different liquids may contain different amounts and types of ions, their conductivity varies. The conductivity of a liquid is an indication of the concentration of ions in it and their type. The measurement of the electrical conductivity of a liquid is accomplished by the use of conductivity meters. These meters use a probe in which two poles are represented by two metallic ends. As an example, these ends could be in the shape of rings. Upon immersing the probe in the liquid medium of interest, the meter generates an electrical current and sends it to two metal ends in the probe. The current is

transferred by the medium from one metallic end to another. The received amount of current is compared to the transmitted one, and the conductivity of the liquid is displayed.

Cheetah multi parameters meter model DZS - 780 is the apparatus used in the present work. It has a wide temperature range for measurements, i.e. from -5 °C up to 135 °C. The meter was calibrated by standard buffer solutions supplied by the manufacturer. The measurements of the electrical conductivities at different temperatures were carried out by placing the DES on a hot plate, equipped with a temperature controller. To ascertain that the temperature displayed by the hot plate was accurate, external thermometers were used to measure the temperature inside the DES medium.

d) Refractive Index

The refractive index n_D is a dimensionless factor which measures the bending of a ray of light when passing from one medium into another (Hale and Querry, 1973). The mathematical expression that is commonly used to calculate refractive index is given in the following equation:

$$n_D = \frac{c}{v} \quad (3.1)$$

where c is the speed of light in vacuum and v is the speed of light in the medium of concern.

The value of n_D for some of the DESs was measured at a specific range of temperatures. This range usually starts from a few degrees Kelvin above the melting temperature of the DES up to a maximum of 363 K. ABBE SASTEC refractometer model number ST-WYA-25 was used to measure the refractive indices. This meter uses

an external oil bath for heating the sample, thus high temperatures can be achieved in the measurement prism. The measurement is achieved when the device sends a beam of light through the lens to the sample and measures the angle by which the reflected light is returning back to the device. This angle is then converted to a refractive index. The meter was calibrated by measuring the refractive index of glycerol at 298 K, which was found to be 1.4746, exactly same as what is reported in the literature (Rheims *et al.*,1997).

3.3 Measuring the Solubility of Sodium Salts in DESs and ILs

The electrochemical separation of the Na⁺ ions from sodium salts is carried out by passing a high voltage electrical current through the electrolyte in which the salt is dissolved. Thus, if DESs or ILs are to be utilized as electrolytes for the production of sodium metal from its common salts, it is important to know the extent in which a sodium salt dissolves in a certain DES or IL.

In the shake flask experiments, the solute is added to the solvent and the mixture is stirred (shaken) vigorously for 24 hours or longer. Continuous observation is required to determine if the solute has completely dissolved or not. If it is completely dissolved, addition of more solute is required and the observation is repeated. Saturation is reached and confirmed by observing the presence of undissolved solute in the solvent after several additions of the solute.

Both the stirring and settling must be performed under the same temperature. Samples from the solution are then taken from the upper part that does not hold suspended undissolved salt. The sample may require filtering if suspended salt is suspected to be present. After filtration, samples are taken for chemical analysis. To prevent crystallization, dilution may be necessary in certain cases of sample preparation. If necessary, the samples are diluted with de-ionized water. Finally, samples are analyzed using Perkin-Elmer Optima 5300DV inductively coupled plasma-atomic

emission spectrometer (ICP-AES). For reasons of accuracy, each analysis should be repeated three times and the average of the three analyses is to be considered.

Shake Flask method was used in this work as it is the most accurate method to determine solubility. In the present work, the solubilities of three different low-cost sodium salts, namely sodium chloride (NaCl), sodium bromide (NaBr) and sodium carbonate (Na₂CO₃) were measured in various DESs and ILs under different temperatures (25°C – 150°C). This was carried out by adding about 0.1 g of sodium salt (anhydrous) to 5 g of DES or IL and stirred for 24 – 48 hours at constant temperature. If the solvent was able to dissolve all the 0.1 g of the sodium salt, more salt was added and observation was focused to ensure that a saturated solution was achieved. During these measurements, three important factors were taken into consideration. Firstly, the solvent and sodium salt must be of high purity. This is because any amount of impurities, no matter how small, will affect the measured solubility. For this reason, all the chemicals used in the present work were of synthesis grade. Secondly, the samples withdrawn from the saturated solutions did not contain any undissolved salt. Lastly, the temperature during stirring was carefully controlled. The uncertainty of the ICP is estimated to be ± 0.02 for solubility >20wt% and ± 0.05 for solubility < 10 wt%.

3.4 Measuring the Conductivities of Sodium Solutions

The conductivity of the solutions of sodium salts in different DESs is important for the final selection of the most suitable DES for sodium metal production. As this production process is electrochemical, high conductivity of the electrolytic solution is favorable. Accordingly, some of the solutions of sodium salts in DESs were subjected to electrical conductivities measurements. The measurement here is from the measurement of electrical conductivity described in Subsection 3.2 (b). The difference here is that the electrical conductivity was measured for a solution of sodium salt in a DES, while it was for pure DES earlier.

3.5 Measuring the Stability of Sodium Metal in DESs

It is well known that sodium metal is highly reactive when it is in its pure form. For this reason, sodium metal cannot be found in a pure form in nature, but in the form of compounds. This is due to the reaction of pure sodium with other elements or compounds to form sodium halides, nitrate and oxides. Thus, it is important to know whether the sodium metal proposed to be produced DES is going to react with the DES or remain intact, i.e. stable.

The stability of sodium inside the proposed DESs was studied by placing approximately 0.5 g of pure sodium metal in 5 ml of each DES in a glove box and monitoring the results of this addition over a time span of one week.

3.6 Cyclic Voltammetry

Cyclic voltammetry is the most widely used technique for acquiring qualitative information about electrochemical behavior of electrolytes (Wibowo et al., 2010, Barrosse-Antle et al., 2010). It offers a rapid location of redox potentials of the electroactive species. In the current work, the electrolytic behavior of ZnCl₂-based DESs in electrolysis of sodium chloride were investigated in those possess high solubility and high conductivity of sodium chloride at optimum thermal conditions. The electrochemical cell consisted of a typical three-electrode set-up. The counter electrode was a Pt wire, and an Ag wire (immersed in 65% HNO₃ prior to experiments, then rinsed thoroughly with water and ethanol) was used as a quasi-reference electrode. A glassy carbon (GC, 3 mm diameter) were used as working electrodes. The working electrodes were carefully polished before each voltammetric experiment with 0.25 M alumina suspensions and ultrasonically rinsed in acetone. All electrochemical

experiments were performed using a computer-controlled *i*-Autolab potentiostat (PGSTAT302N) and experiments were carried out inside a Faraday cage.

CHAPTER IV

RESULTS AND DISCUSSION

Different types of DESs have been synthesized in the present work and some of these DESs have not been reported before. Their novelty is due to the unique combinations of chemicals used in their synthesis. Most of the DESs that have been investigated and reported in the literature were synthesized from a salt and a hydrogen-bond donor (HBD). However, in the present work, some of the DESs were synthesized from a salt and a metal halide. Moreover, one DES was synthesized from a combination of a salt and two metal halides. The DESs used in the present study along with their abbreviations are summarized in Table 4.1.

Table 4.1: DESs studied in this work with their abbreviations.

Salt:HBD	Mole ratios				Abbreviation
Choline chloride:Ethylene glycol	4:7	4:8	4:9	4:10	DES1
Choline chloride:Glycerol	2:2	2:3	2:4	2:5 2:6	DES2
N,Ndiethylethanolammonium chloride:Ethylene glycol	2:5	2:6	2:8	2:9	DES3
N,Ndiethylethanolammonium chloride:Glycerol	2:4	2:5	2:6	2:8	DES4
Choline chloride:Zinc chloride	1:1	1:2	1:3	1:4	DES5
Choline chloride:Tin chloride	1:3				DES6
Choline chloride:Zinc chloride:Tin chloride	1:1:1				DES7
N,Ndiethylethanolammonium chloride:Zinc chloride	1:1	1:2	1:3	1:4	DES8
N,Ndiethylethanolammonium chloride:Iron(III) chloride	1:3				DES9
Methyltriphenylphosphonium bromide:Ethylene Glycol	1:3	1:4	1:5		DES10
Methyltriphenylphosphonium bromide:Glycerol	2:4	2:6	2:7	2:8	DES11
Ethyltriphenylphosphonium bromide:Zinc chloride	1:2	1:3	1:4	1:5	DES12
Ethyltriphenylphosphonium bromide:Zinc bromide	1:2	1:3	1:4		DES13
Ethyltriphenylphosphonium bromide:Iron (III) chloride	1:3	1:4	1:5		DES14
Tetrabutylphosphonium bromide:Zinc chloride	1:2	1:3	1:4	1:5	DES15
Tetrabutylphosphonium bromide:Iron(III) chloride	1:3	1:4	1:5		DES16

The solubility of NaCl in selected ILs was also investigated. The ILs employed are listed in Table 4.2.

Table 4.2: ILs studied for the solubility of NaCl.

No	IL	Structure	Common name	M.wt. g/mol	m.p. °C
1	1-Ethyl-3-methylimidazolium ethylsulfate		[emim] [EtSO ₄]	236.29	< -20
2	1-Ethyl-3-methylimidazolium methanesulfonate		[emim] [MeSO ₃]	206.27	35
3	1-Ethyl-3-methylimidazolium dimethylphosphate		[emim] [DMP]	264.26	20
4	1-Ethyl-2,3-dimethylimidazolium chloride		[edmi] [Cl]	160.65	96
5	1-Butyl-3-methylimidazolium chloride		[bmim] [Cl]	174.67	70
6	1-Butyl-3-methylimidazolium dicyanamide		[bmim] [DCA]	205.26	-6
7	1-Butyl-3-methylimidazolium trifluoromethanesulfonate		[bmim] [TfO]	288.29	16.4
8	1-Butyl-3-methylimidazolium tetrafluoroborate		[bmim] [BF ₄]	226.02	-71
9	1-Butyl-3-methylimidazolium bis (trifluoromethylsulfonyl)-imide		[bmim] [Tf ₂ N]	419.36	1
10	1-Octyl-3-methylimidazolium chloride		[C ₈ mim] [Cl]	230.78	NA
11	1-Butyl-1-methylpyrrolidinium dicyanamide		[bmp] [DCA]	208.31	-55
12	1-Butyl-1-methylpyrrolidinium trifluoroacetate		[bmp] [TfA]	255.28	31
13	1-Butyl-1-methylpyrrolidinium trifluoromethanesulfonate		[bmpyr] [CF ₃ SO ₃]	291.33	3
14	N-Butyl-3-methylpyridinium dicyanamide		[bmpy] [DCA]	216.29	16
15	N-Butyl-3-methylpyridinium methylsulfate		[bmpy] [MSO ₄]	261.34	NA
16	(2-Hydroxyethyl) trimethylammonium dimethylphosphate		[EtOHNMe ₃] [Me ₂ PO ₄]	229.21	40

The results of this study are presented in two main sections. Section 4.1 shows the results of the synthesis and characterization of some of the DESs summarized in Table 4.1 while Section 4.2 presents the results of the assessment of the solubilities of sodium salts in ILs and DESs as electrolytic solvents for the potential production of sodium metal by electrolysis. Section 4.2 also reports the application of the non-random two liquid (NRTL) activity coefficients model to predict the solubilities of sodium salts in some of the ILs and DESs.

4.1 Synthesis and Characterization of Selected DESs

Some of the DESs synthesized in this work were characterized for their physical properties. This is to obtain a clear view of their significant behaviours if they were to be used for application in chemical processes.

It has been shown in Section 3.1 that it is possible to synthesize different DESs from the same salt and HBD combination by varying the salt:HBD mole ratio. The effect of the mole ratio on the physical properties of DESs was investigated. The results confirmed that the physical properties of the synthesized DESs are dependent on the salt:HBD mole ratio.

4.1.1 Melting Temperatures

The melting temperatures were measured for DESs 5, 8, 12 and 15. These DESs were all synthesized from ZnCl_2 which was used as the complexing agent. The measured melting temperatures are listed in Table 4.3 and plotted as a function of molar ratio in Figure 4.1.

Table 4.3: Melting temperatures T_m (K) for DESs 5, 8, 12 and 15.

DES5	1:1	1:2	1:3	1:4
T_m	314.77	325.33	320.37	318.97
DES8	1:1	1:2	1:3	1:4
T_m	313.39	307.56	310.47	312.26
DES12	1:2	1:3	1:4	1:5
T_m	341.5	338.98	340.27	345.29
DES15	1:2	1:3	1:4	1:5
T_m	340.95	343.01	341.55	344.99

Figure 4.1 shows that the melting point of the DES is dependent on the salt:HBD mole ratio. The minimum melting point for each DES occurs at different salt:HBD mole ratio.

It is obvious that the DESs based on phosphonium salts have higher melting points than those based on ammonium salts. This is agreement with results reported by Shahbaz et al. (2012a and 2012b). It has been shown that, in general, the phosphonium-based DESs possess melting temperatures are higher than those of the ammonium-based DESs. For instance, the ammonium-based DESs reported by Shahbaz, et al. (2012a and 2012b) were of melting temperatures lower than 323 K while the phosphonium-based ones were of melting temperatures more than 333 K.

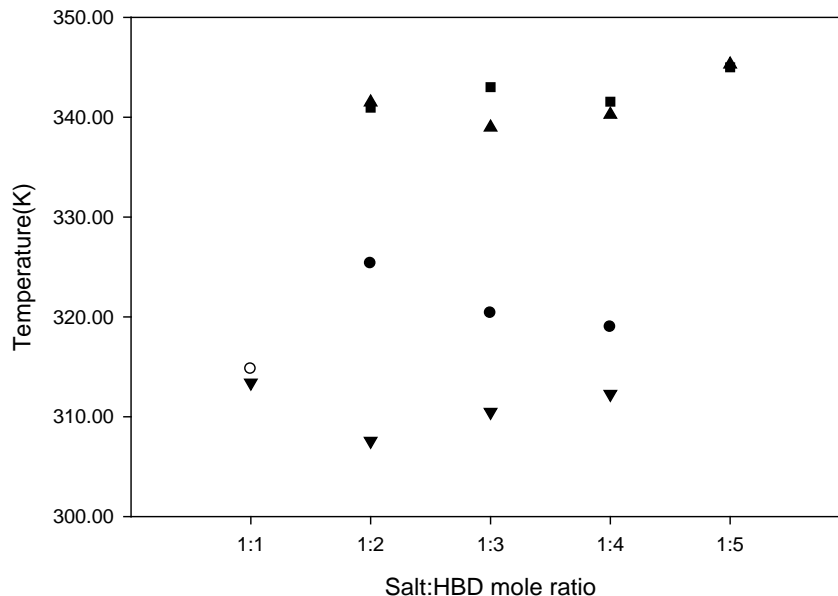


Figure 4.1 Melting temperatures of DES5 (●), DES8 (▼), DES12 (▲) and DES15 (■) as a function of salt:HBD mole ratio.

4.1.2 Viscosities

The viscosity of a fluid varies with temperature in an inverse proportional pattern, i.e. becoming smaller as temperature is elevated. Research on this physical phenomenon has been carried out to understand the relationship between the temperature and the viscosity (Giap, 2010). One model assumed that this relationship is governed by an “Arrhenius-like” equation, as shown below (Choi and Yoo, 2009, Saeed et al., 2009):

$$\mu = \mu_o e^{\frac{E_\mu}{RT}} \quad (4.1)$$

where μ is the viscosity in Pa.s and R is the ideal gas constant in $\text{kPa.L.mol}^{-1}.\text{K}^{-1}$. In the case of DESs of this work, μ_o is a specific constant for each DES with the units of viscosity and E_μ is the activation energy of viscosity, which is constant for each DES in $\text{Pa.m}^3.\text{mol}^{-1}$.

The viscosity of various ILs and DESs was a subject for many characterization studies (Kareem et al., 2010, Dai et al., 2009, Hayyan et al., 2013, Pereiro et al., 2007).

This is due to the need for such data in the references and literature if a certain process utilizing ILs or DESs is to be designed.

In the present work, the viscosity of selected DESs was measured experimentally at temperatures between 343.15 and 368.15 K and presented in Table 4.4. The experimental values of the viscosity were plotted as a function of the temperature, Figures 4.2 – 4.5. Individual series of viscosity values for each DES were fitted by Equation 4.1 above. Although the values of the constants μ_o and E_μ are different for each DES, all the series were fitted with high accuracy, as can be seen in Figures 4.2 – 4.5. The values of μ_o and E_μ are listed in Table 4.5.

Table 4.4: Experimental results for viscosity (Pa.S) of DESs 5, 8, 12, and 15 at different molar ratios and temperatures.

T/K	DES5 (1:1)	DES5 (1:2)	DES5 (1:3)	DES8 (1:2)	DES8 (1:3)	DES8 (1:4)
343.15	0.8278	13.9887	3.4654	0.5053	0.9954	2.2885
348.15	0.6648	9.5433	2.5171	0.3891	0.7679	1.5433
353.15	0.522	7.1962	1.8269	0.3116	0.5956	1.1122
358.15	0.396	5.6353	1.3993	0.2445	0.4687	0.8376
363.15	0.3168	4.0271	1.2456	0.1828	0.3612	0.6068
368.15	0.2842	3.0392	1.2148	0.1423	0.2916	0.4601
T/K	DES12 (1:2)	DES12 (1:3)	DES12 (1:4)	DES15 (1:2)	DES15 (1:3)	DES15 (1:4)
343.15	76.8437	19.7389	23.8818	44.0712	66.0198	49.64
348.15	39.4883	12.3299	16.6789	31.6102	55.2216	38.6791
353.15	25.484	8.7249	10.0123	20.5574	31.335	25.7027
358.15	20.0837	8.013	8.9119	13.2642	19.4016	18.1887
363.15	15.5391	7.1931	7.2456	10.9159	10.5504	11.5157
368.15	7.9785	6.8769	6.9125	9.0304	5.3145	6.4118

Table 4.5: Values of μ_o and E_μ for the fitting by Equation 4.1.

DES	Ratio	μ_o (Pa.S)	E_μ (Pa.m ³ .mol ⁻¹)
5	1:1	4.16×10^{-08}	$4.80 \times 10^{+04}$
5	1:2	2.37×10^{-09}	$6.41 \times 10^{+04}$
5	1:3	2.79×10^{-08}	$5.31 \times 10^{+04}$
8	1:2	7.25×10^{-09}	$5.15 \times 10^{+04}$
8	1:3	1.29×10^{-08}	$5.18 \times 10^{+04}$
8	1:4	6.55×10^{-11}	$6.92 \times 10^{+04}$
12	1:2	5.88×10^{-14}	$9.92 \times 10^{+04}$
12	1:3	9.43×10^{-08}	$5.44 \times 10^{+04}$
12	1:4	3.97×10^{-09}	$6.42 \times 10^{+04}$
15	1:2	2.28×10^{-10}	$7.42 \times 10^{+04}$
15	1:3	1.24×10^{-11}	$8.38 \times 10^{+04}$
15	1:4	4.19×10^{-10}	$7.29 \times 10^{+04}$

As can be seen in Figure 4.2, the viscosity of DES5 1:2 has a large value at low temperatures in comparison to DES5 1:1 and 1:3. However, it decreases sharply with increasing temperature and reaches a value of around 3.03 Pa.s at 368.15 K. Both DES5 1:1 and 1:3 show lower viscosities than DES5 1:2 at all measured temperatures. In addition, DES5 1:2 has a melting temperature of 325.33 K which is higher than both DES5 1:1 and 1:3, i.e. 314.77 K and 320.37 K, respectively.

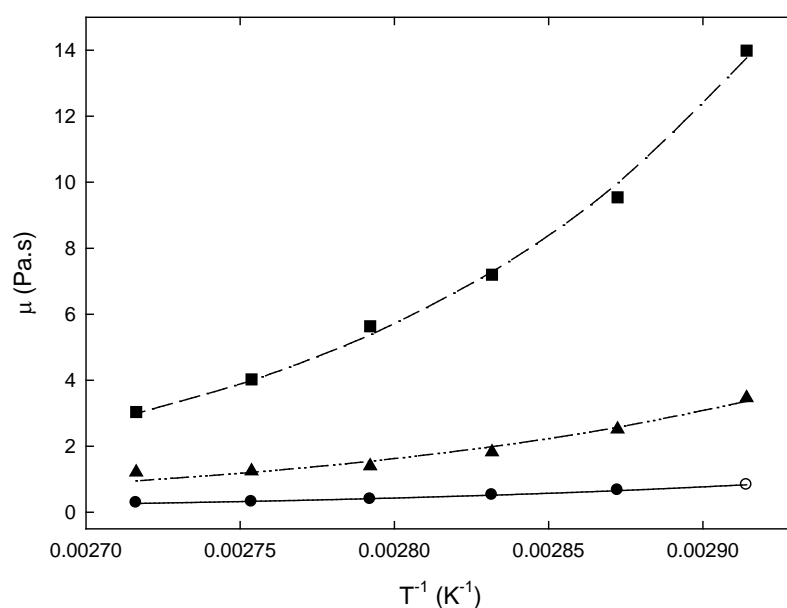


Figure 4.2 Viscosity μ of DES5 1:1 (\bullet), 1:2 (\blacksquare) and 1:3 (\blacktriangle) as a function of inversed temperature T^{-1} . Curves represent fitting by Equation 4.1.

Figure 4.3 depicts the profiles of viscosity for DES8 1:2, 1:3 and 1:4. The increased mole percentage of ZnCl_2 from 66% in DES8 1:2 to 80% in DES8 1:4 has a clear and uniform effect on the viscosity. It increases from around 0.5 Pa.s for DES8 1:2 at 343.15 K to 2.28 Pa.s for DES8 1:4 at the same temperature. Thus, the relationship between the mole percentage of ZnCl_2 in DES8 1:2, 1:3, and 1:4 and the viscosity is a direct proportional relationship. At higher temperatures, the same observation applies, whereby DES8 1:4 possesses a higher viscosity than DES8 1:2 and 1:3.

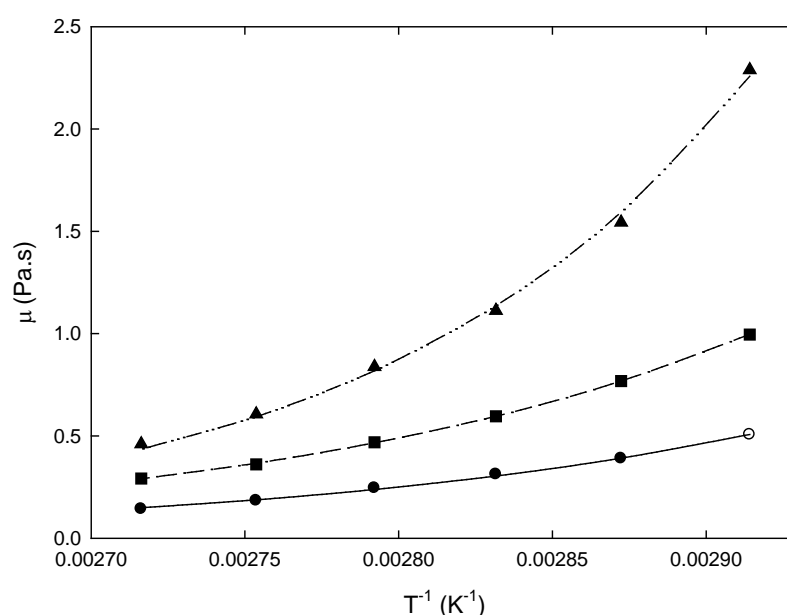


Figure 4.3 Viscosity μ of DES8 1:2 (●), 1:3 (■) and 1:4 (▲) as a function of inversed temperature, T^{-1} . Curves represent fitting by Equation 4.1.

Viscosity profiles for DES12 and DES15 are shown in Figure 4.4 and Figure 4.5, respectively. DES12 1:3 was found that possessed lower viscosity than that of 1:2 and 1:4, it means that by approaching to the eutectic ratio of salt:metal halide viscosity decreases to its minimum point. For instance, it decreases from 7.98 Pa.s for 1:2 under 368.15K to 6.88 Pa.s at ratio of 1:3 and then increases to 6.91 Pa.s at that of 1:4 under same operating temperature. Significantly, the same trend was observed in table 4.3 for the melting point of DES12 1:3.

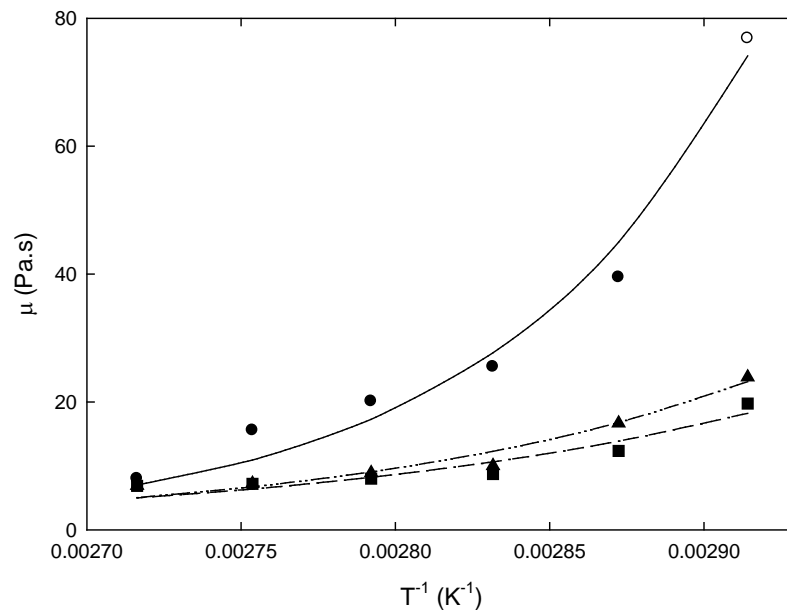


Figure 4.4 Viscosity μ of DES12 1:2 (\bullet), 1:3 (\blacksquare) and 1:4 (\blacktriangle) as a function of inversed temperature, T^{-1} . Curves represent fitting by Equation 4.1.

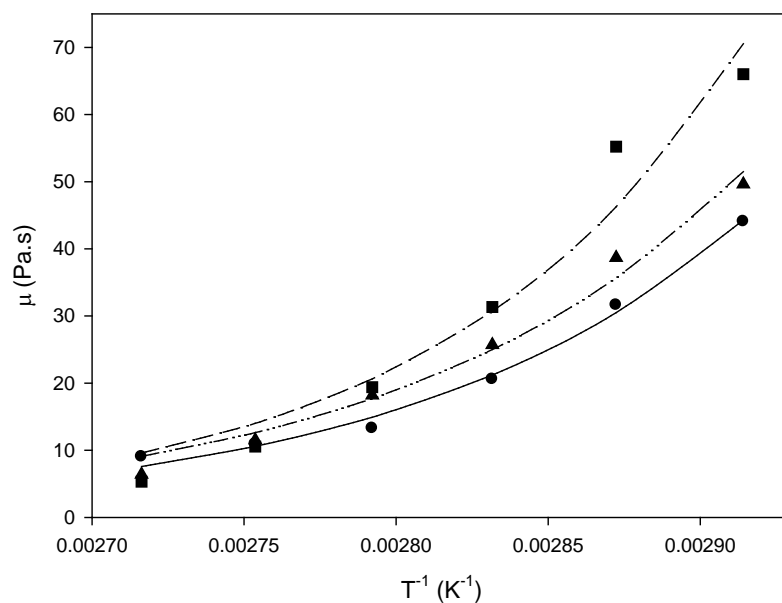


Figure 4.5 Viscosity μ of DES15 1:2 (\bullet), 1:3 (\blacksquare) and 1:4 (\blacktriangle) as a function of inversed temperature, T^{-1} . Curves represent fitting by Equation 4.1.

Figure 4.6 shows a comparison between the viscosity of DESs 5, 8, 12, and 15 when the salt:HBD is 1:2, and this is to illustrate the difference in viscosities between phosphonium and ammonium-based DESs. It can be seen that phosphonium-based DESs, i.e. DES12 and DES15, possess relatively higher viscosities than ammonium-

based DESs, i.e. DES5 and DES8. The difference is very big in some cases, reaching up to 80 folds at low temperatures. This finding reduces the search for potential solvents for the extraction of sodium metal from its common salts to a fewer number of DESs. This is because the viscosity of the successful DES candidate at the proposed moderate temperatures should be within an acceptable range.

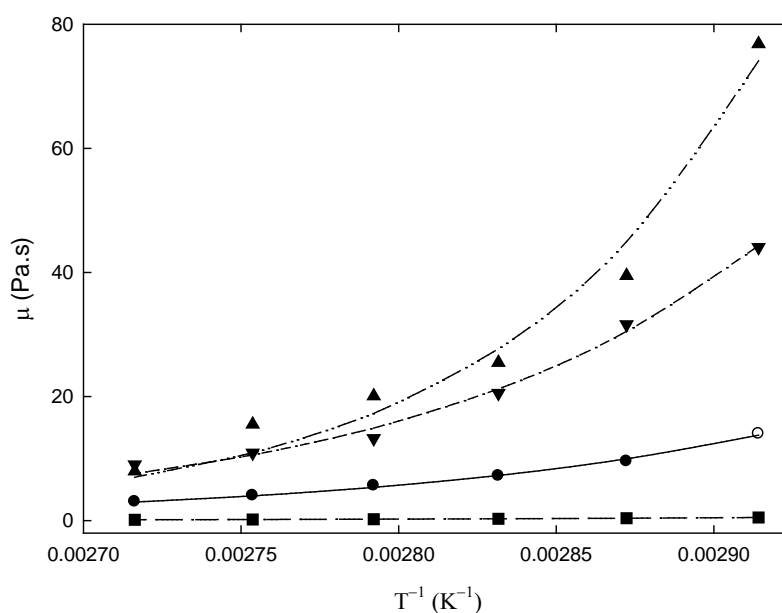


Figure 4.6 Viscosity μ of DES5 1:2 (\bullet), DES8 1:2 (\blacksquare), DES12 1:2 (\blacktriangle), DES15 1:2 (\blacktriangledown) as a function of inversed temperature, T^{-1} . Curves represent fitting by Equation 4.1.

4.1.3 Electrical Conductivity

As the intended use of the DESs of the present study is as solvents for electrolytic production of sodium metal, the electrical conductivity σ is thus an important physical property that, together with other factors, can decide the eligibility of a solvent to serve for the intended task.

σ is measured from a temperature above the melting temperature of each DES. Table 4.6 to 4.10 presents the experimental result of measured electrical conductivity for some of the DESs listed in Table 4.1. The conductivity is found to have a consistent trend of increasing with increasing temperature for DESs. This is an expected behaviour

for most materials, as the increase in temperature charges the molecules of the matter with additional energy and sets the electrons of the molecules in an active state. This situation leads to an improved electrical conductivity.

Figures 4.7 – 4.16 show the profiles of $\ln(\sigma)$ as function of inverse of temperature (T^{-1}) for DES1 1:1.75, 1:2, and 1:2.5; DES2 1:1, 1:2, and 1:3; DES3 1:2.5, 1:3, and 1:4; DES4 1:2, 1:3, and 1:4; DES5 1:1, 1:2, 1:3, and 1:4; DES8 1:1, 1:2, 1:3 and, 1:4; DES10 1:3, 1:4, and 1:5; DES11 1:2, 1:3, and 1:4; DES12 1:2, 1:3, 1:4, and, 1:5; and DES15 1:2, 1:3, 1:4, and 1:5. From the plots, the temperature dependence of σ is obvious. An adoption of the original Arrhenius-like equation for conductivity which was given by Ying et al., (2001), was used to represent this dependence:

$$\ln(\sigma) = \ln(\sigma_{\infty}) - \frac{E_{\sigma}}{kT} \quad (4.2)$$

where σ_{∞} is the electrical conductivity as T reaches infinity, E_{σ} is the electron mobility of the DES in me.V, k is the Boltzmann's constant in which meV.K⁻¹, and T is the temperature in Kelvin (Vila et al., 2007). This equation is used to fit the conductivity profiles for the above mentioned ten DESs. Individual series of σ possess their own σ_{∞} and E_{σ} , and these are given in Table 4.11. The fitted series are also plotted in Figures 4.7 – 4.16. The accuracy of this fitting is obvious from the plots, as the curves are very close to the experimental points. Due to the high accuracy found for this fitting, it could be used as a predictive method for the values of electrical conductivity at a given temperature.

Table 4.6: Experimental results of electrical conductivity (mS cm^{-1}) for DESs 1 and 2 at different molar ratios.

T/K	DES1 (1:1.75)	DES1 (1:2)	DES1 (1:2.5)	DES2 (1:1)	DES2 (1:2)	DES2 (1:3)
298.15	6.801	7.332	8.317	1.929	1.749	1.463
303.15	9.138	10.191	10.665	2.191	1.951	1.553
308.15	10.857	11.407	12.070	3.161	2.549	2.035
313.15	12.935	13.553	14.133	3.680	3.004	2.570
318.15	14.794	15.895	16.558	4.603	3.991	3.112
323.15	16.335	17.185	17.977	5.864	5.120	3.816
328.15	18.393	20.227	21.257	6.668	6.046	4.811
333.15	20.102	22.991	24.247	7.805	7.187	5.757
338.15	21.773	24.200	25.152	8.980	8.160	6.717
343.15	23.474	25.599	26.275	9.863	8.955	7.805
348.15	24.750	27.065	27.799	11.548	10.629	9.286
353.15	26.043	28.072	28.690	12.954	12.191	10.800

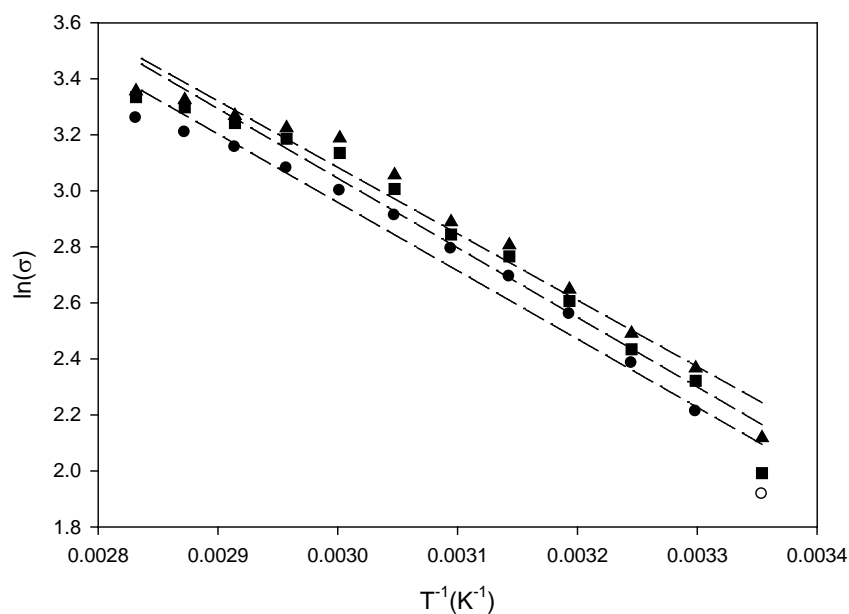


Figure 4.7 Electrical conductivity σ of DES1 1:1.75 (\bullet), 1:2 (\blacksquare), and 1:2.5 (\blacktriangle) as a function of the inversed temperature. Curves represent fitting by Equation 4.2.

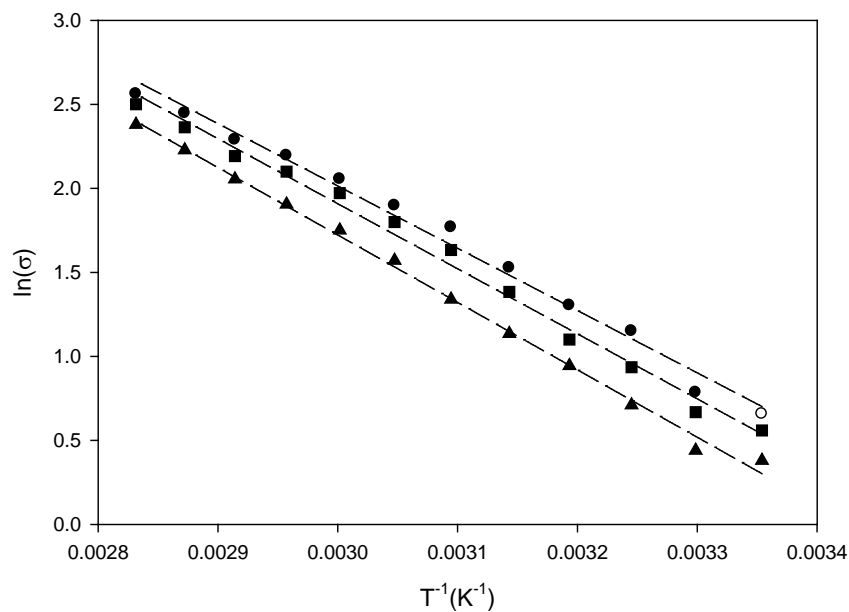


Figure 4.8 Electrical conductivity σ of DES2 1:1 (●), 1:2 (■), and 1:3 (▲) as a function of the inversed temperature. Curves represent fitting by Equation 4.2.

Table 4.7: Experimental results of electrical conductivity (mS cm^{-1}) for DESs 3 and 4 at different molar ratios.

T/K	DES3 (1:2.5)	DES3 (1:3)	DES3 (1:4)	DES4 (1:2)	DES4 (1:3)	DES4 (1:4)
298.15	5.120	5.429	5.661	0.750	0.602	0.487
303.15	6.627	6.878	6.994	1.177	0.958	0.780
308.15	7.940	8.305	8.245	1.635	1.041	1.099
313.15	9.283	9.486	9.699	2.067	1.562	1.387
318.15	10.955	11.339	11.579	2.716	2.112	1.878
323.15	12.539	13.147	13.408	3.381	2.637	2.357
328.15	14.330	14.769	15.086	3.903	3.426	2.716
333.15	16.161	16.664	17.137	4.878	4.086	3.246
338.15	17.779	18.395	18.755	5.754	4.916	3.962
343.15	19.417	19.900	20.286	6.521	5.748	4.646
348.15	21.347	21.924	22.262	7.754	6.474	5.335
353.15	23.097	23.667	24.053	9.109	7.100	6.095

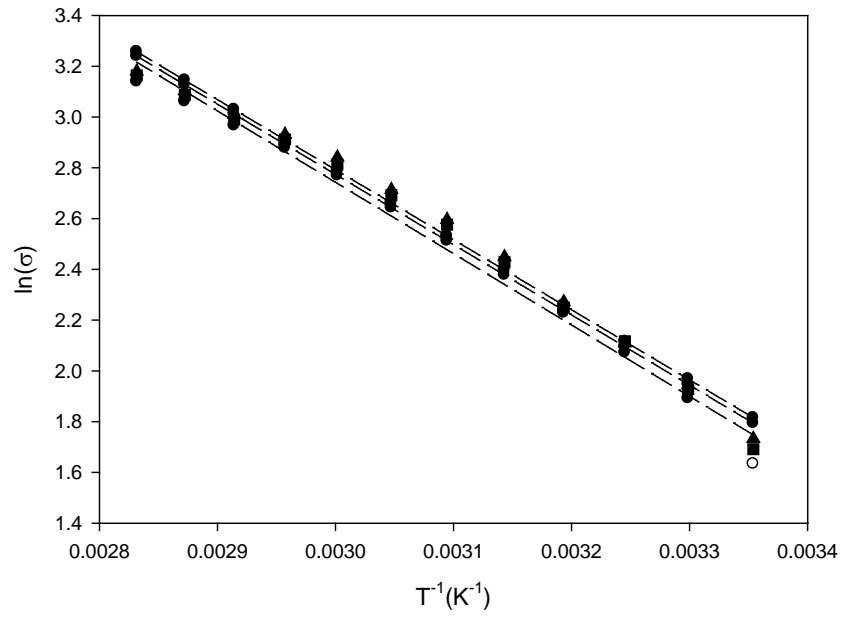


Figure 4.9 Electrical conductivity σ of DES3 1:2.5 (\bullet), 1:3 (\blacksquare), and 1:4 (\blacktriangle) as a function of the inversed temperature. Curves represent fitting by Equation 4.2.

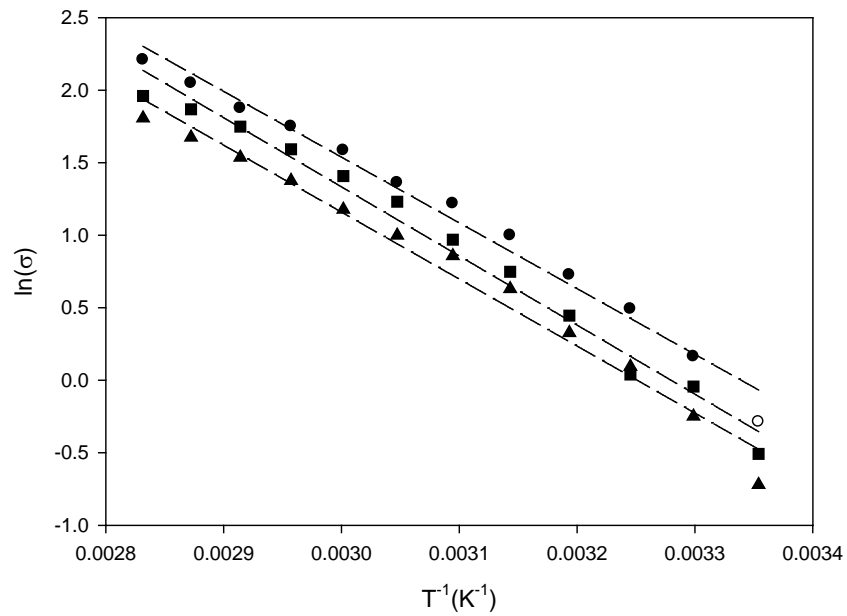


Figure 4.10 Electrical conductivity σ of DES4 1:2 (\bullet), 1:3 (\blacksquare), and 1:4 (\blacktriangle) as a function of the inversed temperature. Curves represent fitting by Equation 4.2.

Table 4.8: Experimental results of electrical conductivity (mS cm^{-1}) for DESs 5 and 8 at different molar ratios.

T/K	DES5 (1:1)	DES5 (1:2)	DES5 (1:3)	DES5 (1:4)	DES8 (1:1)	DES8 (1:2)	DES8 (1:3)	DES8 (1:4)
328.15	0.574	0.481	0.325	0.212	0.512	0.376	0.345	0.316
348.15	1.548	1.418	1.216	0.959	1.852	1.717	1.180	0.929
373.15	2.403	2.235	1.861	1.116	3.267	2.877	2.468	2.060
393.15	3.518	3.348	2.730	1.948	4.360	3.845	3.453	2.770
408.15	4.779	4.631	3.780	2.270	5.200	4.723	4.105	3.170

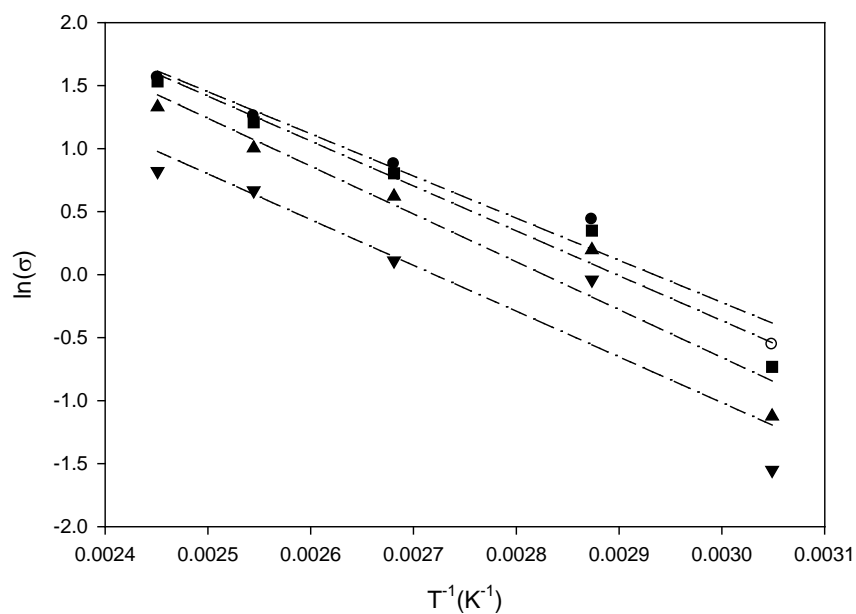


Figure 4.11 Electrical conductivity σ of DES5 1:1 (\bullet), 1:2 (\blacksquare), 1:3 (\blacktriangle), and 1:4 (\blacktriangledown) as a function of the inversed temperature. Curves represent fitting by Equation 4.2.

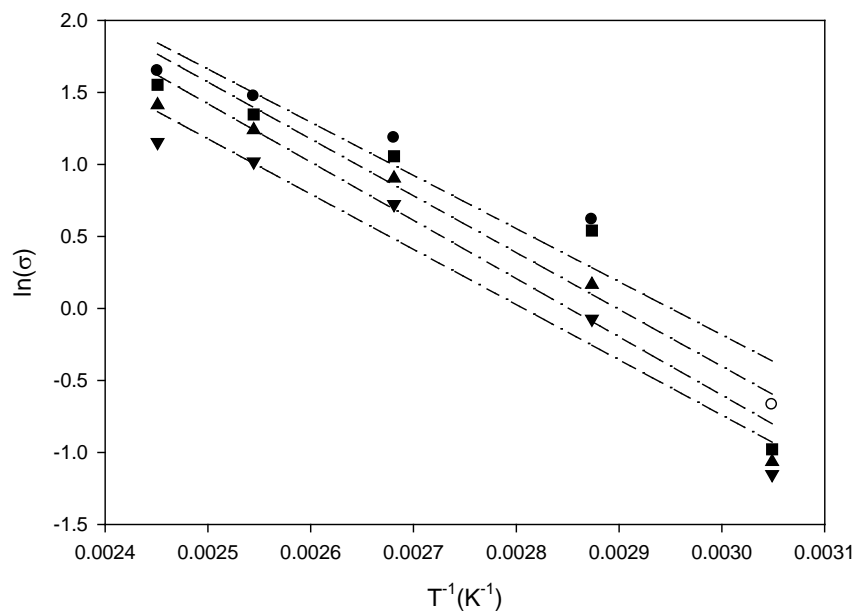


Figure 4.12 Electrical conductivity σ of DES8 1:1 (\bullet), 1:2 (\blacksquare), 1:3 (\blacktriangle), and 1:4 (\blacktriangledown) as a function of the inversed temperature. Curves represent fitting by Equation 4.2.

Table 4.9: Experimental results of electrical conductivity (mS cm^{-1}) for DESs 10 and 11 at different molar ratios.

T/K	DES10 (1:3)	DES10 (1:4)	DES10 (1:5)	DES11 (1:2)	DES11 (1:3)	DES11 (1:4)
298.15	1.092	1.557	1.942	0.062	0.103	0.116
303.15	1.598	2.193	2.570	0.124	0.172	0.198
308.15	1.914	2.649	3.103	0.186	0.319	0.370
313.15	2.502	3.246	3.845	0.277	0.394	0.410
318.15	2.964	3.858	4.437	0.405	0.549	0.607
323.15	3.265	4.405	5.072	0.496	0.719	0.816
328.15	4.307	5.395	6.279	0.701	0.927	0.965
333.15	5.129	6.221	7.110	0.858	1.124	1.233
338.15	5.797	7.423	8.169	1.160	1.487	1.608
343.15	6.723	8.192	9.496	1.493	1.778	1.971
348.15	7.372	9.074	10.31	1.811	2.196	2.874
353.15	8.114	10.027	11.196	2.154	2.599	3.594

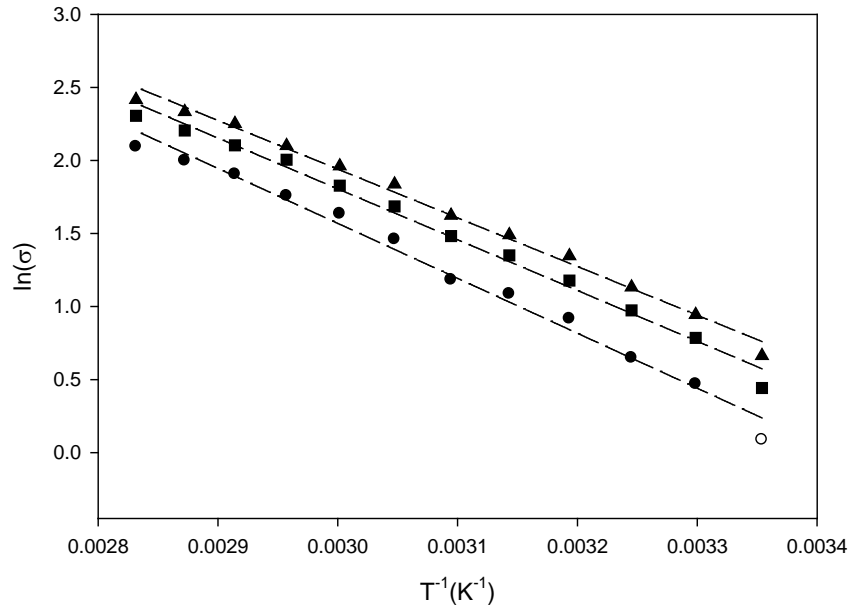


Figure 4.13 Electrical Conductivity σ of DES10 1:3 (\bullet), 1:4 (\blacksquare), and 1:5 (\blacktriangle) as a function of the inversed temperature. Curves represent fitting by Equation 4.2.

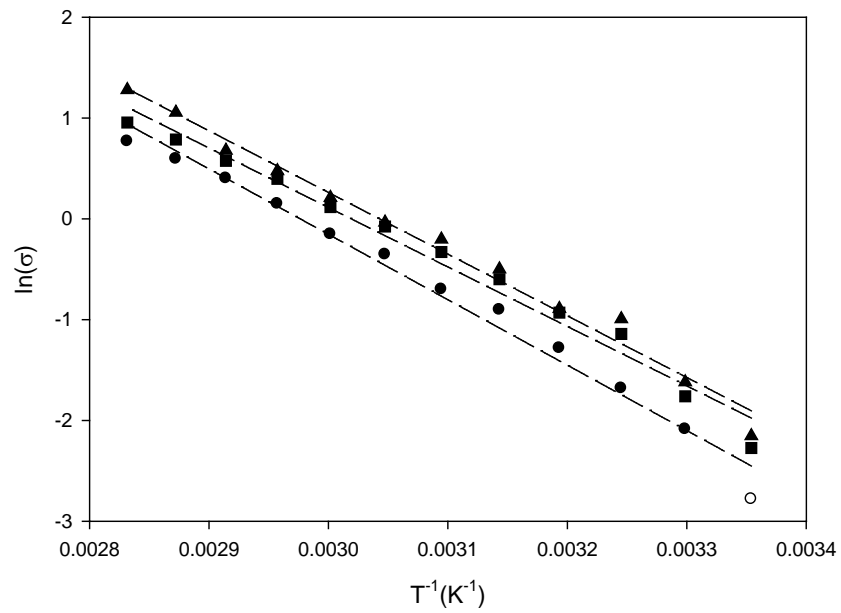


Figure 4.14 Electrical conductivity σ of DES11 1:2 (\bullet), 1:3 (\blacksquare), and 1:4 (\blacktriangle) as a function of the inversed temperature. Curves represent fitting by Equation 4.2.

Table 4.10: Experimental results of electrical conductivity (mS cm^{-1}) for DESs 12 and 15 at different molar ratios.

T/K	DES12 (1:2)	DES12 (1:3)	DES12 (1:4)	DES12 (1:5)	DES15 (1:2)	DES15 (1:3)	DES15 (1:4)	DES15 (1:5)
353.15	0.101	0.124	0.152	0.175	0.330	0.363	0.417	0.465
363.15	0.257	0.377	0.493	0.601	0.406	0.440	0.518	0.597
373.15	0.387	0.550	0.733	0.860	0.471	0.524	0.608	0.680
393.15	0.650	0.840	1.086	1.302	0.602	0.716	0.822	0.964
408.15	0.930	1.150	1.379	1.707	0.768	0.911	1.081	1.351

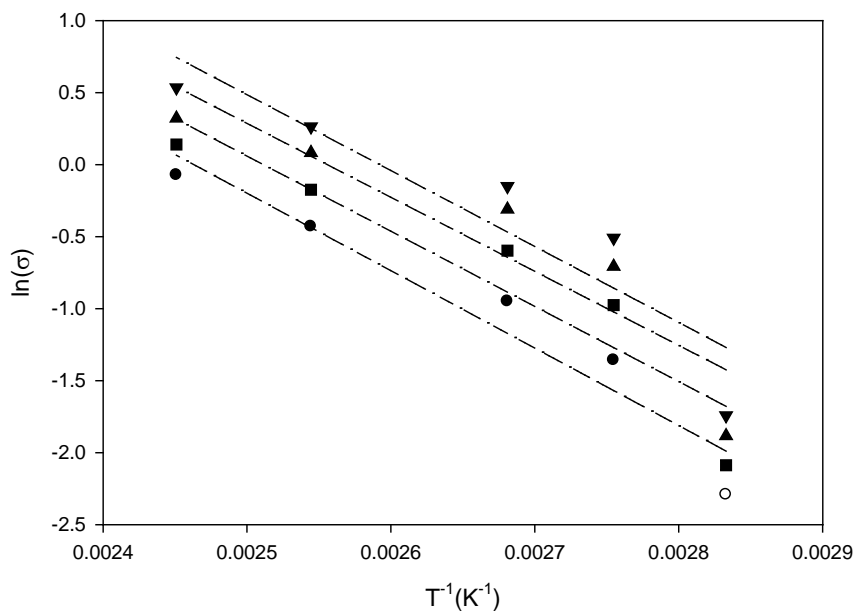


Figure 4.15 Electrical conductivity σ of DES12 1:2 (\bullet), 1:3 (\blacksquare), 1:4 (\blacktriangle), and 1:5 (\blacktriangledown) as a function of the inversed temp. Curves represent fitting by Equation 4.2.

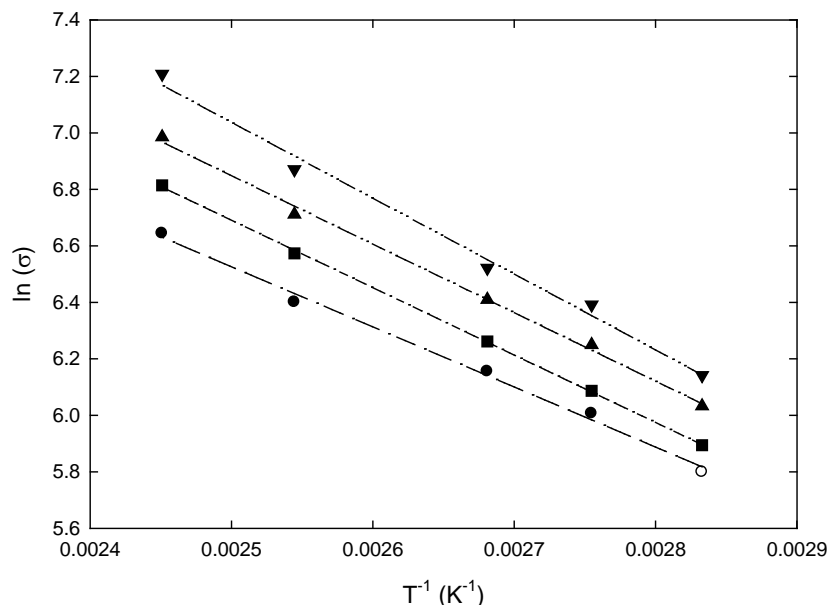


Figure 4.16 Electrical conductivity σ of DES15 1:2 (●), 1:3 (■), 1:4 (▲), and 1:5 (▼) as a function of the inversed temp. Curves represent fitting by Equation 4.2.

It can be observed from Figures 4.7 – 4.16 that the electrical conductivity for most ammonium based DESs is higher than that for the corresponding phosphonium based DESs. The maximum conductivity achieved in this research was for DES1 1:2.5 at 353.15 K which is 28.69 mS.cm^{-1} . As expected the electrical conductivity of DESs increased with increasing the salt concentration in the mixture. This can be attributed to the increase of the number of charge-carriers in the solution. This behavior can be seen in Tables 4.6, 4.7 and 4.8 for ammonium based DESs with glycerol or zinc chloride as complexing agent, i.e. DESs 2, 4, 5, and 8. On the other hand, DESs 1 and 3 which are composed of ammonium salt and ethylene glycol together with the phosphonium based DESs, i.e. DESs 10, 11, 12, and 15, showed an opposite trend. At higher salt concentrations in the DESs mixtures, the electrical conductivity was found to be decreasing. This decrease could be due to the strong influence of ion pairs, ion triplets, and higher ion aggregations that reduces the overall mobility and number of the effective charge carriers.

Table 4.11: Values of σ_∞ and E_σ for the fitting by Equation 4.2.

DES	Ratio	$\sigma_\infty(\text{ms.cm}^{-1})$	$E_\sigma(\text{meV})$
1	1:1.75	$2.91 \times 10^{+04}$	$2.10 \times 10^{+02}$
1	1:2	$3.63 \times 10^{+04}$	$2.14 \times 10^{+02}$
1	1:2.5	$2.69 \times 10^{+04}$	$2.04 \times 10^{+02}$
2	1:1	$5.08 \times 10^{+04}$	$3.20 \times 10^{+02}$
2	1:2	$7.44 \times 10^{+05}$	$3.34 \times 10^{+02}$
2	1:3	$9.46 \times 10^{+05}$	$3.46 \times 10^{+02}$
3	1:2.5	$7.16 \times 10^{+04}$	$2.42 \times 10^{+02}$
3	1:3	$6.48 \times 10^{+04}$	$2.38 \times 10^{+02}$
3	1:4	$6.42 \times 10^{+04}$	$2.37 \times 10^{+02}$
4	1:2	$3.77 \times 10^{+06}$	$3.90 \times 10^{+02}$
4	1:3	$6.13 \times 10^{+06}$	$4.11 \times 10^{+02}$
4	1:4	$3.33 \times 10^{+06}$	$3.98 \times 10^{+02}$
5	1:1	$1.82 \times 10^{+04}$	$2.88 \times 10^{+02}$
5	1:2	$3.03 \times 10^{+04}$	$4.62 \times 10^{+02}$
5	1:3	$4.52 \times 10^{+04}$	$3.27 \times 10^{+02}$
5	1:4	$1.93 \times 10^{+04}$	$3.13 \times 10^{+02}$
8	1:1	$5.36 \times 10^{+04}$	$3.18 \times 10^{+02}$
8	1:2	$9.29 \times 10^{+04}$	$3.40 \times 10^{+02}$
8	1:3	$1.01 \times 10^{+05}$	$3.49 \times 10^{+02}$
8	1:4	$4.75 \times 10^{+04}$	$3.31 \times 10^{+02}$
10	1:3	$3.80 \times 10^{+04}$	$3.24 \times 10^{+02}$
10	1:4	$2.06 \times 10^{+04}$	$3.00 \times 10^{+02}$
10	1:5	$1.53 \times 10^{+04}$	$2.87 \times 10^{+02}$
11	1:2	$2.45 \times 10^{+08}$	$5.59 \times 10^{+02}$
11	1:3	$5.42 \times 10^{+07}$	$5.08 \times 10^{+02}$
11	1:4	$1.20 \times 10^{+08}$	$5.27 \times 10^{+02}$
12	1:2	$5.68 \times 10^{+05}$	$4.63 \times 10^{+02}$
12	1:3	$4.93 \times 10^{+05}$	$4.50 \times 10^{+02}$
12	1:4	$5.08 \times 10^{+05}$	$4.43 \times 10^{+02}$
12	1:5	$8.55 \times 10^{+05}$	$4.54 \times 10^{+02}$
15	1:2	$1.38 \times 10^{+02}$	$1.83 \times 10^{+02}$
15	1:3	$3.14 \times 10^{+02}$	$2.06 \times 10^{+02}$
15	1:4	$4.03 \times 10^{+02}$	$2.09 \times 10^{+02}$
15	1:5	$9.34 \times 10^{+02}$	$2.31 \times 10^{+02}$

In general, the conductivities of the ammonium-based DESs are higher than those of the phosphonium-based DESs. Together with the finding that ammonium-based DESs possessed lower melting temperatures and lower viscosities than the phosphonium-based DESs, it is more evident now that the production of sodium metal

from its common salts at moderate temperatures has more potential to be carried out in ammonium-based DESs.

4.1.4 Refractive Index

Refractive index n_D is an important property in many optical applications and it can reflect how pure the measured medium is. The typical relationship between the refractive index and temperature is an inversed proportional relationship. This means that the refractive index decreases with increasing temperature (Kareem et al., 2010, Hayyan et al., 2013). At elevated temperatures, the density of the medium decreases, allowing more freedom for the movement of light. This translates in an increase for the speed of light in that medium and thus a lower refractive index is observed. Hence, the following expression is valid:

$$T \propto \rho^{-1} \propto n_D^{-1} \quad (4.3)$$

where T , ρ and n_D are temperature, density and refractive index, respectively. Accordingly, the refractive index could be used as an indication for the density of the DES at a given temperature. This requires a single measurement of the density at a temperature at which the refractive index is measured as well. Table 4.12 presents experimental results of refractive indices at different molar ratios as a function of temperature.

Figures 4.17, 4.18, 4.19, and 4.20 show the profiles of the refractive indices at different molar ratios for DESs 5, 8, 12, and 15, respectively. It was found that the refractive indices are directly proportional to the ZnCl_2 molar ratios in ammonium based DESs, i.e. DES5 and DES8. In phosphonium based DESs, i.e. DES12 and DES 15, the same trend was observed for salt:metal halide molar ratios of 1:3, 1:4, and 1:5. While for the salt:metal halide ratio of 1:2, the refractive indices are higher than those of 1:3, 1:4, and 1:5. It is worth mentioning that the refractive indices decrease to a minimum when approaching the eutectic point of DESs. The relationships between the refractive indices and the temperature were fitted by a straight-line equation in the form:

$$n_D = a + bT(K) \quad (4.4)$$

where a and b are fitting parameters which are different for each individual DES.

Table 4.12: Experimental refractive indices n_D of DESs 5, 8, 12, and 15 at different molar ratios.

T/K	DES5 (1:1)	T/K	DES5 (1:2)	T/K	DES5 (1:3)	T/K	DES5 (1:4)
339.15	1.5161	336.15	1.5371	333.15	1.5533	333.15	1.5683
340.15	1.5156	340.15	1.5358	339.15	1.5518	339.15	1.5668
346.15	1.5143	348.15	1.5337	344.15	1.5505	344.15	1.5655
351.15	1.5131	353.15	1.5325	349.15	1.5492	349.15	1.5642
359.15	1.5112	357.15	1.5312	353.15	1.5482	353.15	1.5632
362.15	1.5105	361.15	1.5301	358.15	1.5469	358.15	1.5619
				362.15	1.5459	362.15	1.5609
T/K	DES8 (1:1)	T/K	DES8 (1:2)	T/K	DES8 (1:3)	T/K	DES8 (1:4)
338.15	1.5106	338.15	1.513	331.15	1.5221	323.15	1.5304
348.15	1.5073	348.15	1.5103	338.15	1.5202	329.15	1.5292
353.15	1.5057	353.15	1.5092	348.15	1.5179	333.15	1.5279
358.15	1.5041	357.15	1.5082	358.15	1.5154	339.15	1.5264
363.15	1.5024	362.15	1.5073	362.15	1.5145	343.15	1.5255
						348.15	1.5244
						353.15	1.5229
						359.15	1.5213
T/K	DES12 (1:2)	T/K	DES12 (1:3)	T/K	DES12 (1:4)	T/K	DES12 (1:5)
348.15	1.5525	343.15	1.5205	343.15	1.5365	343.15	1.5412
353.15	1.5508	348.15	1.5185	348.15	1.5337	348.15	1.5384
358.15	1.5492	353.15	1.5169	353.15	1.5329	353.15	1.5369
362.15	1.5475	358.15	1.5153	358.15	1.5306	358.15	1.5353
		362.15	1.5136	362.15	1.5291	362.15	1.5335
T/K	DES15 (1:2)	T/K	DES15 (1:3)	T/K	DES15 (1:4)	T/K	DES15 (1:5)
343.15	1.5390	331.15	1.5068	331.15	1.5221	343.15	1.5355
348.15	1.5373	338.15	1.5050	338.15	1.5202	348.15	1.5338
353.15	1.5362	348.15	1.5027	348.15	1.5179	353.15	1.5327
358.15	1.5349	358.15	1.5002	358.15	1.5154	358.15	1.5314
362.15	1.5341	362.15	1.5001	362.15	1.5145	362.15	1.5306

Equation 4.4 was used to fit the refractive index values in Table 4.12. Table 4.13

shows the values of a and b for the fitted values.

Table 4.13: Values of a and b for the fitting by Equation 4.4.

DES	Salt:metal halide	a	b (K)
DES5	1:1	1.597	-2.38×10^{-04}
	1:2	1.630	-2.75×10^{-04}
	1:3	1.639	-2.56×10^{-04}
	1:4	1.654	-2.56×10^{-04}
DES8	1:1	1.621	-3.27×10^{-04}
	1:2	1.594	-2.40×10^{-04}
	1:3	1.603	-2.44×10^{-04}
	1:4	1.612	-2.53×10^{-04}
DES12	1:2	1.675	-3.52×10^{-04}
	1:3	1.642	-3.54×10^{-04}
	1:4	1.664	-3.73×10^{-04}
	1:5	1.673	-3.85×10^{-04}
DES15	1:2	1.626	-2.55×10^{-04}
	1:3	1.603	-2.44×10^{-04}
	1:4	1.581	-2.24×10^{-04}
	1:5	1.623	-2.55×10^{-04}

Figures 4.17, 4.18, 4.19, and 4.20 show plots for the profiles of the refractive indices along with the calculated values using Equation 4.4 for DESs 5, 8, 12, and 15; respectively. The regression coefficient, R^2 , was not less than 0.99 for all the systems. This means that the regressed models are highly suitable for representing the n_D values as the temperature varies. The plots in the Figures show this fact as the fitting curves are passing through almost all of the experimental data points.

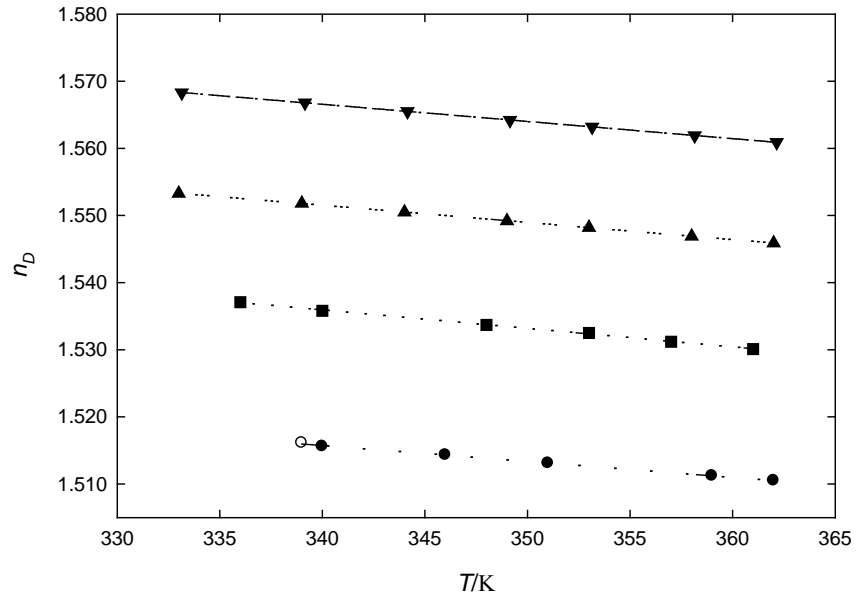


Figure 4.17 Refractive index n_D of DES5 1:1 (●), 1:2 (■), 1:3 (▲), and 1:4 (▼) as a function of temperature. Lines represent fitting by Equation 4.4.

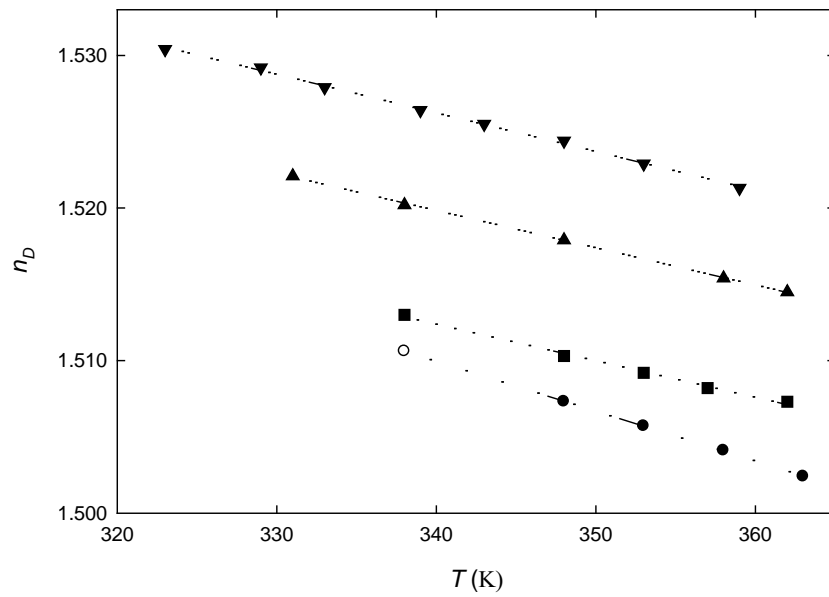


Figure 4.18 Refractive index n_D of DES8 1:1 (●), 1:2 (■), 1:3 (▲), and 1:4 (▼) as a function of temperature. Lines represent fitting by Equation 4.4.

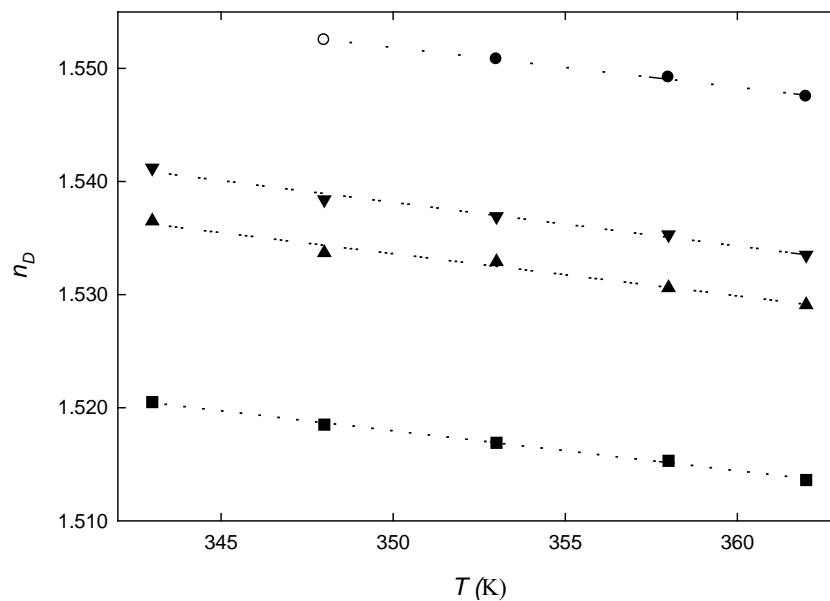


Figure 4.19 Refractive index n_D of DES12 1:2 (●), 1:3 (■), 1:4 (▲), and 1:5 (▼) as a function of temperature. Lines represent fitting by Equation 4.4.

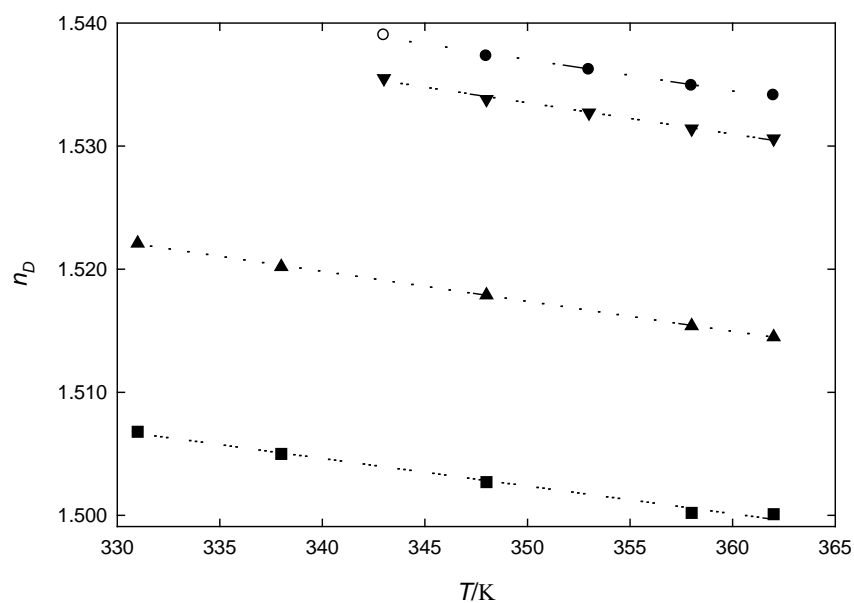


Figure 4.20 Refractive index n_D of DES15 1:2 (●), 1:3 (■), 1:4 (▲), and 1:5 (▼) as a function of temperature. Lines represent fitting by Equation 4.4.

4.2 Solubility of Different Sodium Salts in ILs and DESs

Three important factors must be taken into account when choosing the proper solvent for the production of sodium metal electrochemically. These are: i) the high

solubility of commercially available sodium salts in the solvent, ii) reasonable electrical conductivity of the resulting solution, and iii) the stability of the produced sodium metal in the solution. The most important part of the present work was the measurement of the solubility of different sodium salts in ILs and DESs. This section was divided into three main subsections to handle the size of the experimental results obtained. They are:

- 4.2.1 Solubility of sodium chloride, sodium bromide, and sodium carbonate in ammonium-based DESs
- 4.2.2 Solubility of sodium chloride in phosphonium-based DESs
- 4.2.3 Solubility of sodium chloride in different ILs

4.2.1 Solubility of Sodium Chloride, Sodium Bromide, and Sodium Carbonate in Ammonium-Based DESs

The method used to measure the solubility of a sodium salt in DES or IL was given in Section 3.3. In this Subsection, ammonium-based DESs mentioned in Table 4.1 were synthesized and the solubility of sodium chloride (NaCl), sodium bromide (NaBr), and sodium carbonate (Na_2CO_3) was measured experimentally in these DESs and tabulated in Tables 4.14 through 4.21.

Several solubility measurements were done repeatedly to increase the reliability of the experimental results. The results were classified according to solvent structure, range of temperature and stability of the solution. Figures 4.21 through 4.28 depict the results of solubility as a function of temperature.

The studied ammonium DESs were shown in Table 4.1 as DESs 1 – 9.

Figure 4.21 shows the solubility of NaCl, NaBr and Na_2CO_3 in DES1, i.e. choline chloride:ethylene glycol. This DES has a maximum solubility of 0.25 wt. % of Na_2CO_3 while the solubility of NaCl and NaBr are 0.06 and 0.04 wt. %, respectively. The solubility increases by increasing the temperature from ambient to 308.15°C, and then

slowly increasing to a temperature of 333.15 K. The slight decrease in solubility noticed at 50°C for a number of cases can be neglected and considered as experimental error. This is because it happened in certain cases but not in all. At temperatures higher than 333.15 K the DES started to lose ethylene glycol and thus became unstable. There is no clear trend in the solubility of all three salts in DES1 with the change of salt:HBD molar ratio.

Table 4.14: Solubility(wt%) of sodium chloride, sodium carbonate, and sodium bromide in DES1 at different temperatures.

T/K	1:1.75	1:2	1:2.25	1:2.5
NaCl				
298.15	5.076×10^{-03}	5.224×10^{-03}	4.386×10^{-03}	5.424×10^{-03}
308.15	3.390×10^{-02}	4.630×10^{-02}	5.230×10^{-02}	6.660×10^{-02}
323.15	3.350×10^{-02}	4.180×10^{-02}	5.130×10^{-02}	5.670×10^{-02}
333.15	4.020×10^{-02}	4.770×10^{-02}	5.650×10^{-02}	6.600×10^{-02}
Na ₂ CO ₃				
298.15	3.090×10^{-02}	1.570×10^{-02}	1.250E-02	1.490E-02
308.15	2.159×10^{-02}	1.621×10^{-02}	1.469E-01	1.825E-01
323.15	2.246×10^{-02}	1.504×10^{-02}	1.442E-01	1.548E-01
333.15	2.486×10^{-02}	1.755×10^{-02}	1.620E-01	1.789E-01
NaBr				
298.15	4.061E-03	4.701×10^{-02}	3.114×10^{-02}	1.190×10^{-02}
308.15	2.710E-02	3.980×10^{-02}	3.710×10^{-02}	1.478×10^{-02}
323.15	2.680E-02	3.520×10^{-02}	3.640×10^{-02}	1.176×10^{-02}
333.15	3.220E-02	4.720×10^{-02}	4.010×10^{-02}	1.414×10^{-02}

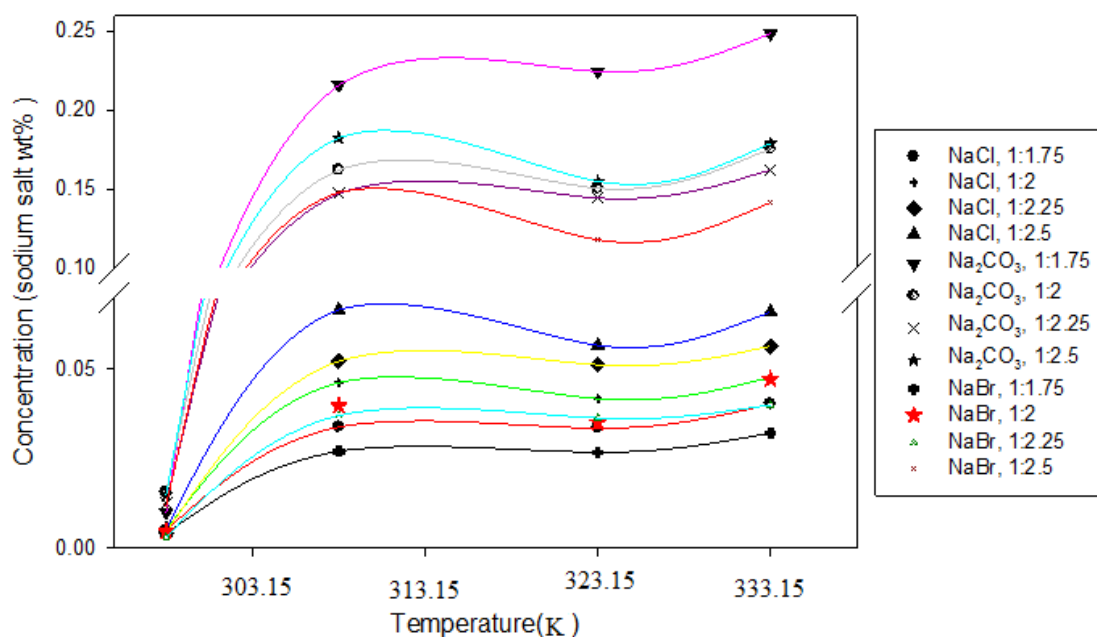


Figure 4.21 Solubility of NaCl, NaBr and Na₂CO₃ in DES1 as a function of temperature. The continuous line is drawn through the experimental data of the same system for visual clarity.

For DES2, i.e. choline chloride:glycerol, the solubility of sodium salts decreases smoothly by increasing temperature. DES2 dissolves a maximum of 1.09 wt% of NaCl and 0.97 wt% of NaBr, as can be seen in Figure 4.22. Thus, it is clear that the type of the HBD does affect the solubility of sodium salts in DES.

Table 4.15: Solubility(wt%) of sodium chloride and sodium bromide in DES2 at different temperatures.

T/K	1:1.5	1:2	1:2.5	1:3
NaCl				
298.15	0.365		0.870	1.090
323.15	0.361	0.427	0.862	1.088
348.15	0.333	0.423	0.842	1.074
373.15	0.319	0.402	0.804	1.039
393.15	0.312	0.399	0.798	0.979
414.15	0.307	0.400	0.776	0.960
NaBr				
298.15	0.329			
323.15	0.325	0.385	0.776	0.979
348.15	0.299	0.381	0.756	0.966
373.15	0.287	0.362	0.723	0.935
393.15	0.281	0.359	0.718	0.881
414.15			0.658	

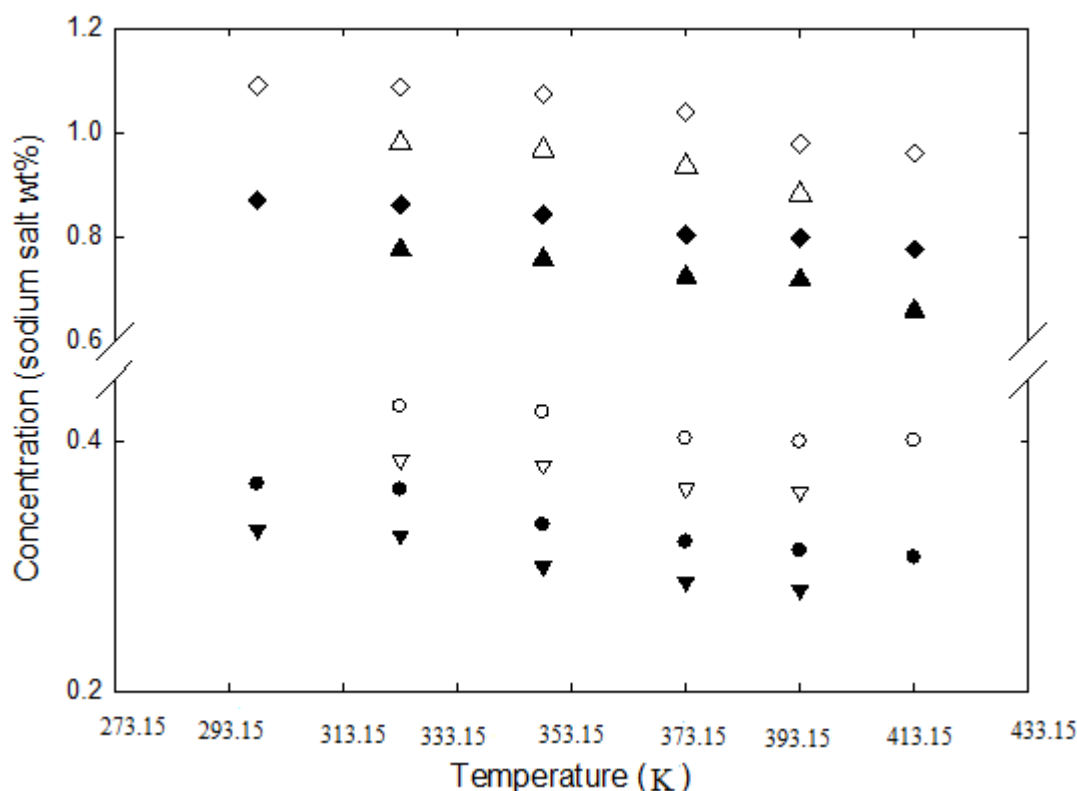


Figure 4.22 Solubility profiles of NaCl and NaBr in DES2 as a function of temperature. NaCl series, for salt:HBD ratios 1:1.5 (●), 1:2 (○), 1:2.5 (◆) and 1:3 (◇). NaBr series, for salt:HBD ratios 1:1.5 (▼), 1:2 (▽), 1:2.5 (▲) and 1:3 (△).

In order to investigate the effect of the salt used in the synthesis of the DES on the solubility of sodium chloride, choline chloride was replaced by N,N-diethylethanolammonium chloride with ethylene glycol as HBD, and this is designated DES3. The maximum solubility of NaCl at 328.15 K was approximately 0.55 wt%. This is higher than that for DES1, under the same conditions. The maximum solubility of NaCl in DES3 was 1.15 wt% at 25°C for the salt:HBD molar ratio of 1:4. Surprisingly, the solubility of NaCl in DES3 decreased with an increase of temperature and increased with an increase of the HBD molar ratio in the DES from 2.5 to 4, as illustrated in Figure 4.23. The use of N,N- diethylethanolammonium chloride increased the stability of the DES to much higher temperatures which enabled the measurement of the solubility at temperatures up to 423.15 K.

Table 4.16: Solubility of sodium chloride in DES3 at different temperatures.

T/K	1:2.5	1:3	1:4	1:4.5
	NaCl			
298.15	0.442	0.529	1.044	1.153
323.15	0.399	0.524	0.980	1.066
348.15	0.366	0.509	0.950	1.061
373.15	0.319	0.494	0.860	0.989
398.15	0.278	0.442	0.804	0.886
423.15	0.213	0.407	0.700	0.800

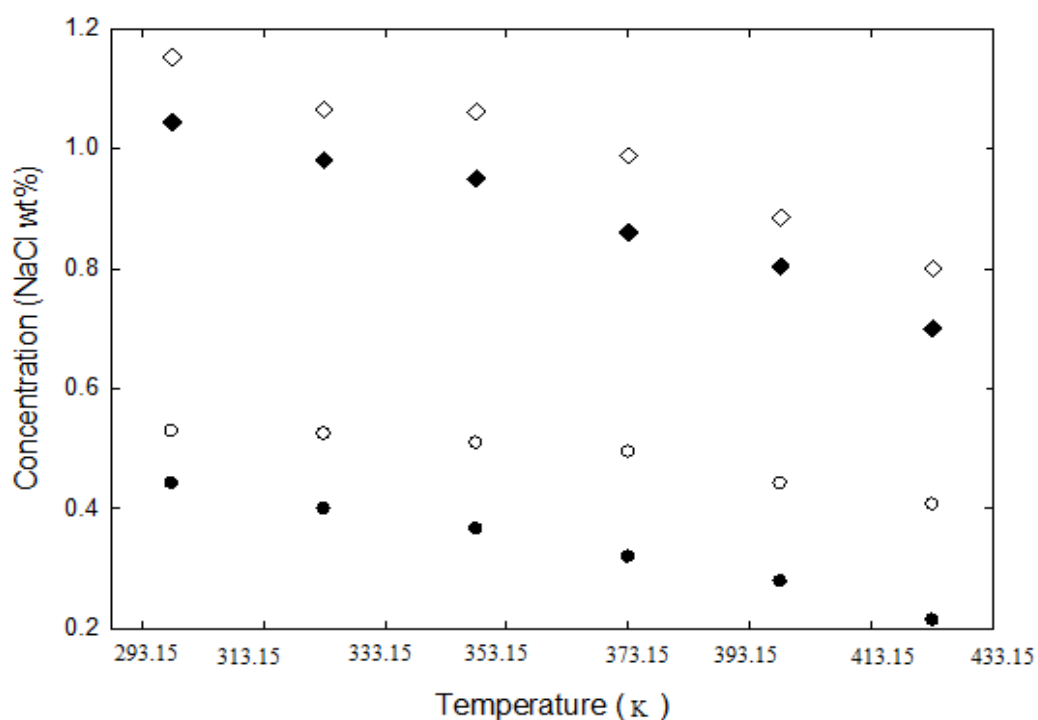


Figure 4.23 Solubility profiles of NaCl in DES3 as a function of temperature. NaCl series, for salt:HBD ratios 1:2.5 (●), 1:3 (○), 1:4 (◆) and 1:4.5 (◇).

The solubility of NaCl in DES4 was 2.08 and 2.53 wt% at 298.15 K and 423.15 K, respectively, as shown in Figure 4.24.

Table 4.17: Solubility of sodium chloride in DES4 at different temperatures.

T/K	1:2.5	1:3	1:4
	NaCl		
298.15	1.050	1.141	2.047
323.15	1.097	1.198	2.228
348.15	1.181	1.264	2.361
373.15	1.200	1.326	2.402
398.15	1.270	1.374	2.451
423.15	1.314	1.425	2.529

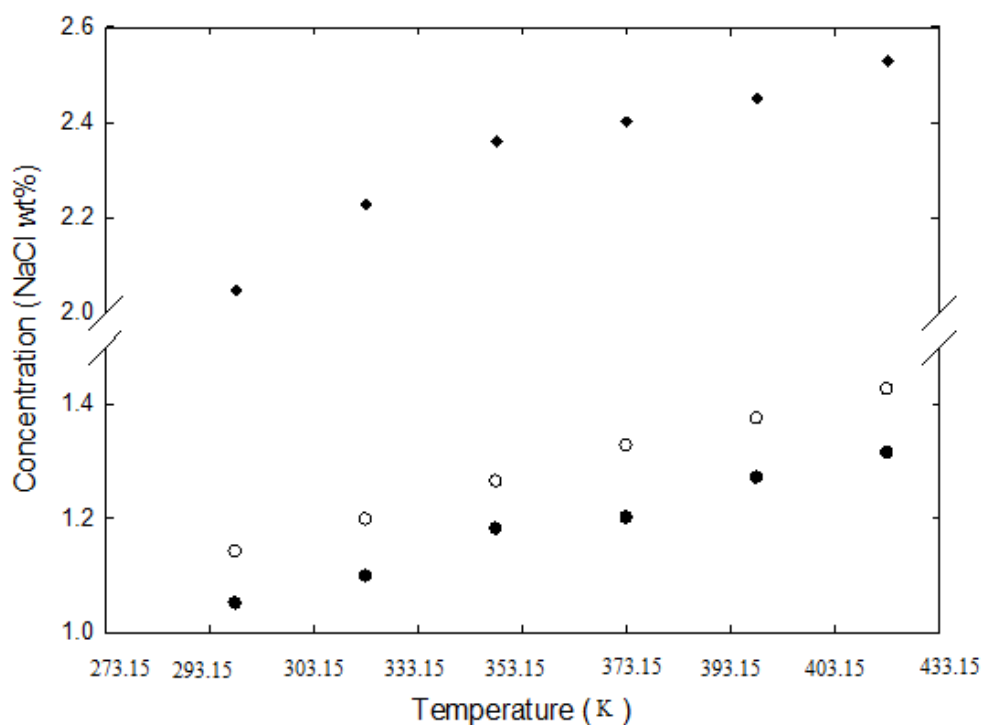


Figure 4.24 Solubility (Concentration) profiles of NaCl in DES4 as a function of temperature. NaCl series, for salt:HBD ratios 1:2.5 (●), 1:3 (○), 1:4 (◆).

Moreover, the solubility of NaCl increased with an increase of temperature and the decrease of HBD molar ratio in the DES. It is clear from Figures 4.21 – 4.24 that for the same salt, the solubility of NaCl in DESs using glycerol as HBD is higher than that when ethylene glycol is used as HBD.

The relatively low NaCl solubility in the DESs studied so far motivated the investigation in to other types of DESs, namely the DESs resulting from mixing ammonium based salts with metal halides. This group of DESs was synthesized and used for different applications by Abbott et al. (2004b). The solubility of NaCl and NaBr in choline chloride:zinc chloride DES, i.e. DES5, was measured at different temperatures and different salt:metal halide ratios. Interestingly, it was found that the solubility of NaCl and NaBr in DES5 is very high, reaching a maximum of 67 and 56 wt%, respectively, as illustrated in Figure 4.25.

Table 4.18: Solubility of sodium chloride and sodium bromide in DES5 at different temperatures.

T/K	1:1	1:2	1:3
NaCl			
323.15	42.56	58.00	60.00
333.15	43.68	60.00	63.00
348.15	44.85	63.00	66.00
383.15	46.00	65.60	68.15
398.15	45.24	63.00	67.00
408.15	44.95	62.50	66.00
NaBr			
T/K	1:1	1:2	1:3
323.15	41.50	50.40	53.40
328.15	42.30	51.20	54.00
333.15	43.00	52.30	55.50
343.15	44.00	53.60	56.70
363.15	44.70	54.90	58.30
393.15	44.20	54.00	57.00
403.15	44.10	53.80	56.80

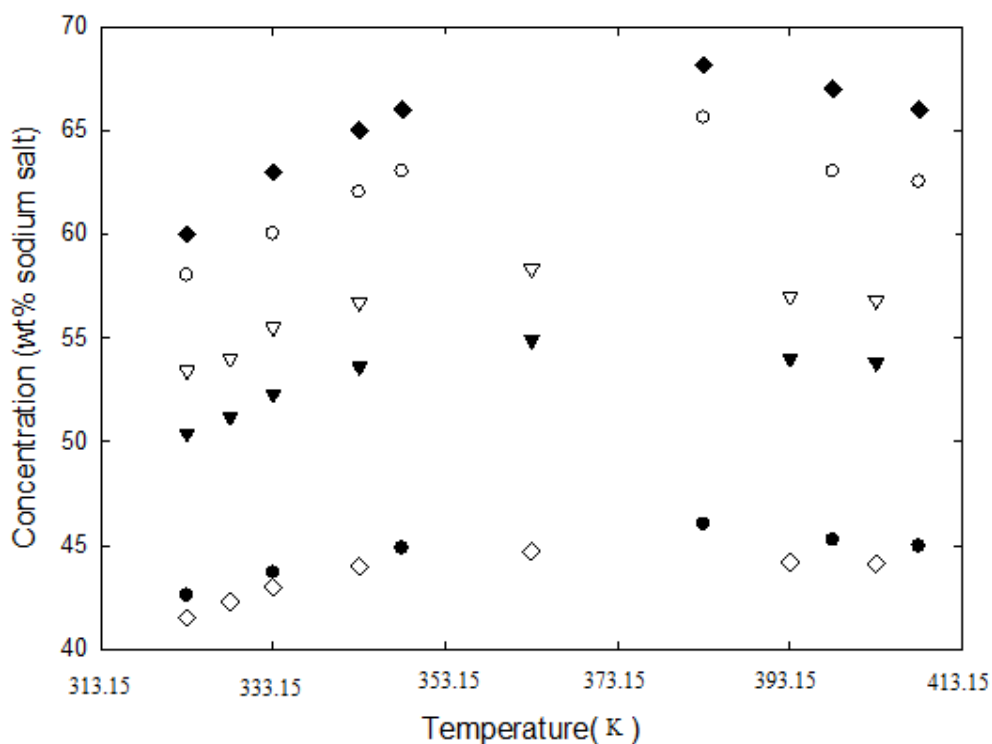


Figure 4.25 Solubility profiles of NaCl and NaBr in DES5 as a function of temperature. NaCl series, for salt:HBD ratios 1:1 (●), 1:2 (○), and 1:3 (◆). NaBr series, for salt:metal halide ratios 1:1 (◇), 1:2 (▼), and 1:3 (▽).

Again, the solubility of NaBr is less than that of NaCl under the same conditions for all ratios and temperatures. It is to be noted that the solubility of both NaCl and NaBr increased with the increase of metal halide molar ratio. On the other hand, the solubility increased with the increase of temperature up to a maximum temperature, and then it started to decrease slowly. Special analytical techniques are to be employed in order to understand this behaviour. Such techniques include the analysis by Fourier Transform Infrared (FTIR), Nuclear Magnetic Resonance (NMR) and X-ray Diffraction (XRD).

The high solubility in the DES synthesised from an ammonium salt and a metal halide instead of a typical HBD is very promising.

These significant finding led to the extension of the research into the utilization of another metal halide, namely tin chloride, and the investigation into the solubility of different sodium salts in the resulting DESs. DES6 in Table 4.1 is the result of mixing choline chloride with tin chloride. Following the procedure described earlier, different molar ratios were investigated. In Figure 4.26, the solubility of NaCl in DESs 5, 6 and 7 at 333.15 K is shown. From this, it can be inferred that the solubility of NaCl in tin chloride-based DES, which is 2.07 wt %, is much lower than that in zinc chloride-based DES. Both $ZnCl_2$ and $SnCl_2$ were used with choline chloride in the synthesis of DES7. NaCl solubility in this DES at 333.15 K is included in Figure 4.26. It is approximately 4.27 wt%, which is again not as good as DES5. Thus, further investigation of NaCl's solubility at different temperatures in this DES was not carried out.

Table 4.19. Comparison of solubility of sodium chloride in DESs 5, 6, and 7 at 333.15 K.

DES and ratio	Solubility
DES5, 1:1	43.68
DES5, 1:2	60.00
DES5, 1:3	63.00
DES6, 1:3	2.08
DES7, 1:1:1	4.27

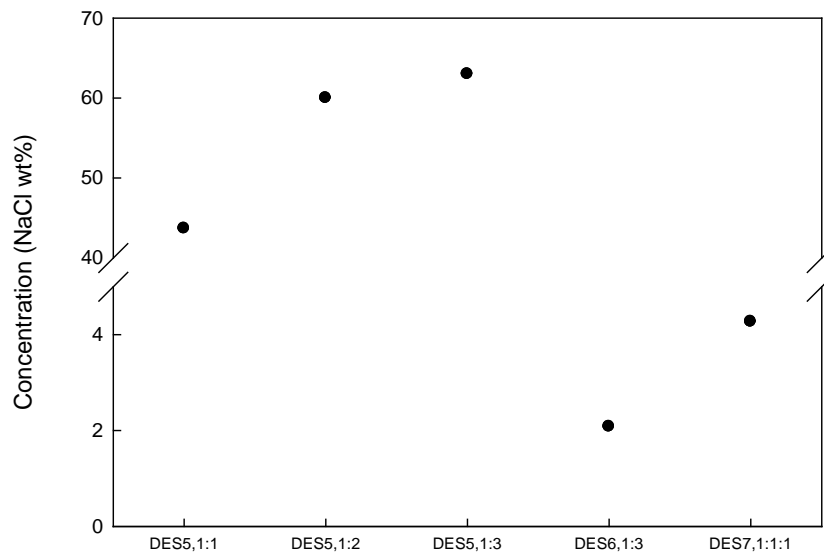


Figure 4.26: Comparison of solubility (Concentration) of NaCl in DES5, 6 and 7 at 333.15 K.

Due to the high NaCl solubility in DES5, another ammonium salt, i.e. N,N-diethylethanolammonium chloride, was chosen to synthesize a novel DES with zinc chloride. This new DES was abbreviated as DES8. As in DES5, NaCl solubility profiles with temperature showed two regions of increase and decrease, from 323.15 K to 358.15 K and from 358.15 K to 398.15 K, respectively, as illustrated in Figure 4.27. The solubility of NaCl in DES8 has a maximum value of approximately 80 wt%. The NaCl solubility in this DES increased when the metal halide's molar ratio in this DES increased from 1 to 3. However, the solubility decreased when the metal halide's molar ratio was further increased to 4. On the other hand, by approaching to the eutectic ratio in DES8, solubility of NaCl in DES increased to its maximum point.

Following the study on the effect of metal halide on the solubility of NaCl, zinc chloride was replaced by iron (II) chloride to give a new DES, i.e. DES9. Figure 4.28 shows the variation in NaCl solubility with temperature in DES9. A maximum solubility of 10.8 wt% at 368.15 K was observed. On the other hand, for DES8 (1:3) with the same salt, i.e. N,N-diethylethanolammonium chloride, but using zinc chloride

as the metal halide, 80 wt% of solubility was observed. Thus, no further investigation was carried out on other salt:metal halide ratios of DES9.

Table 4.20: Solubility of sodium chloride in DES8 at different temperatures.

T/K	1:1	1:2	1:3	1:4
323.15	67.00	76.00	77.70	50.42
333.15	67.60	76.70	78.40	50.80
348.15	68.10	77.20	79.30	51.10
358.15	68.80	77.25	80.00	51.20
363.15	68.20	76.80	79.30	51.10
383.15	67.96	74.97	78.60	51.00
403.15	67.30	74.30	77.90	50.87

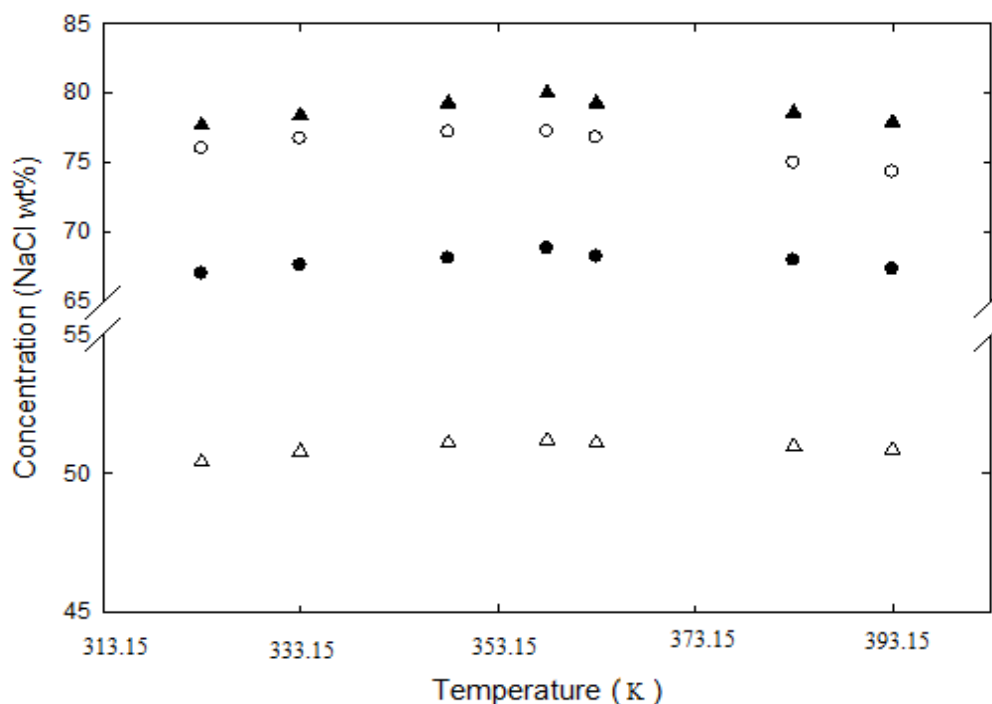


Figure 4.27 Solubility (Concentration) profiles of NaCl in DES8 as a function of temperature. NaCl series, for salt:metal halide ratios 1:1 (●), 1:2 (○), 1:3 (▲) and 1:4 (△).

Table 4.21. Solubility of sodium chloride in DES9 at different temperatures.

T(K)	1:3
317.15	3.57
328.15	4.72
350.15	10.21
368.15	10.40

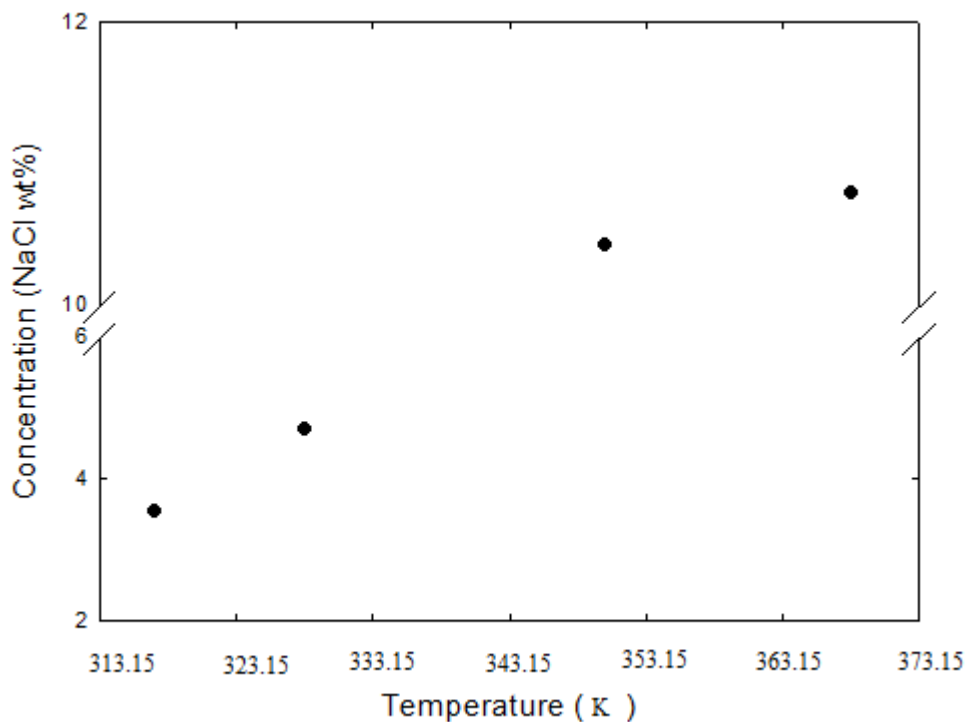


Figure 4.28 Solubility profile of NaCl in DES9 (salt:metal halide molar ratio 1:3) as a function of temperature.

4.2.1.1 Stability of Sodium Metal in DESs 1 – 9

As expected, sodium metal reacted with DESs containing ethylene glycol and glycerol as HBDs, i.e. DES1 to DES4. This is due to the presence of the hydroxyl group in these HBDs, and the fact that sodium metal in its pure state reacts instantly with oxygen, hydroxyl or halides (Banks, 1990). However, DESs synthesized from metal halides, i.e. DES5 to DES9, were stable and did not react with the sodium metal. Even though a halide group existed, it seems that the DES's structure held it strongly and prevented it from reacting. These results narrow down the search for a potential DES to conduct the task of sodium metal production.

4.2.1.2 Solubility Modelling

The basic equation for predicting the saturation mole fraction of a solid in a liquid is given by the general equation (Prausnitz et al., 1999, Sandler, 1999):

$$\ln(x_1\gamma_1) = -\frac{\Delta H^{fus}(T_m)}{RT} \left[1 - \frac{T}{T_m}\right] - \frac{1}{RT} \int_{T_m}^T \Delta C_p dT + \frac{1}{R} \int_{T_m}^T \frac{\Delta C_p}{T} dT \quad (4.5)$$

The subscript 1 denotes the solid solute, x_1 and γ_1 its molar composition (solubility at equilibrium) and activity coefficient in the mixture, respectively. T_m is the melting temperature of the solid. T is the temperature of the system at equilibrium. ΔH^{fus} and ΔC_p are the respective enthalpy and heat capacity changes from the solid to the liquid state of the solute.

Without introducing appreciable error, we can assume that ΔC_p is independent of temperature. Thus, equation 4.5 becomes:

$$\ln(x_1) = -\ln \gamma_1 - \left\{ \frac{\Delta H^{fus}(T_m)}{RT} \left[1 - \frac{T}{T_m} \right] + \frac{\Delta C_p}{RT} \left[1 - \frac{T_m}{T} + \ln \left(\frac{T_m}{T} \right) \right] \right\} \quad (4.6)$$

This equation can be used based on the assumption of simple eutectic mixtures with complete miscibility in the liquid and immiscibility in the solid phases. However, due to the lack of suitable data representing the difference in heat capacity (ΔC_p) between the solute in the two states, the simplified version of the solubility without the ΔC_p term was applied:

$$\ln x_1 = -\ln \gamma_1 - \left\{ \frac{\Delta H^{fus}(T_r)}{RT} \left[1 - \frac{T}{T_r} \right] \right\} \quad (4.7)$$

where T_r is reduction

The expected error resulting from neglecting ΔC_p usually depends on the compound under consideration. For conventional molecular compounds, the error does not exceed 2%.

If the liquid mixture is ideal, $\gamma_1 = 1$ and the solubility can be computed from the thermodynamic data (ΔH^{fus} and ΔC_p) for the solid species near the melting point. For non-ideal solutions, γ_1 must be estimated from either experimental data or liquid solution models, such as NRTL or UNIFAC model.

The latent heat of fusion of pure sodium chloride and its melting temperature are $\Delta H^{fus} = 28.3$ kJ/mol and $T_m = 1073.95$ K, respectively (Yamada et al, 1993).

The Non-Random Two Liquid (NRTL) model (Renon and Prausnitz, 1968) was used to calculate the activity coefficient at equilibrium. This model has three parameters, τ_{ij} , τ_{ji} and α_{ij} , for each pair of components in the multi-component mixture.

The model development was achieved by utilizing the Simulis[®] thermodynamics environment which is a thermo-physical properties calculation server, provided by ProSim (www.prosim.net, 2013). The deep eutectic solvent was considered as a pseudo component. In the present work, we proposed the hypothesis that $\tau_{ij} = \tau_{ji}$ and the non-randomness parameter referred to as α_{ij} was taken equal to 0.20, a commonly used value. The binary interaction parameters τ_{ij} were estimated from the N experimental data points at each temperature for NaCl with DES2, DES3, DES4 and DES5, respectively. An iterative procedure was used for each temperature by minimizing the squared relative error (criterion) between the calculated and the experimental solubilities:

$$Criterion = \frac{1}{N} \sum_N \left(\frac{x_1^{exp} - x_1^{cal}}{x_1^{exp}} \right)^2 \quad (4.8)$$

Linear temperature dependence was obtained for the binary interaction parameters expressed by the following correlation:

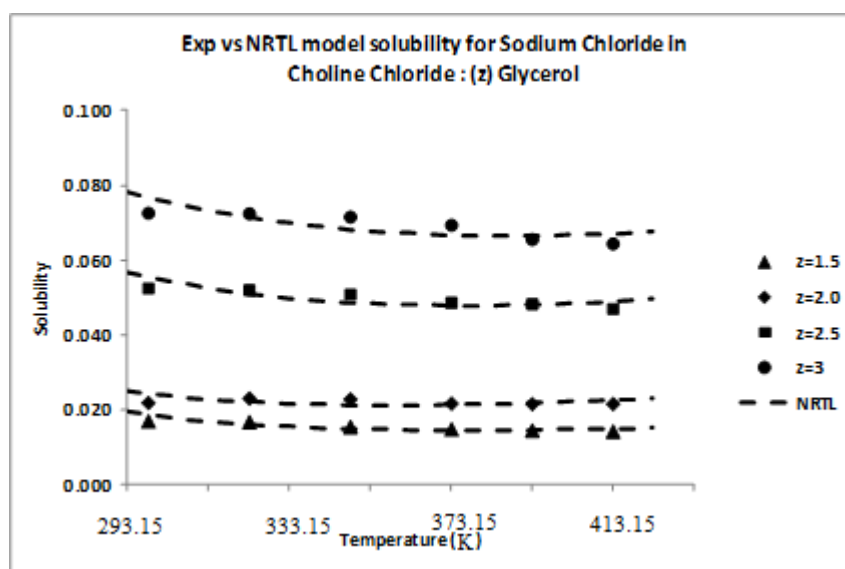
$$\tau_{ij} = \tau_{ij0} + \tau_{ijT} \cdot (T - 273.15) \quad T/K \quad (4.9)$$

The optimized parameters τ_{ij0} and τ_{ijT} for each DES and the different molar ratios are listed in Table 4.22. A comparison of the calculated values from the model with experimental data is presented in Figure 4.29 for NaCl solubility in DES2, DES3, DES4 and DES5. The calculated solubilities by the model show a good agreement with experimental measured solubilities.

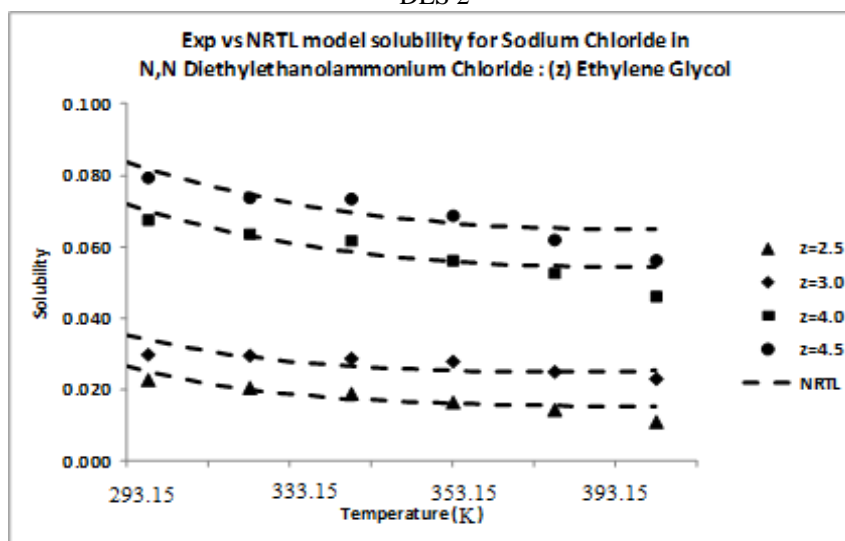
It must be noted that the modeling procedure has been tested and validated for NaCl with a number of DESs, but it could be easily applied to fit NaBr and Na₂CO₃ solubilities with other DESs, provided that the number of experimental data is representative.

Table 4.22: NRTL binary interaction parameters between NaCl and DES2 to DES5 for different molar ratios ($i \equiv \text{NaCl}$ and $j \equiv \text{DES}$).

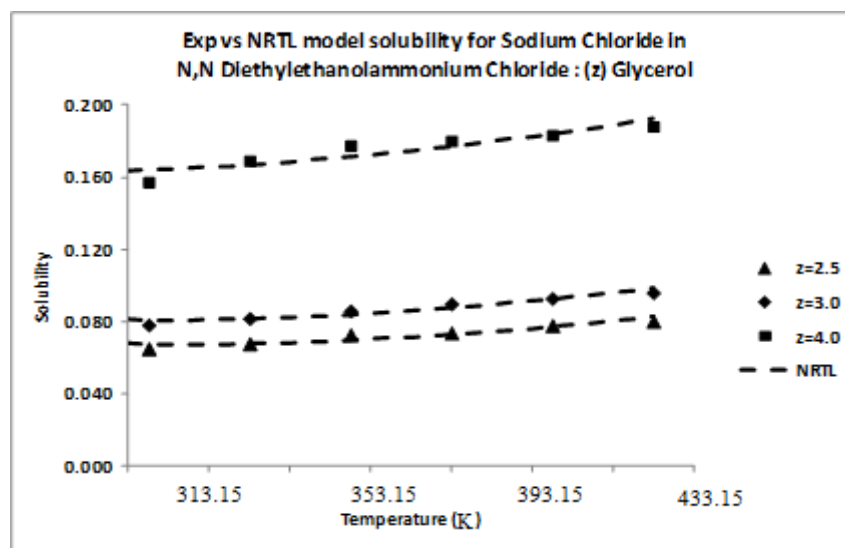
τ_{ij0}	τ_{ijT}	τ_{ij0}	τ_{ijT}	τ_{ij0}	τ_{ijT}	τ_{ij0}	τ_{ijT}
DES2							
1:1.5		1:2		1:2.5		1:3	
-623.9	3.194	-647.3	2.767	-764.9	2.446	-829.6	2.368
DES3							
1:2.5		1:3		1:4		1:4.5	
-668.5	3.472	-698.9	2.987	-816.2	2.636	-849.5	2.569
DES4							
1:2.5		1:3		1:4		-	
-785.3	1.709	-822.7	1.601	-1063.6	1.267	-	-
DES5							
1:1		1:2		1:3		-	
-3718.9	-4.531	-4542.7	-10.282	-4847.4	-12.939	-	-



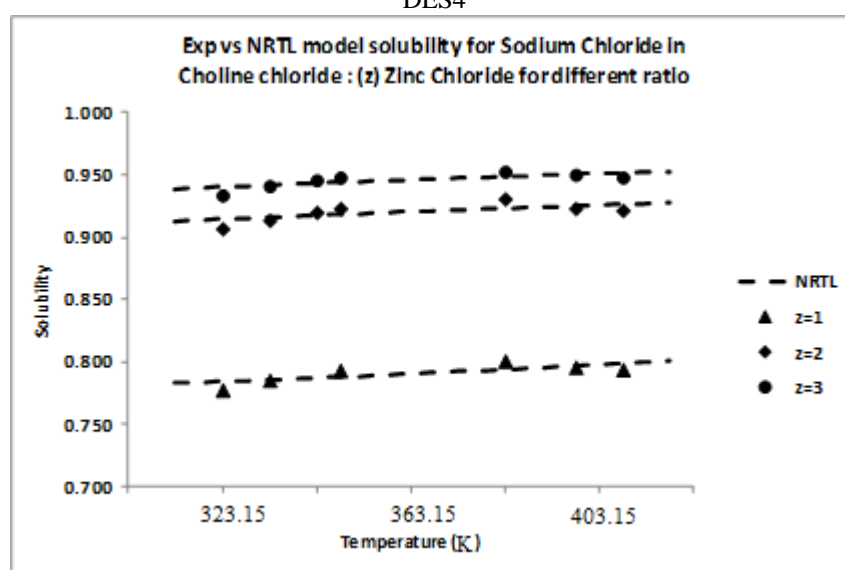
DES 2



DES3



DES4



DES5

Figure 4.29 Calculated (NRTL) vs experimental solubilities mole fraction, of sodium chloride in DES2, DES3, DES4, and DES5 for different ratios and at different temperatures. z is the ratio of the HBD in the DES considering that the salt's ratio is always 1.

4.2.2 Solubility of Sodium Chloride in Phosphonium-Based DESs

Phosphonium-based DESs were synthesized and the solubility of sodium chloride (NaCl) was measured experimentally in these DESs at different temperatures, i.e. 293.15 K to 433.15 K. The phosphonium DESs are shown in Table 4.1 as DESs 10 – 16.

The results are classified according to the solvent structure, temperature, and the solution stability. Figures 4.30 to 4.36 show plots for the measured NaCl solubility in

the mentioned DESs at different temperatures. As a large amount of experimental results have been generated, the results for each DES are shown in individual figures.

Figure 4.30 shows the solubility of NaCl in DES10. The solubility of NaCl increases as the salt:HBD ratio for the DES increases. However, the increase in solubility when the mole ratio increases from 1:3 to 1:4 is much less than that when the mole ratio increases from 1:4 to 1:5. This is because a ratio of 1:5 is close to the DES eutectic point. For all salt:HBD mole ratios, the solubility of NaCl increased with temperature. The maximum NaCl solubility was approximately 0.47 wt% at a salt:HBD ratio of 1:5.

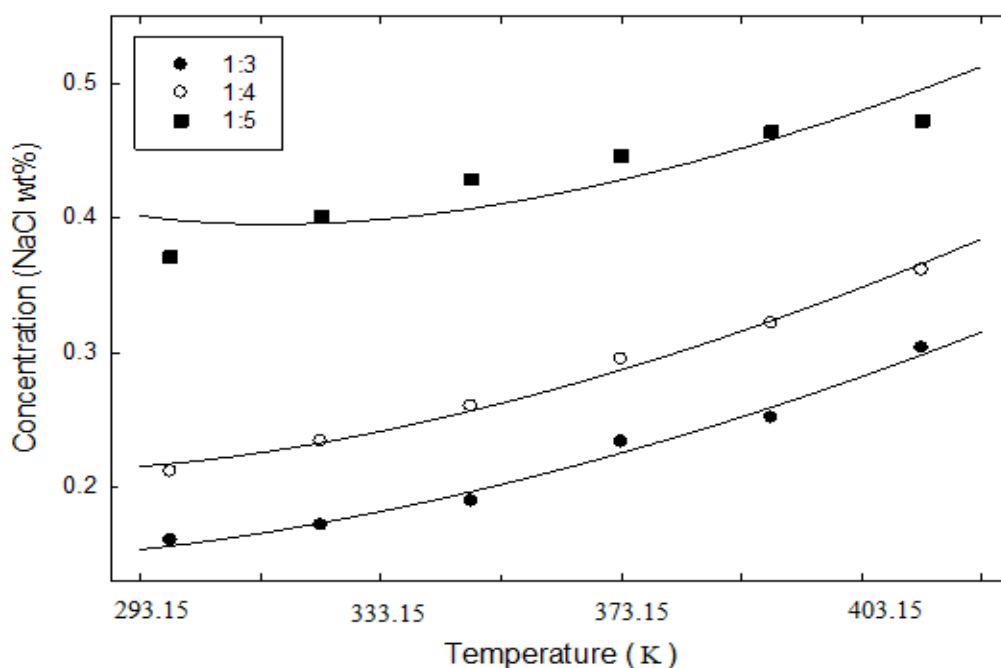


Figure 4.30 Solubility profiles of NaCl in DES10 as a function of temperature (passed lines are based on NRTL calculations).

For DES11, the solubility of NaCl increases with a smooth gradient from ambient temperature to 353.15 K, where it reaches 0.2 at a salt:HBD molar ratio of 1:4, as shown in Figure 4.31. The solubility of NaCl increased with the increase in salt:HBD molar ratio. However, DES10 exhibited a larger molar ratio effect. DES10 and DES11 produced low NaCl solvation capacities, i.e. less than the capacities required to commercially produce sodium metal.

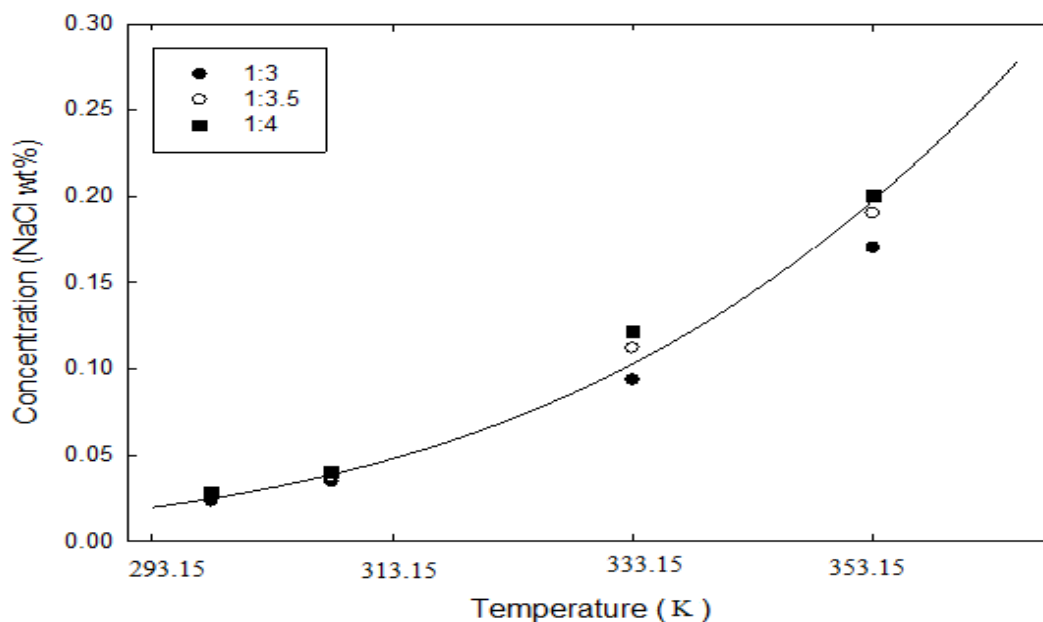


Figure 4.31 Solubility profiles of NaCl in DES11 as a function of temperature (passed line is based on NRTL calculations).

The low NaCl solubility in these DESs could be attributed to the low electronegativity of the DESs due to the use of neutral HBD as well as the presence of alkyl groups in the neutral molecules of HBDs which negatively affected the solubility term. This prompted the investigation of NaCl solubility in other types of DESs.

Using metal halides as complexing agents instead of HBDs produces a unique type of DES. Although metal halides cannot share hydrogen, they form a complex with phosphonium salts and yield a different type of DES. This is the first time ever that this type of DES was synthesised. Abbott et al. (2004b) produced a similar type of DES by using ammonium salts instead of phosphonium salts. Zinc chloride ($ZnCl_2$), zinc bromide ($ZnBr_2$), and iron(III) chloride ($FeCl_3$) were used to synthesize DES12, DES13, DES14, DES15, and DES16.

The solubility of NaCl in DES12 under different temperatures and salt:metal halide ratios is shown in Figure 4.32. The solubility of NaCl in DES12 is higher than in DES10 and DES11, reaching a maximum of 88.5 wt% at 383.15 K. The solubility increased with temperature, reaching a maximum at 383.15 K. Figure 4.31 shows that

the solubility of NaCl increases with the amount of metal halide used in the DES. This confirms the observations from DES10 and DES11. A DES composed of a metal halide exhibits a higher melting temperature than a DES composed of ethylene glycol and glycerine. Thus, the solubility of NaCl was measured in DES12 starting from 82 °C onwards, as shown in Figure 4.31. However, this does not affect the use of these DESs in the production of sodium metal because the minimal process temperature is approximately 120 °C.

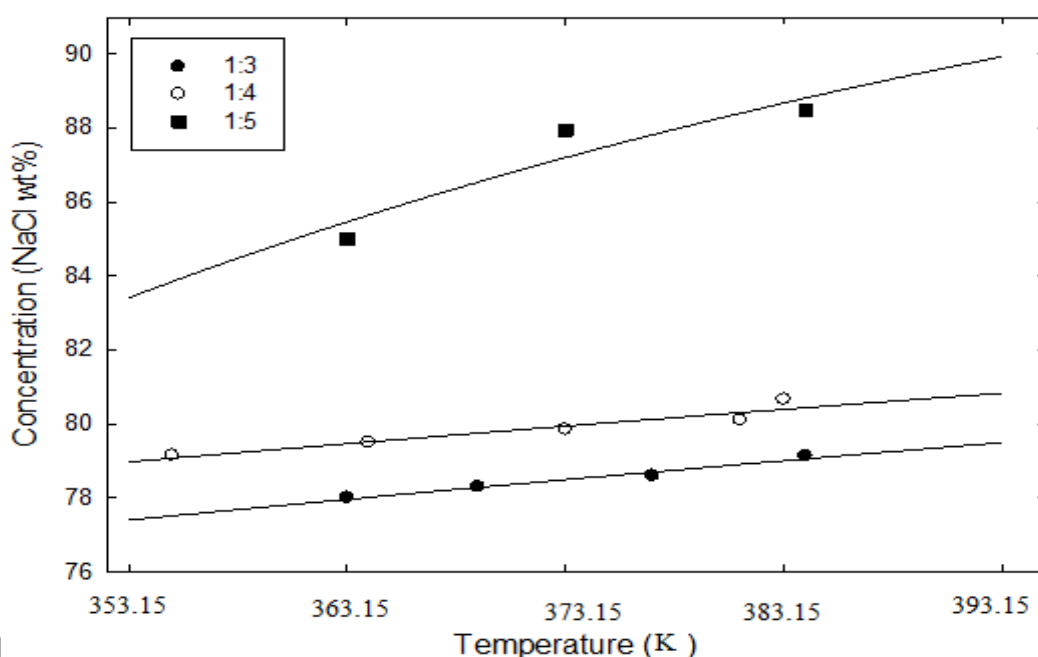


Figure 4.32 Solubility profiles of NaCl in DES12 as a function of temperature (passed lines are based on NRTL calculations).

In order to evaluate the effect of the halide ion in the molecule of metal halide on the solubility on NaCl in DESs, $ZnBr_2$ was used instead of $ZnCl_2$ to synthesize DES13. Figure 4.33 shows that the solubility of NaCl in DES13 increases uniformly with temperature and with the $ZnBr_2$ molar ratio. When the metal halide ratio in the DES increase from 2 to 3, the solubility of NaCl increased by approximately 5 wt% at the same temperature. Increasing this ratio to 1:4 increased the solubility by approximately 1 wt% at the same temperature. The maximal solubility for NaCl in this DES, i.e. 75.4

wt%, occurred at a salt:metal halide ratio of 1:4 and a temperature of 393.15 K. At the same temperature and molar ratio, DES12 has a solubility of 88.8 wt%. This shows that the type of halide ion affects the solubility of NaCl in DESs.

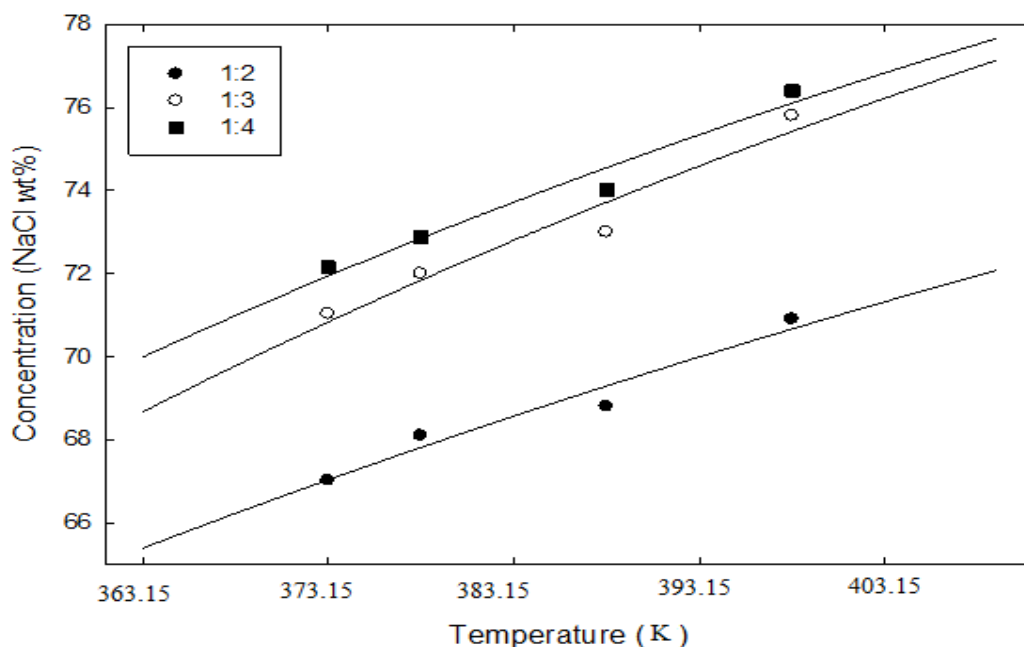


Figure 4.33 Solubility profiles of NaCl in DES13 as a function of temperature (passed lines are based on NRTL calculations).

To investigate the effect of the type of metal in the metal halide on NaCl solubility, FeCl_3 and ethyltriphenylphosphonium bromide were used to synthesize DES14. Figure 4.34 shows the variation of NaCl solubility in DES14 as a function of temperature and DES composition. The solubility of NaCl increases sharply from 6.2 wt% at 90 °C to 66.6 wt% at 423.15 K. The solubility increases also with the increase of the metal halide molar ratio in the DES. The maximal NaCl solubility in DES14 at 393.15 K was approximately 68 wt%. This value is lower than that achieved by DES12 under the same temperature and metal halide molar ratio.

Lastly, an examination for the effect of the salt used in the DES on NaCl solubility was carried out. Ethyltriphenylphosphonium bromide was replaced by tetrabutylphosphonium bromide. The salt was combined with ZnCl_2 and FeCl_3 to

synthesize DES15 and DES16, respectively. Figures 4.35 and 4.36 show the solubility profiles of NaCl as a function of temperature in DES15 and DES16, respectively. As expected, NaCl solubility increases with temperature and the metal halide ratio. DES15 and DES16 have lower NaCl solubilities than DES12 and DES14 at the same temperature. DES15 has a higher NaCl solubility than DES16 under the same conditions. This is similar to the findings for DES12 and DES14.

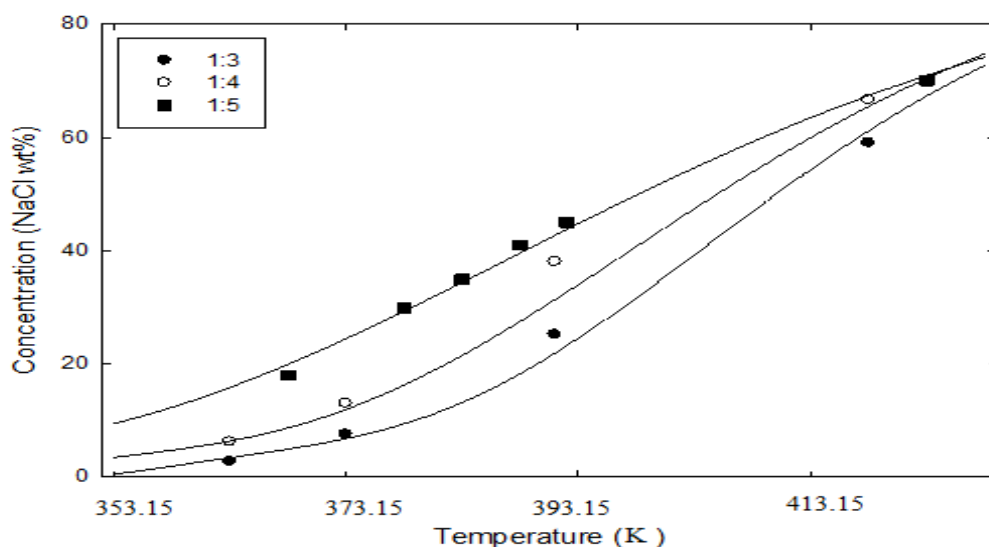


Figure 4.34 Solubility profiles of NaCl in DES14 as a function of temperature (passed lines are based on NRTL calculations).

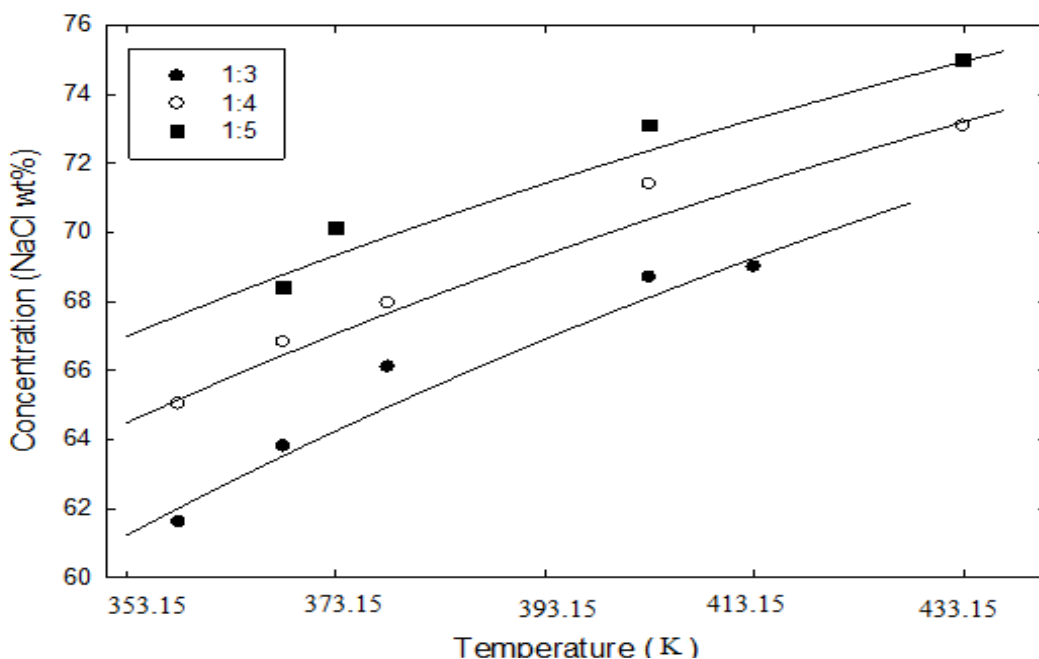


Figure 4.35 Solubility profiles of NaCl in DES15 as a function of temperature (passed lines are based on NRTL calculations).

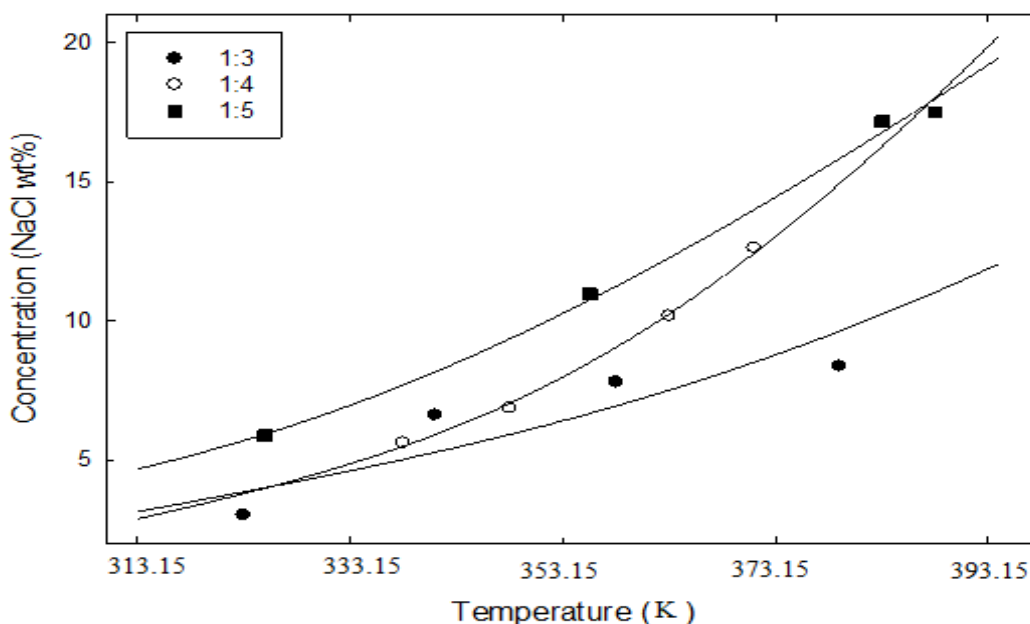


Figure 4.36 Solubility profiles of NaCl in DES16 as a function of temperature (passed lines are based on NRTL calculations).

4.2.2.1 Stability of Sodium Metal in DESs 10 – 16

Sodium metal reacts with DESs containing ethylene glycol and glycerol as HBDs, i.e. DES10 and DES11. This is expected to occur because of the hydroxide group in the HBDs and because sodium metal reacts instantly with oxygen, hydroxides, halides, alcohols, and other compounds (Banks, 1990). Sodium metal was stable in DESs containing metal halides, i.e. DES12, DES13, DES14, DES15 and DES16. This means that a reaction does not occur between the pure sodium metal and the DESs, despite the presence of a halide group. This is attributed to the strong interaction between the halide group and the salt, preventing it from reacting with the sodium metal.

4.2.2.2 Solubility Modelling

The procedure described in Subsection 4.2.1.2 is followed here for the application of the non-random two-liquid (NRTL) model to calculate the solubilities of NaCl in DESs 10 – 17.

Table 4.23 shows the optimized parameters τ_{ij0} and τ_{ijT} for each DES and different molar ratios. For DES11, the unique interaction parameters, $\tau_{ij0} = 269.15$ and $\tau_{ijT} = 2.076$, were regressed to fit the solubilities obtained in the DES regardless of the HBD molar ratio. The calculated solubilities are plotted in Figures 4.30 – 4.36 as curves. Excellent agreement between the experimental and calculated solubilities are obtained.

DES10 and DES15 exhibited a relationship between the binary interaction parameters and the HBD or metal halide mole fraction in the DES. The remaining DESs did not exhibit any clear trends.

Tables 4.24 – 4.30 show comparisons between the calculated solubilities by the NRTL model and the experimental values with the percentage differences between the values. The percentages were lower than 10% in most of the cases, indicating high agreement between the calculated and experimental solubilities, except for the case of DES16 where the percentages reached a maximum of 27.7% for 1:3 molar ratio.

Table 4.23: NRTL binary interaction parameters between NaCl and DES10, DES12 – DES16 for different molar ratios ($i \equiv \text{DES}$ and $j \equiv \text{NaCl}$).

DES10	τ_{ij0}	τ_{ijT}	DES14	τ_{ij0}	τ_{ijT}
1:3	-423.3	2.964	1:3	6286.7	-76.059
1:4	-450.8	3.017	1:4	5925.4	-75.935
1:5	-517.6	3.147	1:5	3083.2	-57.074
DES12	τ_{ij0}	τ_{ijT}	DES15	τ_{ij0}	τ_{ijT}
1:2	-4504.1	-12.378	1:3	-3431.3	-12.471
1:3	-4523.9	-12.075	1:4	-3565.2	-11.996
1:4	-3371.6	-30.060	1:5	-3649.9	-11.970
DES13	τ_{ij0}	τ_{ijT}	DES16	τ_{ij0}	τ_{ijT}
1:2	-3677.1	-16.176	1:3	-576.1	-6.044
1:3	-3411.5	-20.541	1:4	147.1	-16.677
1:4	-3530.7	-19.687	1:5	-202.6	-14.970

Table 4.24: Comparison of NRTL and experimental solubilities of NaCl in DES10 at different molar ratios.

T/K	1:3			1:4			1:5		
	exp.	cal.	Differ.(%)	exp.	cal.	Differ.(%)	exp.	cal.	Differ.(%)
298.15	0.160	0.156	2.56	0.212	0.217	2.74	0.371	0.399	7.55
323.15	0.172	0.173	0.99	0.234	0.233	0.47	0.402	0.396	1.37
348.15	0.190	0.197	3.69	0.260	0.257	1.27	0.429	0.407	5.08
473.15	0.234	0.225	3.55	0.295	0.287	2.61	0.446	0.428	3.95
498.15	0.252	0.259	3.14	0.322	0.324	0.56	0.464	0.458	1.19
523.15	0.303	0.298	1.65	0.361	0.366	1.36	0.472	0.496	4.95

Table 4.25: Comparison of NRTL and experimental solubilities of NaCl in DES11 at 1:3.5 molar ratio.

T/K	1:3.5		
	exp.	cal.	Differ.(%)
298.15	0.026	0.025	3.846
308.15	0.037	0.039	3.876
333.15	0.112	0.103	8.438
353.15	0.190	0.198	3.991

Table 4.26: Comparison of NRTL and experimental solubilities of NaCl in DES12 at different molar ratios.

1:2				1:3				1:4			
T(K)	exp.	cal.	Differ.(%)	T(K)	exp.	cal.	Differ.(%)	T(K)	exp.	cal.	Differ.(%)
363.15	78	77.97	0.043	355.15	79.15	79.079	0.089	363.15	85	85.47	0.551
369.15	78.3	78.29	0.130	364.15	79.5	79.52	0.025	373.15	87.95	87.21	0.236
377.15	78.6	78.71	0.136	373.15	79.85	79.946	0.120	384.15	88.5	88.82	0.355
384.15	79.13	79.06	0.087	381.15	80.1	80.311	0.264				
				383.15	80.66	80.401	0.321				

Table 4.27: Comparison of NRTL and experimental solubilities of NaCl in DES13 at different molar ratios.

1:3				1:4			1:5		
T(°C)	exp.	cal.	Differ.(%)	exp.	cal.	Differ.(%)	exp.	cal.	Differ.(%)
373.15	67.02	67.04	0.030	71.03	70.84	0.267	72.16	71.94	0.305
378.15	68.1	67.82	0.411	72	71.84	0.222	72.88	72.85	0.041
388.15	68.8	69.3	0.727	73	73.72	0.986	74.02	74.56	0.730
398.15	70.9	70.67	0.324	75.8	75.43	0.488	76.4	76.11	0.380

Table 4.28: Comparison of NRTL and experimental solubilities of NaCl in DES14 at different molar ratios.

1:3				1:4				1:5			
T(°C)	exp.	cal.	Differ.(%)	T(°C)	exp.	cal.	Differ.(%)	T(°C)	exp.	cal.	Differ.(%)
363.15	2.7	3.4	25.926	363.15	6.21	6.36	2.415	368.15	18	19.9	10.556
373.15	7.5	6.78	9.600	373.15	13	11.95	8.077	378.15	29.88	29.3	1.941
391.15	25.1	21.91	12.709	398.15	38	40.72	7.158	383.15	34.9	34.39	1.461
418.15	59.01	61.17	3.660	418.15	66.6	65.48	1.682	388.15	41	39.58	3.463
								392.15	45	43.73	2.822
								423.15	70	70.95	1.357

Table 4.29: Comparison of NRTL and experimental solubilities of NaCl in DES15 at different molar ratios.

1:3				1:4				1:5			
T(°C)	exp.	cal.	Differ.(%)	T(°C)	exp.	cal.	Differ.(%)	T(°C)	exp.	cal.	Differ.(%)
358.15	61.6	62.3	1.136	358.15	65.03	65.47	0.677	368.15	68.4	69.09	1.009
368.15	63.8	63.81	0.016	368.15	66.82	66.75	0.105	373.15	70.12	69.65	0.670
378.15	66.1	65.22	1.331	378.15	67.95	67.96	0.015	403.15	73.1	72.67	0.588
403.15	68.7	68.38	0.466	403.15	71.4	70.67	1.022	433.15	75	75.23	0.307
413.15	69	69.52	0.754	433.15	73.08	73.47	0.534				

Table 4.30: Comparison of NRTL and experimental solubilities of NaCl in DES16 at different molar ratios.

1:3				1:4				1:5			
T(°C)	exp.	cal.	Differ.(%)	T(°C)	exp.	cal.	Differ.(%)	T(°C)	exp.	cal.	Differ.(%)
323.15	3.03	3.87	27.723	338.15	5.61	5.51	1.783	325.15	5.88	5.95	1.190
341.15	6.61	5.29	19.970	348.15	6.88	7.05	2.471	355.65	10.96	10.76	1.825
358.15	7.8	6.95	10.897	363.15	10.18	10.26	0.786	383.15	17.16	16.78	2.214
379.15	8.37	9.64	15.173	371.15	12.62	12.45	1.347	388.15	17.5	17.98	2.743
				377.15	17.25	14.29	17.159				

4.2.3 Solubility of Sodium Chloride in Different ILs

Table 4.2 summarized the names and chemical structures of the sixteen ILs investigated. Experimental solubilities of NaCl in these ILs are listed in Table 4.31 and illustrated in Figures 4.37 to 4.40.

Table 4.31: Experimental solubilities of NaCl in studied ILs.

[emim][EtSO ₄]		[emim][MeSO ₃]		[emim][DMP]		[edmi][Cl]	
<i>T</i> / K	<i>s</i> / wt%	<i>T</i> / K	<i>s</i> / wt%	<i>T</i> / K	<i>s</i> / wt%	<i>T</i> / K	<i>s</i> / wt%
298.15	0.56	298.15	0.33	303.15	0.67	378.15	0.2
333.15	0.74	333.15	0.52	323.15	2.55	389.15	0.22
358.15	1.11	358.15	0.71	342.15	2.97	398.15	0.26
378.15	1.27	378.15	1.31	359.15	3.66	408.15	0.33
383.15	1.30	383.15	2.18	368.15	3.73		
		298.15	2.34	378.15	4.67		
				388.15	6.28		
				398.15	8.96		
[bmim][Cl]		[bmim][DCA]		[bmim][TfO]		[bmim][BF ₄]	
<i>T</i> / K	<i>s</i> / wt%	<i>T</i> / K	<i>s</i> / wt%	<i>T</i> / K	<i>s</i> / wt%	<i>T</i> / K	<i>s</i> / wt%
348.15	0.07	303.15	0.37	298.15	0.02	303.15	0.05
383.15	0.10	333.15	0.38	333.15	0.03	333.15	0.07
396.15	0.14	363.15	0.40	358.15	0.04	363.15	0.09
408.15	0.16	393.15	0.45	378.15	0.05	393.15	0.11
423.15	0.22	423.15	0.50	383.15	0.05	423.15	0.14
[bmim][Tf ₂ N]		[C ₈ mim][Cl]		[bmp][DCA]		[bmp][TfA]	
<i>T</i> / K	<i>s</i> / wt%	<i>T</i> / K	<i>s</i> / wt%	<i>T</i> / K	<i>s</i> / wt%	<i>T</i> / K	<i>s</i> / wt%
298.15	0.02	363.15	1.28	298.15	0.22	303.15	0.59
323.15	0.02	373.15	1.96	318.15	0.26	333.15	0.62
353.15	0.03	383.15	2.63	348.15	0.30	363.15	0.68
385.15	0.03	393.15	3.38	393.15	0.39	393.15	0.71
390.15	0.03	403.15	3.94			423.15	0.74
403.15	0.05	363.15					
[bmpyr][CF ₃ SO ₃]		[bmpy][DCA]		[bmpy][MSO ₄]		[EtOHNMe ₃][Me ₂ PO ₄]	
<i>T</i> / K	<i>s</i> / wt%	<i>T</i> / K	<i>s</i> / wt%	<i>T</i> / K	<i>s</i> / wt%	<i>T</i> / K	<i>s</i> / wt%
303.15	0.08	303.15	0.71	298.15	0.27	298.15	1.21
333.15	0.08	333.15	0.74	318.15	0.35	313.15	1.70
363.15	0.08	363.15	0.81	345.35	0.42	333.15	1.81
393.15	0.09	393.15	0.86	373.15	0.53	348.15	2.06
423.15	0.09	423.15	0.89			363.15	2.37
						379.15	3.34

Figure 4.37 shows the results of NaCl solubility in several imidazolium-based ILs at different temperatures. The solubility of NaCl in the ILs increased with temperature, and

different ILs showed different solubility profile trends. The IL structure affected these trends. For instance, IL2, IL3, and IL10 exhibited a sharp increase in NaCl solubility with increasing temperature whereas IL4, IL5, IL8, and IL9 exhibited the lowest NaCl solubilities of the imidazolium ILs. The NaCl solubility in these ILs did not exceed 0.05 wt% at all temperatures. One of the factors that affect NaCl solubility is the type of anion of the IL. IL3 which composes a dimethylphosphate anion provided the highest NaCl solubility of 8.96 wt% at 398.15 K. These findings confirm the data available in the literature (AlNashef, 2001). AlNashef (2001) examined the solubility of NaCl in dimethylimidazolium dimethylphosphate, concluding that its solubility increases with temperature, similar to the results illustrated in Figure 4.37.

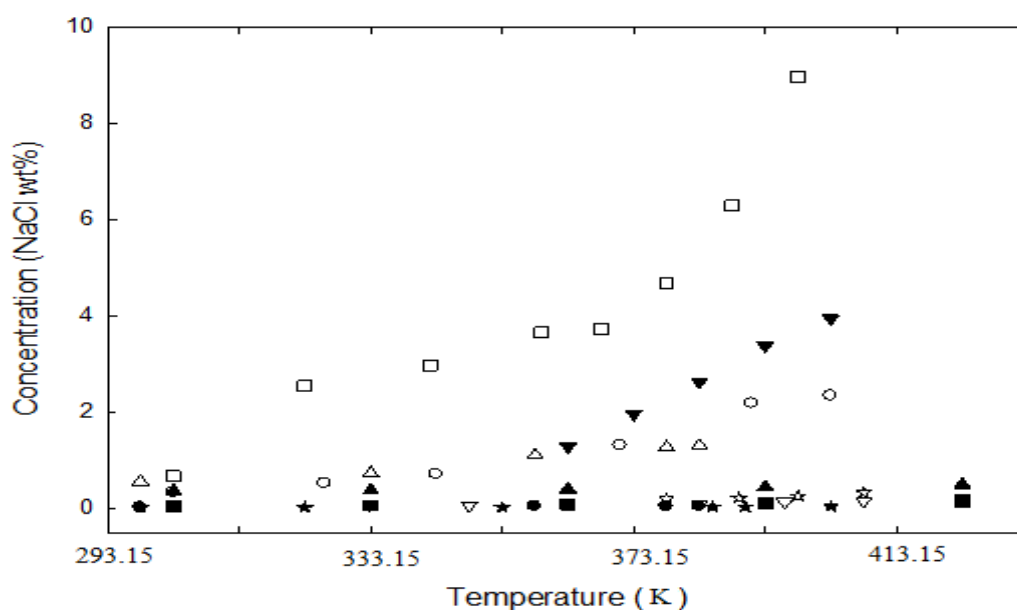


Figure 4.37 Experimental solubility (Concentration) of NaCl in imidazolium-based ILs. (Δ) IL1, (o) IL2, (\square) IL3, (\star) IL4, (∇) IL5, (\blacktriangle) IL6, (\bullet) IL7, (\blacksquare) IL8, (\star) IL9, (\blacktriangledown) IL10.

The results from this study and from AlNashef show that the dimethylphosphate anion significantly increases the solubility of NaCl in ILs. Substituents on the imidazolium cation can also affect the solubility of NaCl in ILs. This is reflected by IL5 and IL10. The IL5 cation has a butyl group and produces a NaCl solubility of 0.098 wt% at 110 °C. IL10 has an octyl group instead of the butyl group and produces a NaCl

solubility of 2.629 wt% at 383.15 K. It can be explained by the strength of C/H bond in IL10 which is more than in IL5 (Yu et al., 2008); Therefore, it significantly affects the Cl⁻ ion from NaCl. The mutual electro negativity item in IL10 is more obvious than in IL5.

The effect of changing the anion on NaCl solubility in imidazolium-based ILs was also investigated. The ethylsulfate anion in IL1 was replaced by a methanesulfonate anion in IL2 and a dimethylphosphate anion in IL3. The NaCl solubilities in these ILs were compared at 358.15 K. The solubility increased from approximately 1.102 wt% in IL1 and 0.982 wt% in IL2 to 3.66 wt% in IL3. Figure 4.30 shows that imidazolium-based ILs with a 1-butyl-3-methyl group in the cation resulted in low solubility, i.e. less than 0.5 wt%.

Figure 4.38 shows an assessment of NaCl solubility in pyrrolidinium-based ILs. It shows that solubility is directly proportional to temperature.

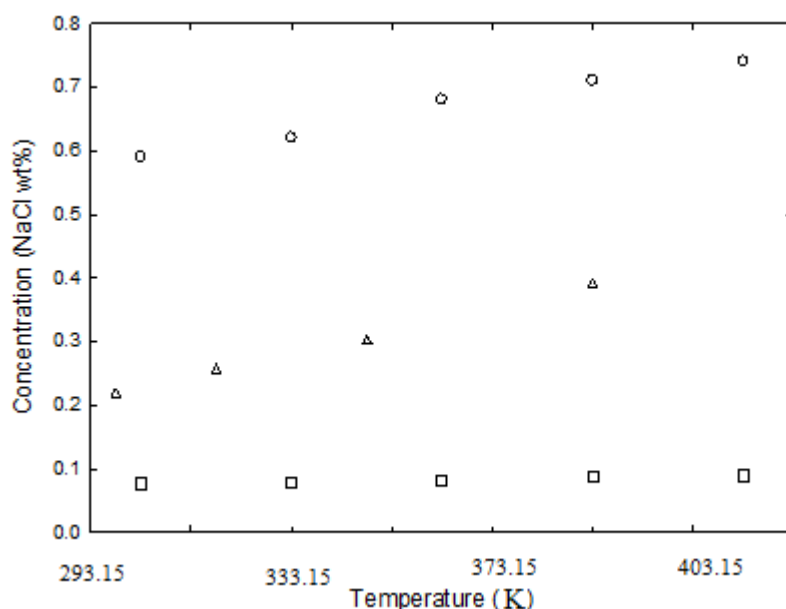


Figure 4.38 Experimental solubility (Concentration) of NaCl in pyrrolidinium-based ILs. (Δ) IL11, (o) IL12, (\square) IL13.

To determine the effects of anions on NaCl solubility, the dicyanamide anion in IL11 was replaced with a trifluoroacetate and trifluoromethanesulfonate anions in IL12

and IL13, respectively. At 393.15 K, IL12 had the highest NaCl solubility of 0.71 wt%. Under the same temperature, IL11 and IL13 produced lower NaCl solubilities of approximately 0.4 wt% and 0.09 wt%, respectively. This shows that the trifluoroacetate anion is more attracted to sodium ions (Na^+) than the dicyanamide or trifluoromethanesulfonate anions.

Figure 4.39 shows NaCl solubility plots for IL14 and IL15, which are based on pyridinium cations. The solubilities increased sharply with temperature.

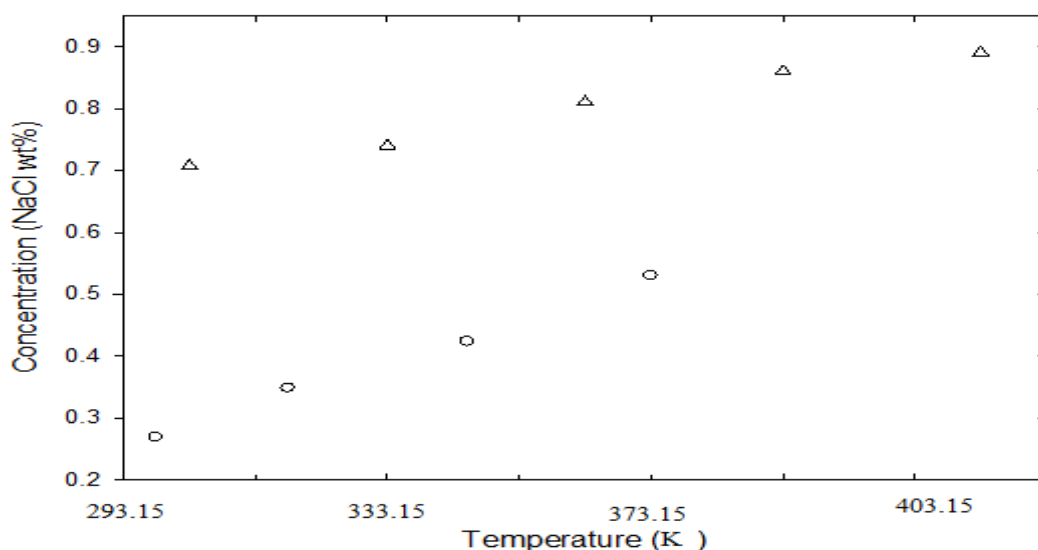


Figure 4.39 Experimental solubility (Concentration) of NaCl in pyridinium-based ILs. (Δ) IL14, (o) IL15.

IL6, IL11 and IL14 contained dicyanamide anions. Comparing NaCl solubilities in these ILs allows the comparison of the effects of the parent groups on NaCl solubility. To compare the changes in NaCl solubility with a fixed anion and a variable cation, NaCl solubility in IL6, IL11, and IL14 were compared at similar temperatures. IL6 and IL11 produced NaCl solubilities of approximately 0.448 wt% and 0.389 wt% at 393.15 K, respectively. IL14 produced the highest solubility of 0.86 wt%. This shows that a N-butyl-3-methyl pyridinium cation exhibits more Na^+ affinity than the other cations.

Figure 4.40 shows the solubility of NaCl in IL16 as a function of temperature. NaCl solubility in this IL is approximately 3.34 wt% at 379.15 K. Comparing IL3 and IL16

which are both having the dimethylphosphate anion, it is noticed that NaCl solubility in IL3 is higher than that in IL16. However, the difference in solubility is not significant. This may be attributed to the difference in the cation. It can therefore be concluded that the presence of dimethylphosphate anion in the IL increases its ability to dissolve NaCl. It is to be noted that the highest NaCl solubility achieved was in IL3 which has the dimethylphosphate anion with imidazolium-based cation.

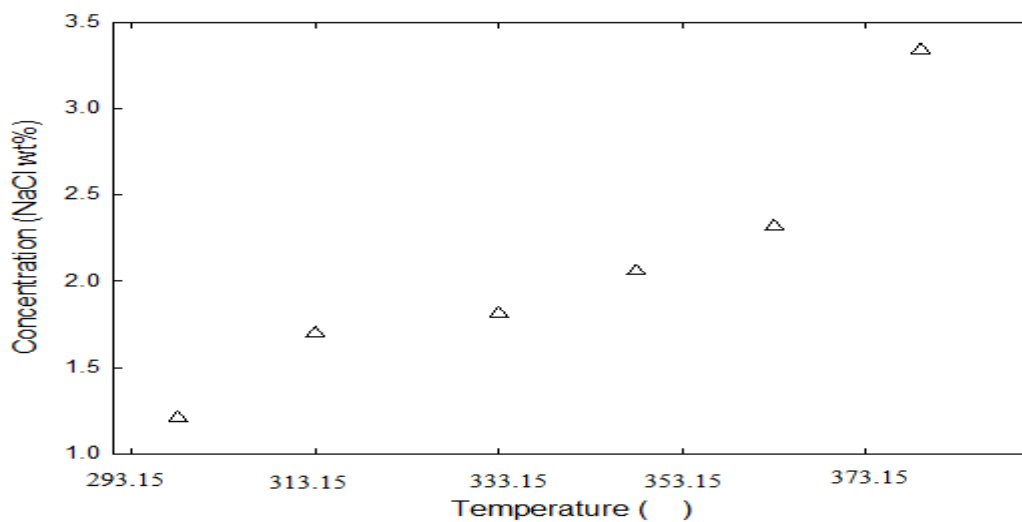


Figure 4.40 Experimental solubility of NaCl in IL16 (Δ).

4.2.3.1 Solubility Modelling

Solubility modelling in ILs is different from the one shown for DESs. Taking the same equation presented in Subsection 4.2.1.2, the basic equation for calculating the saturation mole fraction of a solid in a liquid is:

$$\ln(x_1\gamma_1) = -\frac{\Delta H^{fus}(T_m)}{RT} \left[1 - \frac{T}{T_m}\right] - \frac{1}{RT} \int_{T_m}^T \Delta C_P dT + \frac{1}{R} \int_{T_m}^T \frac{\Delta C_P}{T} dT \quad (4.5)$$

where subscript 1 is the solid solute; x_1 and γ_1 are its molar composition (solubility at equilibrium) and activity coefficient in the mixture, respectively. T_m is the melting point temperature; T is the temperature of the system at equilibrium; and ΔH^{fus} and ΔC_P are the enthalpy and heat capacity changes when the solute changes from a solid to a liquid state, respectively.

Two approximations were made without introducing appreciable error. The first assumption is that ΔC_p is independent of temperature. Therefore, Equation (4.5) is simplified to:

$$\ln(x_1\gamma_1) = - \left\{ \frac{\Delta H^{fus}(T_m)}{RT} \left[1 - \frac{T}{T_m} \right] + \frac{\Delta C_p}{RT} \left[1 - \frac{T_m}{T} + \ln \left(\frac{T_m}{T} \right) \right] \right\} \quad (4.10)$$

Because the melting temperature T_m at any pressure and the triple point temperature T_r are only slightly different for most solids, Equation (4.10) can be rewritten as Equation (4.11) below:

$$\ln x_1 = - \ln \gamma_1 - \left\{ \frac{\Delta H^{fus}(T_r)}{RT} \left[1 - \frac{T}{T_r} \right] + \frac{\Delta C_p}{RT} \left[1 - \frac{T_r}{T} + \ln \left(\frac{T_r}{T} \right) \right] \right\} \quad (4.11)$$

- If the liquid mixture is ideal, $\gamma_1 = 1$ and the solubility can be calculated by using the thermodynamic data, ΔH^{fus} and ΔC_p , for the solid species near the melting point.
- For non-ideal solutions, γ_1 must be estimated from either experimental data or liquid solution models, such as the UNIFAC model.

This equation may be used, assuming that the ILs exhibit full miscibility in the liquid phase and immiscibility in the solid phase. Due to the lack of appropriate data representing the difference in ΔC_p between the heat capacities of the solute in the solid and liquid states for systems containing ILs, especially in systems where the IL represents the solid phase, the simple solubility version without the ΔC_p term was used in Equation 4.12:

$$\ln x_1 = - \ln \gamma_1 - \left\{ \frac{\Delta H^{fus}(T_r)}{RT} \left[1 - \frac{T}{T_r} \right] \right\} \quad (4.12)$$

The expected error from ignoring ΔC_p usually depends on the substance. For normal molecular compounds, this error does not exceed 2%.

The latent heat from pure sodium chloride fusion and its melting temperature are $\Delta H^{fus} = 28.3$ kJ/mol and $T_m = 1073.95$ K, respectively (Yamada et al., 1993).

The non-random 2-liquid (NRTL) model is an activity coefficient model frequently used in chemical engineering to calculate phase equilibria (Renon and Prausnitz, 1968). This model presumes that, within a liquid solution, local compositions account for the short-range order and non-random molecular orientations resulting from molecular size and intermolecular force differences.

The NRTL equation is expressed for a multi-component system in terms of activity coefficients in Equation 4.13:

$$\ln\gamma_i = \frac{\sum_j \tau_{ji} G_{ji} x_j}{\sum_j G_{ji} x_j} + \sum_j \frac{G_{ij} x_j}{\sum_k G_{kj} x_k} \left(\tau_{ij} - \frac{\sum_k \tau_{kj} G_{kj} x_k}{\sum_k G_{kj} x_k} \right) \quad (4.13)$$

with: $\ln G_{ij} = -\alpha_{ij} \tau_{ij}$, $\alpha_{ij} = \alpha_{ji}$, $\tau_{ii} = 0$

Equation 4.13 includes three parameters, i.e. τ_{ij} , τ_{ji} , and α_{ij} , for each pair of components in the multi-component mixture. Therefore, modifying the NRTL equation for a binary system produces Equation 4.14:

$$\ln\gamma_1 = x_2^2 \left(\tau_{21} \left(\frac{G_{21}}{x_1 + x_2 G_{21}} \right)^2 + \frac{\tau_{12} G_{12}}{(x_2 + x_1 G_{12})^2} \right) \quad (4.14)$$

The model was developed within the Simulis® Thermodynamics environment, a thermo physical property calculation server created by ProSim and available as an MS-Excel add-in (www.prosim.net, 2013).

The non-randomness parameter α_{12} was set to 0.2. Then, the binary interaction parameters τ_{ij} and τ_{ji} were estimated temperature from the Na^+ experimental data points.

An iterative process was used at each temperature. The quadratic relative criterion between the calculated and experimental solubilities was minimized using Equation 4.8:

$$\text{Criterion} = \frac{1}{N} \sum_N \left(\frac{x_1^{\text{exp}} - x_1^{\text{cal}}}{x_1^{\text{exp}}} \right)^2 \quad (4.8)$$

This methodology was applied to estimate the binary interaction parameters τ_{12} for only the ionic liquids showing NaCl solubility greater than 1 wt%, i.e. IL1, IL2, IL3,

IL10 and IL16. The results show linear temperature dependence for τ_{ij} parameter expressed by the following correlation:

$$\tau_{ij} = \tau_{ij}^0 + \tau_{ij}^T \cdot (T - 273.15) \quad (4.15)$$

The optimized parameters τ_{ij}^0 and τ_{ij}^T are listed in Table 4.32. Figures 4.41 and 4.42 show comparisons between the experimental and calculated solubilities, expressed in mole fractions. Overall, these data are in very good agreement, confirming that the NRTL model can be used to predict the solubility of NaCl in various ILs.

Table 4.32: NRTL binary interaction parameters between NaCl and different ILs (1 \equiv NaCl and 2 \equiv IL).

IL	τ_{12}^0	τ_{12}^T
[emim][EtSO ₄]	-585.33	0.6662
[emim][MeSO ₃]	-420.74	-1.0891
[emim][DMP]	-479.47	-3.9415
[C ₈ mim][Cl]	-86.52	-5.2329
[EtOHNMe ₃][Me ₂ PO ₄]	-651.25	-0.8478

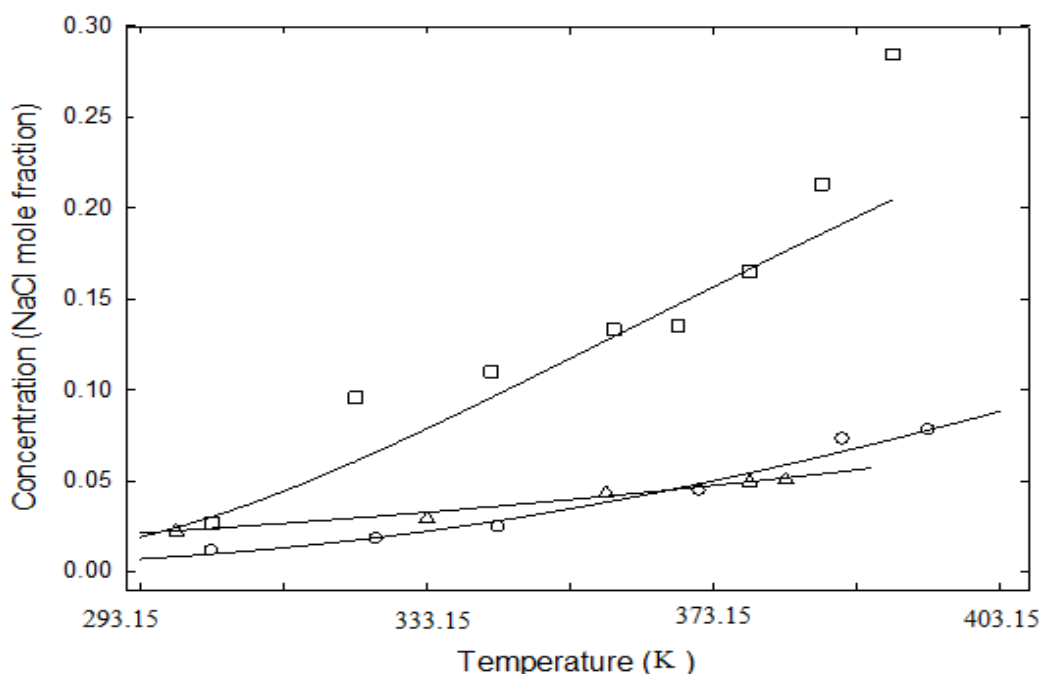


Figure 4.41: Experimental and calculated solubilities (mole fraction) by NRTL for NaCl in imidazolium-based ILs. (Δ) IL1, (\circ) IL2, (\square) IL3. Line represents NRTL data.

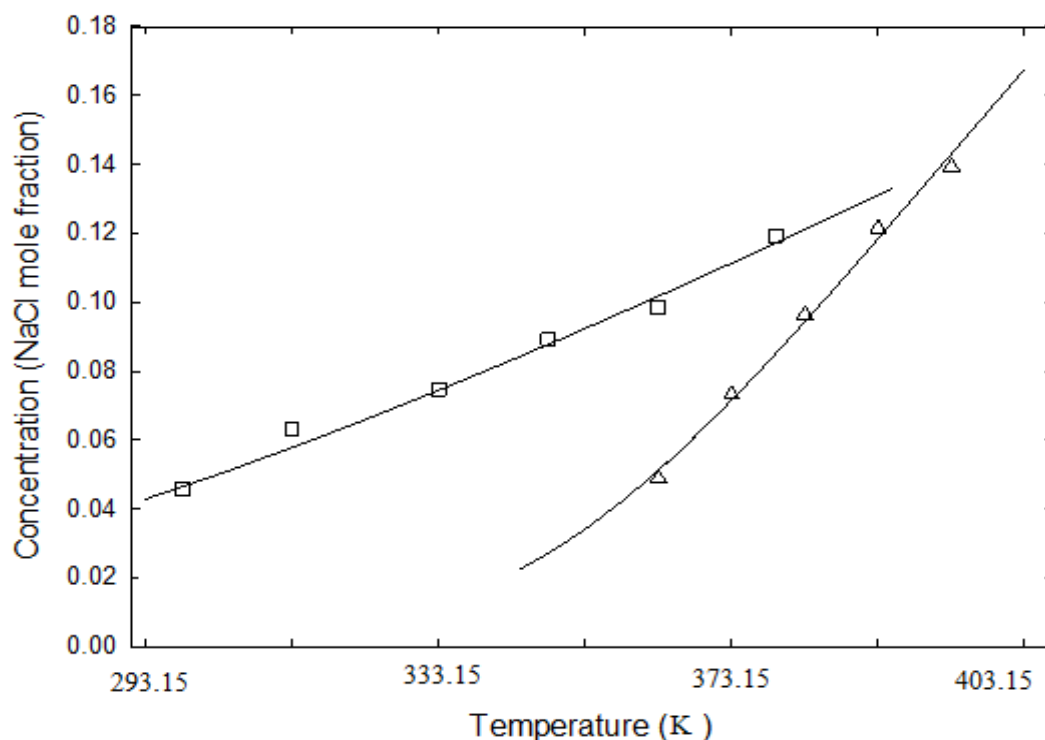


Figure 4.42: Experimental and calculated solubilities (mole fraction) by NRTL for NaCl in (Δ) IL10, (\square) IL16. Lines represent NRTL data.

The experimental and calculated data for IL1, IL2, IL4, and IL5 are in good agreement, with the exception of the data for IL3. However, this does not affect the overall suitability of the developed model.

4.3 Electrical Conductivity of Sodium Chloride Saturated in DESs

Electrical conductivity is one of the essential factors of electrolytes since it determines the level of ohmic drop in cyclic voltammetric analysis (Faridbod et al., 2011). Thus, measuring ionic mobility of saturated solutions of sodium chloride in DESs is highly important to evaluate the electrolytic behaviour of DESs. The electrical conductivity of saturated NaCl solutions in DESs 1 - 5, 8, 10 - 12, and 15 was measured within a range of temperatures. Experimental measurements were done repeatedly to increase the reliability of the obtained values. The results were classified according to solvent structure, range of temperature and stability of the solution. Experimental results

are tabulated in Tables 4.33 through 4.37. Similar to the electrical conductivity of blank DESs, the electrical conductivity of NaCl solutions in DESs was found to be directly proportional to the temperature. Additionally, it depended significantly on the salt, HBD or metal halide used to synthesize a DES.

Figures 4.43 through 4.52 show the profiles of $\ln(\sigma)$ versus the inverse of temperature for NaCl solutions in DESs at different salt:HBD or metal halide ratios and under different temperatures.

Similar to the electrical conductivity of blank DESs, the electrical conductivity of NaCl solutions in DESs were fitted using the same equation used to fit the conductivity profiles in Section 4.1.3, i.e. Equation 4.2. The values of σ_{∞} and E_{σ} for each solution are given in Table 4.38. The fitted series were also plotted in Figures 4.43 – 4.52. The fitting showed a high accuracy when plotted, as it showed a high proximity to the experimental points.

The addition of NaCl to blank DESs until saturation was expected to increase the electrical conductivity of each DES used. This was ascertained by measuring the conductivity of saturated solutions and comparing them to that of blank DESs. An enhancement was obviously noticed in the values of conductivity when compared at the same temperatures. However, in some saturated solutions when the salt concentration was high in the DES, the electrical conductivity decreased when the DES became a saturated solution of NaCl. This was true for DESs 1, 10, 11, and 12. This reduction is caused by the strong influence of ion pairs and ion triplets, together with the higher ion aggregations, which all reduce the overall mobility of ions and the number of effective charge carriers.

The electrical conductivity of ammonium based DESs was increased by a magnitude bigger than the magnitude in which it was increased in phosphonium based DESs. This can be seen when the values in Tables 4.6 - 4.10, blank DES, and Tables

4.33 - 4.37, NaCl solutions in DESs, are compared. For instance, the conductivity of DES8(1:1) increased sharply from 4.36 mS.cm⁻¹ for blank DES to 11.81 mS.cm⁻¹ when the DES became a saturated solution under 398.15 K. However, the conductivity of DES12(1:2) slightly increased from 0.257 mS.cm⁻¹ to 0.360 mS.cm⁻¹ under 363.15 K in saturated NaCl solution.

Considering the practical range of electrical conductivity in electrochemical processes, the electrical conductivity of selected DESs for the present work ought to be higher than 0.1 mS.cm⁻¹ (Faridbod et al., 2011). In this study, all measured electrical conductivities of DESs were found to be in the aforesaid range of electrical conductivity, except for DES15 at 1:4 and 1:5 molar ratios of salt:metal halide under temperatures below 373.15 K and 368.15 K, respectively.

Table 4.33: Experimental electrical conductivity (mS cm⁻¹) of saturated NaCl in DESs 1 and 2 at different molar ratios.

T/K	DES 1 (1:1.75)	DES1 (1:2)	DES1 (1:2.5)	DES2 (1:1)	DES2 (1:2)	DES2 (1:3)
298.15	8.500	8.925	9.996	1.701	1.405	1.264
308.15	11.300	11.865	13.289	2.614	2.160	1.944
318.15	14.120	14.826	16.605	4.453	3.680	3.312
328.15	17.500	18.375	20.580	7.889	6.520	5.868
338.15	20.464	21.487	24.070	14.387	11.890	10.701
348.15	23.018	24.168	27.069	20.546	16.980	15.282

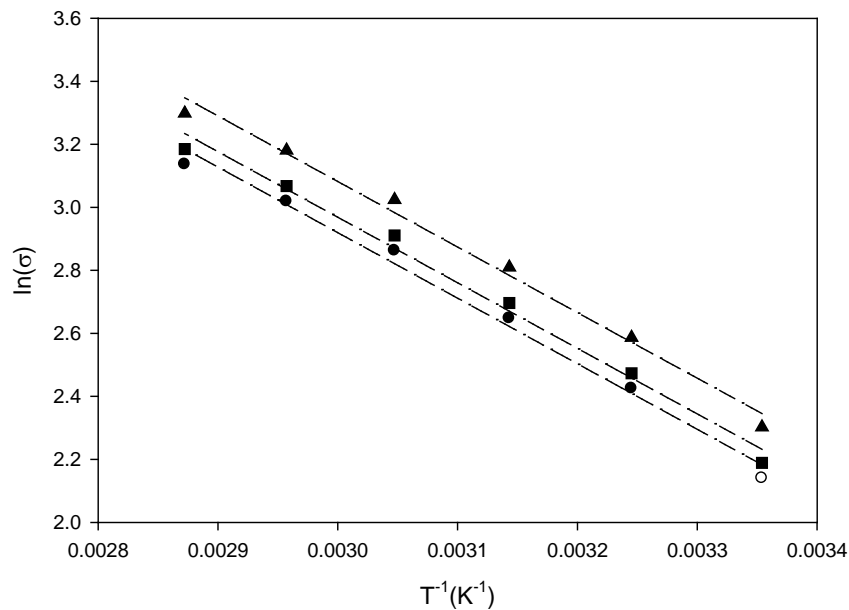


Figure 4.43 Electrical conductivity σ of saturated NaCl in DES1 1:1.75 (●), 1:2 (■), and 1:2.5 (▲) as a function of the inversed temperature. Curves represent fitting by Equation 4.2.

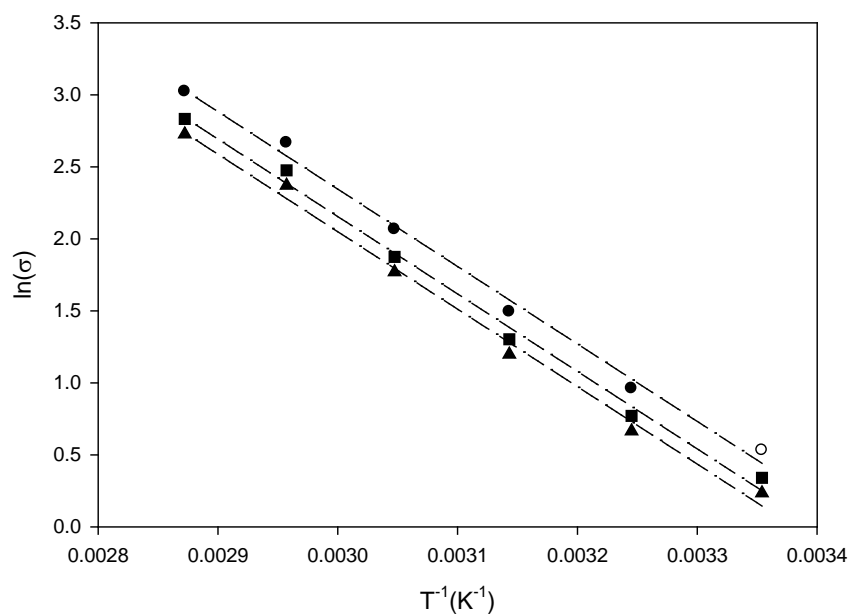


Figure 4.44 Electrical conductivity σ of saturated NaCl in DES2 1:1 (●), 1:2 (■), and 1:3 (▲) as a function of the inversed temperature. Curves represent fitting by Equation 4.2.

Table 4.34: Experimental electrical conductivity (mS cm^{-1}) of saturated NaCl in DESs 3 and 4 at different molar ratios.

T/K	DES3 (1:2.5)	DES3 (1:3)	DES3 (1:4)	DES4 (1:2)	DES4 (1:3)	DES4 (1:4)
298.15	6.360	5.490	5.460	0.707	0.587	0.547
308.15	8.640	7.937	7.260	1.504	1.093	0.995
318.15	11.000	10.324	9.980	2.700	2.050	1.780
328.15	15.750	14.370	13.200	5.300	4.400	3.500
338.15	17.073	16.840	15.847	7.930	5.500	4.910
348.15	20.634	19.641	19.100	11.380	9.830	8.950

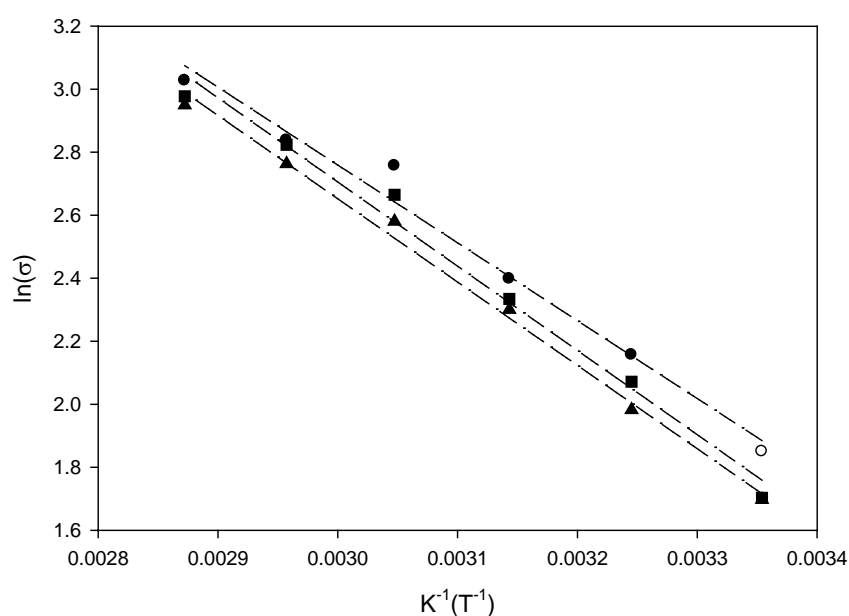


Figure 4.45 Electrical conductivity σ of saturated NaCl in DES3 1:2.5 (\bullet), 1:3 (\blacksquare), and 1:4 (\blacktriangle) as a function of the inversed temperature. Curves represent fitting by Equation 4.2.

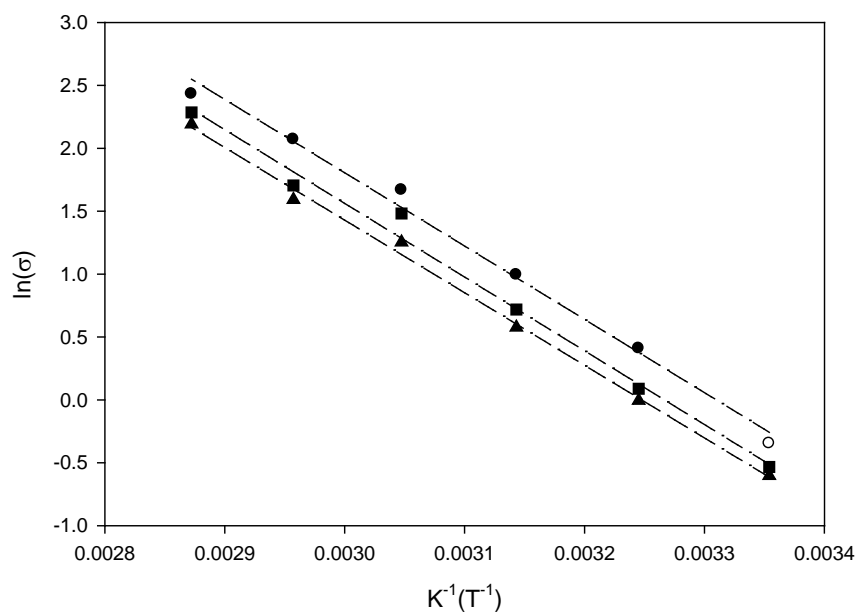


Figure 4.46 Electrical conductivity σ of saturated NaCl in DES4 1:2 (●), 1:3 (■), and 1:4 (▲) as a function of the inversed temperature. Curves represent fitting by Equation 4.2.

Table 4.35: Experimental electrical conductivity (mS cm^{-1}) of saturated NaCl in DESs 5 and 8 at different molar ratios.

T/K	DES5 (1:1)	DES5 (1:2)	DES5 (1:3)	DES5 (1:4)	DES8 (1:1)	DES8 (1:2)	DES8 (1:3)	DES8 (1:4)
363.15	0.924	0.912	0.770	0.580	3.760	2.850	0.207	0.980
368.15	1.308	1.207	0.890	0.730	4.490	3.905	0.650	1.560
373.15	1.628	1.572	1.300	1.100	6.200	5.400	0.854	2.900
378.15	2.080	2.018	1.575	1.400	7.070	6.100	1.097	4.200
383.15	2.550	2.561	1.831	1.798	8.580	7.200	1.823	5.600
388.15	3.940	3.219	2.618	2.246	10.400	9.010	2.180	6.400
393.15	4.640	4.011	3.206	2.900	11.810	10.800	2.960	7.500
398.15	4.810	4.961	4.050	3.700	14.880	12.600	3.560	9.300
403.15	6.180	6.093	5.110	4.500	16.100	13.500	4.800	10.200

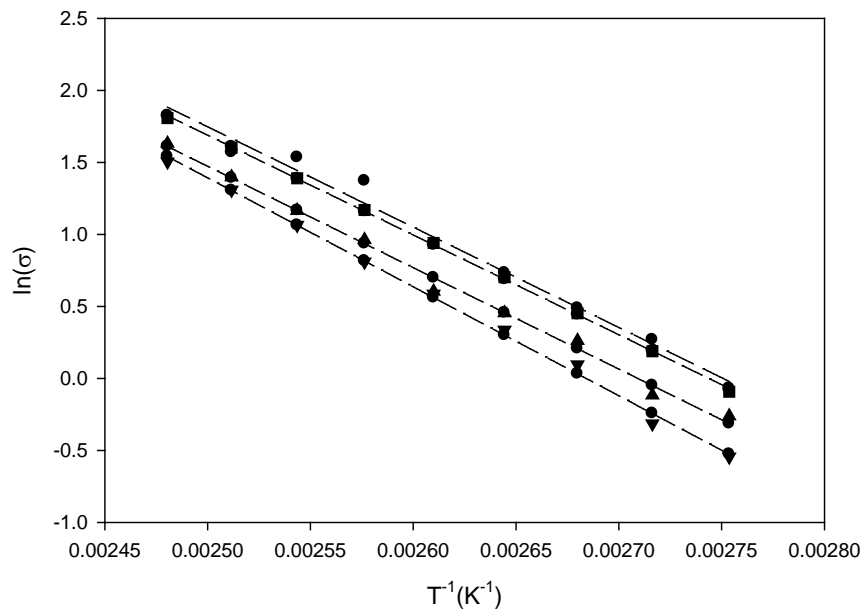


Figure 4.47 Electrical conductivity σ of saturated NaCl in DES5 1:1 (\bullet), 1:2 (\blacksquare), 1:3 (\blacktriangle), and 1:4 (\blacktriangledown) as a function of the inversed temperature. Curves represent fitting by Equation 4.2.

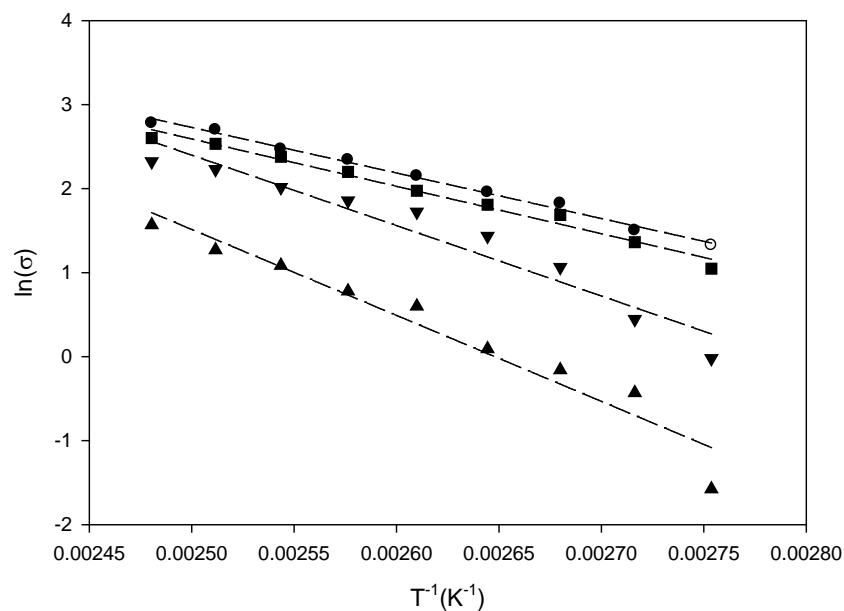


Figure 4.48 Electrical conductivity σ of saturated NaCl in DES8 1:1 (\bullet), 1:2 (\blacksquare), 1:3 (\blacktriangle), and 1:4 (\blacktriangledown) as a function of the inversed temperature. Curves represent fitting by Equation 4.2.

Table 4.36: Experimental electrical conductivity ($\text{mS}\cdot\text{cm}^{-1}$) of saturated NaCl in DESs 10 and 11 at different molar ratios.

T/K	DES10 (1:3)	DES10 (1:4)	DES10 (1:5)	DES11 (1:2)	DES11 (1:3)	DES11 (1:4)
303.15	1.454	2.351	2.920	0.120	0.132	0.185
313.15	1.887	3.155	3.531	0.266	0.340	0.390
323.15	2.920	4.300	5.250	0.462	0.502	0.566
333.15	4.390	5.420	6.730	0.725	0.855	1.067

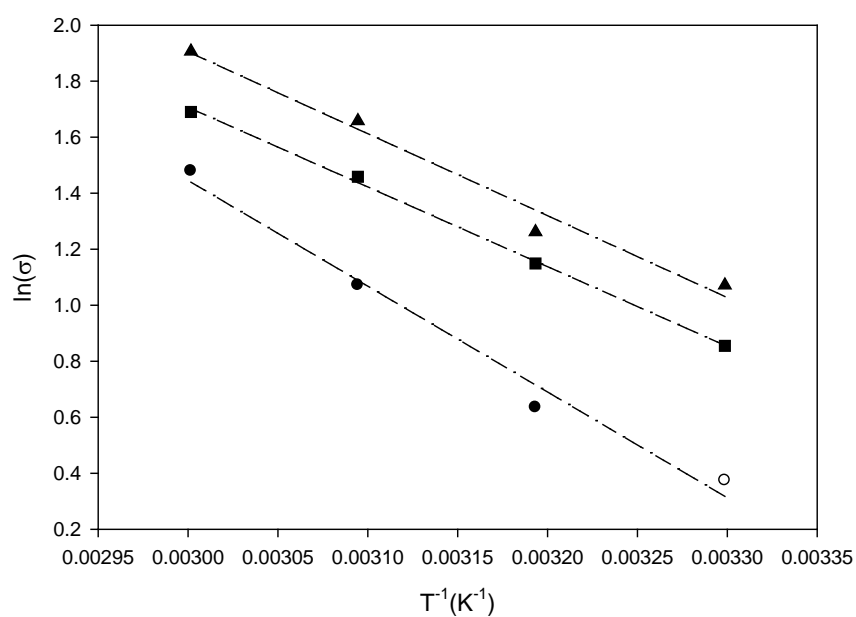


Figure 4.49 Electrical Conductivity σ of saturated NaCl in DES10 1:3 (●), 1:4 (■), and 1:5 (▲) as a function of the inversed temperature. Curves represent fitting by Equation 4.2.

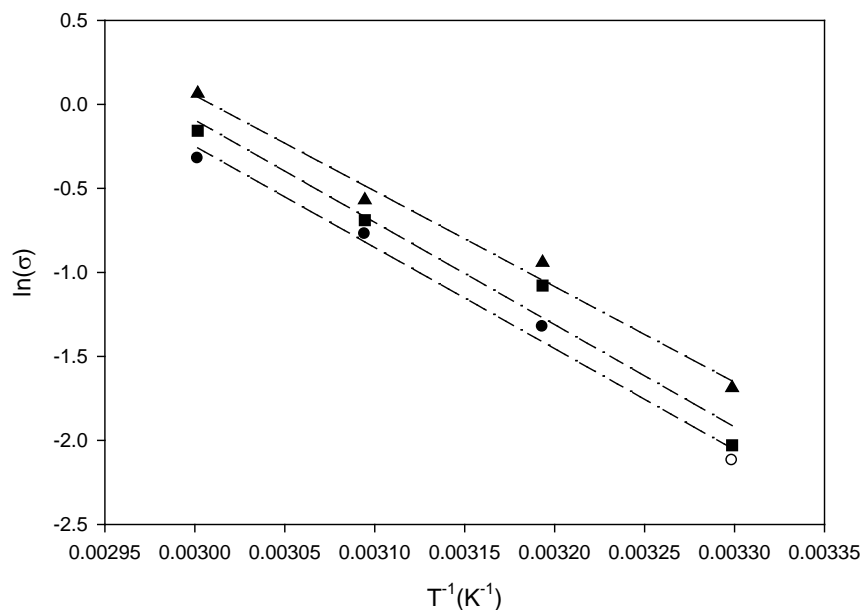


Figure 4.50 Electrical conductivity σ of saturated NaCl in DES11 1:2 (●), 1:3 (■), and 1:4 (▲) as a function of the inversed temperature. Curves represent fitting by Equation 4.2.

Table 4.37: Experimental electrical conductivity (mS cm^{-1}) of saturated NaCl in DESs 12 and 15 at different molar ratios.

T/K	DES12 (1:2)	DES12 (1:3)	DES12 (1:4)	DES12 (1:5)	DES15 (1:2)	DES15 (1:3)	DES15 (1:4)	DES15 (1:5)
363.15	0.297	0.365	0.410	0.534	0.416	0.320	0.059	0.047
368.15	0.360	0.442	0.498	0.647	0.503	0.387	0.081	0.065
373.15	0.425	0.522	0.588	7.645	0.524	0.403	0.103	0.082
378.15	0.448	0.551	0.619	0.805	0.588	0.452	0.166	0.133
383.15	0.525	0.645	0.726	0.944	0.651	0.501	0.197	0.158
388.15	0.598	0.735	0.827	1.075	0.806	0.620	0.267	0.214
393.15	0.705	0.867	0.975	1.268	0.940	0.723	0.324	0.259
398.15	0.780	0.959	1.079	1.403	1.037	0.798	0.399	0.319
403.15	0.930	1.143	1.286	1.672	1.294	0.995	0.460	0.368

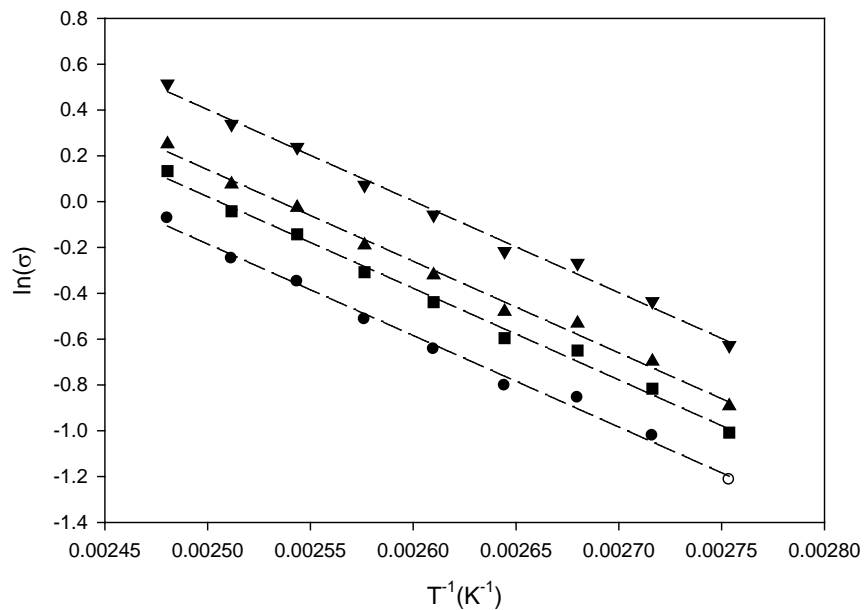


Figure 4.51 Electrical conductivity σ of saturated NaCl in DES12 1:2 (●), 1:3 (■), 1:4 (▲), and 1:5 (▼) as a function of the inversed temp. Curves represent fitting by Equation 4.2.

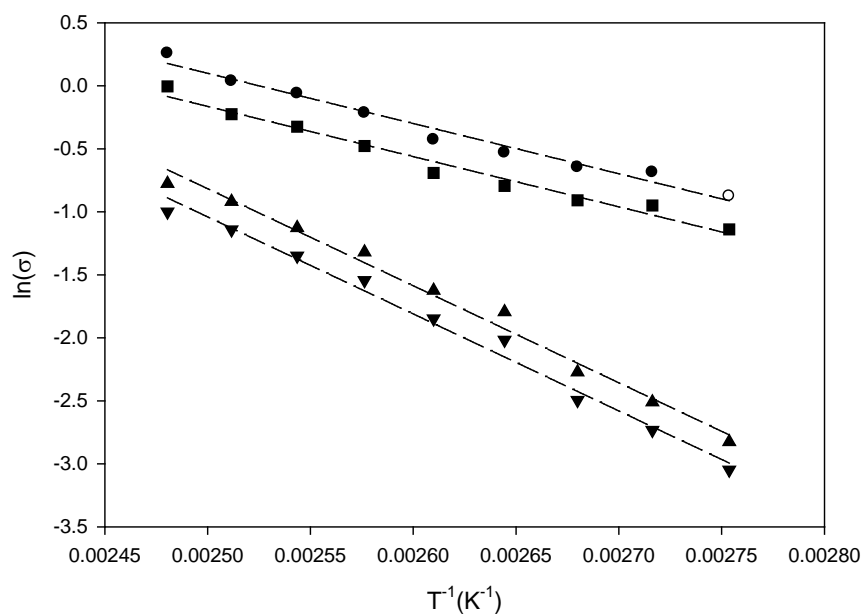


Figure 4.52 Electrical conductivity σ of saturated NaCl in DES15 1:2 (●), 1:3 (■), 1:4 (▲), and 1:5 (▼) as a function of the inversed temp. Curves represent fitting by Equation 4.2.

Table 4.38: Values of σ_{∞} and E_{σ} for the fitting by Equation 4.2 in the system of NaCl(saturated)/DES.

DES	Ratio	σ_{∞} (ms.cm ⁻¹)	E_{σ} (meV)
1	1:1.75	$9.52 \times 10^{+3}$	$1.79 \times 10^{+2}$
1	1:2	$1.00 \times 10^{+4}$	$1.80 \times 10^{+2}$
1	1:2.5	$1.12 \times 10^{+4}$	$1.81 \times 10^{+2}$
2	1:1	$1.06 \times 10^{+8}$	$1.06 \times 10^{+2}$
2	1:2	$8.77 \times 10^{+7}$	$4.63 \times 10^{+2}$
2	1:3	$7.93 \times 10^{+7}$	$4.64 \times 10^{+2}$
3	1:2.5	$2.61 \times 10^{+4}$	$2.12 \times 10^{+2}$
3	1:3	$4.57 \times 10^{+4}$	$2.30 \times 10^{+2}$
3	1:4	$3.97 \times 10^{+4}$	$2.27 \times 10^{+2}$
4	1:2	$2.38 \times 10^{+8}$	$5.09 \times 10^{+2}$
4	1:3	$2.05 \times 10^{+8}$	$5.04 \times 10^{+2}$
4	1:4	$1.39 \times 10^{+8}$	$4.97 \times 10^{+2}$
5	1:1	$2.11 \times 10^{+8}$	$6.00 \times 10^{+2}$
5	1:2	$1.80 \times 10^{+8}$	$5.95 \times 10^{+2}$
5	1:3	$1.93 \times 10^{+8}$	$6.06 \times 10^{+2}$
5	1:4	$6.61 \times 10^{+8}$	$6.51 \times 10^{+2}$
8	1:1	$1.18 \times 10^{+7}$	$4.67 \times 10^{+2}$
8	1:2	$1.77 \times 10^{+7}$	$4.86 \times 10^{+2}$
8	1:3	$5.88 \times 10^{+11}$	$8.81 \times 10^{+2}$
8	1:4	$1.41 \times 10^{+10}$	$7.22 \times 10^{+2}$
10	1:3	$3.55 \times 10^{+5}$	$3.25 \times 10^{+2}$
10	1:4	$2.80 \times 10^{+4}$	$2.45 \times 10^{+2}$
10	1:5	$4.34 \times 10^{+4}$	$2.52 \times 10^{+2}$
11	1:2	$5.48 \times 10^{+7}$	$5.19 \times 10^{+2}$
11	1:3	$7.78 \times 10^{+7}$	$5.24 \times 10^{+2}$
11	1:4	$2.72 \times 10^{+7}$	$4.90 \times 10^{+2}$
12	1:2	$1.80 \times 10^{+4}$	$3.44 \times 10^{+2}$
12	1:3	$2.24 \times 10^{+4}$	$2.44 \times 10^{+2}$
12	1:4	$2.50 \times 10^{+4}$	$2.44 \times 10^{+2}$
12	1:5	$3.25 \times 10^{+4}$	$3.44 \times 10^{+2}$
15	1:2	$2.36 \times 10^{+4}$	$3.43 \times 10^{+2}$
15	1:3	$1.81 \times 10^{+4}$	$3.43 \times 10^{+2}$
15	1:4	$1.01 \times 10^{+8}$	$6.63 \times 10^{+2}$
15	1:5	$8.10 \times 10^{+7}$	$6.63 \times 10^{+2}$

4.4 The Electrochemical Potential Windows of ZnCl₂ Based DESs

It was shown throughout this chapter that zinc chloride based DESs are potential candidates for the production of sodium metal. This is mainly because of the high NaCl

solubility and their high electrical conductivity. Additionally, experiments in our labs showed that pure sodium metal was stable in these DESs.

Another important property of the solvent to be used in electrochemical processes is the electrochemical window. The electrochemical window can be defined as the potential range within which the material is stable. In this work, the electrochemical windows of these DESs were measured using cyclic voltammetry.

Table 4.39 gives a summary of the findings for each DES at different experimental conditions.

Table 4.39: Electrochemical windows obtained at Pt counter electrode, glassy carbon working electrode, and a silver wire quasi reference electrode for DESs 5, 8, 12, and 15.

DES	Salt:metal halide molar ratio	Temperature (°C)	Anodic Limit (V)	Cathodic Limit (V)	Electrochemical window (V)
DES 5	1:1	100	1.69	-0.97	2.66
		110	2.13	-1.06	3.19
		130	2.47	-1.27	3.74
	1:3	100	1.3	-0.95	2.25
		110	1.37	-1.02	2.39
		130	1.65	-1.36	3.01
DES 8	1:1	100	1.33	-0.69	2.02
		110	1.37	-0.74	2.11
		130	1.4	-0.97	2.37
	1:2	100	1.32	-0.48	1.8
		110	1.21	-0.66	1.87
		130	1.41	-0.6	2.01
	1:3	100	1.26	-0.41	1.67
		110	1.34	-0.51	1.85
		130	1.38	-0.57	1.95
DES12	1:2	100	1.87	-1.06	2.93
		110	1.91	-1.09	3.00
		130	1.93	-1.11	3.04
	1:3	100	1.51	-0.8	2.31
		110	1.6	-0.82	2.42
		130	1.64	-0.84	2.48
DES15	1:2	100	1.6	-1.17	2.77
		110	1.73	-1.24	2.97
		130	1.8	-1.26	3.06
	1:3	100	1.17	-1.07	2.24
		110	1.23	-1.08	2.31
		130	1.31	-1.13	2.44

Figures 4.53 through 4.64 depict the electrochemical windows and cyclic voltammeteries of saturated solutions of sodium in DESs at different molar ratios and temperatures. This is achieved by using a glassy carbon (GC) electrode with a diameter of 3 mm as working electrode, a silver (Ag) wire as reference electrode, and a platinum (Pt) electrode as counter electrode at a scan rate of 100 mV s⁻¹.

The electrochemical windows of DES5 for ratios of 1:1 and 1:3 in the temperature range of 100 °C to 130 °C were plotted in Figures 4.53 and 4.54. The effect of increasing the concentration of ZnCl₂ as the complexing agent in the DES was evaluated together with the effect of varying the temperature. It was found that the electrochemical windows of DES5 are strong functions of temperature. For instance, in DES5(1:1), the electrochemical window increased sharply from 2.66 V at 100 °C to 3.19 V and 3.74 V at 110 °C and 130 °C, respectively. In addition, the same trend was obtained for DES5(1:3). The electrochemical window increased from 2.25V at 100 °C to 2.39V and 3.01V at 110 °C and 130 °C, respectively. In contrast, the electrical electrochemical window of DES5 decreased significantly by increasing the molar ratio of ZnCl₂ in the DES. The maximum electrochemical window of DES5 (1:1) at 130 °C was 3.74 V while it was 3.01 V for the molar ratio 1:3 under the same temperature.

Figure 4.55 depicted the cyclic voltammetry of saturated sodium in DES5 at 130 °C as the minimum temperature which attained a electrochemical window of 3.74 V. The sodium reduction potential peak was detected at -0.40 V vs. Ag reference electrode.

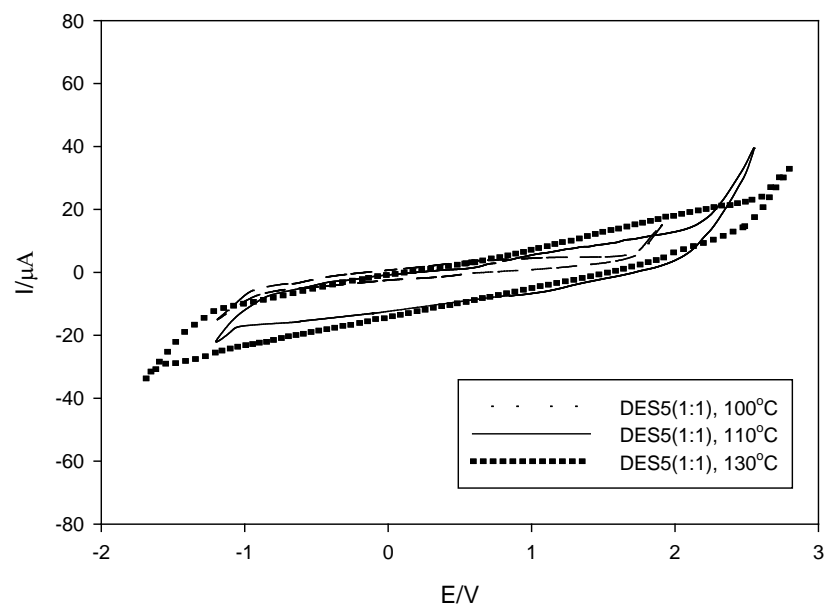


Figure 4.53: Electrochemical window of DES5 (1:1) as a function of temperature on a GC (3 mm) working electrode/ Ag reference electrode/ Pt counter electrode at scan rate of 100 mV s⁻¹.

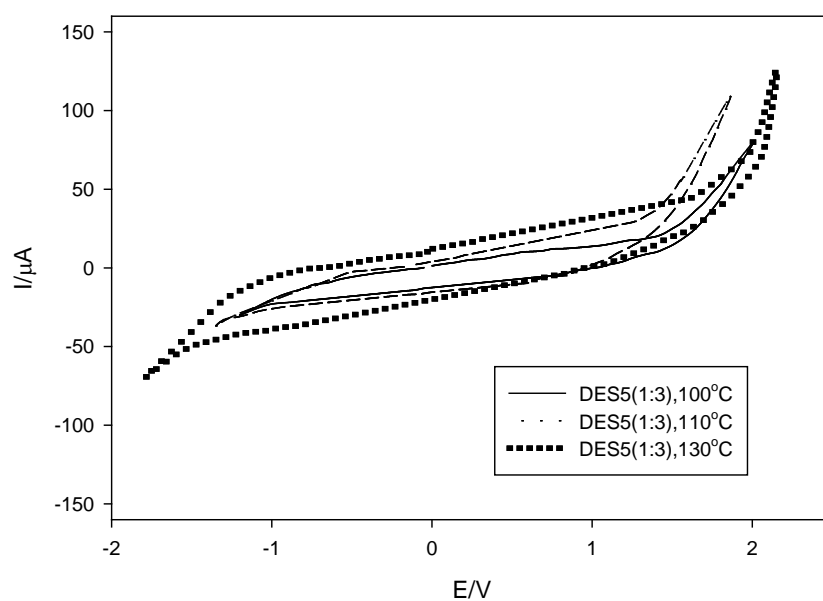


Figure 4.54: Electrochemical window of DES5 (1:3) as a function of temperature on a GC (3 mm) working electrode/ Ag reference electrode/ Pt counter electrode at scan rate of 100mV s⁻¹.

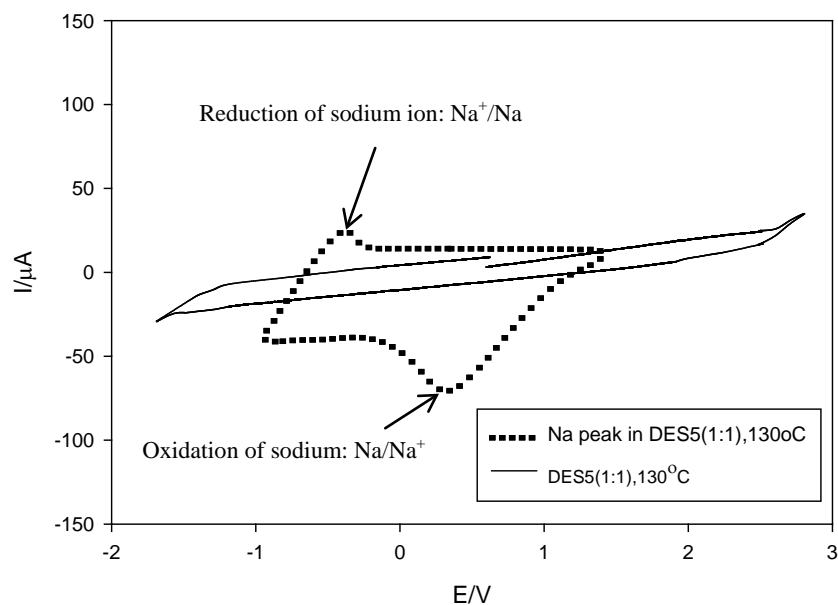


Figure 4.55: Cyclic voltammetry for the reduction of saturated sodium chloride in DES5 (1:1) at 130°C on a GC (3 mm) working electrode/ Ag reference electrode/ Pt counter electrode at scan rate of 100mV s⁻¹.

To evaluate the effect of the salt on the electrochemical window, choline chloride as salt in DES5 was replaced by N,N diethylethanolammonium chloride in DES8. It is clearly shown in Figures 4.56, 4.57, and 4.58 that for the same salt and complexing agent in DES8 but at different molar ratios, the electrochemical windows were influenced noticeably by the concentration of ZnCl_2 and temperature. By changing the molar ratio of DES8 from 1:1 to 1:2 and then to 1:3 at 130 °C, the electrochemical window declined from 2.37 V to 2.01 V and 1.95 V, respectively. However, it was found that the electrochemical windows of DES8 for each molar ratio depended significantly on the operating temperature similar to DES5. On the contrary, the electrochemical window in DES8 increased by increasing the temperature. Table 4.39 and Figure 4.56 shows that in DES8 with molar ratio of 1:1, the electrochemical window grow from 2.02 V under 100 °C to 2.11 V under 110 °C, and afterward it reaches to its maximum potential at 2.37 V under 130°C. The same trend of electrochemical windows are presented in Figures 4.57 and 4.58 for DES8 with the molar ratios 1:2 and 1:3.

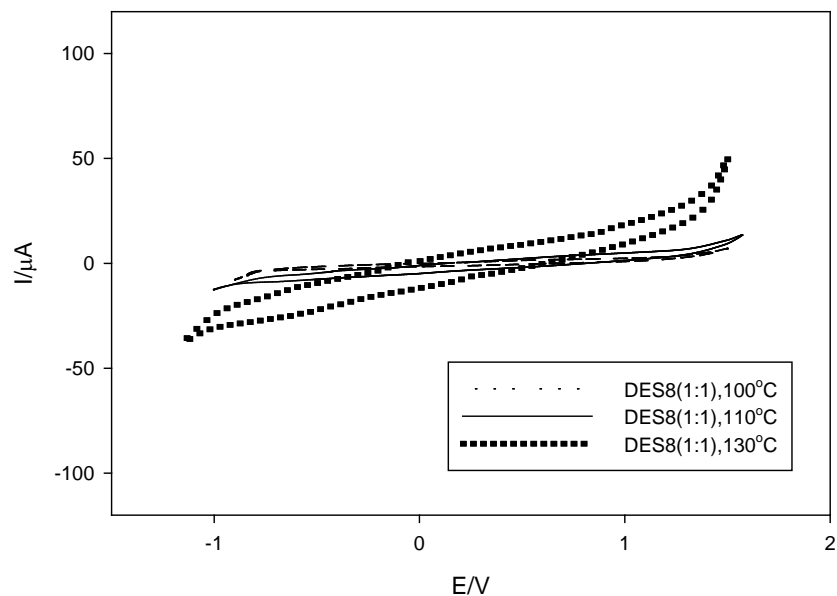


Figure 4.56: Electrochemical window of DES8(1:1) as a function of temperature on a GC (3 mm) working electrode/ Ag reference electrode/ Pt counter electrode at scan rate of 100 mV s⁻¹.

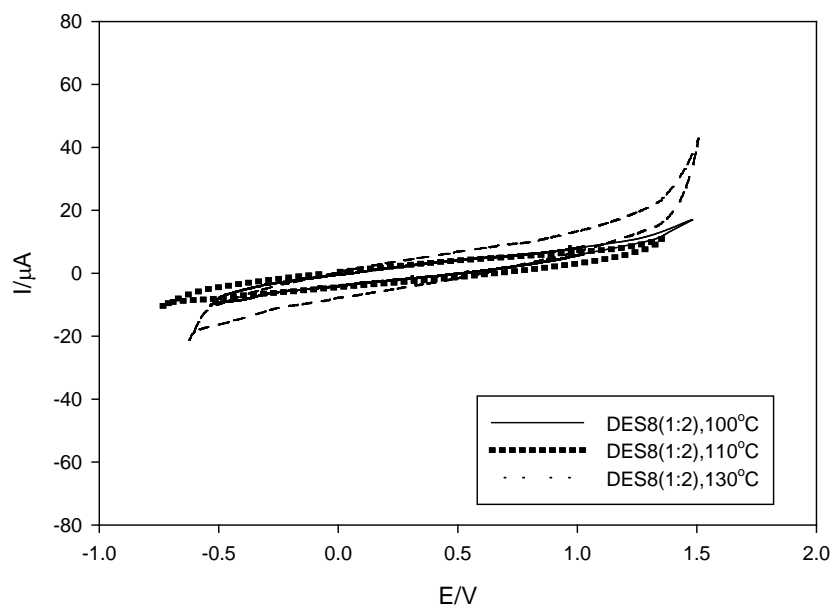


Figure 4.57: Electrochemical window of DES8(1:2) as a function of temperature on a GC (3 mm) working electrode/ Ag reference electrode/ Pt counter electrode at scan rate of 100 mV s⁻¹.

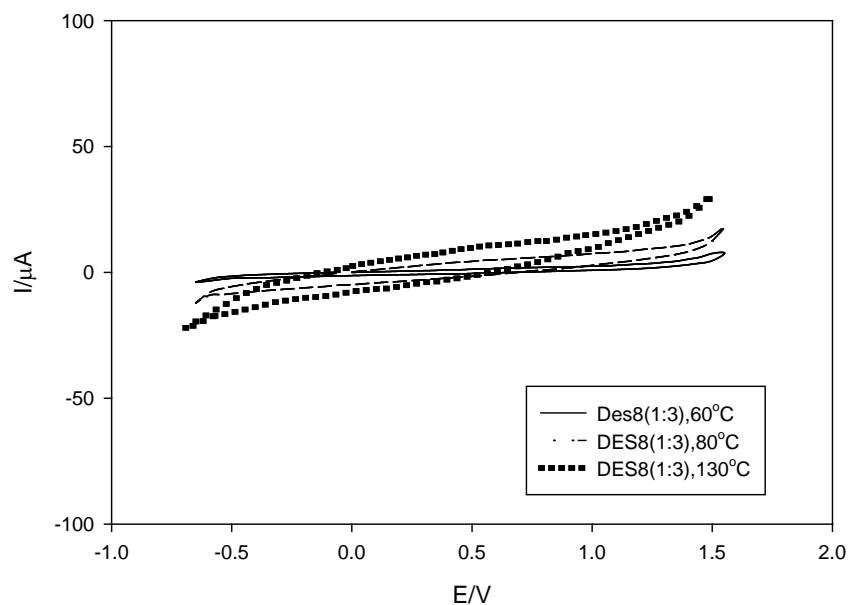


Figure 4.58: Electrochemical window of DES8(1:3) as a function of temperature on a GC (3 mm) working electrode/ Ag reference electrode/ Pt counter electrode at scan rate of 100 mV s⁻¹.

In a comparison between the effect of different ammonium salts on the cyclic voltammetry of ZnCl₂ based DESs, it was found that the electrochemical window in N,N diethylethanolammonium chloride:ZnCl₂ DES was less than the corresponding ChCl:ZnCl₂ DES. From Table 4.39 it can be seen that the maximum electrochemical window for DES 8 (1:1) at 130°C is 2.37 V. However, it is 3.74 V for DES5 (1:1) at the same temperature.

Surprisingly, the cyclic voltammetry of saturated solutions of sodium chloride in DES8 at different molar ratios and different temperatures below 130°C did not give any peak for the reduction of sodium ion. It may give peak at temperatures higher than 130°C. However, owing to equipment limitations the analysis was not carried out at temperatures more than 130°C.

Following the discussion of the effect of the salt on the electrochemical window of ZnCl₂ based DES, the ammonium salts in DESs 5 and 8 were replaced by phosphonium salts, namely, ethyltriphenylphosphonium bromide and tetrabutylphosphonium bromide

for DESs 12 and 15, respectively. The electrical electrochemical windows of ethyltriphenylphosphonium bromide: ZnCl_2 , DES12, at two molar ratios of salt:complexing agent, 1:2 and 1:3, are plotted in Figures 4.59 and 4.60, respectively. Similar to the electrical windows of the ammonium based DESs, i.e. DES5 and DES8, the electrical windows of DES12 are influenced directly by the temperature change. The obtained electrochemical window for DES12 with a mole ratio of 1:2, Figure 4.59 and Table 4.39, increased from 2.93 V at 100 °C to 3 V and 3.04V at 110 °C and 130 °C, respectively. Additionally, the same trend was attained in the cyclic voltammetry test for DES12 using a 1:3 ratio, as observed in Figure 4.60 and Table 4.39. The detected electrochemical window at 100 °C was 2.31V, which increased to 2.42 V and 2.48 V at 110 °C and 130 °C, respectively. Furthermore, the electrochemical windows of this DES decreased sharply by decreasing the molar ratio of ethyltriphenylphosphonium bromide: ZnCl_2 . For instance, from Table 4.39, the maximum electrochemical window for DES12 with a molar ratio of 1:2 is 3.04 V at 130 °C in comparison with a electrochemical window of 2.48 V for the same DES at a molar ratio of 1:3 and under the same temperature.

Figure 4.61 shows the cyclic voltammetry of saturated solution of sodium chloride in DES12 at 100 °C as the minimum temperature, which had the electrochemical window of 2.93 V. The sodium reduction potential peaked at -0.35 V vs. Ag reference electrode.

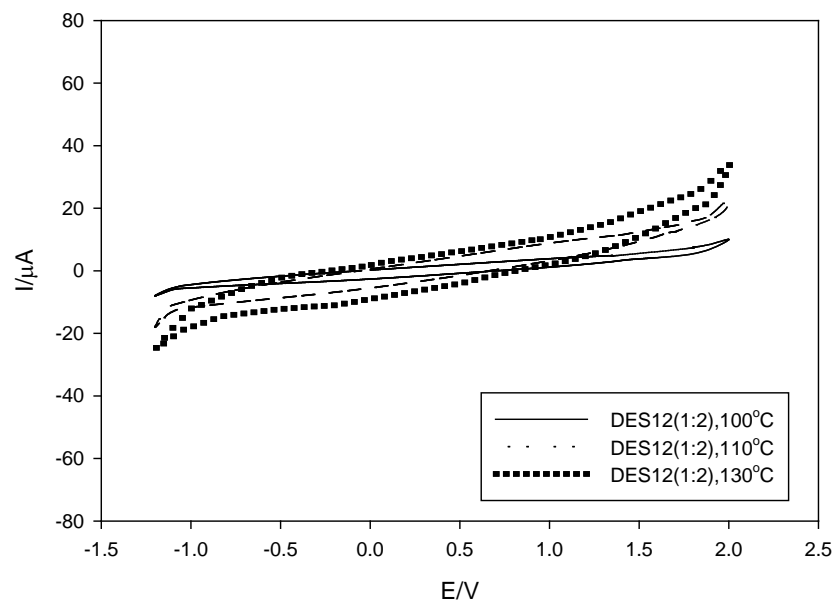


Figure 4.59: Electrochemical window of DES12 (1:2) as a function of temperature on a GC (3 mm) working electrode/ Ag reference electrode/ Pt counter electrode at scan rate of 100 mV s^{-1} .

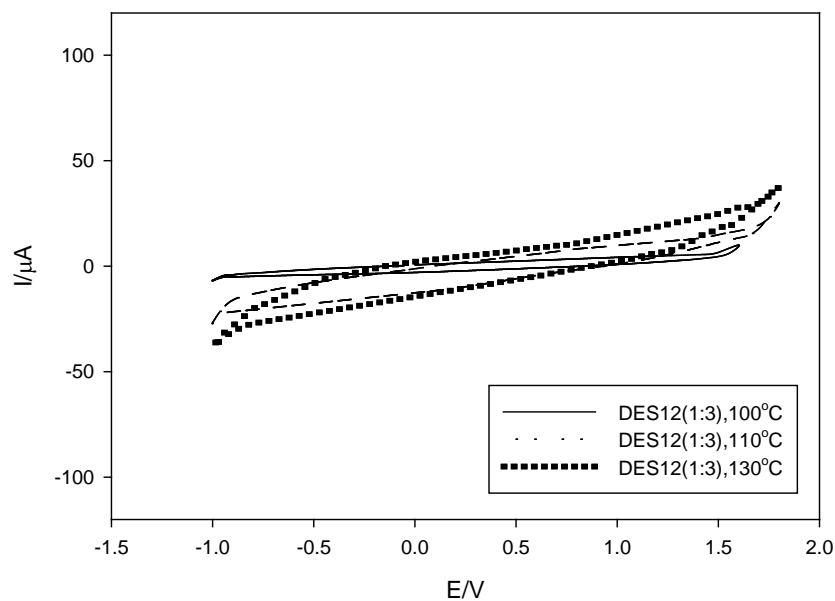


Figure 4.60: Electrochemical window of DES12 (1:3) as a function of temperature on a GC (3 mm) working electrode/ Ag reference electrode/ Pt counter electrode at scan rate of 100 mV s^{-1} .

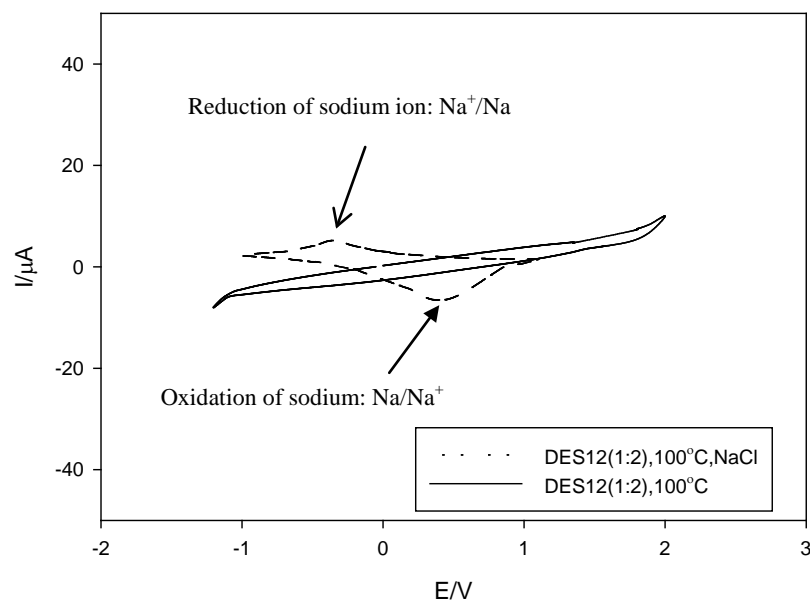


Figure 4.61: Cyclic voltammetry for the reduction of saturated sodium in DES12 (1:2) at 100 °C on a GC (3 mm) working electrode/ Ag reference electrode/ Pt counter electrode at scan rate of 100 mV s⁻¹.

Cyclic voltammetry analysis for electrochemical windows of DES15 are shown in Figures 4.62 and 4.63. The electrical electrochemical windows of DES 15(1:2 and 1:3) decline by the increase in ZnCl₂ molar composition in the DES and increase slightly as the temperature increases. For instance, in Table 4.39, the detected electrochemical window for DES 15 (1:2) was 3.06V at 130 °C while it was 2.44 V for DES 15(1:3) under the same operating temperature. In Table 4.39 and Figure 4.62, the electrochemical window of DES15 (1:2) is 2.77 V at 100°C and increases to 2.97 V at 110 °C and finally reached to 3.06V under 130 °C. Similarly, Figure 4.63 shows that the electrochemical windows of DES15 (1:3) increase from 2.24 V at 100 °C to 2.31 V and 2.44 V at 110 °C and 130 °C, respectively. The maximum detected electrochemical window for DES15 was 3.06 V at 130 °C and 1:2 molar ratio.

Figure 4.64 depicts the cyclic voltammetry of saturated solution of sodium chloride in DES15 at 130 °C . The reduction potential peaks at -0.42 V vs. Ag reference electrode.

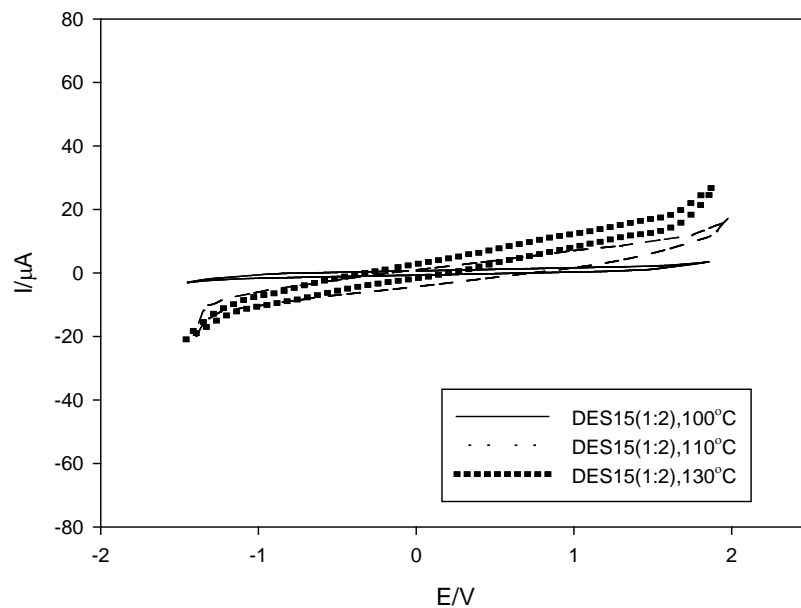


Figure 4.62: Electrochemical window of DES15 (1:2) as a function of temperature on a GC (3 mm) working electrode/ Ag reference electrode/ Pt counter electrode at scan rate of 100 mV s⁻¹.

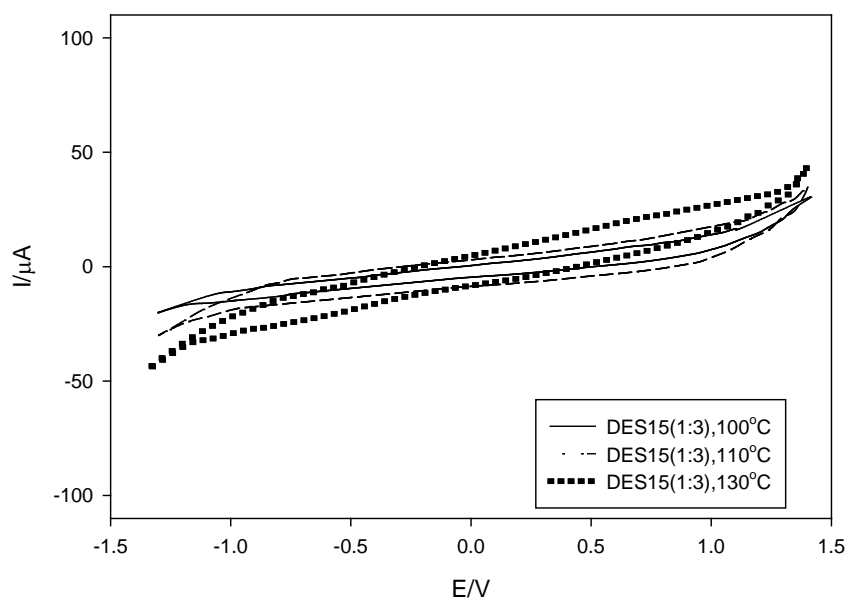


Figure 4.63 Electrochemical window of DES15 (1:3) as a function of temperature on a GC (3 mm) working electrode/ Ag reference electrode/ Pt counter electrode at scan rate of 100 mV s⁻¹.

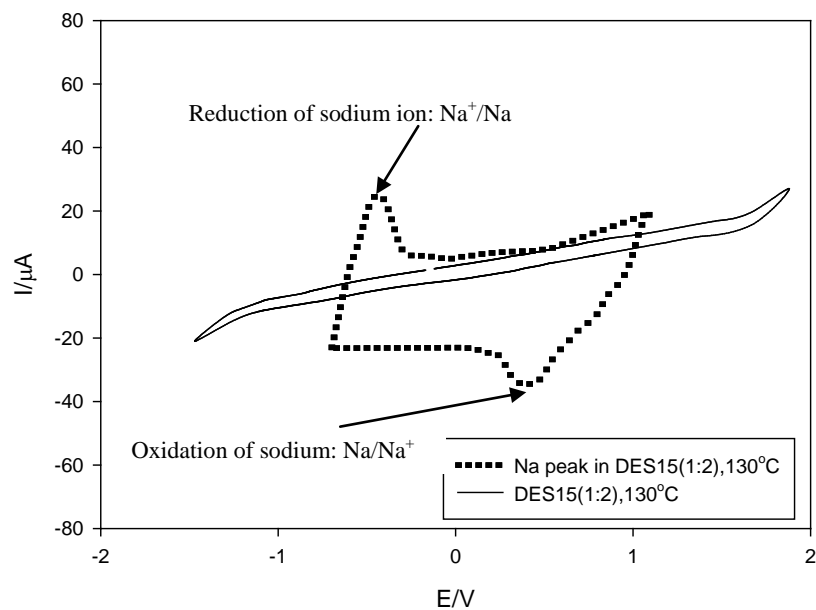


Figure 4.64: Cyclic voltammetry for the reduction of saturated sodium in DES15(1:2) under 130°C on a GC (3 mm) working electrode/ Ag reference electrode/ Pt counter electrode at scan rate of 100 mV s⁻¹.

It can be concluded that the electrical windows in the studied ammonium based DESs, i.e. DES5 and DES8, were more affected by the change in temperature in comparison with the phosphonium based DESs, i.e. DES12 and 15. For instance, for DES5(1:1), the electrochemical window increased from 2.66V at 100 °C to 3.19V and 3.74V at 110 °C and 130 °C, respectively. While it increased slightly for DES12(1:2) from 2.93V at 100 °C to 3V and 3.04V at 120 °C and 130 °C, respectively.

As a conclusion from this electrochemical study, DES5(1:1) at 130 °C possessed the widest electrochemical window among the studied DESs, which was 3.74 V.

ZnCl₂-DESs with high solubility for NaCl in DESs, high electrical conductivity of NaCl in DESs as well as stability of sodium metal in DESs were selected for this application.

CHAPTER V

CONCLUSIONS

The present study investigated the suitability of selected ILs and DESs to serve as electrolytes for the production of sodium metal by electrolysis of common sodium salts. Sixteen ILs and sixteen DESs at various salt:HBD or metal halide molar ratios were utilized in this study, and the results obtained are promising. A number of conclusions can be drawn from this study.

5.1 A Simple and Efficient Method Can be Used for the Synthesis of DESs

DESs were simply produced by mixing a salt and a HBD or a metal halide. The procedure was straight forward and did not require sophisticated equipment. The components of the DES were mixed while the mixing vessel was heated, and this resulted in the formation of a DES. All the mass of the starting materials were utilized in the formation of a DES without a side product, meaning a 100% yield. The purity of the resulting DES depended totally on the purity of the mixed components.

5.2 Different Conditions are Needed for the Synthesis of DESs of Different Combinations

Different ammonium and phosphonium salts were utilized to synthesize the sixteen DESs. By combining these salts with different HBDs and metal halides, and by varying the molar ratios of these combinations, a large variety of DESs was produced.

The important parameters that determine the successful synthesis of a DES are the mixing time, mixing type and mixing temperature. These parameters are of importance for the synthesis of various DESs.

5.3 Physical Properties of DESs are Temperature and Component Dependent

The physical properties, such as electrical conductivity, viscosity and refractive index, are temperature-dependent. The variation of the temperature affected the measured physical properties either linearly or exponentially. Some of the DESs possessed good electrical conductivities, especially the DESs synthesized from ZnCl_2 as complexing agent. In addition, DESs of ammonium salts and ZnCl_2 have low viscosities which is very important in industrial applications.

Additionally, they depended also on the salt of the DES. In general, the DESs synthesized from phosphonium-based salts had melting temperatures above 338 K, while those synthesized from ammonium-based salts had melting temperatures below 326 K. The ammonium-based DESs also had lower viscosities than those of the phosphonium-based DESs. In certain cases, the viscosities of phosphonium-based DESs were 90 folds higher than that of the corresponding ammonium DESs under the same conditions. Moreover, the DESs synthesized from ammonium salts showed higher electrical conductivities than those made from phosphonium salts.

5.4 Solubility of Sodium Salts in ILs or DESs Depended on Various Parameters

In most cases, the solubility of sodium salt increased as the temperature increased and the salt:HBD or metal halide mole ratios decreased. The chemical structure of the DES has a significant effect on the solubility of sodium salts. The solubility of sodium salts in DESs that have ethylene glycol or glycerol as HBD, i.e. neutral molecules, was very small. On the other hand, the solubility of sodium salts in DESs containing ammonium salts and metal halides was very high. This is especially observed for a DES synthesized using ZnCl_2 as complexing agent.

When ILs were analyzed, it was found that both the anion and the cation of a IL affect the solubility of NaCl in the IL. The solubility of NaCl was measured in 16 ILs at different temperatures. Similar to solubility in DESs, the solubility of NaCl in ILs was found to be directly proportional to the temperature. Imidazolium-based ILs had higher NaCl solubilities than pyridinium, pyrrolidinium, and ammonium-based ILs.

5.5 NRTL Activity Coefficients Model Can be Applied Successfully for the Studied Systems

NRTL model was applied successfully to correlate the solubilities of NaCl in some of the tested DESs and ILs. The experimental and predicted values showed very good agreement in most cases. This indicates that the NRTL model can be successfully applied to correlate the solubility of salts in DES or IL.

5.6 ZnCl₂ –based DESs Had a High Potential for Being Electrolytes for Sodium Production

Sodium metal was stable in ZnCl₂-based DESs. The cyclic voltammetry study on saturated NaCl solutions in these DES showed a reduction peak through a quasi-reversible reaction. This peak confirmed the suitability of these DESs to be electrolytes for NaCl decomposition.

CHAPTER VI

RECOMMENDATIONS FOR FUTURE WORK

The recommendations for future work are as follows:

- 1- DESs of the present work can be applied in electrolysis cell so as to produce sodium metal under 130 °C.
- 2- Pilot plant-scale experiments can be carried out to assess the applicability of the studied systems in the batch process.
- 3- The parameters of the process can be optimized to achieve better productivity. Such parameters are the temperature of the separation and the salt:HBD mole ratio.
- 4- In addition to the production of sodium metal, DESs of the present work can also be applied for the production of zinc from zinc halides.

Bibliography

- Abbott, A. P., Barron, J. C., Frisch, G., Ryder, K. S., Silva, A. F. (2011b). The effect of additives on zinc electrodeposition from deep eutectic solvents. *Electrochimica Acta*. 56, 5272–5279.
- Abbott, A. P., Bell, T. J., Handa, S., Stoddart, B. (2006a). Cationic functionalisation of cellulose using a choline based ionic liquid analogue. *Green Chemistry*. 8, 784–786
- Abbott, A. P., Boothby, D., Capper, G., Davies, D. L., Rasheed, R. K. (2004a). Deep eutectic solvents formed between choline chloride and carboxylic acids: Versatile alternatives to ionic liquids. *Journal of American Chemical Society*. 126 (29), 9142–9147.
- Abbott, A. P., Capper, G., Davies, D. L., McKenzie, K. J., Obi, S. U. J. (2006a). Solubility of metal oxides in deep eutectic solvents based on choline chloride. *Journal of Chemical and Engineering Data*. 51, 1280–1282.
- Abbott, A. P., Capper, G., Davies, D. L., Munro, H., Rasheed, R. K., Tambyrajah, V. (2003b). Ionic liquids as green solvents: progress and prospects. *ACS Symposium Series, American Chemical Society: Washington D.C.* 439–452.
- Abbott, A. P., Capper, G., Davies, D. L., Rasheed R. (2004b). Ionic liquids based upon metal halide/substituted quaternary ammonium salt mixtures. *Inorganic Chemistry*. 43, 3447–3452.
- Abbott, A. P., Capper, G., Davies, D. L., Rasheed, R. K., Tambyrajah, V. (2003a). Novel solvent properties of choline chloride/urea mixtures. *Chemical Communications*. 70–71.
- Abbott, A. P., Capper, G., Davies, D. L., Rasheed, R. K., Tambyrajah, V. (2001). Novel ambient temperature ionic liquids for zinc and zinc alloy electrodeposition. *Transactions of the Institute of Metal Finishing*. 79, 204–206.
- Abbott, A. P., Capper, G., Glidle, A., Ryder, K. S. (2006b). Electropolishing of stainless steels in a choline chloride based ionic liquid: an electrochemical study with surface characterisation using SEM and atomic force microscopy. *Physical Chemistry and Chemical Physics*. 8, 4214–4221.
- Abbott, A. P., Capper, G., McKenzie, K. J., Ryder, K. S. (2006c). Voltammetric and impedance studies of the electropolishing of type 316 stainless steel in a choline chloride based ionic liquid. *Electrochimica Acta*. 51, 4420–4425.
- Abbott, A. P., Capper, G., McKenzie, K. J., Ryder, K. S. (2007a). Electrodeposition of zinc–tin alloys from deep eutectic solvents based on choline chloride. *Journal of Electroanalytical Chemistry*. 599 (2), 288–294.
- Abbott, A. P., Cullis, P. M., Gibson, M. J., Harris, R. C., Raven, E. (2007c). Extraction of glycerol from biodiesel into a eutectic based ionic liquid. *Green Chemistry*. 9, 868–872.

- Abbott, A. P., Eardley, A. C. (1999). Solvent properties of liquid and supercritical hydrofluorocarbons. *Journal of Physical Chemistry*. 103, 2504-2509.
- Abbott, A. P., El Taib, K., Frisch, G., McKenzie, K. J., Ryder, K. S. (2009). Electrodeposition of copper composites from deep eutectic solvents based on choline chloride. *Physical Chemistry and Chemical Physics*. 11, 4269–4277.
- Abbott, A. P., Griffith, J., Nandhra, S., O'Connor, C., Postlethwaite, S., Ryder, K. S., Smith, E. L. (2008). Sustained electroless deposition of metallic silver from a choline chloride-based ionic liquid. *Surface & Coatings Technology*. 202 (10), 2033–2039.
- Abbott, A. P., Harris, R. C., Ryder, K. S., Agostino, C. D, Gladden, L. F., Mantle, M. D. (2011a). *Glycerol eutectics as sustainable solvent systems*. *Green Chemistry*. 13, 82–90.
- Abbott, A. P., Nandhra, S., Postlethwaite, S., Smith, E. L., Ryder, K. S. (2007b). Electroless deposition of metallic silver from a choline chloride-based ionic liquid: a study using acoustic impedance spectroscopy, SEM and atomic force microscopy. *Physical Chemistry and Chemical Physics*. 9, 3735–3743.
- Abu-lebdeh, Y., Davidosn, I. (2013). Nanotechnology for lithium-ion batteries. Springer, New York. ISSN 1571-5744. ISBN 978-4614-4604-0.
- Akella, A.K., Sharma, M.P., Saini, R.P. (2007). Optimum utilization of renewable energy sources in a remote area. *Renewable and Sustainable Energy Reviews*. 11, 894–908.
- Aki, S. N. V. K., Brennecke, J. F., Samanta, A. (2001). How polar are room temperature ionic liquids? *Chemical Communications*. 413–414.
- AlNashef, I. M. (2010). Solubility and electrical conductivity of common sodium salts in selected ionic liquids. *Advanced Materials Research*. 233–235, 2760–2764.
- Anastas, P. T. Green Solvents Set II, Volumes 4–6, Boxed Set. (2010). Wiley-VCH Verlag GmbH. ISBN 9783527325924.
- Anastas, P. T., Zimmerman, J. B. (2003). Design through the twelve principles of green engineering. *Environmental Science and Technology*. 37 (5), 94A-101A.
- Aquilina, G., Bories, G., Chesson, A. (2011). Scientific opinion on safety and efficacy of choline chloride as a feed additive for all animal species. *European Food Safety Authority Journal*. 9 (9), 2353–2367.
- Arce, A., Earle, M. J., Rodríguez, H., Seddon, K. R. (2007). Separation of aromatic hydrocarbons from alkanes using the ionic liquid 1-ethyl-3-methylimidazolium bis{(trifluoromethyl) sulfonyl}amide. *Green Chemistry*. 9, 70–74.
- Armand, M., Endres, F., MacFarlane, D. R., Ohno, H., Scrosati, B. (2009). Ionic-liquid materials for the electrochemical challenges of the future. *Nature Materials*. 8, 621–629.
- Awwad, A. M., AlDujaili, A. H. (2001). Density, refractive index, permittivity, and related properties for *N*-formylmorpholine + ethyl acetate and + butanone at 298.15 K. *Journal of Chemical and Engineering Data*. 46 (6), 1349–1350.

- Azizi, N., Gholibeglo, E., Babapour, M., Ghafuri, H., Bolourtchian, S., M. (2012) Deep eutectic solvent promoted highly efficient synthesis of N, N'-diarylamidines and formamides. *Comptes Rendus Chimie*. 15, 768-773.
- Balducci, A., Bradi, U., Caporali, S., Mastragostino, M., Soavi, F. (2004). Ionic liquids for hybrid supercapacitors. *Electrochemistry Communications*. 6 (6), 566-570.
- Banks, A. (1990). Sodium. *Journal of Chemical Education*. 67 (12), 1046.
- Bao, W. L., Wang, Z. M., Li, Y. X. (2003). Synthesis of chiral ionic liquids from natural amino acids. *Journal of Organic Chemistry*. 68, 591-593.
- Barrosse-Antle, L. E., Bond, A. M., Compton, R. G., O'Mahony, A. M., Rogers, E. I., Silvester, D. S. (2010). Voltammetry in room temperature ionic liquids: comparisons and contrasts with conventional electrochemical solvents. *Chemistry An Asian Journal*. 5, 202-230.
- Buzzeo, M. C., Hardacre, C., Compton, R. G. (2004). Use of room temperature ionic liquids in gas sensor design. *Analytical Chemistry*. 76 (15), 4583-4588.
- Cai, Q., Xian, Y., Li, H., Yang-ming, T., Jin, T. (2001). Studies on a sulfur dioxide electrochemical sensor with ionic liquid as electrolyte. *Journal of East China Normal University*. 3, 57-60.
- Carmichael, A. J., Seddon, K. R. (2000). Polarity study of some 1-alkyl-3-methylimidazolium ambient-temperature ionic liquids with the solvatochromic dye, Nile red. *Journal of Physical and Organic Chemistry*. 13, 591-595.
- Carriazo, D., Serrano, M. C., Gutiérrez, M. C., Ferrer, M. L., del Monte, F. (2012). Deep-eutectic solvents playing multiple roles in the synthesis of polymers and related materials. *Chemical Society Reviews*. 41, 4996-5014.
- Chandran, K., Nithya, R., Sankaran, K., Gopalan, A., Ganesan, V. (2006). Synthesis and characterization of sodium alkoxides. *Bulltin of Material Science*. 29 (2), 173-179.
- Chen C. (2001). Synthesis and characterization of new cathode materials for lithium ion batteries. Thesis, Binghamton University, New York.
- Chen, Z., Zhu, W., Zheng, Z., Zou, X. (2010). One-pot α -nucleophilic fluorination of acetophenones in a deep eutectic solvent. *Journal of Fluorine Chemistry*. 131 (3), 340-344.
- Choi, H. M., Yoo, B. (2009). Steady and dynamic shear rheology of sweet potato starch-xanthan gum mixtures. *Food Chemistry*. 116 (3), 638-643.
- Citron, M. L., Gabel, C., Stroud, C., Stroud, C. (1977). Experimental study of power broadening in a two-level atom. *Physical Review A*. 16 (4), 1507.
- Clare, B. R., Bayley, P. M., Best, A. S., Forsyth, M., MacFarlane, D. R. (2008). Purification or contamination? The effect of sorbents on ionic liquids. *Chemical Communications*. 2689-2691.
- Coll, C., Labrador, R. H., Manez, R. M., Soto, J., Sancenon, F., Segui, M. J., Sanchez, E. (2005). Ionic liquids promote selective responses towards the highly

- hydrophilic anion sulfate in PVC membrane ion-selective electrodes. *Chemical Communications*. 3033–3035.
- Cooper, E. I., O’Sullivan, E. J. M. (1992). Proceedings of the eighth international symposium of molten salts, Physical and high temperature materials division proceedings. *Electrochemical Society*. 386–396.
- Dai, Y., van Spronsen, J., Witkamp, G. J., Verpoorte, R., Choi, Y. H. (2013). Natural deep eutectic solvents as new potential media for green technology. *Analytica Chimica Acta*. 66, 61–68.
- Davies, J. A. (1996). *Synthetic coordination chemistry: Principles and practice*. World Scientific. ISBN 978-981-02-2084-6.
- Dawodu, O. F., Meisen, A. (1996). Degradation of aqueous diethanolamine solutions by carbon disulfide. *Gas Separation & Purification*. 10 (1), 1 – 11.
- Ding, J., Zhou, D., Spinks, G., Wallace, G., Forsyth, S., Forsyth, M., MacFarlane, D. (2003). Use of ionic liquids as electrolytes in electromechanical actuator systems based on inherently conducting polymers. *Chemistry of Materials*. 15, 2392–2398.
- Durand, E., Lecomte, J., Barea, B., Piombo, G., Dubreucq, E., Villeneuve, P. (2012) Evaluation of deep eutectic solvents as new media for *Candida antarctica* B lipase catalyzed reactions. *Process Biochemistry*. 47, 2081-2089.
- Earle, M. J., Seddon, K. R. (2000). Ionic liquids. Green solvents for the future. *Pure and Applied Chemistry*. 72 (7), 1391–1398.
- Eggeman, T. (2007). Sodium and sodium alloys. *Kirk-Othmer encyclopedia of chemical technology*. John Wiley & Sons. ISBN: doi:10.1002/0471238961.1915040912051311.a01.pub2.
- Endres, F. (2002). Ionic liquids: solvents for the electrodeposition of metals and semiconductors. *A European Journal of Chemical Physics and Physical Chemistry*. 3 (2), 144–154.
- Endres, F. (2004). Ionic liquids: promising solvents for electrochemistry. *Zeitschrift für Physikalische Chemie*. 218, 255–283.
- Fanning, T. H. (2007). Sodium as a fast reactor coolant. U.S. Nuclear Regulatory Commission. Topical Seminar Series on Sodium Fast Reactors.
- Faridbod, M. R. G. F., Norouzi, P., Riahi, S., Rashedi, H. Application of room temperature ionic liquids in electrochemical sensors and biosensors, ionic liquids: applications and perspectives. (2011). Intech Publications. ISBN 978-953-307-248-7.
- Forsyth, S. A., Pringle, J. M., MacFarlane, D. R. (2004). Ionic liquids-an overview. *Australian Journal of Chemistry*. 57, 113–119
- Frackowiak, E., Lota, G., Pernak, J. (2005). Room-temperature phosphonium ionic liquids for supercapacitor application. *Applied Physics Letters*. 86, 164104–164106.

- Galiński, M., Lewandowski, A., Stępnia, I. (2006). Ionic liquids as electrolytes. *Electrochimica Acta*. 51 (26) 5567 – 5580.
- Gan, Q., Rooney, D., Zou, Y. (2006). Supported ionic liquid membranes in nanopore structure for gas separation and transport studies. *Desalination*. 199, 535–537.
- Ganjali, M. R., Khoshshafar, H., Shirzadmehr, A., Javanbakht, M., Faridbod, F. (2009). Improvement of carbon paste ion selective electrode response by using room temperature ionic liquids (RTILs) and multi-walled carbon nanotubes (MWCNTs). *International Journal of Electrochemical Science*. 4 (3), 435–443.
- Gatti, M., Tokatly, I., Rubio, A. (2010). Sodium: A charge-transfer insulator at high pressures. *Physical Review Letters*. 104 (21), 216–404.
- George, A., Tran, K., Morgan, T. J., Benke, P. I., Berruoco, C., Lorent, E., Wu, B. C., Keasling, J. D., Simmons, B. A., Holmes, B. M. (2011). The effect of ionic liquid cation and anion combinations on the macromolecular structure of lignins. *Green Chemistry*. 13, 3375–3385
- Giap, S. G. E. (2010). The hidden property of arrhenius-type relationship: viscosity as a function of temperature. *Journal of Physical Science*, 21 (1), 29–39.
- Gorke, J., Srienc, F., Kazlauskas, R. (2010). Toward advanced ionic liquids. Polar, enzyme-friendly solvents for biocatalysis, *Biotechnology and Bioprocess Engineering*. 15, 40–53.
- Gray, M. L., Champagne K. J., Fauth, D., Baltrus, J. P., Pennline, H. (2008). Performance of immobilized tertiary amine solid sorbents for the capture of carbon dioxide. *International Journal of Greenhouse Gas Control*. 2 (1), 3 – 8.
- Greaves, T. L., Drummond, C. J. (2008). Protic ionic liquids: properties and applications. *Chemical Reviews*. 108, 206–237.
- Greenlee, K. W., Henne, A. L., Fernelius, W. C. (1946). Sodium amide. *Inorganic Syntheses*. 2, 128–135.
- Greenwood, N. N., Earnshaw, A. (1997). Chemistry of the elements. (2nd ed.). Butterworth–Heinemann. 819–824. ISBN 0750633654.
- Hagiwara, R., Ito, Y. (2000). Room temperature ionic liquids of alkylimidazolium cations and fluoroanions. *Journal of Fluorine Chemistry*. 105, 221–227.
- Hale, G. M., Querry, M. R. (1973). Optical constants of water in the 200-nm to 200- μ m wavelength region. *Applied Optics*. 12, (3) 555–563.
- Handy, T. S. (2011). Applications of ionic liquids in science and technology. Intech publications. ISBN 978-953-307-605-8.
- Hayward, T. (2010). British petroleum statistical review of world energy.
- Hayyan, A., Mjalli, F. S., AlNashef, I. M, Al-Wahaibi, T., Al-Wahaibi, Y. M., Hashim, M. A. (2012). Fruit sugar-based deep eutectic solvents and their physical properties. *Thermochimica Acta*. 541, 70– 75.

- Hayyan, A., Mjalli, F. S., AlNashef, I. M., Al-Wahaibi, Y. M., Al-Wahaibi, T., Hashim, M. A. (2013). Glucose-based deep eutectic solvents: physical properties. *Journal of Molecular Liquids*. 178, 137 – 141.
- Holbrey, J. D., Reichert, W. M., Reddy, R. G., Rogers, R. D. (2003). Heat capacities of ionic liquids and their applications as thermal fluids. *ACS Symposium Series: Ionic Liquids as Green Solvents*. 856, 121–133.
- Holleman, A. F., Wiberg, E. (2001). Inorganic chemistry. Academic Press: San Diego. ISBN-10:0123526515.
- Hou, Y., Gu, Y., Zhang, S., Yang, F., Ding, H., Shan, Y. (2008). Novel binary eutectic mixtures based on imidazole. *Journal of Molecular Liquids*. 143, 154–159.
- Houshmand, A., Shafeeyan, M. S., Arami-Niya, A., Daud, W. M. A. W. (2013). Anchoring a halogenated amine on the surface of a microporous activated carbon for carbon dioxide capture. *Journal of the Taiwan Institute of Chemical Engineers*. <http://dx.doi.org/10.1016/j.jtice.2013.01.014>
- <http://www.prosim.net>
- Huang, J-F., Chen, P-Y., Sun, I-W., Wang, S. P. (2001). NMR evidence of hydrogen bond in 1-ethyl-3-methylimidazolium-tetrafluoroborate room temperature ionic liquid, *Spectroscopy Letters*. 34, 591–603.
- IAEA. (2007). Liquid metal cooled reactors: Experience in design and operation. IAEA-TECDOC-1569, VIENNA, ISBN 978-92-0-107907-7, ISSN 1011-4289.
- Ilgen, F., Ott, D., Kralish, D., Reil, C., Palmberger, A., König, B. (2009). Conversion of carbohydrates into 5-hydroxymethylfurfural in highly concentrated low melting mixtures. *Green Chemistry*. 11, 1948–1954.
- Irvin, D. J., Stenger-Smith, J. D. (2007). Electrochemical supercapacitors based on poly(xylyl viologen). *Polymer Preprints*. 48, 150-XXX.
- Johnson, K. E. (2007). What's an Ionic Liquid? *The electrochemical society interface*. 16,38–40.
- Ju, Y. J., Lien, C. H., Chang K. H., Hu, C. C., Wong, D. S. H. (2012). Deep eutectic solvent-based ionic liquid electrolytes for electrical double-layer capacitors. *Journal of the Chinese Chemical Society*. DOI: 10.1002/jccs.201100698
- Kareem, M. A., Mjalli, F. S., Hashim, M. A., AlNashef, I. M. (2010). Phosphonium-based ionic liquids analogues and their physical properties. *Journal of Chemical and Engineering Data*. 55, 4632–4637.
- Kareem, M. A., Mjalli, F. S., Hashim, M. A., AlNashef, I. M. (2012a). Liquid-liquid equilibria for the ternary system (phosphonium based deep eutectic solvent-benzene-hexane) at different temperatures: a new solvent introduced. *Fluid Phase Equilibria*. 314, 52–59.
- Kareem, M. A., Mjalli, F. S., Hashim, M. A., Hadj-Kali, M. K. O., Bagh, F. S. G., AlNashef, I. M. (2012b). Phase equilibria of toluene/heptane with tetrabutylphosphonium bromide based deep eutectic solvents for the potential

- use in the separation of aromatics from naphtha. *Fluid Phase Equilibria*. 333, 47–54.
- Ke, C., Li, J., Li, X., Shao, Z., Yi, B. (2012). Protic ionic liquids: an alternative proton-conducting electrolyte for high temperature proton exchange membrane fuel cells. *RSC Advances*, 2, 8953–8956.
- Keppler, S. J., Messing, T. A., Proulx, K. B., Jain, D. K. (2003). Molten salt electrolysis of alkali metals. U.S. Patent 6,669,836B2.
- Keskin, S., Kayrak-Talay, D., Akman, U., Hortaçsu, Ö. (2007). A review of ionic liquids towards supercritical fluid applications. *Journal of Supercritical Fluids*. 43, 150–180.
- Kim, T. Y., Lee, H. W., Stoller, M., Dreyer, D. R., Bielawski, C. W., Ruoff, R. S., Suh, K. S. (2011). High-performance supercapacitors based on poly(ionic liquid)-modified graphene electrodes. *ACS Nano*. 5 (1), 436–442.
- Klemm, D., Heublein, B., Fink, H. P., Bohn, A. (2005). Cellulose: fascinating biopolymer and sustainable raw material. *Angewandte Chemie International Edition*. 44, 3358–3393.
- Kölle, P., Dronskowski, R. (2004). Synthesis, crystal structures and electrical conductivities of the ionic liquid compounds butyl dimethylimidazolium tetrafluoroborate, hexafluoroborate and hexafluoroantimonate. *European Journal of Inorganic Chemistry*. 2313–2320.
- Kroschwitz, J. I. (1995). Kirk-Othmer encyclopedia of chemical technology. John Wiley & Sons (New York). ISBN: 9780471238966.
- Lewandowski, A., Swiderska-Mocek, A. (2009). Ionic liquids as electrolytes for Li-ion batteries—An overview of electrochemical studies. *Journal of Power Sources*. 194 (2), 601–609.
- Li, X., Hou, M., Han, B., Wang, X., Zou, L. (2008). Solubility of CO₂ in a choline chloride + urea eutectic mixture. *Journal of Chemical and Engineering Data*. 53, 548–550.
- Lindberg, D., Revenga, M. F., Widersten, M. (2010). Deep eutectic solvents (DESs) are viable cosolvents for enzyme-catalyzed epoxide hydrolysis. *Journal of Biotechnology*. 147, 169–171.
- Mavrovic, I., Shirley, R., Coleman, G. (2010). Urea, Kirk-Othmer encyclopedia of chemical technology, John Wiley & Sons (New York). ISBN:13-978-0-9827779-7-8
- Morrison, H. G., Sun, C. C., Neervannan, S. (2009). Characterization of thermal behavior of deep eutectic solvents and their potential as drug solubilization vehicles. *International Journal of Pharmaceutics*. 378, 136–139.
- Namisnyk, A. M. (2003). A survey of electrochemical supercapacitor technology. Project paper, University of Sydney.
- Noda, A., Susan, M. A. B. H., Kudo, K., Mitsushima, S., Hayamizu, K., Watanabe, M. (2003). Brønsted acid–base ionic liquids as proton-conducting nonaqueous electrolytes. *The Journal of Physical Chemistry B*. 107 (17), 4024–4033.

- Palmieri, V., Mondin, G., Rampazzo, V., Rizzetto, D., Rupp, V., Stivanello, S., Deambrosis, S., Rossi, A. A. (2009). Niobium electropolishing by ionic liquids: What are the naked facts? *Proceedings of SRF2009, Berlin, Germany, Cavity preparation and production*. 463–465.
- Pandey, S. (2006). Analytical applications of room-temperature ionic liquids: A review of recent efforts. *Analytica Chimica Acta*. 556, 38–45
- Paterson, D. S., Chance, M. (1966). Production of sodium, U.S. patent 3,257,297.
- Pearson, D. R., Aranoff, S. L., Okun, D. T., Lane, C. R., Williamson, I. A., Pinkert, D. A. (2008). Sodium metal from France. US International Trade Commission. Investigation No. 731-TA-1135.
- Peng, B., Zhu, J., Liu, X., Qina, Y. (2008). Potentiometric response of ion-selective membranes with ionic liquids as ion-exchanger and plasticizer. *Sensors and Actuators B*. 133, 308–314.
- Pereiro, A. B., Legido, J. L., Rodriguez, A. (2007). Physical properties of ionic liquids based on 1-alkyl-3-methylimidazolium cation and hexafluorophosphate as anion and temperature dependence. *The Journal of Chemical Thermodynamics*. 39 (8), 1168–1175.
- Pesaran, A. A., Markel, T., Tataria, H. S., Howell, D. (2007). Battery requirements for plug-in hybrid electric vehicles - analysis and rationale. 23rd International Electric Vehicle Symposium. California.
- Petkovic, M., Seddon, K. R., Rebelo, L. P. N., Pereira, C. S. (2011). Ionic liquids: a pathway to environmental acceptability. *Chemical Society Reviews*. 40, 1383–1403
- Plechkova, N. V., Seddon, K. R. (2007). Applications of ionic liquids in the chemical industry. *Chemical Society Reviews*. 37, 123–150.
- Prausnitz, J. M., Lichtenthaler, R. N., de Azevedo, E. G. (1999). Molecular thermodynamics of fluid-phase equilibria. 3rd Edition. Prentice Hall, London, UK. International. ISBN-10: 0139777458.
- Pringle, J. M., Forsyth, M., MacFarlane, D. R., Wagner, K., Hall, S. B., Officer, D. L. (2005). The Influence of the monomer and the ionic liquid on the electrochemical preparation of polythiophene. *Polymer*. 46, 2047–2058.
- Reinhardt, D., Ilgen, F., Kralisch, D., König B., Kreisel, G. (2008). Evaluating the greenness of alternative reaction media. *Green Chemistry*. 10, 1170–1181.
- Ramesh, S., Shanti, R., Morris E. (2012). Studies on the plasticization efficiency of deep eutectic solvent in suppressing the crystallinity of corn starch based polymer electrolytes. *Carbohydrate Polymers*, 87, 701-706.
- Renfrow Jr, W. B., Hauser, C. R. (1939). Sodium triphenylmethyl. *Organic Syntheses*. 2, 607.

- Renon, H., Prausnitz, J. M. (1968). Local compositions in thermodynamic excess functions for liquid mixtures. *Journal of American Institute of Chemical Engineers*. 14 (3), 135–144.
- Rui, C. (2010). Recovery of ionic liquids from lignocellulosic samples. Thesis. Central Ostrobothnia University of Applied Sciences.
- Saeed, R., Uddin, F., Masood, S., Asif, N. (2009). Viscosities of ammonium salts in water and ethanol + water systems at different temperatures. *Journal of Molecular Liquids*. 146 (3), 112–115.
- Sandler, S. L. (1999). Chemical and engineering thermodynamics, 3rd Edition. John Wiley & sons. ISBN 10: 0471017744.
- Santos, L. M. N. B. F., Lopes, J. N. C., Coutinho, J. A. P., Esperança, J. M. S. S., Gomes, L. R., Marrucho, I. M., Rebelo, L. P. N. (2007). Ionic liquids: first direct determination of their cohesive energy. *Journal of the American Chemical Society*. 129, 284–285.
- Saravanan, G., Mohan, S. (2011). Electrodeposition of Fe-Ni-Cr alloy from deep eutectic system containing choline chloride and ethylene glycol. *International Journal of Electrochemical Science*. 6, 1468 – 1478.
- Schach, M. O., Schneider, R., Schramm, H., Repke, J. U. (2010). Techno-economic analysis of postcombustion processes for the capture of carbon dioxide from power plant flue gas. *Industrial Engineering Chemistry and Research*. 49 (5), 2363 – 2370.
- Seddon, K. R., Stark, A., Torres, M. J. (2000). Influence of chloride, water, and organic solvents on the physical properties of ionic liquids. *Pure and Applied Chemistry*. 72, 2275–2287.
- Shahbaz, K., Baroutian, S., Mjalli, F. S., Hashim, M. A., AlNashef, I. M. (2012b). Prediction of glycerol removal from biodiesel using ammonium and phosphonium based deep eutectic solvents using artificial intelligence techniques. *Chemometrics and Intelligent Laboratory Systems*. doi:10.1016/j.chemolab.2012.06.005
- Shahbaz, K., Baroutian, S., Mjalli, F. S., Hashim, M. A., AlNashef, I. M. (2012c). Densities of ammonium and phosphonium based deep eutectic solvents: Prediction using artificial intelligence and group contribution techniques. *Thermochimica Acta*. 527, 59–66.
- Shahbaz, K., Ghareh Bagh, F. S., Mjalli, F. S., AlNashef, I. M., Hashim, M. A. (2013). Prediction of refractive index and density of deep eutectic solvents using atomic contributions. *Fluid Phase Equilibria*. 354, 304–311.
- Shahbaz, K., Mjalli, F. S., Hashim, M. A., AlNashef, I. M. (2010). Using deep eutectic solvents for the removal of glycerol from palm-oil based biodiesel. *Journal of Applied Sciences*. 10 (24), 3349–3354.

- Shahbaz, K., Mjalli, F. S., Hashim, M. A., AlNashef, I. M. (2011a). Eutectic solvents for the removal of residual palm oil-based biodiesel catalyst. *Separation and Purification Technology*. 81, 216–222.
- Shahbaz, K., Mjalli, F. S., Hashim, M. A., AlNashef, I. M. (2011b). Using deep eutectic solvents based on methyltriphenylphosphonium bromide for the removal of glycerol from palm-oil-based biodiesel. *Energy & Fuels*. 25, 2671–2678.
- Shahbaz, K., Mjalli, F. S., Hashim, M. A., AlNashef, I. M. (2011c). Prediction of deep eutectic solvents densities at different temperatures. *Thermochimica Acta*. 515, 67–72.
- Shahbaz, K., Mjalli, F. S., Hashim, M. A., AlNashef, I. M. (2012a). Prediction of the surface tension of deep eutectic solvents. *Fluid Phase Equilibria*. 319, 48–54.
- Sheldon, R. A., Lau, R. M., Sorgedraeger, F., Rantwijk, K. V., Seddon, K. R. (2002). Biocatalysis in ionic liquids. *Green Chemistry*. 4, 147–151.
- Shvedene, N. V., Borovskaya, S. V., Sviridov, V. V., Plentnev, I. V. (2005). Measuring the solubilities of ionic liquids in water using ion-selective electrodes. *Analytical and Bioanalytical Chemistry*. 381, 427–430.
- Singh, V. V., Nigam, A., Batra, A., Boopati, M., Singh, B., Vijayaraghavan, R. (2012). Applications of ionic liquids in electrochemical sensors and biosensors. *International Journal of Electrochemistry*. 1–19.
- Song, F., Zhao, Y., Cao, Y., Ding, J., Bu, Y., Zhong, Q. (2013). Capture of carbon dioxide from flue gases by amine-functionalized TiO₂ nanotubes. *Applied Surface Science*. 268, 124 – 128.
- Stenger-Smith, J. D., Irvin, J. A. (2009). Ionic liquids for energy storage applications. *Material Matters*. 4.4, 103.
- Stenger-Smith, J. D., Webber, C. K., Anderson, N., Chafin, A. P., Zong, K., Reynolds, J. R. (2002). Poly(3,4-alkylenedioxythiophene)-based supercapacitors using ionic liquids as supporting electrolytes. *Journal of the Electrochemical Society*. 149 (8), A973–A977.
- Streeter, V. L., Wylie, E. B., Bedford K. W. (1998). Fluid Mechanics. McGraw-Hill, New York, USA. ISBN 0-07-062537-9.
- Swatloski, R. P., Holbrey, J. D., Rogers, R. D. (2003). Ionic liquids are not always green: hydrolysis of 1-butyl-3-methylimidazolium hexafluorophosphate. *Green Chemistry*. 5 (4), 361–363.
- Thayer, A. M. (2008). Having the mettle for sodium markets. *Chemical Engineering News*. 86 (43), 20–21.
- Thompson, J. S., Blank, H. M., Simmons, W. J., Bergmann, O. R. (2004). Low temperature alkali metal electrolysis. U.S. Patent 6,730,210B2.
- Tsuda, T., Hussey, C. L. (2007). Electrochemical applications of room-temperature ionic liquids. *The Electrochemical Society, Interface*. 42–49

- Vila, J., Franjo, C., Pico, J. M., Varela, L. M., Cabeza, O. (2007). Temperature behavior of the electrical conductivity of emim-based ionic liquids in liquid and solid states. *Portugaliae Electrochimica Acta*. 25, 163–172
- Wallace, T. (1953). The castner sodium process. *Chemistry and Industry*. 876–882.
- Wang, J. (2007). Properties and applications of ionic liquids. *China Textile Press*. 13, 56–62.
- Wasserscheid, P., Hal, R. V., Bösmann, A. (2002). 1-*n*-butyl-3-methylimidazolium ([bmim]) octylsulfate—an even ‘greener’ ionic liquid. *Green Chemistry*. 4, 400–404.
- Wasserscheid, P., Keim, W. (2000). Ionic liquids—new “Solutions” for transition metal catalysis. *Angewandte Chemie International Edition*. 39, 3773–3789.
- Weaver, K. D., Kim, H. J., Sun, J., MacFarlane D. R., Elliott, G. D. (2010). *Green Chemistry*. 12, 507–513.
- Wells, A. F. (1984). *Structural Inorganic Chemistry*, Oxford: Clarendon Press. ISBN 0-19-855370-6.
- Welton, T. (1999). Room temperature ionic liquids: Solvents for synthesis and catalysis. *Chemical Reviews*. 99, 2071–2084.
- Wibowo, R., Aldous, L., Rogers, E. I., Jones, S. E., W., Compton, R. G. (2010). A study of the Na/Na⁺ redox couple in some room temperature ionic liquids. *Journal of Physical Chemistry C*. 114, 3618–3626.
- Wildman, S. A., Crippen, G. M. (1999). Prediction of physicochemical parameters by atomic contributions. *Journal of Chemical Information and Computer Sciences*. 39, 868–873.
- Wilkes, J. S., Levisky, J. A., Wilson, R. A., Hussey, C. L. (1982). Dialkylimidazolium chloroaluminate melts: a new class of room-temperature ionic liquids for electrochemistry, spectroscopy and synthesis. *Inorganic Chemistry*. 21, 1263–1264.
- Wilkes, J. S., Zaworotko, M. J. (1992). Air and water stable 1-ethyl-3-methylimidazolium based ionic liquids. *Journal of the Chemical Society, Chemical Communications*. 965–967.
- Yamada, M., Tago, M., Fukusako, S., Horibe, A. (1993). Melting point and supercooling characteristics of molten salt. *Thermochimica Acta*. 218, 401–411.
- Yu, Y. H., Lu, X. M., Zhou, Q., Dong, K., Yao, H. W., Zhang. S. J. (2008). Biodegradable naphthenic acid ionic liquids: synthesis, characterization, and quantitative structure– biodegradation relationship. *Chemistry - A European Journal*. 14, 11174–11182.
- Zakeeruddin, S. M., Graetzel, M. (2009). Solvent-free ionic liquid electrolytes for mesoscopic dye-sensitized solar cells. *Advanced Functional Materials*. 19 (14), 2187–2202.

- Zhang, J., Bond, A. M. (2005). Practical considerations associated with voltammetric studies in room temperature ionic liquids. *Analyst*. 130, 1132–1147.
- Zhang, Q., De Oliveira, V. K., Royer, S., Jérôme, F. (2012). Deep eutectic solvents: syntheses, properties and applications. *Chemical Society Reviews*. 41 (21), 7108-7146.
- Zhao, H., Baker, G. A. (2013). Ionic liquids and deep eutectic solvents for biodiesel synthesis: a review. *Journal of Chemical Technology and Biotechnology*. 88 (1), 3–12.
- Zheng, Y. H., Li, Z. F., Feng, S. F., Lucas, M., Wu, G. L., Li, Y., Li, C. H., Jiang, G. M. (2010). Biomass energy utilization in rural areas may contribute to alleviating energy crisis and global warming: A case study in a typical agro-village of Shandong, China. *Renewable and Sustainable Energy Reviews*. 14, 3132–3139.
- Zhou, T., Chen, L. Ye, Y., Chen, L., Qi, Z., Freund, H., Sundmarcher, K. (2012). An overview of mutual solubility of ionic liquids and water predicted by COSMO-RS. *Industrial Engineering and Chemistry Research*. 51 (17), 6256–6264.

Appendix A

Research Outputs

Conferences

- Solubility and electrical conductivity of sodium chloride in selected ionic liquids. The 8th Asia Pacific Conference on Sustainable Energy & Environmental Technologies (APCSEET), Adelaide, Australia. 2011. **F. Saadat Ghareh Bagh**, Farouq S. Mjalli, Mohd Ali Hashim, Inas M. Al-Nashef.
- Solubility of selected sodium salts in ionic liquids. 1st International Conference on Ionic Liquids in Separation and Purification Technology, Sitges, Spain. 2011. **F. Saadat Ghareh Bagh**, Farouq S. Mjalli, Mohd Ali Hashim, Inas M. Al-Nashef.
- Solubility of Sodium Chloride in Benign Solvents. International Congress on Green Process Engineering (GPE), Kuala Lumpur, Malaysia. 2011. **F. Saadat Ghareh Bagh**, Farouq S. Mjalli, Mohd Ali hashim, Inas M. Al-Nashef.
- Solubility and Electrical Conductivity of Common Sodium Salts in Selected Ionic Liquid (SHUSER), Kuala Lumpur, Malaysia. 2011. Inas M. AlNashef, Farouq S. Mjalli, Mohd Ali Hashim, Maan Hayyan, **F. Saadat**.
- Application of Ionic Liquids as Green Solvents in Sodium Metal Production from Common Salts, **F. Saadat Ghareh Bagh**, Farouq S. Mjalli, Mohd Ali Hashim, Inas M. Al-Nashef. (ICERT 2012) 3rd international conference on environmental research and technology, Penang, Malaysia.
- Solubility and Conductivity of Sodium Chloride in Benign Solvents, **F. Saadat Ghareh Bagh**, Farouq S. Mjalli, Mohd Ali Hashim, Inas M. Al-Nashef.(ICPEAM2012) International Conference on Process Engineering and

Advanced Materials, Kuala Lumpur, Malaysia.

- Reducing energy consumption in ethylene production by green solvents' utilization. Mukhtar A. Kareem, Farouq S. Mjalli, Mohd Ali Hashim, Inas M. AlNashef, **Fatemeh S. Ghareh Bagh**. 3rd international conference on environmental research and technology (ICERT 2012), Penang, Malaysia.
- Application of deep eutectic solvents based on ethylene glycol and sulfolane for the extraction of toluene from toluene/heptane mixtures. Mukhtar A. Kareem, Farouq S. Mjalli, Mohd Ali Hashim, Inas M. AlNashef, **Fatemeh S. Ghareh Bagh**. 2nd international conference on process engineering and advanced materials (ICPEAM 2012), Kuala Lumpur, Malaysia.
- A Novel Electrolyte for Separation of Sodium Salt: A Study for Sodium Solubility in Deep Eutectic Solvents, **F. Saadat Ghareh Bagh**, Farouq S. Mjalli, Mohd Ali Hashim, Inas M. Al-Nashef, (Chemeca 2012), Quality of life through chemical engineering, Wellington, New Zealand.

Journal Papers

- Solubility of Sodium Salts in Ammonium-based Deep Eutectic Solvents. Journal of Chemical and Engineering Data. 2013, 58, 2154 – 2162. **Fatemeh Saadat Ghareh Bagh**, Farouq S. Mjalli, Mohd Ali Hashim, Mohamed K.O. Hadj-Kali, Inas M. Alnashef.
- Electrical conductivity of ammonium and phosphonium based deep eutectic solvents: Measurements and artificial intelligence-based prediction. Fluid Phase Equilibria. 2013, 356, 30 – 37. **F.S. Ghareh Bagh**, K. Shahbaz, F.S. Mjalli, I.M. AlNashef, M.A. Hashim.
- Solubility of sodium chloride in ionic liquids. **Fatemeh Saadat Ghareh Bagh**, Farouq S. Mjalli, Mohd Ali Hashim, Mohamed K. O. Hadj-Kali, Inas M.

AlNashef. Industrial Engineering and Chemical Research. 2013, 52, 11488 – 11493.

- Prediction of refractive index and density of deep eutectic solvents using atomic contributions. Fluid Phase Equilibria. 2013, 354, 304 – 311. K. Shahbaz, **F.S. Ghareh Bagh**, F.S. Mjalli, I.M. AlNashef, M.A. Hashim.

Patent

- Mohd. Ali Hashim, Farouq S. Mjalli, Inas M. Al-Nashef, **F. Saadat Ghareh Bagh**, Mukhtar A. Kareem. Electrolysis process for producing Sodium metal at a low operating temperature. Application No: PI 2012700369, Applicant: Universiti Malaya. (Applied through University of Malaya in Patent Cooperation Treaty (PCT) International Application/ Overseas Patent)

Under Review Papers

- Solubility of sodium chloride in phosphonium based deep eutectic solvents. Journal of Fluid Phase Equilibria. **Fatemeh Saadat Ghareh Bagh**, Farouq S. Mjalli, Mohd Ali Hashim, Inas M. Al-Nashef, Mohamed Kamel Omar Hadj-Kali.
- Physical and electrochemical properties of ZnCl₂ based DESs. Finalizing to submit to Journal of Chemical and Engineering Data. **Fatemeh Saadat Ghareh Bagh**, Farouq S. Mjalli, Mohd Ali Hashim, Inas M. Al-Nashef.

Awards

- Selected as Bright Spark student under Bright Spark Unit/University of Malaya, 2011-2013.